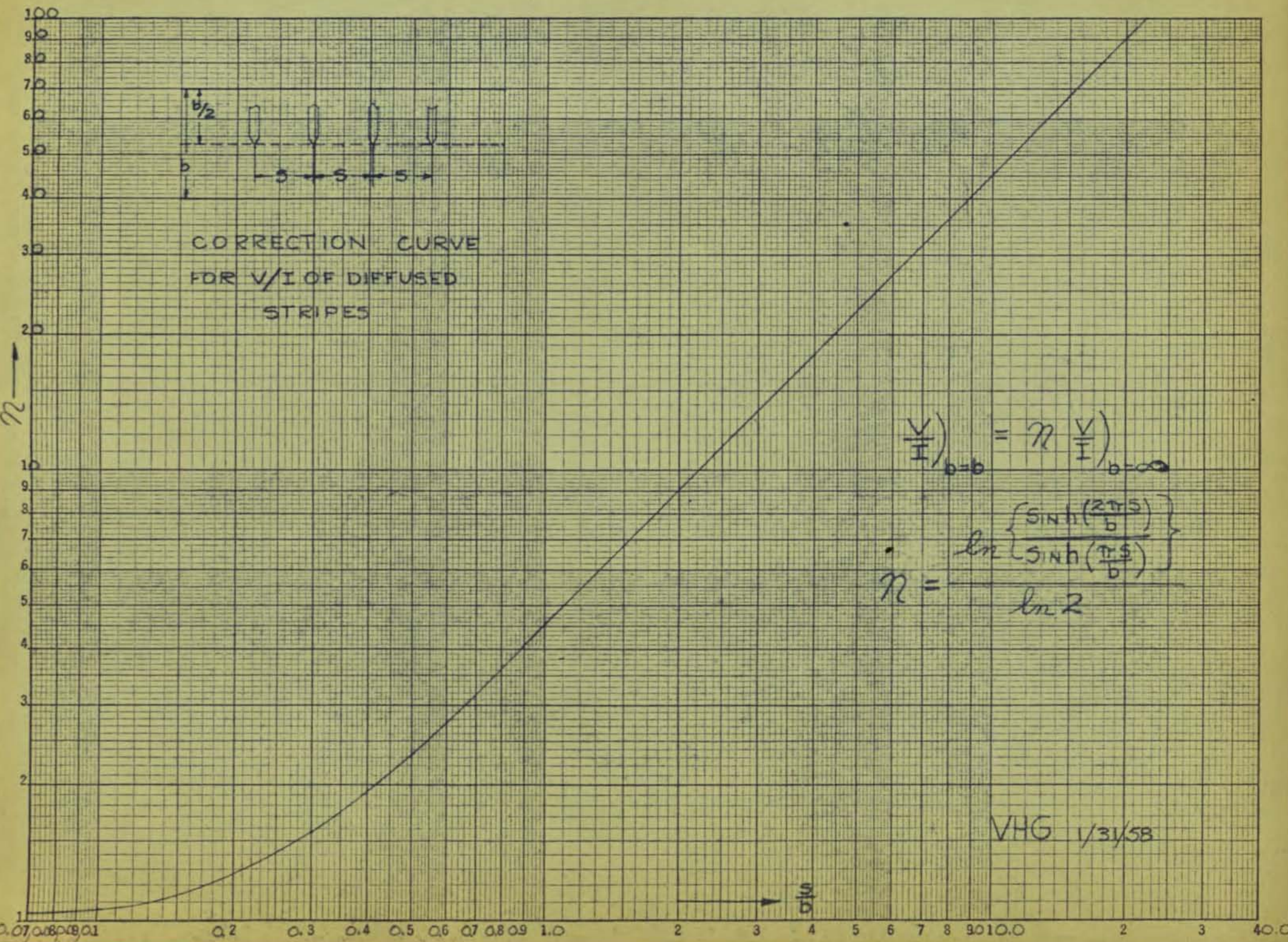
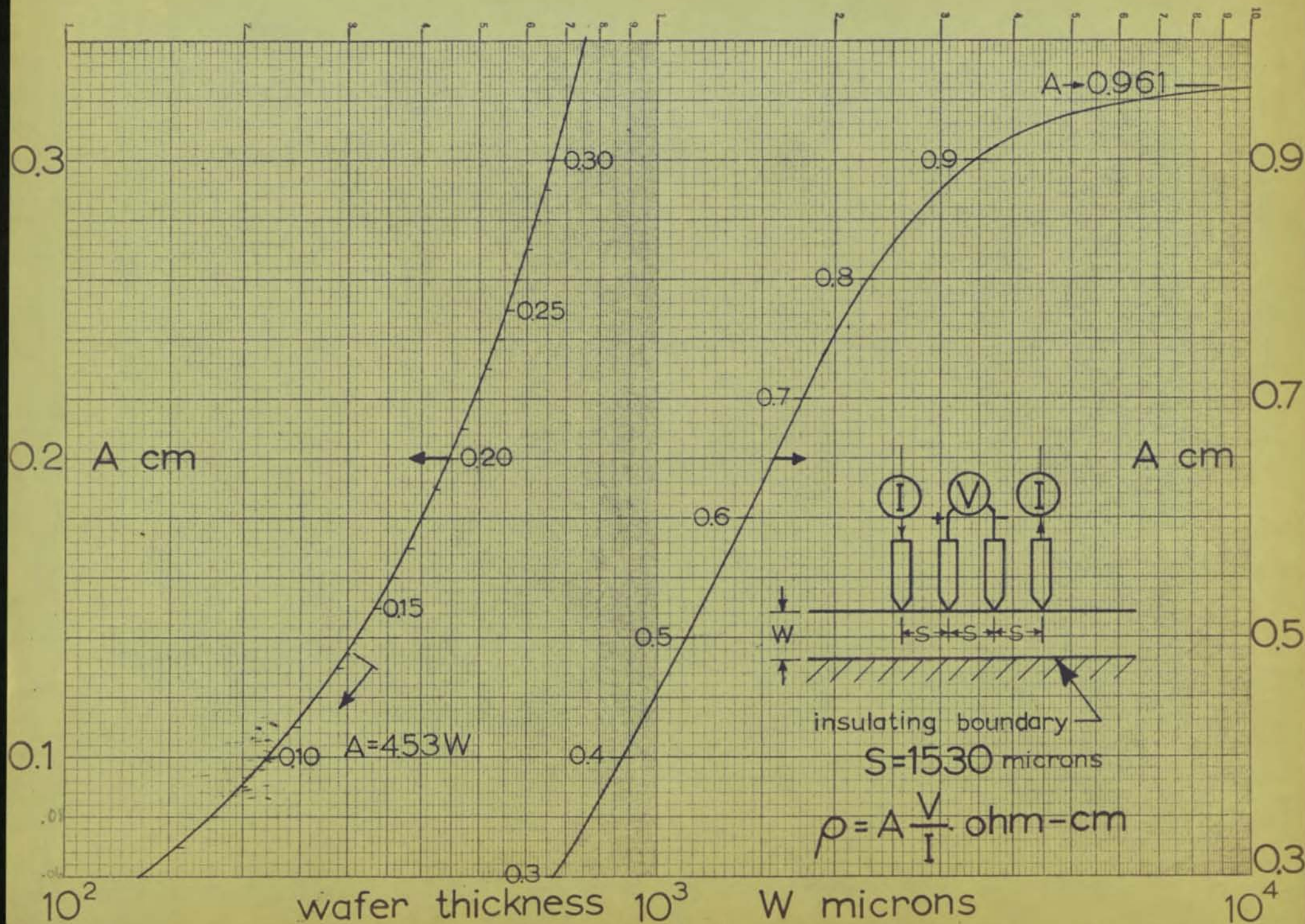
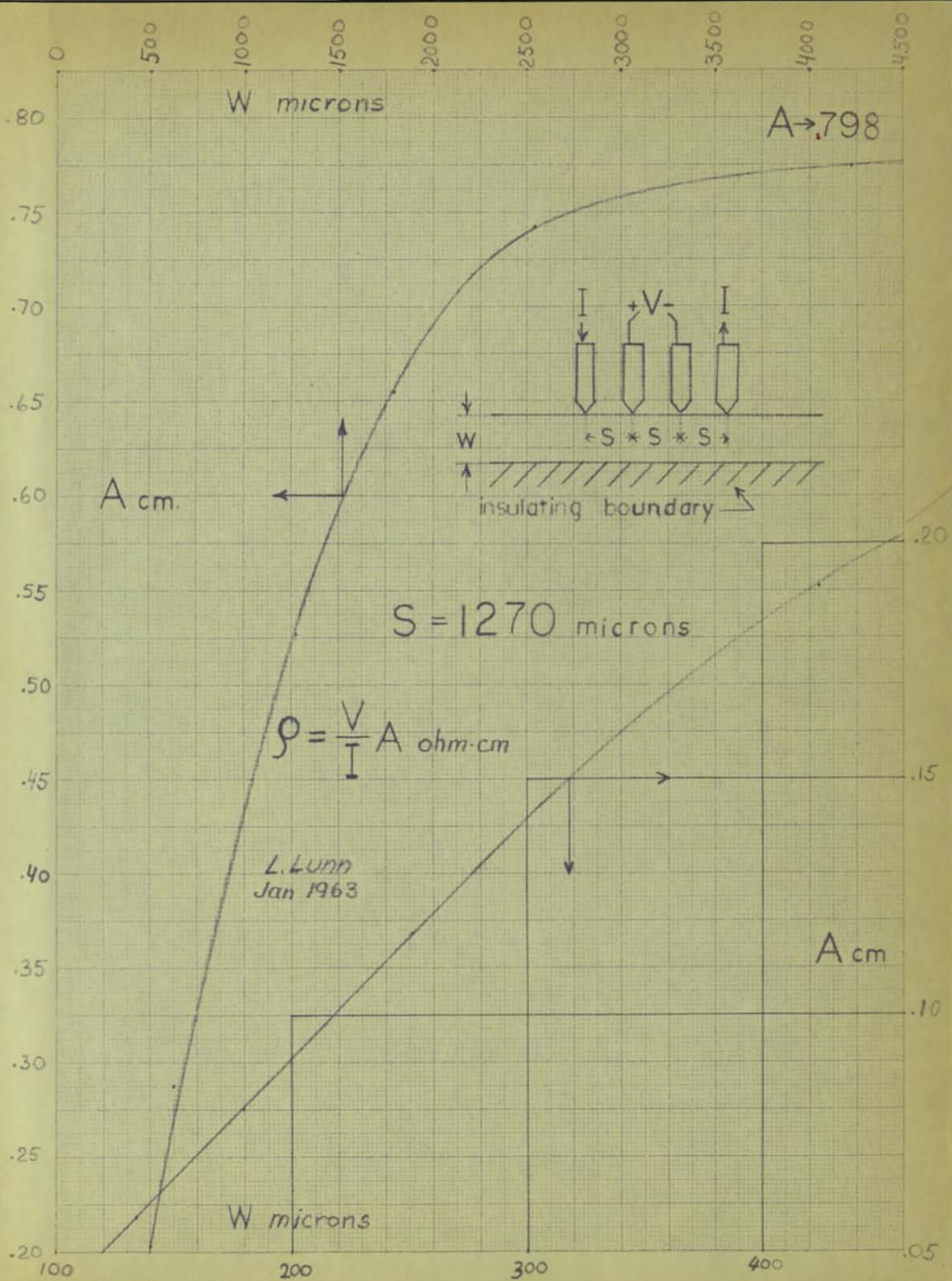
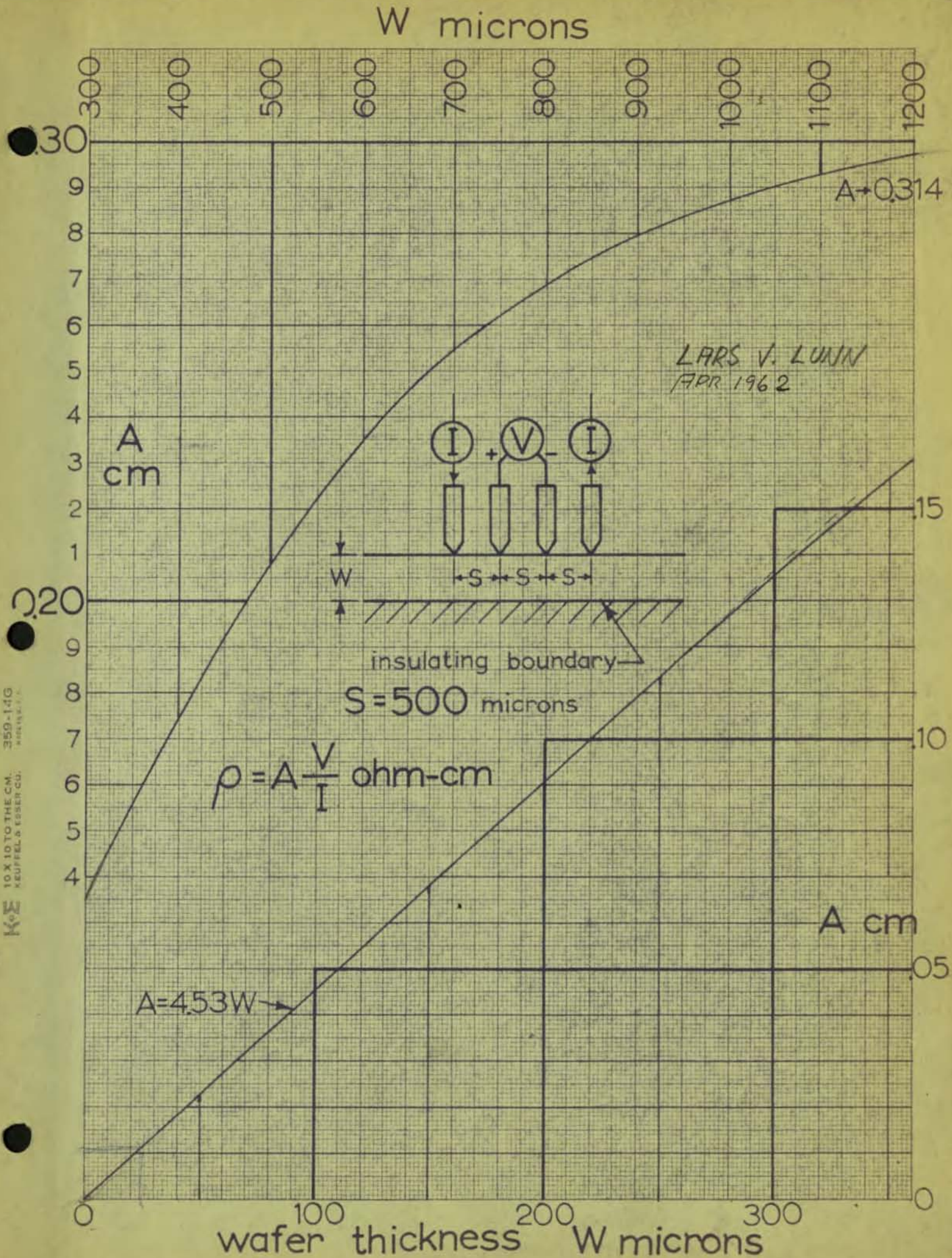


A-FACTOR





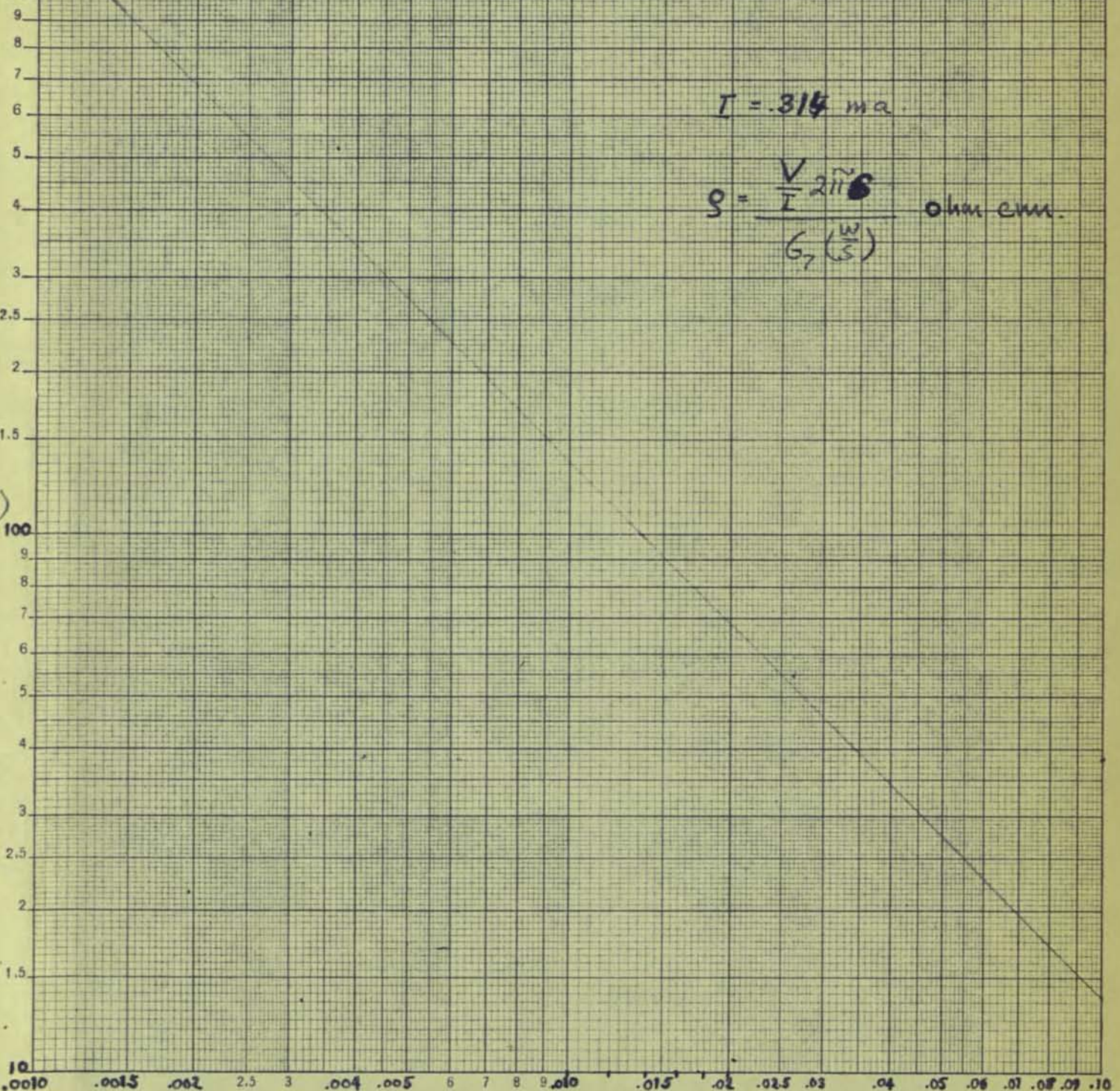




CORRECTION FACTOR

LVL 2-2-62

1000



$$I = .314 \text{ ma.}$$

$$G = \frac{V}{I} \cdot 2\pi \cdot 8 \quad \text{ohm cm.}$$

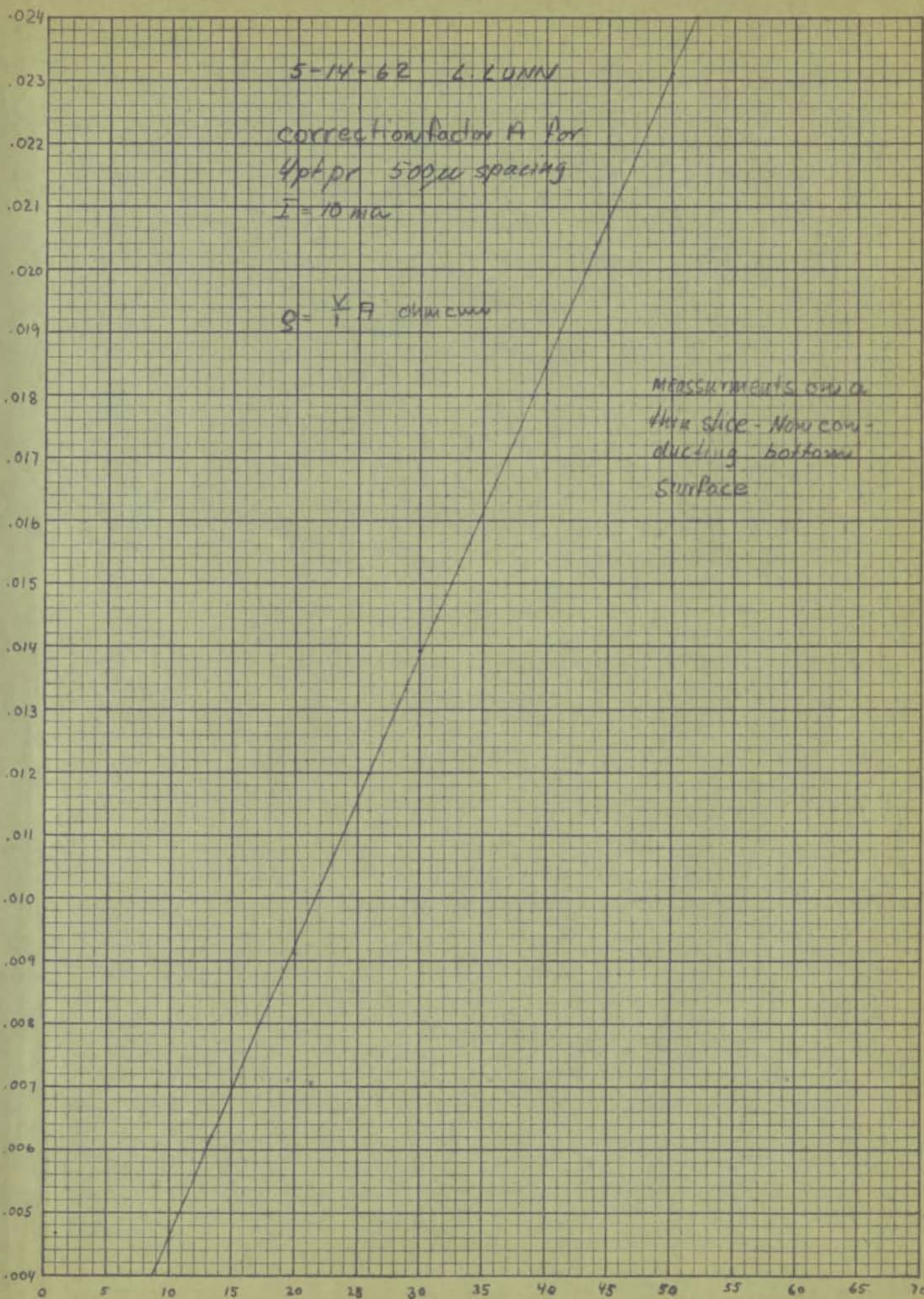
$$G_7 \left(\frac{W}{S} \right)$$

LOGARITHMIC
359-110
KEUFFEL & EBER CO., NEW YORK,
2 X 2 CYCLES

 W 1μ 2μ 3μ 4μ 5μ 6μ 7μ 8μ 9μ 10μ 15μ 20μ 30μ 40μ 50μ

$\frac{W}{S}$ layer thickness
probe spacing

Probe Spacing $S = 508\mu$ or 20 mill



10×10^{-4}

9×10^{-4}

8×10^{-4}

7×10^{-4}

6×10^{-4}

H

5×10^{-4}

4.6×10^{-4}

4×10^{-4}

3×10^{-4}

2×10^{-4}

K.E. 3 X 5 TO THE $\frac{1}{2}$ INCH 359T-6G
KEUPFER & ECKER CO. MADE IN U.S.A.
ALBANY 50

1×10^{-4}

4.6×10^{-5}

O

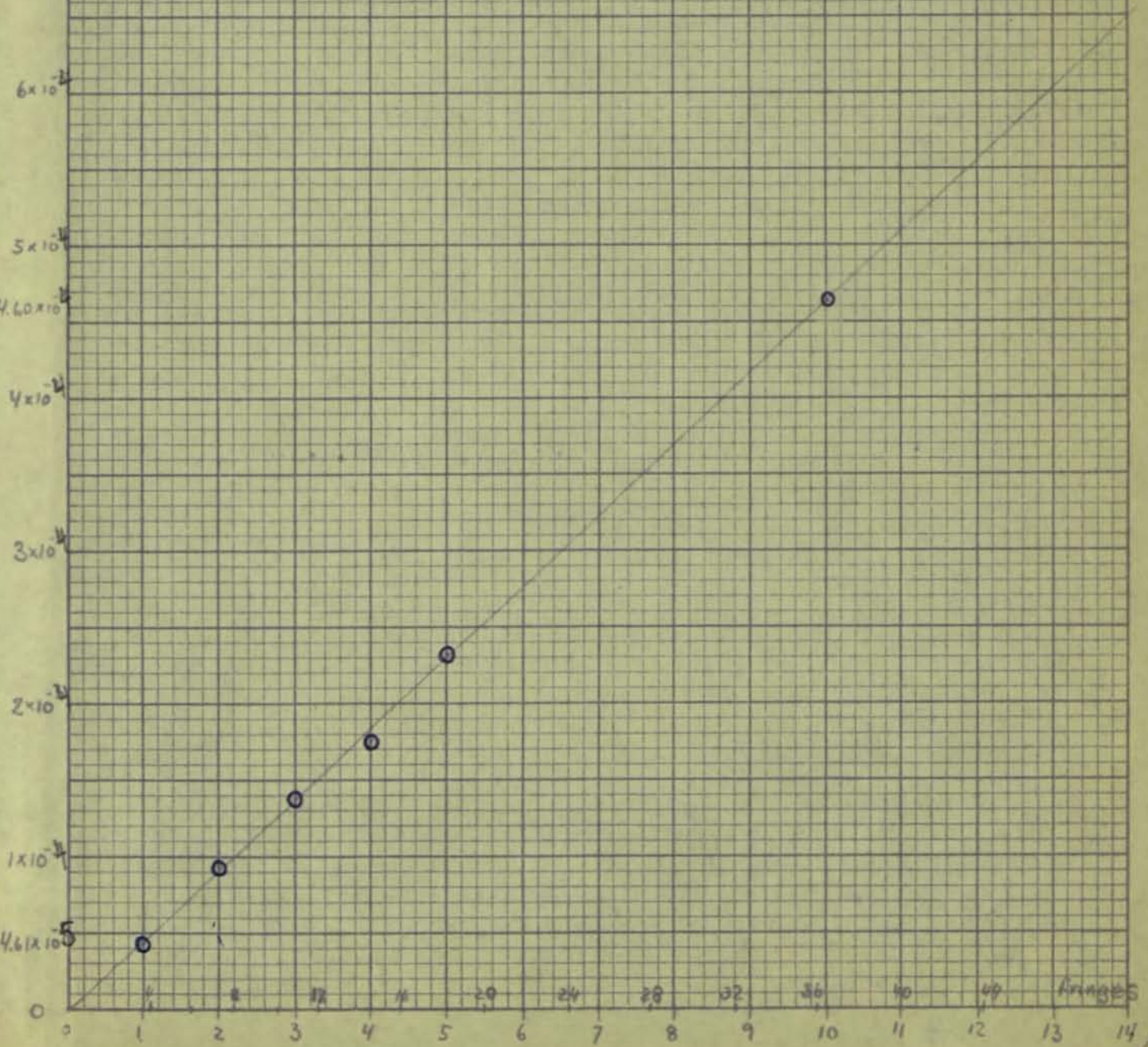
5-14-62 L. LUNN

Correction Factor A Per
4pt or 500 μ spacing

$I = 10 \text{ mA}$ $I = 1 \text{ mA}$ for Amelco
probe

$$g = \frac{H}{I} \times A \text{ ohm cm}$$

MEASUREMENTS ARE ON
THIN SLICE - NON CONDUCTING
bottom Surface



RESISTIVITY/ C b



BELL TELEPHONE SYSTEM

TECHNICAL PUBLICATIONS

Paul Drude's.

Resistivity of bulk silicon and of diffused layers in silicon

by

J. C. Irvin



Published in

THE BELL SYSTEM TECHNICAL JOURNAL

Vol. 41, pp. 387-410, March, 1962

Resistivity of Bulk Silicon and of Diffused Layers in Silicon

By JOHN C. IRVIN

(Manuscript received July 25, 1961)

Measurements of resistivity and impurity concentration in heavily doped silicon are reported. These and previously published data are incorporated in a graph showing the resistivity (at $T = 300^{\circ}\text{K}$) of n- and p-type silicon as a function of donor or acceptor concentration.

The relationship between surface concentration and average conductivity of diffused layers in silicon has been calculated for Gaussian and complementary error function distributions. The results are shown graphically. Similar calculations for subsurface layers, such as a transistor base region, are also given.

I. INTRODUCTION

A diffused layer in silicon is generally characterized by four parameters: the concentration, C_s , of diffused donors or acceptors at the surface, the concentration, C_B , of acceptors or donors originally in the material (background concentration), the depth, x_j , of the resultant junction, and the sheet resistivity, ρ_s , of the layer. A knowledge of the relationship between these parameters is essential to the establishment of device processing recipes, the evaluation of diffusion techniques, and investigations of the thermodynamic properties of silicon.

The desired relationship may be readily calculated, given a knowledge of the distribution of the diffused impurities, the variation of the resistivity of n- and p-type silicon with donor or acceptor density, and a fast electronic computer. The results of such a computation were first

made generally available three years ago, in the form of curves relating C_s to $1/\rho_s x_j$ for a given C_B , for n- and for p-type layers in silicon, and for several common distributions.¹ Recent calculations, however, based on new and more extensive silicon resistivity data, have indicated considerable error in the earlier results. Thus a comprehensive recomputation has been undertaken, the outcome of which is presented herewith.

A necessary adjunct to the calculation is an accurate knowledge of the resistivity of n- and p-type silicon with varying dopant concentration. To this end, most of the extant data have been reviewed and supplemented here and there with some new determinations. The results of this search are also presented here.

II. THE RESISTIVITY OF SILICON AS A FUNCTION OF IMPURITY CONCENTRATION

The variation of the resistivity of silicon at 300°K as a function of the concentration of acceptors or donors is shown in Fig. 1. This graph represents the author's judgment of a most reasonable compromise to

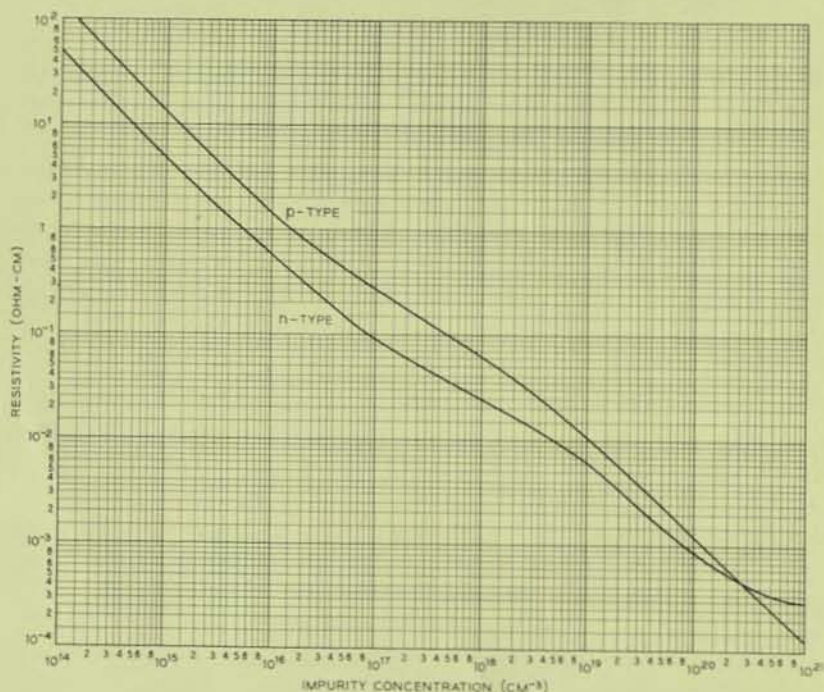


Fig. 1 — Resistivity of silicon at 300°K as a function of acceptor or donor concentration.

TABLE I—RESISTIVITIES AND IMPURITY CONCENTRATIONS
IN SILICON ($T = 300^{\circ}\text{K}$)

Resistivity (ohm-cm)	Impurity	Impurity Concentration (cm^{-3})	Carrier Concentration (cm^{-3})
0.00076	B	1.66×10^{20}	
0.00089	B	1.41×10^{20}	
0.0010	B		
0.0010	B	1.12×10^{20}	1.49×10^{20}
0.0012	B	1.04×10^{20}	
0.0011	B	1.12×10^{20}	
0.0014	B	9.23×10^{19}	
0.0013	B	8.84×10^{19}	
0.0067	B	1.43×10^{19}	
0.0073	B	1.43×10^{19}	
0.013	B	7.41×10^{18}	
0.014	B	7.03×10^{18}	
0.00095	As	1.80×10^{20}	
0.00094	As	1.86×10^{20}	
0.00094	As		
0.00093	As	1.87×10^{20}	1.1×10^{20}
0.00094	As	1.97×10^{20}	
0.00088	As	2.10×10^{20}	
0.00088	As	2.19×10^{20}	
0.00089	As		
0.00083	As	2.30×10^{20}	1.1×10^{20}
0.00083	As	2.20×10^{20}	
0.00080	As	2.46×10^{20}	
0.00082	As	2.44×10^{20}	

the mass of available and not altogether compatible data on the subject. These data include most of the previously published work (Refs. 3–12), recent, unpublished results kindly provided by other investigators,^{2,13} as well as some measurements obtained expressly for the present study.

The last data are shown in Table I. The crystals involved were pulled from quartz crucibles, and hence can not be expected to be particularly low in oxygen content. After dissolution of the boron-doped crystals and separation of the dopant,¹⁴ boron concentrations were determined by a photometric carmine technique essentially similar to published methods.¹⁵ Arsenic concentrations were measured by gamma-ray spectrometry after pile neutron activation. Resistivity measurements were done with a four-point probe. In the case of a few samples, resistivity and carrier concentration were measured in Hall-effect apparatus (where it was assumed $\mu_H/\mu = 1$).

Drawing curves through these many points was accomplished by a succession of smoothing procedures, which were primarily visual. 75 per cent of the data points deviate less than 10 per cent from the curves thus obtained, both for the p-type and the n-type cases. The uncertainty is greatest in the degenerate region. For p-type silicon, suitable data be-

come scarce at dopings greater than 10^{19} cm^{-3} , and none are available beyond $3 \times 10^{20} \text{ cm}^{-3}$. For n-type material, there is an abundance of rather conflicting data representing donor concentrations between 10^{19} cm^{-3} and $6 \times 10^{20} \text{ cm}^{-3}$. In this region a 10 per cent variation in the chosen line still includes 67 per cent of the data, however.

A single pair of curves obviously can not characterize with the same degree of accuracy all silicon material, regardless of dopant employed or degree of compensation. However, over the range $10^{14} \text{ cm}^{-3} \leq N_I \leq 10^{20} \text{ cm}^{-3}$, and subject to the limitations discussed below, Fig. 1 is considered to be within 10 per cent of reality. This graph refers specifically to uncompensated silicon containing a donor or acceptor impurity concentration, N_I , consisting of arsenic, phosphorus, or antimony for n-type, and aluminum, boron, or gallium for p-type material. (Actually, even among samples doped with the aforementioned impurities, small but consistent differences in carrier concentration and mobility, depending on the specific choice of donor or of acceptor, have been reported recently for silicon in the 0.001 ohm-cm region.^{10,12}) In case of moderate compensation, the net impurity density, $|N_A - N_D|$, should be used for N_I . However, heavy compensation requires allowance for the added impurity scattering.

For impurity densities near or greater than 10^{20} cm^{-3} , Fig. 1 can not be considered very reliable. At such concentrations, impurity band conduction is prominent and its effects are apt to differ appreciably depending on choice of impurity. Even more serious are the degrees of impurity precipitation and lattice imperfection which occur in highly doped material and which furthermore vary with growth conditions and history of the crystal. It will be noted with some consternation that the p-type and n-type curves are shown to cross near $N_I = 3 \times 10^{20} \text{ cm}^{-3}$. The paucity of data, of course, casts considerable doubt on this result. However, for what they are worth, such are the indications. Perhaps this can be understood in light of the acceptor action of imperfections, especially vacancies, which are abundant in very highly doped material.

The calculations discussed in the remainder of this paper require a mathematical representation of Fig. 1. Straight-line approximations of the form $(1/\rho) = BN_I^\alpha$ have been obtained, which depart 10 per cent from the desired curve at the turning points and rapidly approach coincidence elsewhere. The parameters B and α are listed in Table II for the respective straight-line regions.

III. DIFFUSION PROFILES AND CALCULATIONS

The diffusion profiles of current practical interest are the complementary error function, $C_x = C_s \operatorname{erfc}(x/2\sqrt{Dt})$, and the Gaussian,

TABLE II — VALUES OF B AND α IN THE EQUATION $(1/\rho) = BN_t^\alpha$,
REPRESENTING STRAIGHT-LINE APPROXIMATIONS TO THE ρ VS
 N_t CURVES OF n-TYPE AND p-TYPE SILICON ($T = 300^\circ\text{K}$)

Region (cm^{-3})	B	α
<i>n-type</i>		
$2.35 \times 10^{20} \leq N_D$	1.04×10^{-6}	0.456
$6.00 \times 10^{19} \leq N_D \leq 2.35 \times 10^{20}$	1.43×10^{-12}	0.744
$9.50 \times 10^{18} \leq N_D \leq 6.00 \times 10^{19}$	2.00×10^{-16}	0.940
$1.00 \times 10^{17} \leq N_D \leq 9.50 \times 10^{18}$	6.93×10^{-9}	0.543
$3.50 \times 10^{15} \leq N_D \leq 1.00 \times 10^{17}$	6.97×10^{-14}	0.837
$N_D \leq 3.50 \times 10^{15}$	2.00×10^{-16}	1.000
<i>p-type</i>		
$1.50 \times 10^{19} \leq N_A$	4.00×10^{-17}	0.966
$2.40 \times 10^{18} \leq N_A \leq 1.50 \times 10^{19}$	1.47×10^{-14}	0.832
$1.50 \times 10^{16} \leq N_A \leq 2.40 \times 10^{18}$	3.30×10^{-11}	0.650
$N_A \leq 1.50 \times 10^{16}$	7.20×10^{-17}	1.000

$C_x = C_s \exp(-x^2/4Dt)$. In these expressions, x , D , and t are the depth, diffusion coefficient (assumed independent of impurity density), and time, respectively. C_x is the concentration of the diffused impurity at depth x and C_s , that at the surface. The former distribution is expected when diffusion takes place with the surface concentration C_s held constant; the latter when the total impurity diffusing is constant. Unfortunately it must be admitted that the accuracy of these expectations is open to question in some situations.^{2,16} Also, precipitation and compensation of impurities near the surface may further distort the distribution. However, it is still useful to solve the problem under these assumptions, leaving corrections for later determination.

The "average conductivity" of a diffused layer (which throughout this paper is assumed to be diffused into a silicon slice of opposite conductivity type and uniform doping C_B) is given by the expression

$$\bar{\sigma} = 1/\rho_s x_j = (1/x_j) \int_0^{x_j} q\mu C dx$$

where q is electronic charge, μ the carrier mobility typical of a total ionized impurity density of $C_x + C_B$, $C = r(C_x - C_B)$ is the density of carriers, r being the fraction of uncompensated diffused impurity atoms which are ionized, and C_x the total density of diffused impurity atoms at depth x . (Possible variation of the mobility as a function of the proximity of the surface is a hazard which should be recognized in passing but is otherwise ignored in the present calculation.) Multiplying and dividing within the integrand by $r'(C_x + C_B)$, where r' is the ionized fraction associated with an uncompensated dopant density of $(C_x + C_B)$, and writing

$$qur'(C_x + C_B) = \sigma_{(Cx+CB)} = B(C_x + C_B)^{\alpha}$$

the average conductivity becomes

$$\bar{\sigma} = (1/x_j) \int_0^{x_j} (r/r')(C_x - C_B)B(C_x + C_B)^{\alpha-1} dx.$$

Now (r/r') represents the ratio of degrees of ionization corresponding to $C_x - C_B$ and $C_x + C_B$ respectively. This ratio is very nearly unity unless C_x and C_B are comparable in magnitude. Such is the case only for the lamina nearest the junction, which contributes negligibly to the conductance of the whole layer. Hence, (r/r') may be justifiably taken as equal to unity, and writing $C_x = C_S f(x)$, where $f(x)$ depends on the profile of interest,

$$\bar{\sigma} = (1/x_j) \int_0^{x_j} [C_S f(x) - C_B]B[C_S f(x) + C_B]^{\alpha-1} dx.$$

A program for the evaluation of this expression has been devised previously by others and employed in the analysis of diffused layers in germanium.¹⁷ With slight additions to facilitate automatic plotting, the same program has been used in the present work. Computations were performed on an IBM 704, and plotting of points was carried out with an Electronic Associates Variplotter.

IV. PRESENTATION OF RESULTS

Of frequent interest in transistor design and in the analysis of diffused layers, are the characteristics of a "subsurface" layer such as illustrated in Fig. 2. This layer, bounded on one side by the junction and on the other by a plane paralleling the junction at depth x , may be characterized by an average conductivity

$$\bar{\sigma} = 1/[\rho_s'(x_j - x)] = \frac{1}{(x_j - x)} \int_x^{x_j} q\mu C dx$$

where ρ_s' is the sheet resistance of the subsurface layer. It will be recognized that the base region of a diffused-base, alloyed-emitter transistor is an example of a subsurface layer. Another example is that portion of a diffused layer remaining after removing the top strata of depth x . Here, however, it must be remembered that the value of C_s specifying this layer pertains to the original surface at $x = 0$.

Since a subsurface layer becomes the entire diffused layer when $x = 0$, it is convenient to display the properties of both in the same plot by introducing the parameter (x/x_j) . On pages 394 to 410 such graphs are presented for n- and p-type diffused layers of Gaussian and complementary error function profile. Each graph contains the family of ten curves $(x/x_j) = 0, 0.1, \dots, 0.9$, and relates the average conductivity of

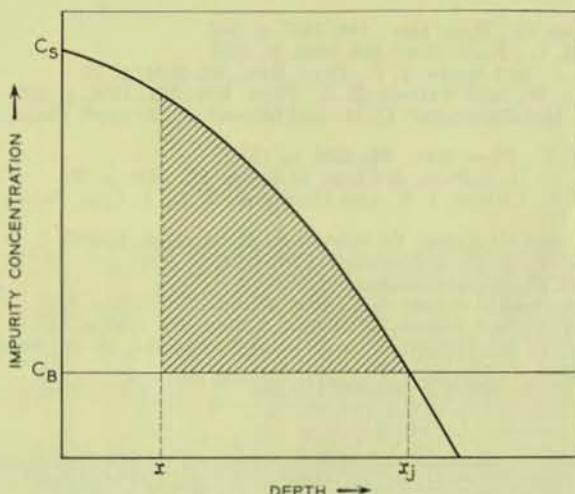


Fig. 2 — Profile of a diffused layer with subsurface layer shaded.

each layer to the surface concentration (at the *original* surface) for a given value of C_B . A separate graph is required for each value of C_B , which in the present work ranges from 10^{14} cm^{-3} to 10^{20} cm^{-3} at one-decade intervals. In each plot the range of surface concentrations spanned is from C_B to 10^{21} cm^{-3} . The so-called "Backenstoss" curve for a particular C_B is simply the right-most line ($x/x_j = 0$) in each graph.

The wiggle in the n-type average conductivity for diffusant concentrations near 10^{19} cm^{-3} is ascribable to the rather large change in slope occurring in the n-type resistivity plot at $N_I = 10^{19} \text{ cm}^{-3}$.

V. ACKNOWLEDGMENTS

It is a pleasure to acknowledge the contributions of many colleagues to this investigation. In particular, the boron determinations, devised and performed by C. L. Luke, were very valuable, as were the radioactive arsenic determinations of Miss K. Wolfstirn and Hall-effect measurements of R. A. Logan and R. L. Johnston. The author is indebted to D. Lassota for the growing of the boron-doped crystals, to D. B. Cuttriss, whose efforts brought about the preparation of the computer program, to Mrs. W. Mammel, for subsequent additions to it, to R. Lilienthal for various measurements, and especially to Mrs. M. S. Boyle for her indefatigable assistance in many measurements and the plotting of hundreds of curves.

REFERENCES

1. Backenstoss, G., B.S.T.J., **37**, 1958, p. 699.
2. Tannenbaum, Eileen, Solid-State Electronics, **2**, 1961, p. 123.

3. Backenstoss, G., Phys. Rev., **108**, 1957, p. 416.
4. Carlson, R. O., Phys. Rev., **100**, 1955, p. 1975.
5. Morin, F. J., and Maita, J. P., Phys. Rev., **96**, 1954, p. 28.
6. Ludwig, G. W., and Watters, R. L., Phys. Rev. **101**, 1956, p. 1699.
7. Long, D., Motchenbacher, C. D., and Meyers, J., J. Appl. Phys., **30**, 1959, p. 353.
8. Prince, M. B., Phys. Rev., **93**, 1954, p. 1204.
9. Wollstirn, K., J. of Phys. & Chem. of Solids, **16**, 1960, p. 279.
10. Logan, R. A., Gilbert, J. F., and Trumbore, F. A., J. Appl. Phys., **32**, 1961, p. 131.
11. Esaki, L., and Miyahara, Y., Solid-State Electronics, **1**, 1960, p. 13.
12. Furukawa, Y., J. Phys. Soc. Japan, **16**, 1961, p. 577.
13. Carlson, R. O., private communication.
14. Luke, C. L., and Flaschen, S. S., Anal. Chem., **30**, 1958, p. 1406.
15. Hatcher, J. T., and Wilcox, L. V., Anal. Chem., **22**, 1950, p. 567.
16. Subashiev, V. K., Landsman, A. P., and Kukharskii, A. A., Soviet Physics-Solid State, **2**, 1961, p. 2406.
17. Cuttriss, D. B., B.S.T.J., **40**, 1961, p. 509.

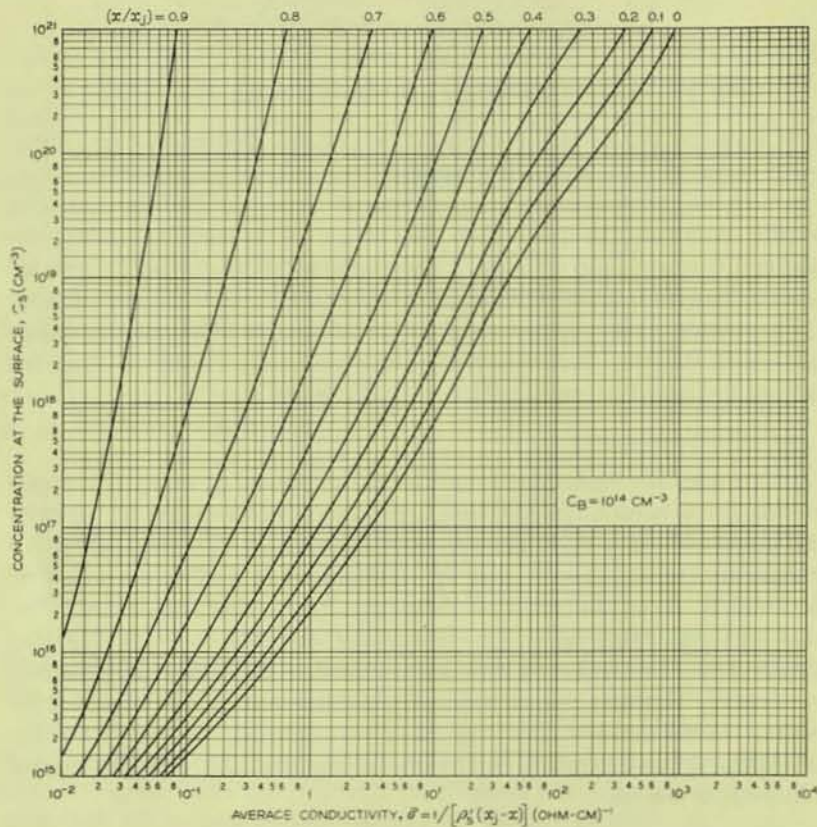


Fig. 3 — Average conductivity of n-type complementary error function layers in silicon.

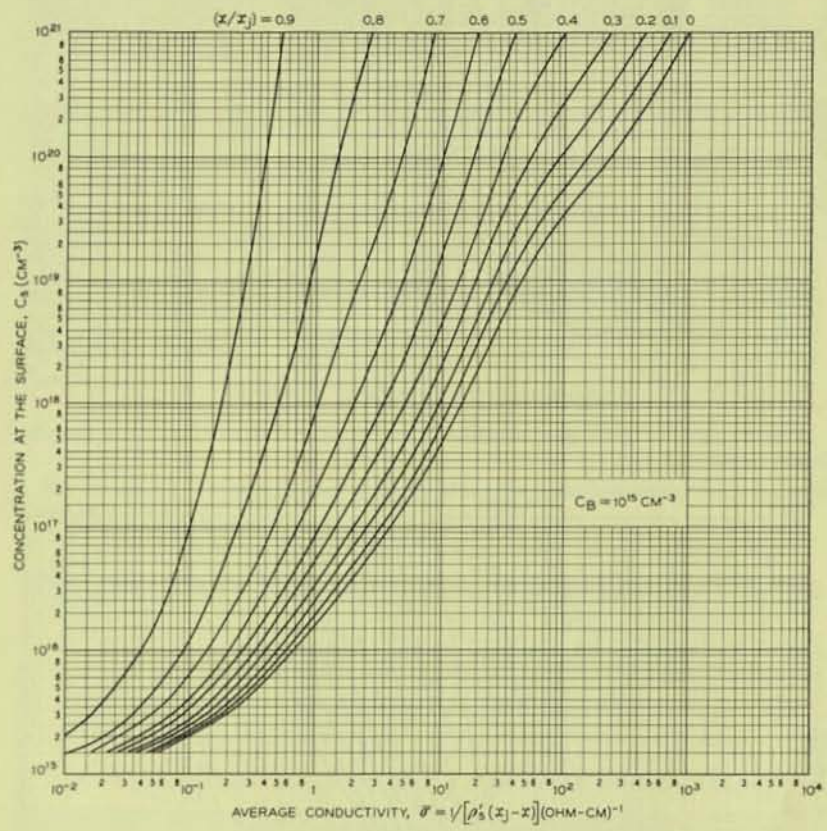


Fig. 3 (cont.) — Average conductivity of n-type complementary error function layers in silicon.

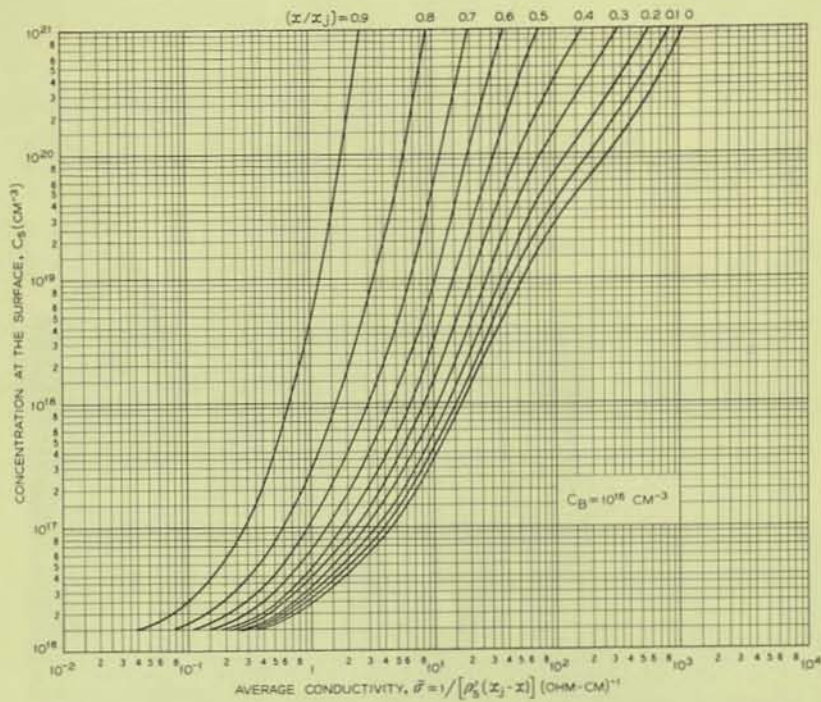


Fig. 3 (cont.) — Average conductivity of n-type complementary error function layers in silicon.

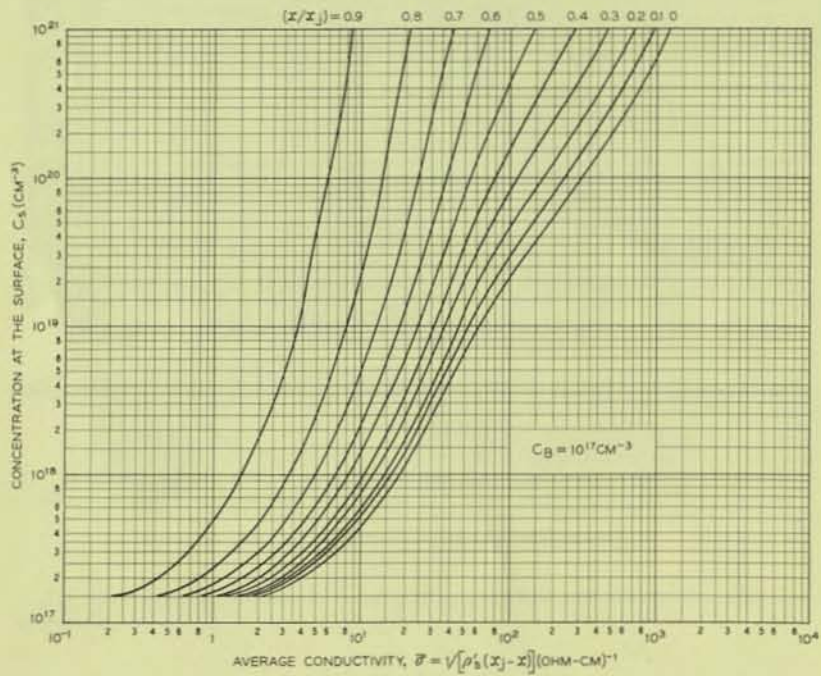


Fig. 3 (cont.) — Average conductivity of n-type complementary error function layers in silicon.

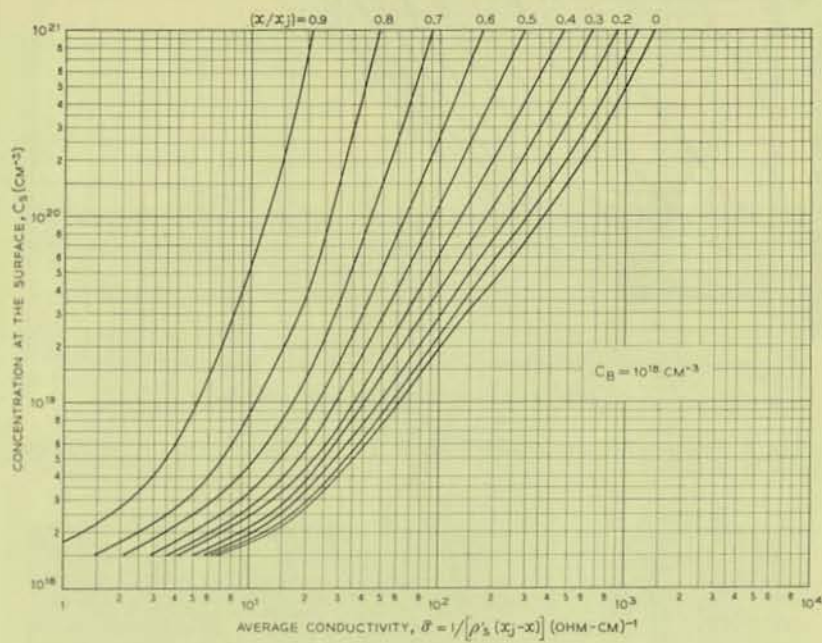


Fig. 3 (cont.) — Average conductivity of n-type complementary error function layers in silicon.

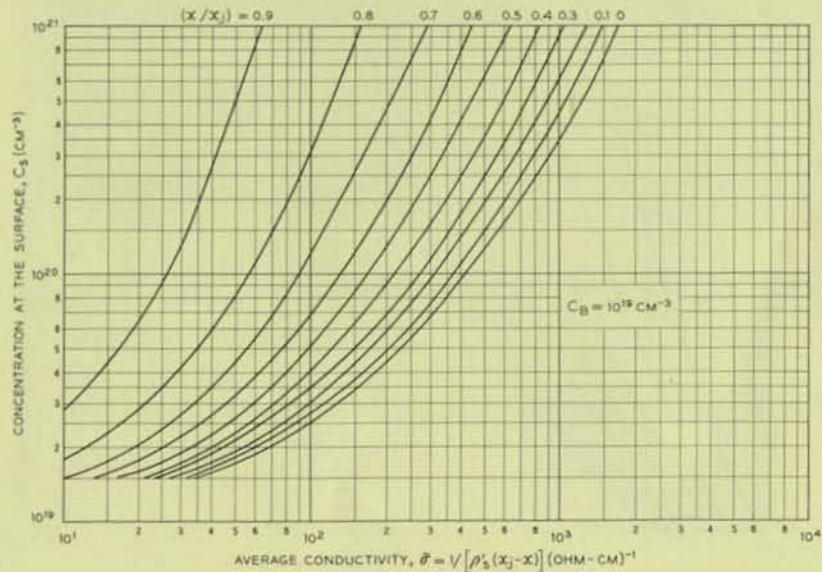


Fig. 3 (cont.) — Average conductivity of n-type complementary error function layers in silicon.

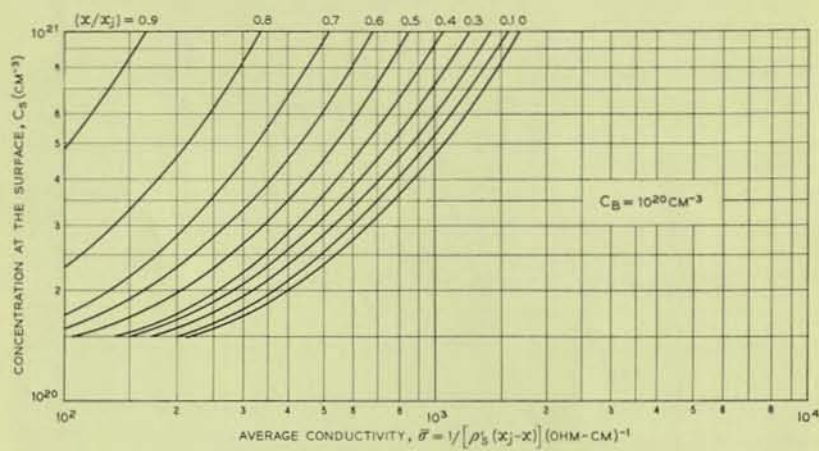


Fig. 3 (cont.) — Average conductivity of n-type complementary error function layers in silicon.

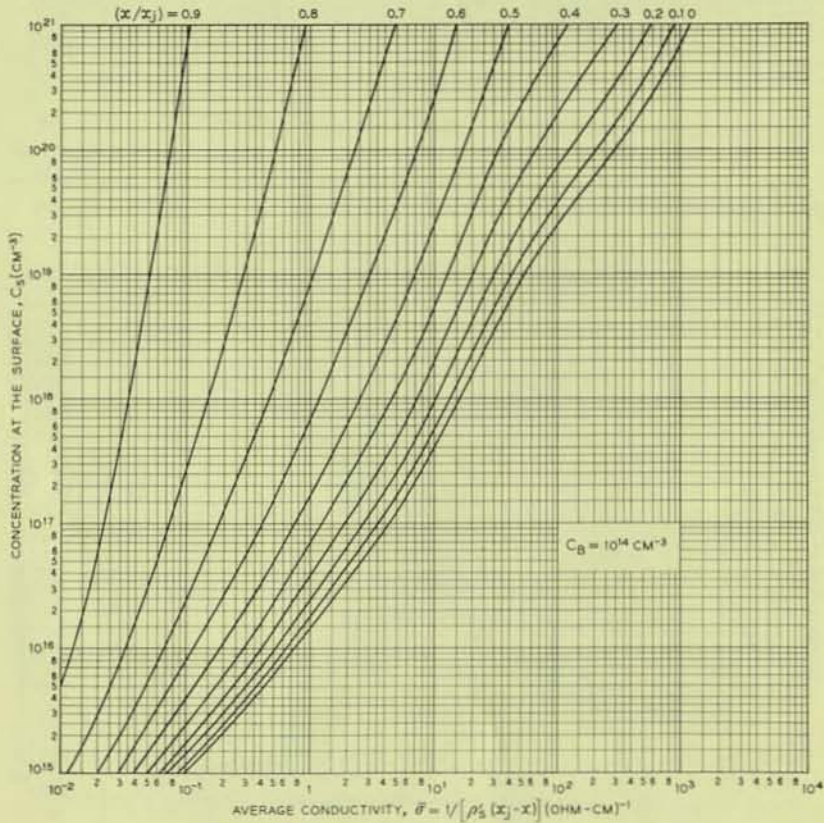


Fig. 4 — Average conductivity of n-type Gaussian layers in silicon.

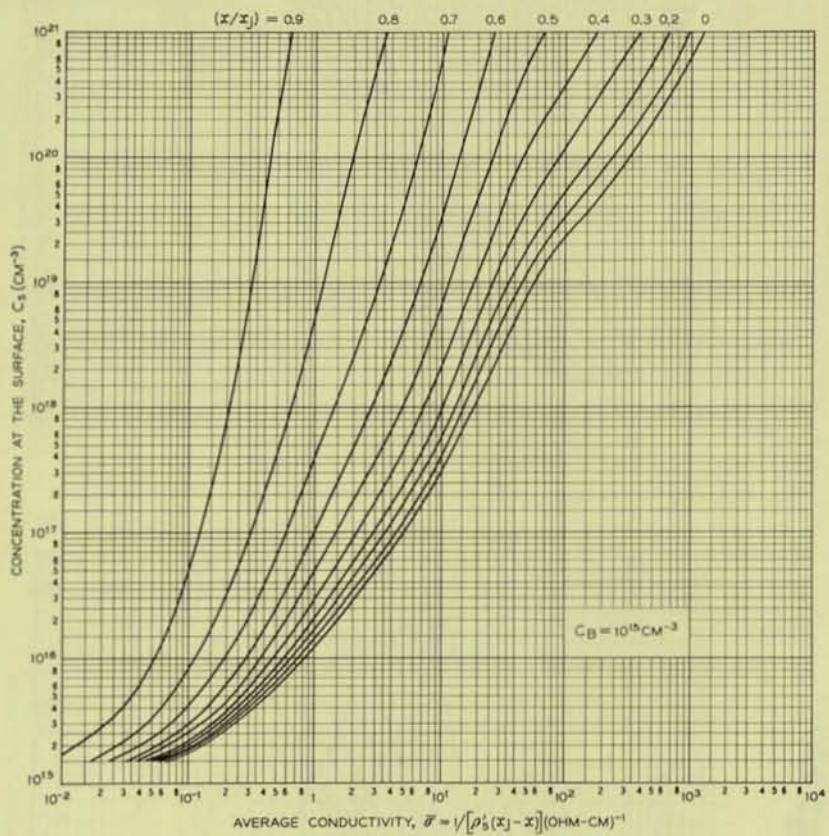


Fig. 4 (cont.) — Average conductivity of n-type Gaussian layers in silicon.

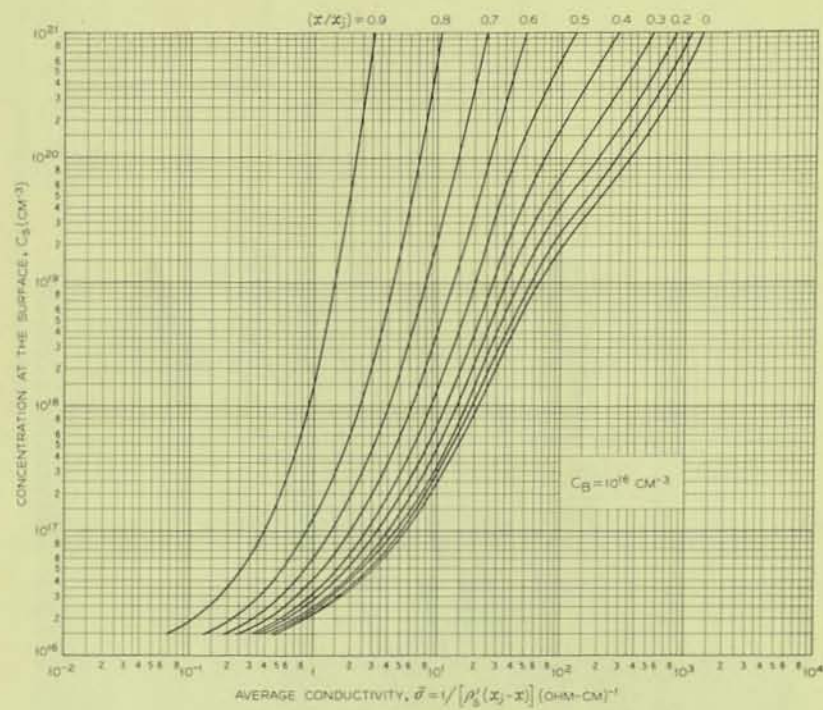


Fig. 4 (cont.) — Average conductivity of n-type Gaussian layers in silicon.

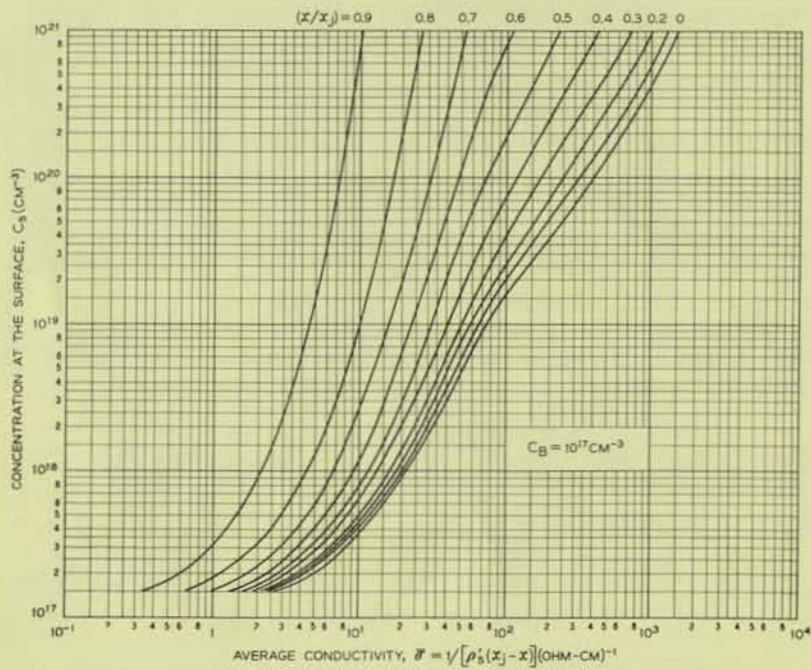


Fig. 4 (cont.) — Average conductivity of n-type Gaussian layers in silicon.

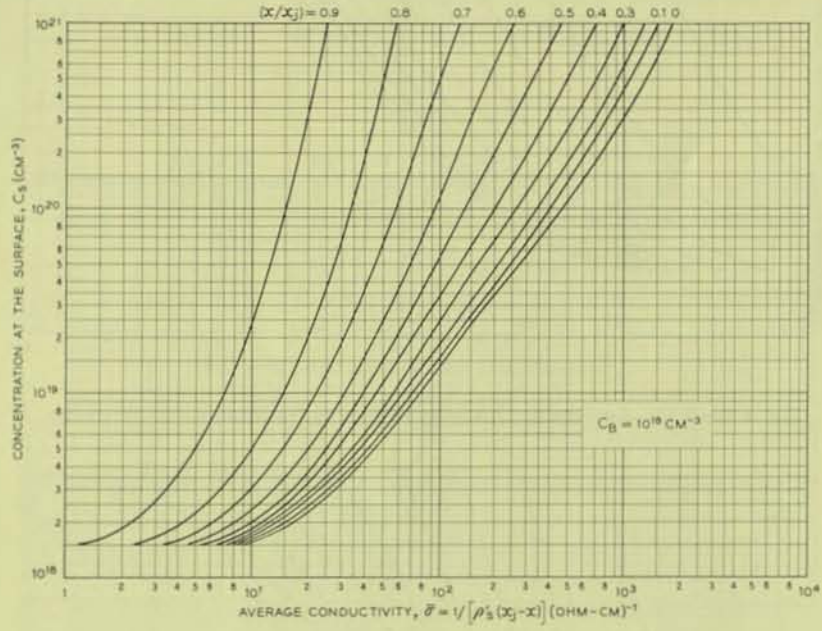


Fig. 4 (cont.) — Average conductivity of n-type Gaussian layers in silicon.

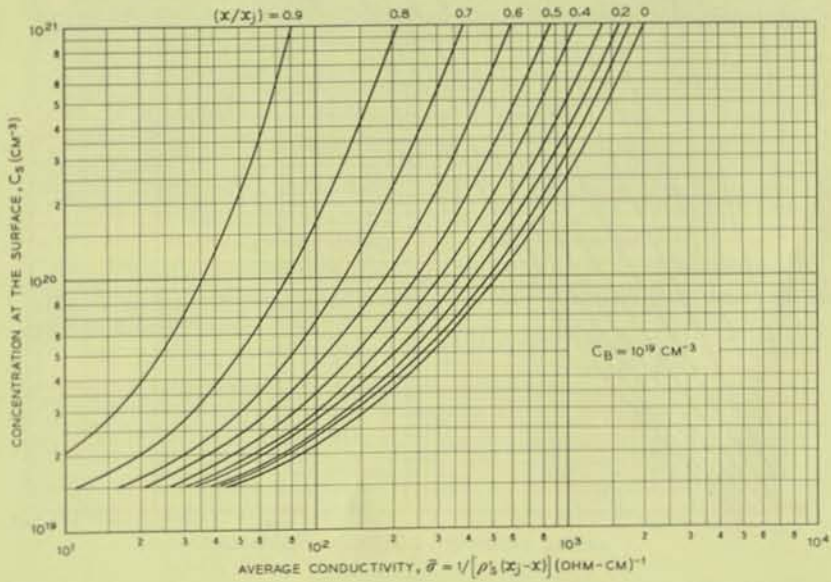


Fig. 4 (cont.) — Average conductivity of n-type Gaussian layers in silicon.

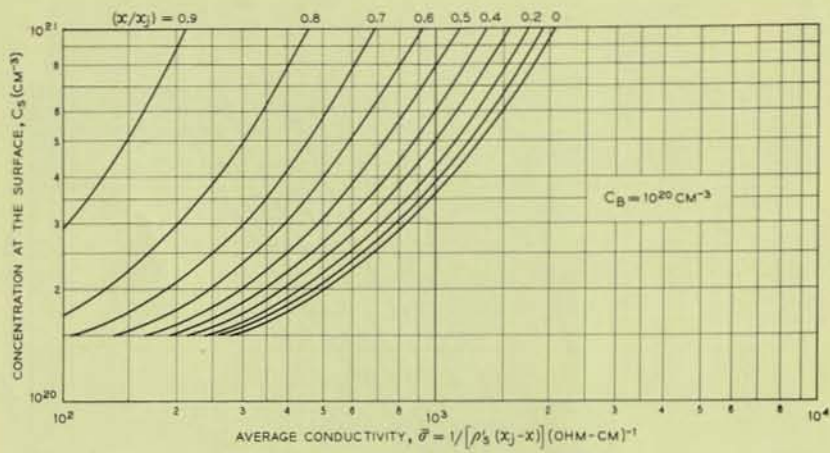


Fig. 4 (cont.) — Average conductivity of n-type Gaussian layers in silicon.

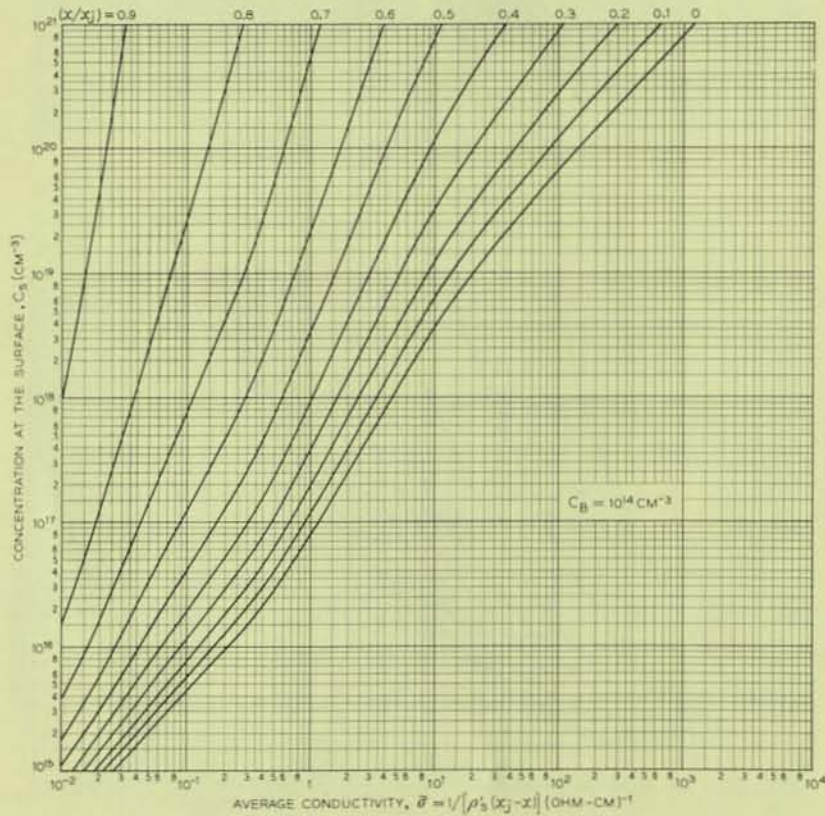


Fig. 5 — Average conductivity of p-type complementary error function layers in silicon.

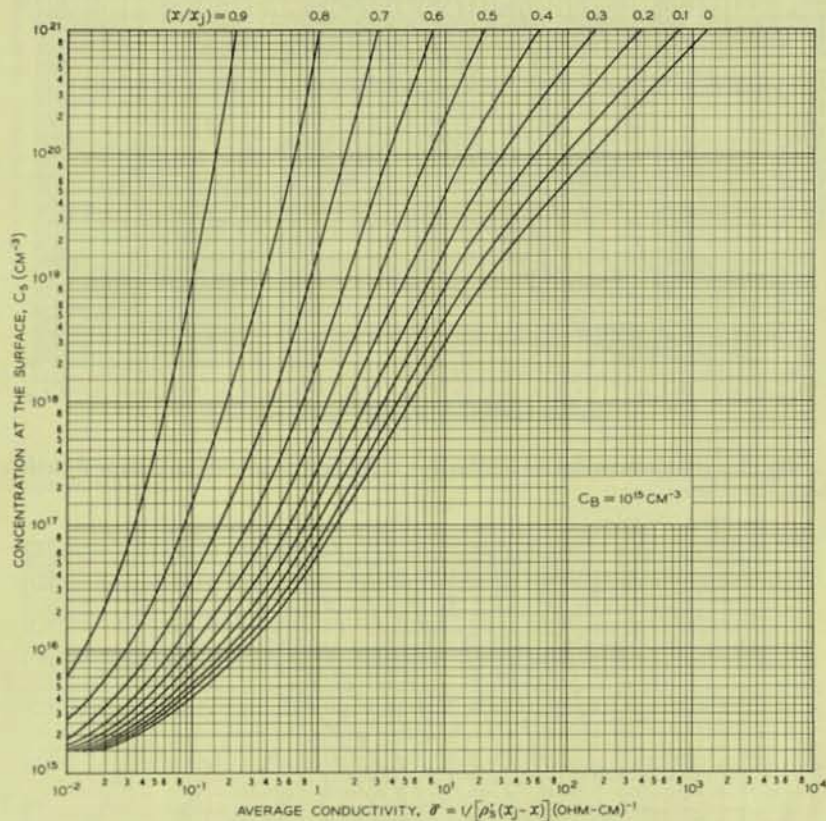


Fig. 5 (cont.) — Average conductivity of p-type complementary error function layers in silicon.

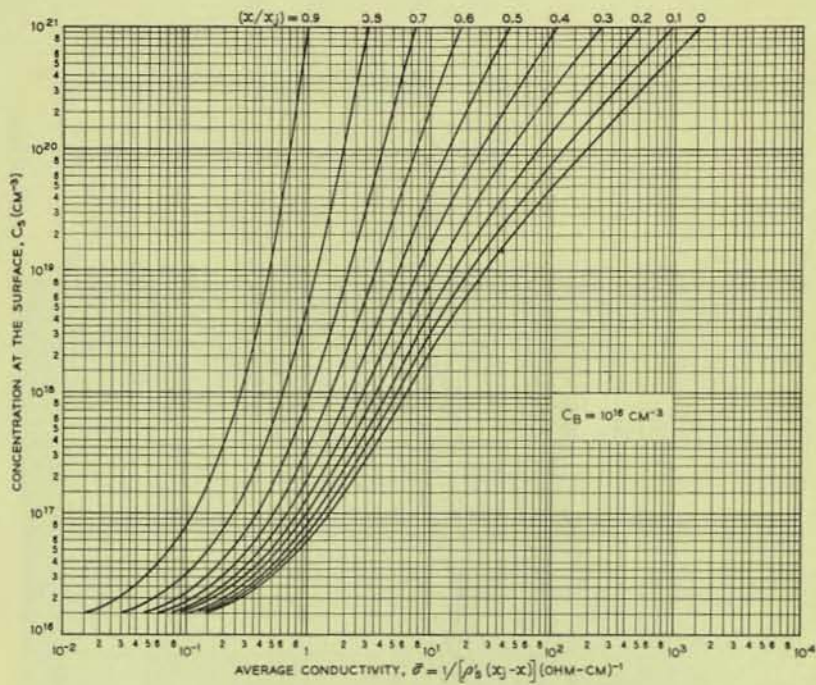


Fig. 5 (cont.) — Average conductivity of p-type complementary error function layers in silicon.

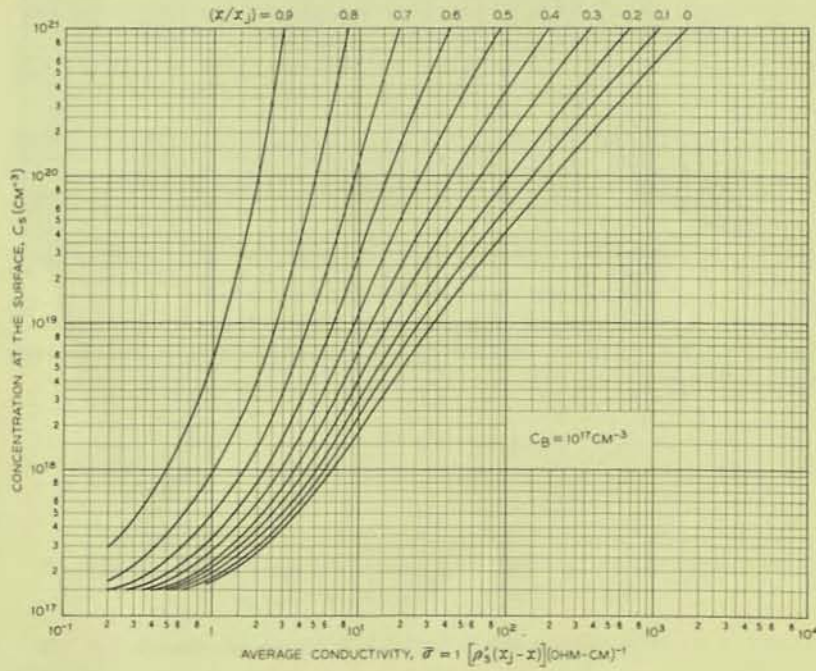


Fig. 5 (cont.) — Average conductivity of p-type complementary error function layers in silicon.

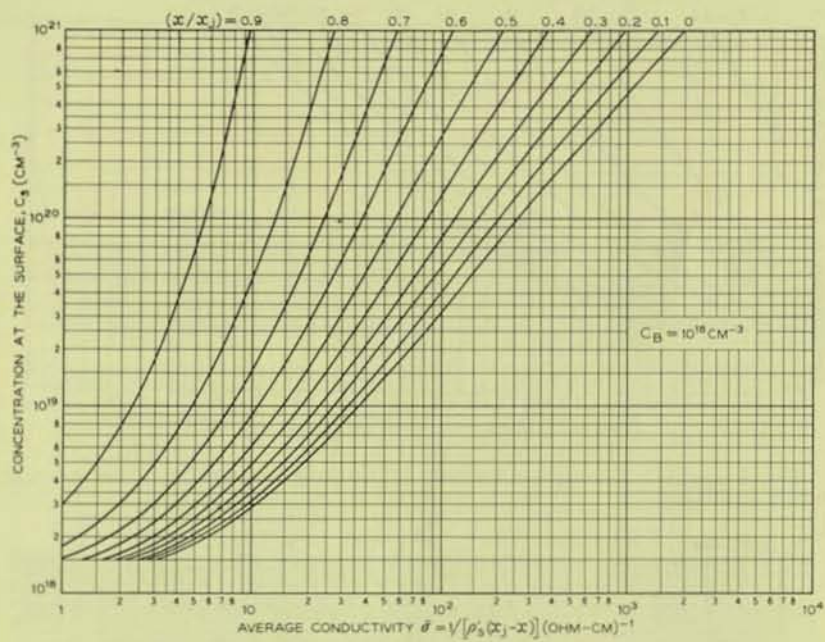


Fig. 5 (cont.) — Average conductivity of p-type complementary error function layers in silicon.

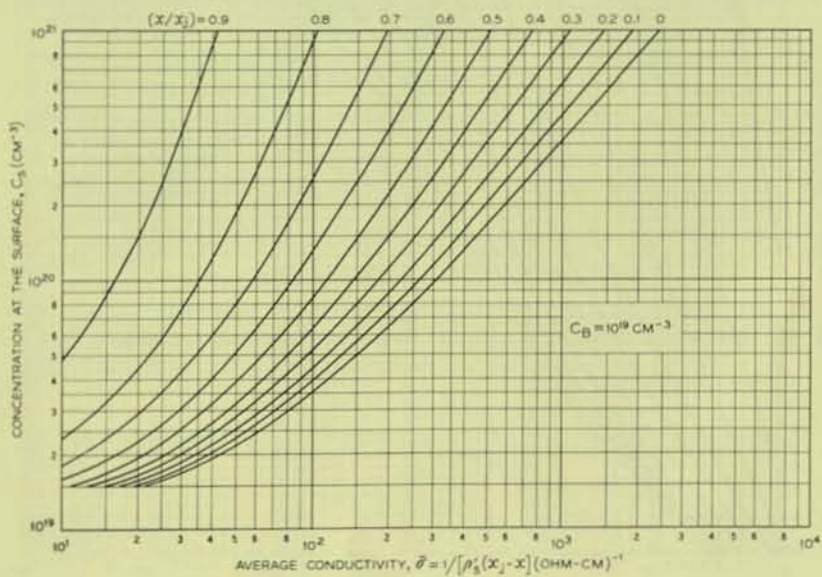


Fig. 5 (cont.) — Average conductivity of p-type complementary error function layers in silicon.

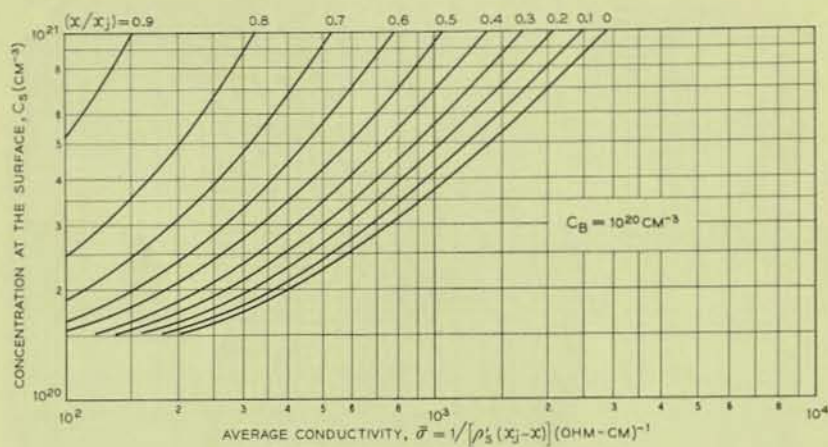


Fig. 5 (cont.) — Average conductivity of p-type complementary error function layers in silicon.

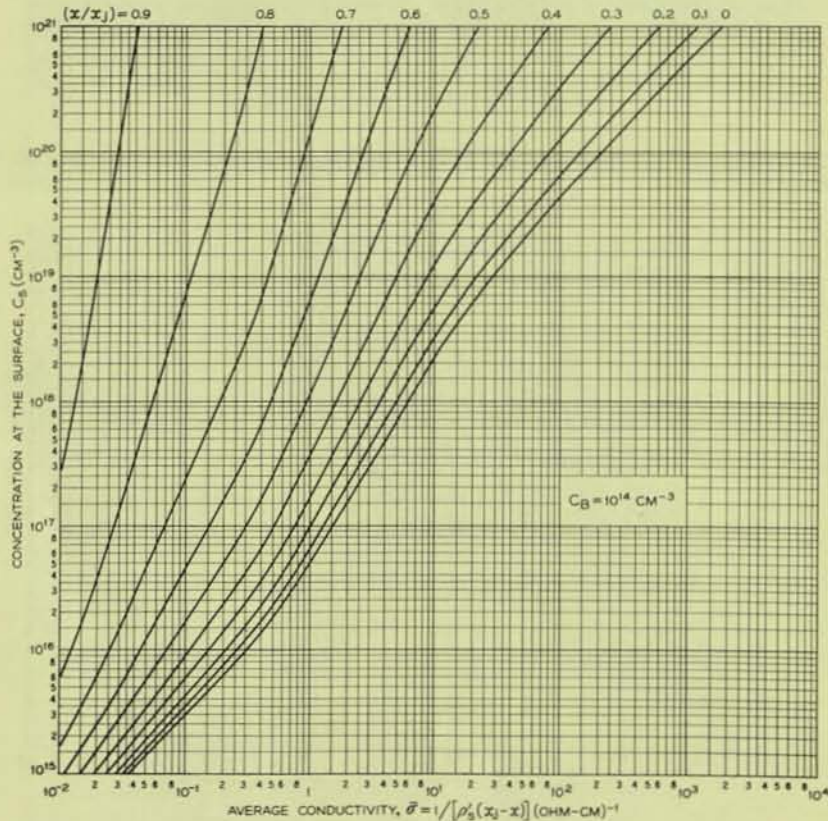


Fig. 6 — Average conductivity of p-type Gaussian layers in silicon.

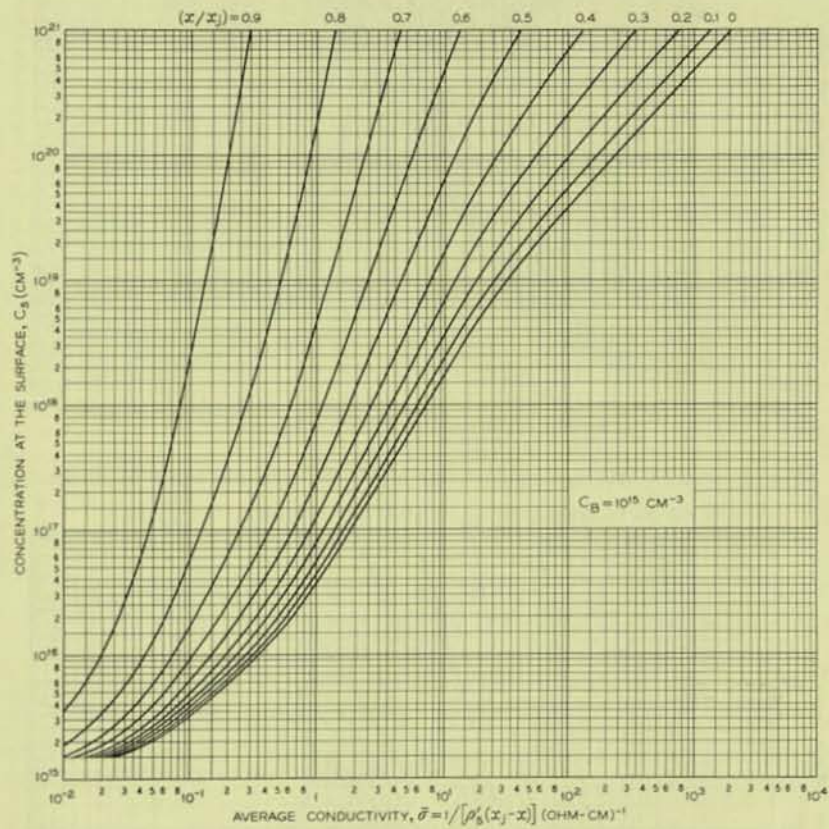


Fig. 6 (cont.) — Average conductivity of p-type Gaussian layers in silicon.

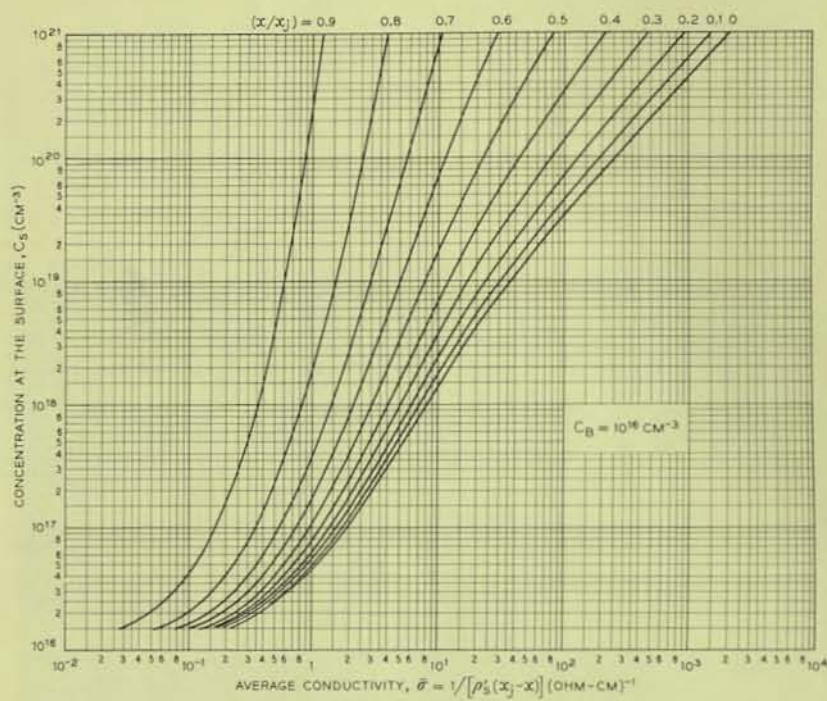


Fig. 6 (cont.) — Average conductivity of p-type Gaussian layers in silicon.

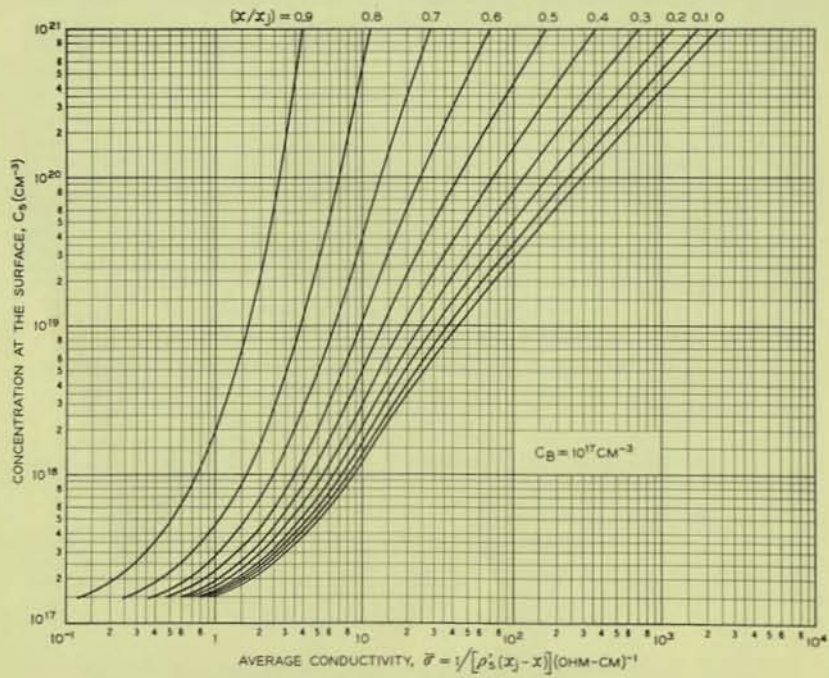


Fig. 6 (cont.) — Average conductivity of p-type Gaussian layers in silicon.

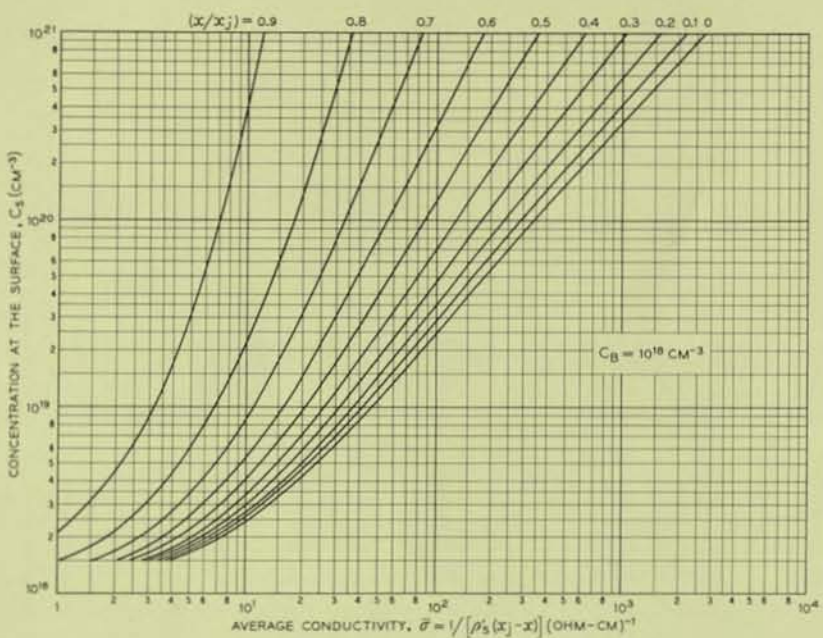


Fig. 6 (cont.) — Average conductivity of p-type Gaussian layers in silicon.

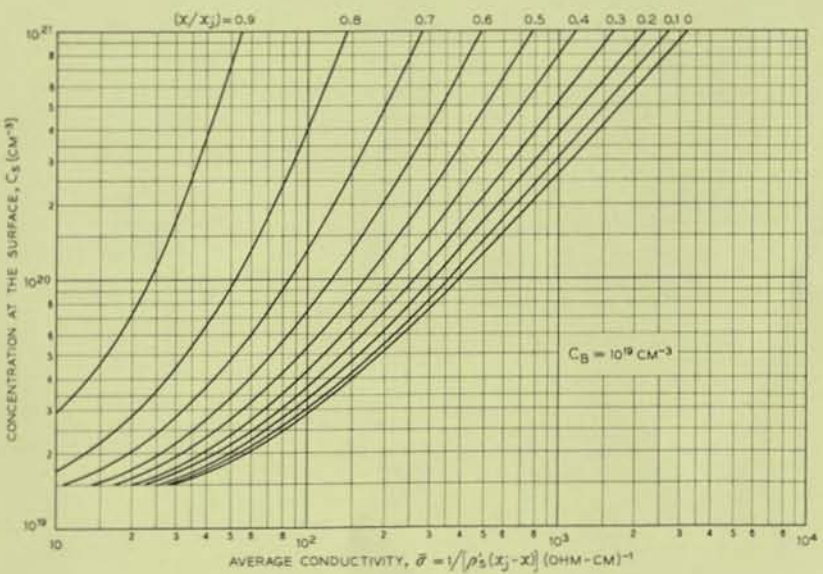


Fig. 6 (cont.) — Average conductivity of p-type Gaussian layers in silicon.

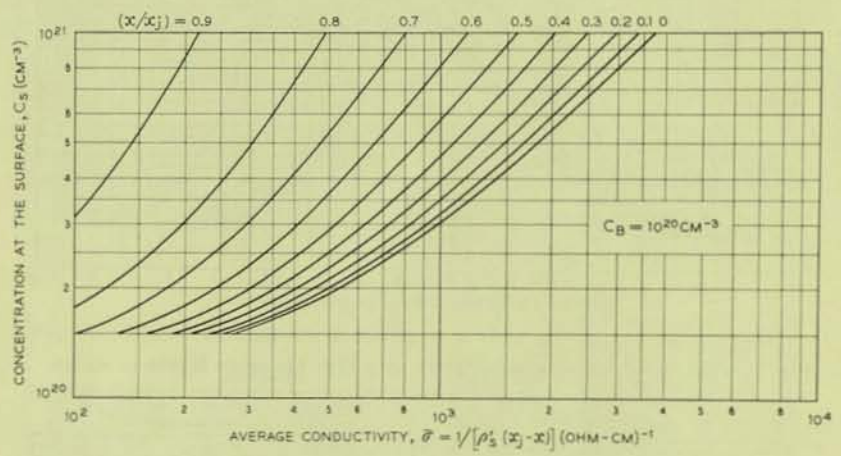


Fig. 6 (cont.) — Average conductivity of p-type Gaussian layers in silicon.

Issued May, 1962

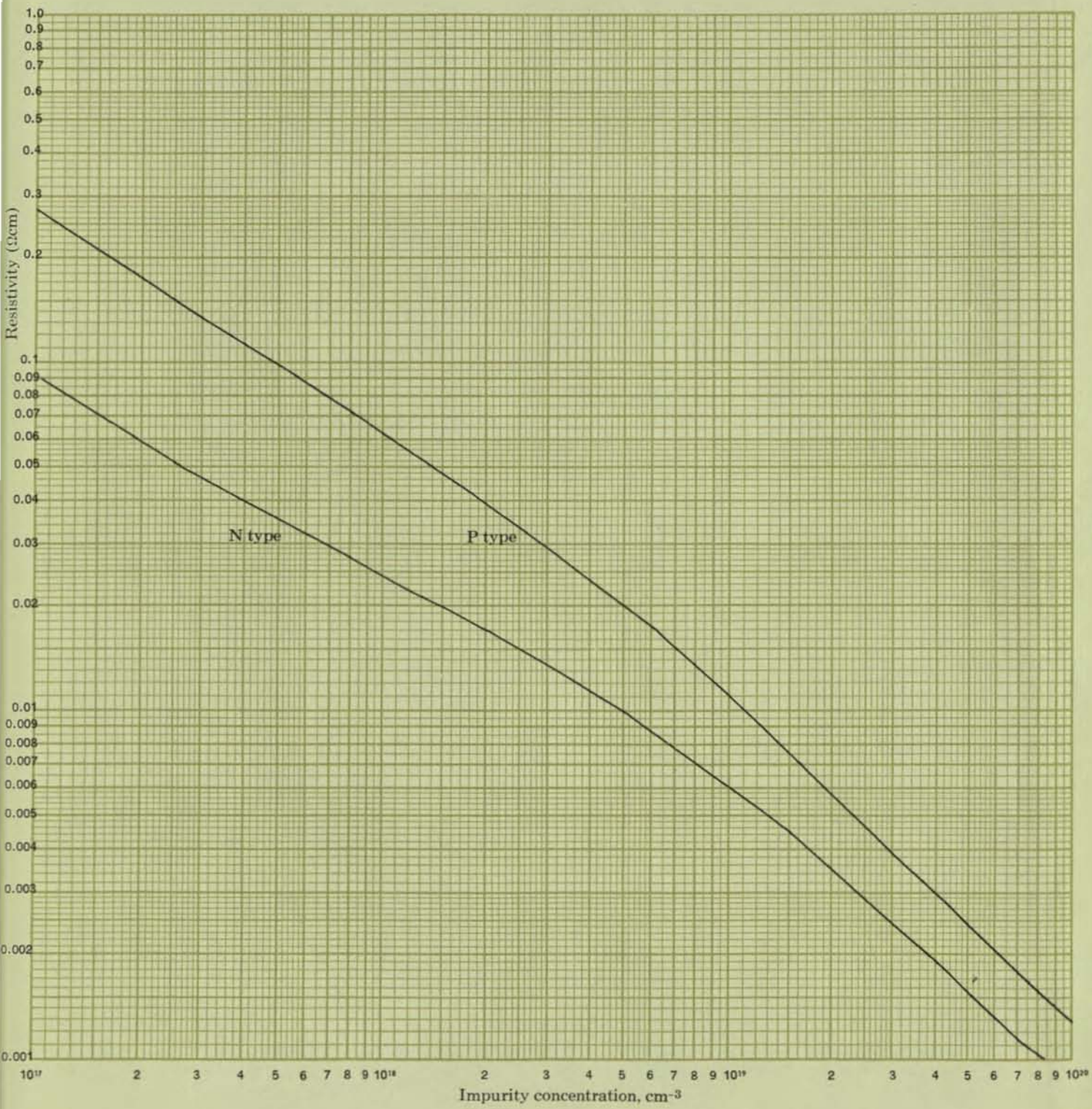
4092: J. C. IRVIN

BELL TELEPHONE LABORATORIES, incorporated

463 West Street, New York 14, N. Y.

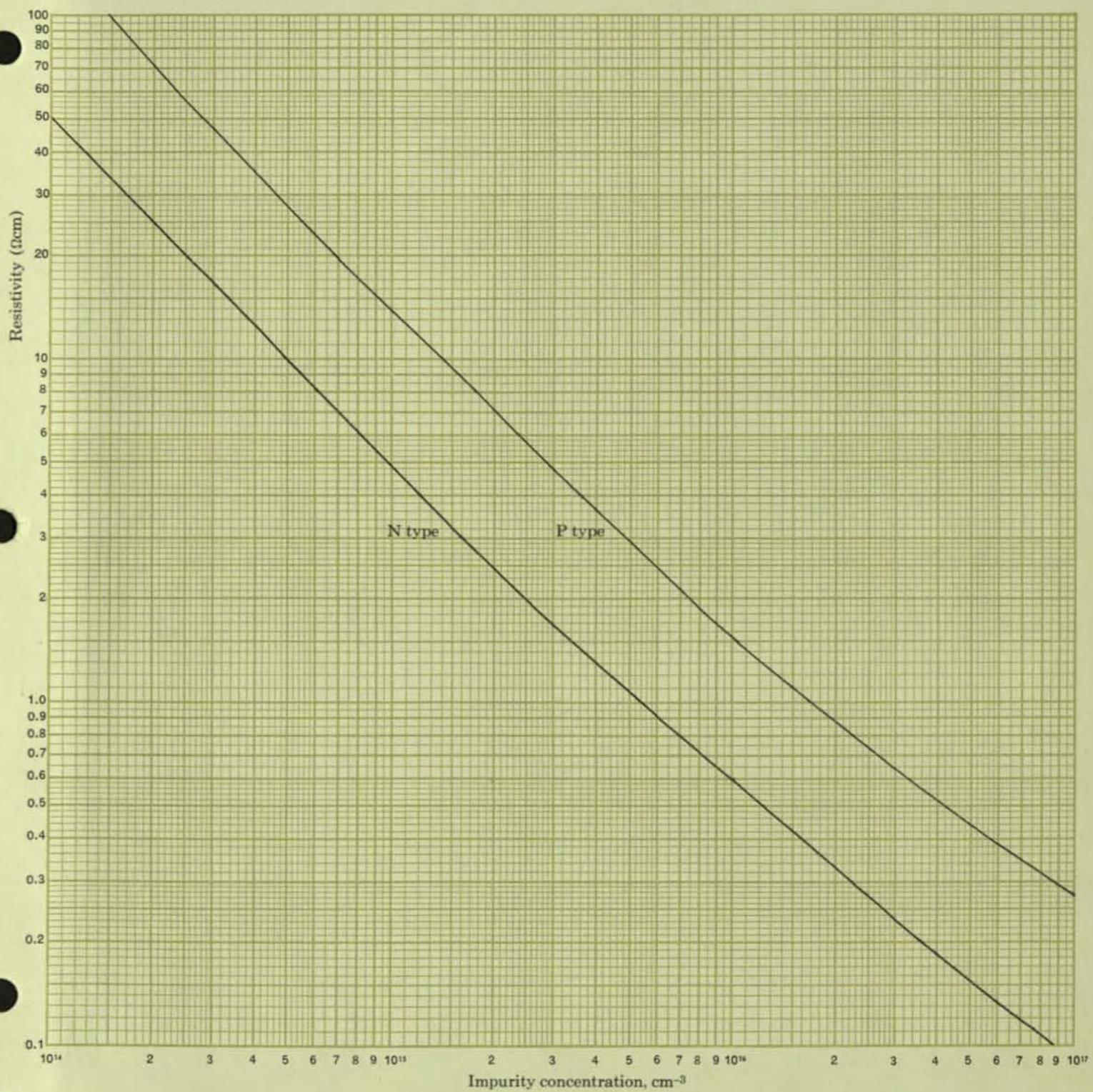
monoSilicon, incorporated

139 East 157th Street Gardena, California

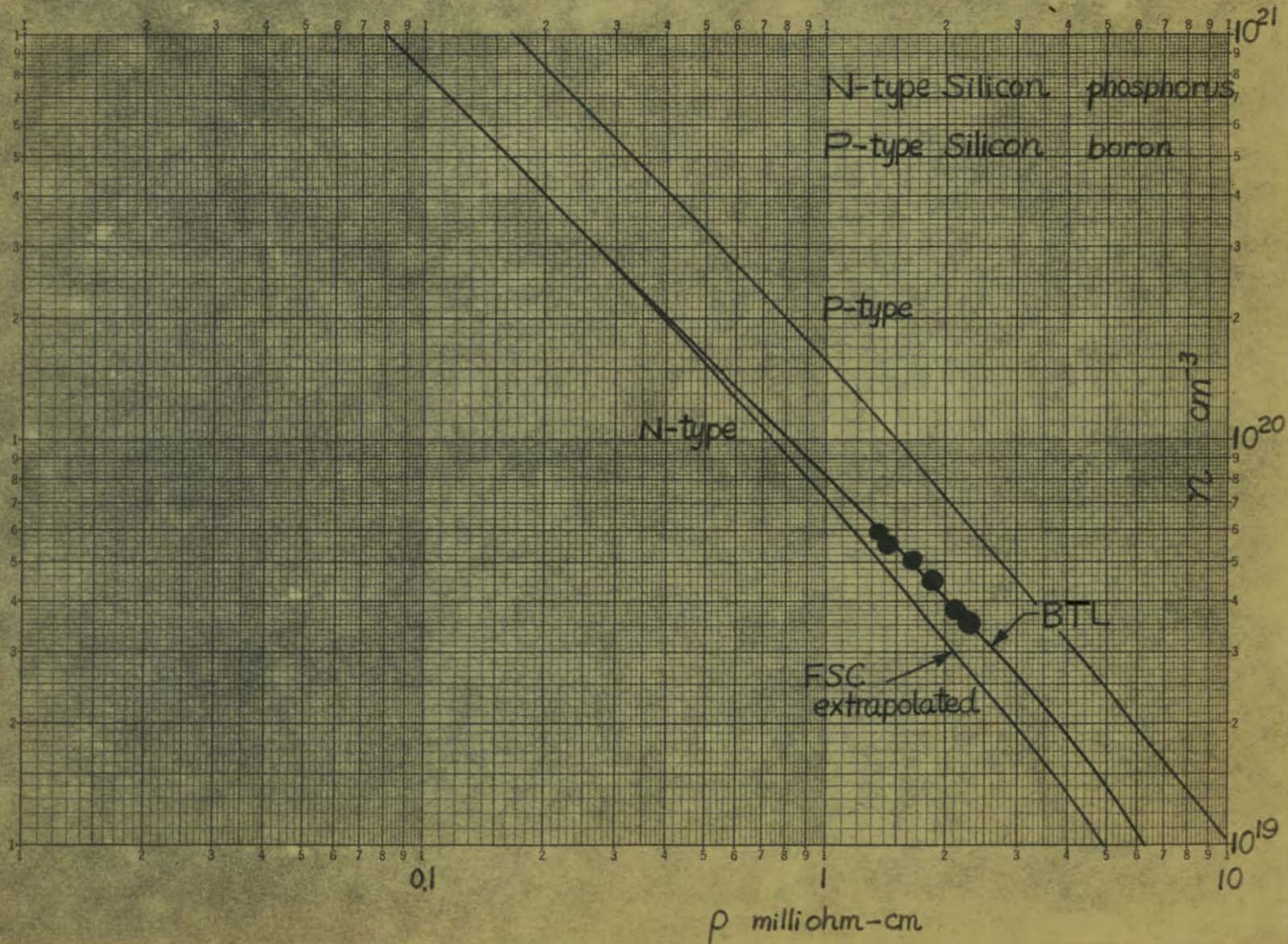


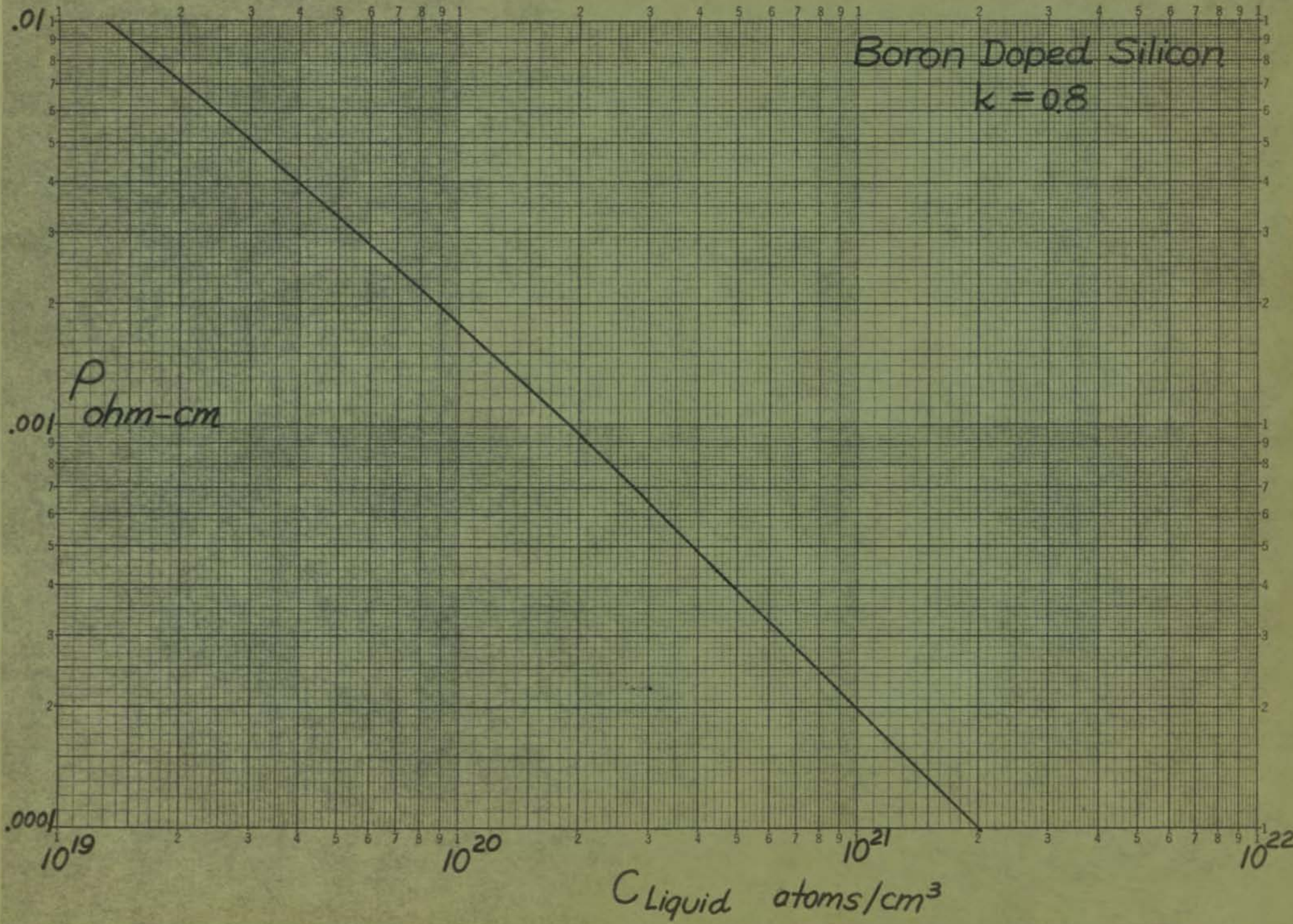
From an article by John C. Irwin in the March 1962 issue of the Bell System Tech. Journal.

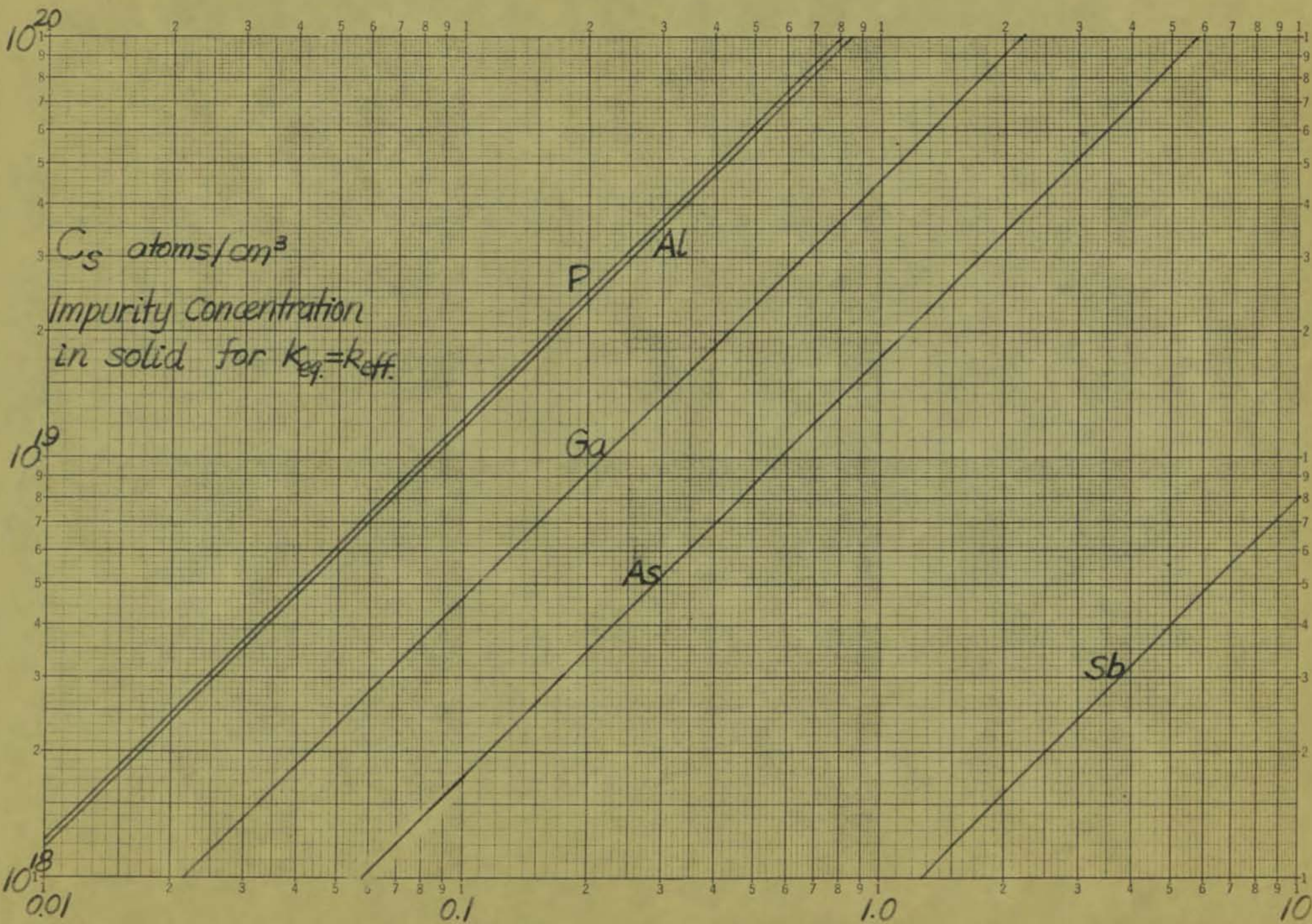
These curves, containing the latest data on the properties of silicon, have been prepared by MonoSilicon, Inc., who pioneered the growth of dislocation free silicon crystals in production quantities. For a review of the effects of dislocations on device characteristics see the article by W. Bardsley, "The Electrical Effects of Dislocations in Semiconductors," Volume 4 of Progress in Semiconductors, A. F. Gibson, Editor, John Wiley & Sons, Publishers, (1960).



Resistivity of Silicon at 300°K. as a function of acceptor or donor concentration.



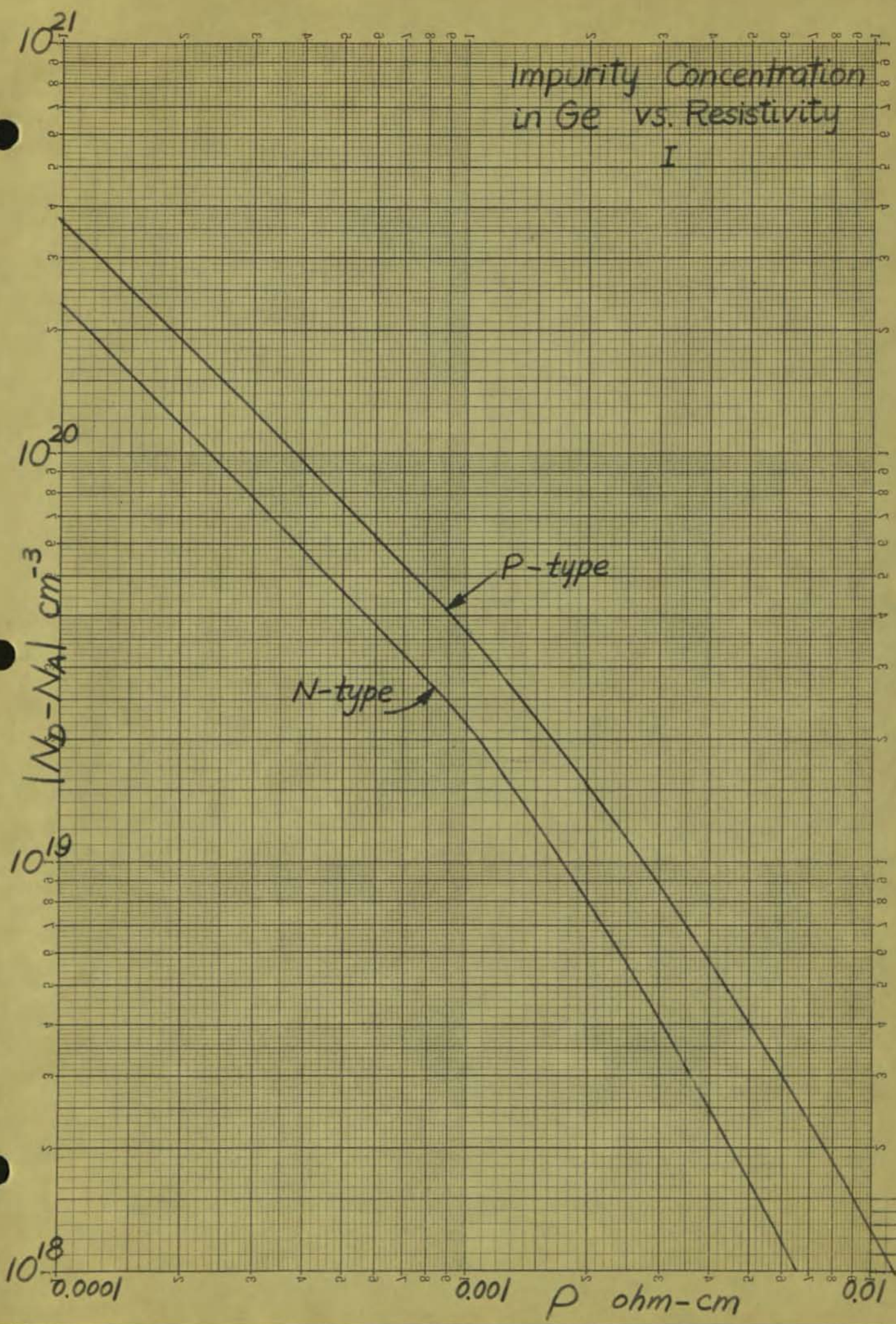




Weight percent of impurity in Ge liquid

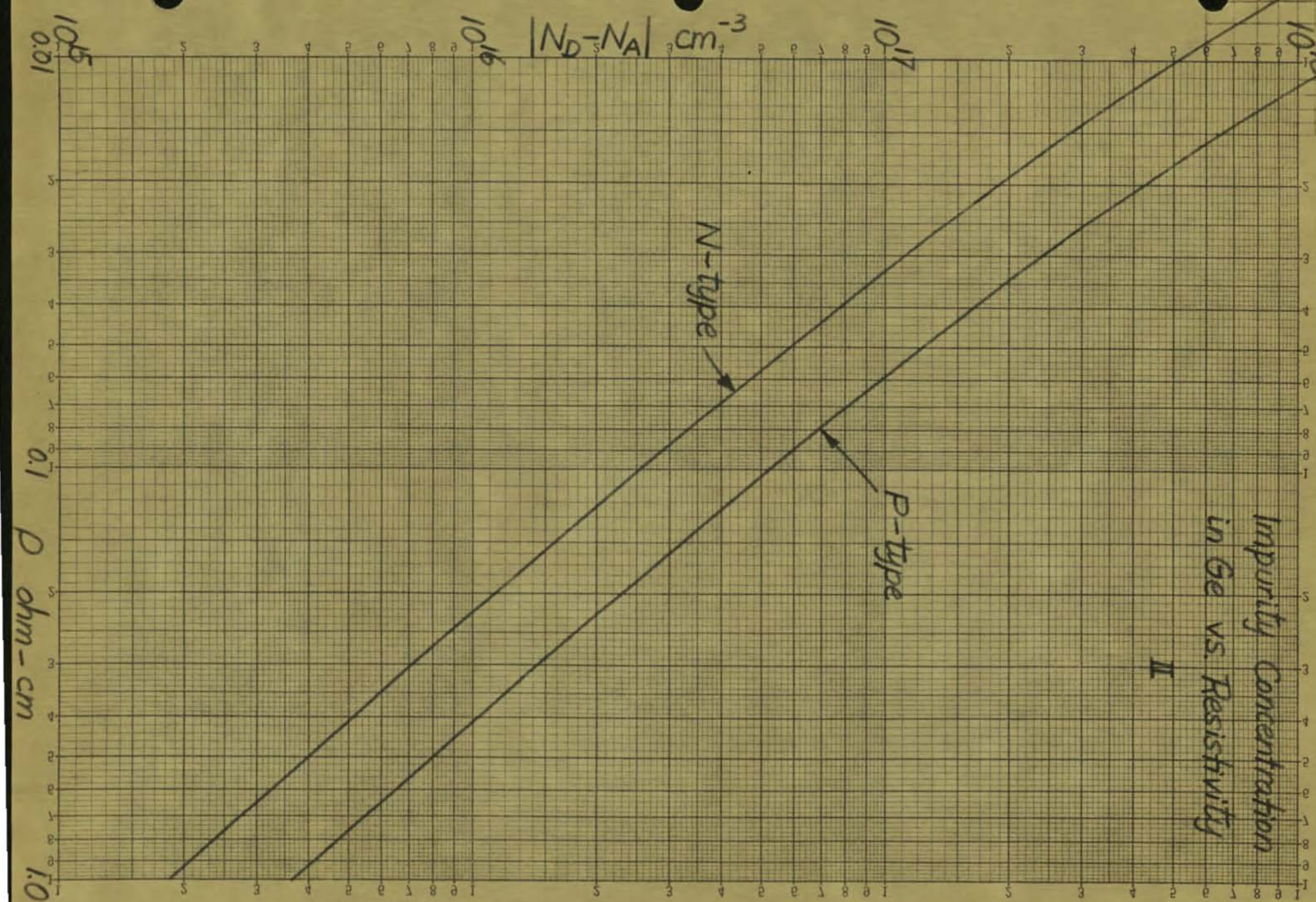
Impurity Concentration
in Ge vs. Resistivity

I



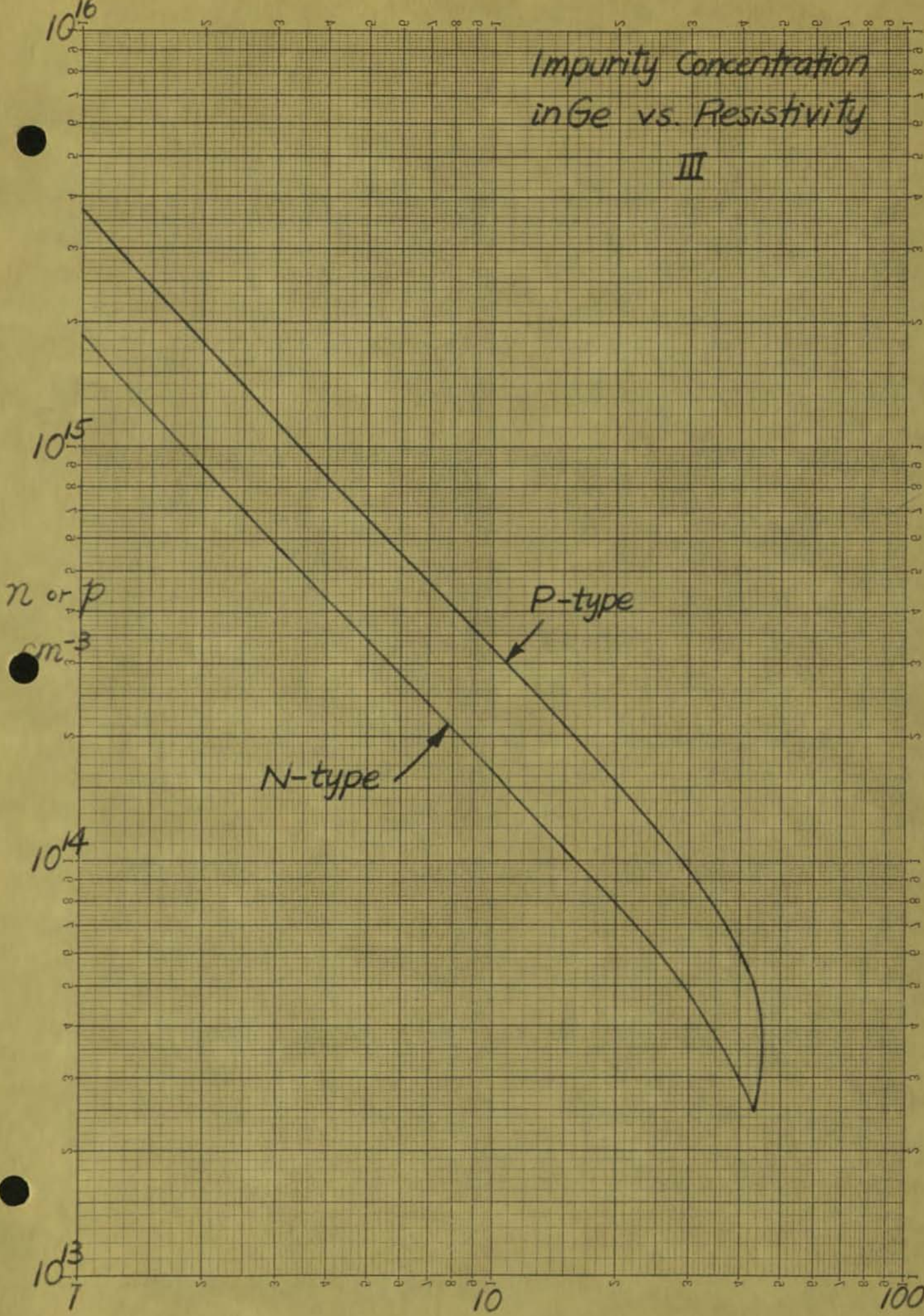
*Impurity Concentration
in Ge vs. Resistivity*

II



*Impurity Concentration
in Ge vs. Resistivity*

III



Sample calculation for Ge doping

W_i = weight of impurity in grams

$$= C_L \frac{\text{atoms}}{\text{cm}^3} \frac{A_w \frac{\text{gm}}{\text{gmat.wt.}}}{N \frac{\text{atoms}}{\text{gmat.wt.}}} \frac{W_{Ge} \text{ gm}}{d_{Ge} \frac{\text{gm}}{\text{cm}^3}}$$

C_L = concentration of impurity in the liquid = k_{eff}^{-1} $C_s = k_{\text{eq.}}^{-1} \frac{(k_{\text{eff}})^{-1}}{(k_{\text{eq.}})} C_s$

A_w = atomic weight of impurity element

N = avagadro's number = 6.06×10^{23}

W_{Ge} = weight of germanium in melt in gram = 100 gm

d_{Ge} = weight density of germanium in gm per cm^3 . = 5.32 gm/cm^3

element	A_w	$\frac{A_w}{N} \frac{W_{Ge}}{d_{Ge}}$	$k_{\text{eq.}}$	$k_{\text{eq.}} \frac{A_w W_{Ge}}{N d_{Ge}}$
B	10.82	3.37×10^{-22}	17	1.98×10^{-23}
Al	26.98	8.38×10^{-22}	0.1	8.38×10^{-21}
Ga	69.72	2.17×10^{-21}	0.1	2.17×10^{-20}
P	30.98	9.63×10^{-22}	0.12	8.02×10^{-21}
As	74.91	2.33×10^{-21}	0.04	5.82×10^{-20}
Sb	121.76	3.78×10^{-21}	0.003	1.26×10^{-18}

Resistivity Profile of Phosphorus Doped
Silicon

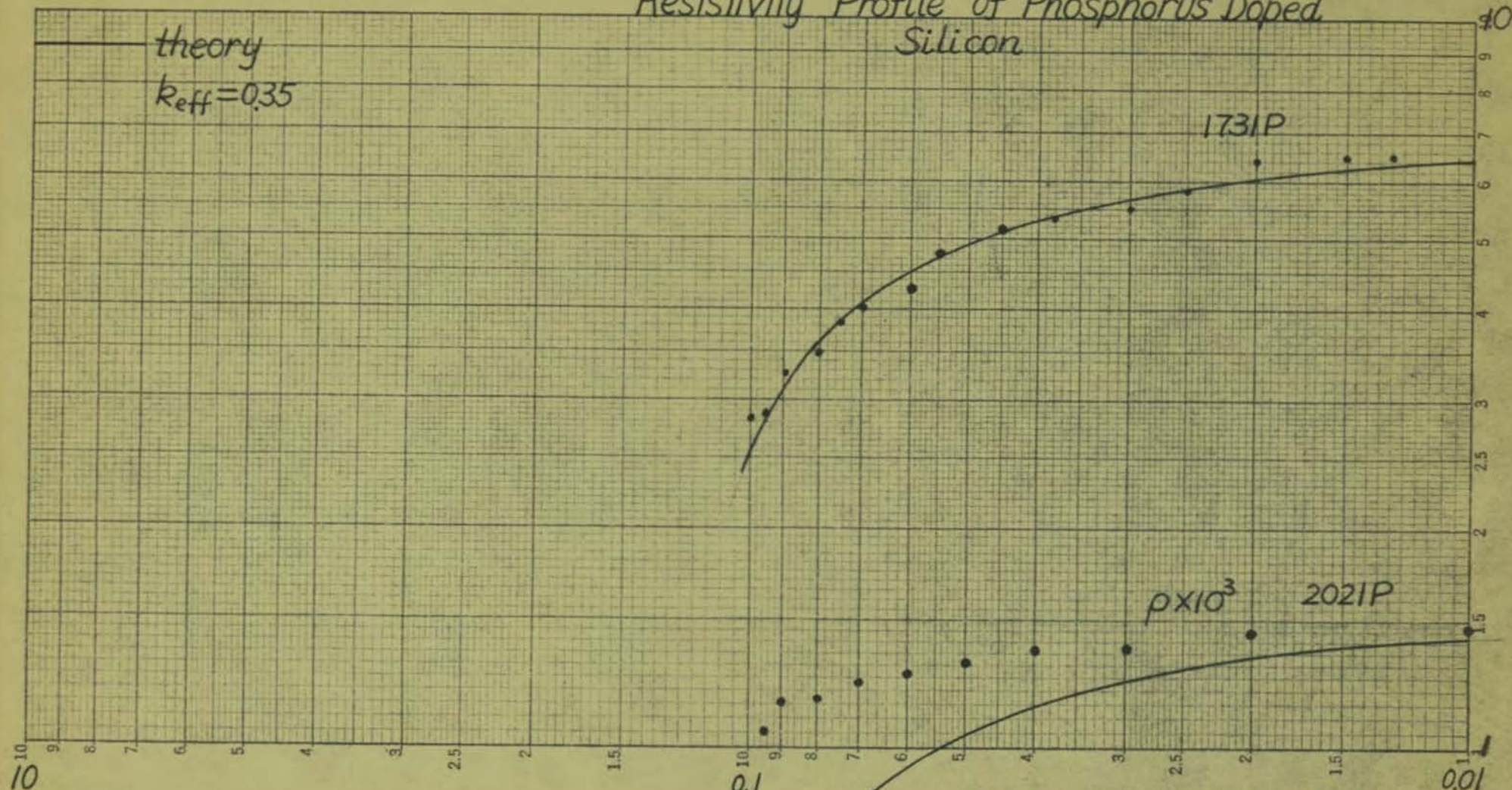
theory

$k_{eff} = 0.35$

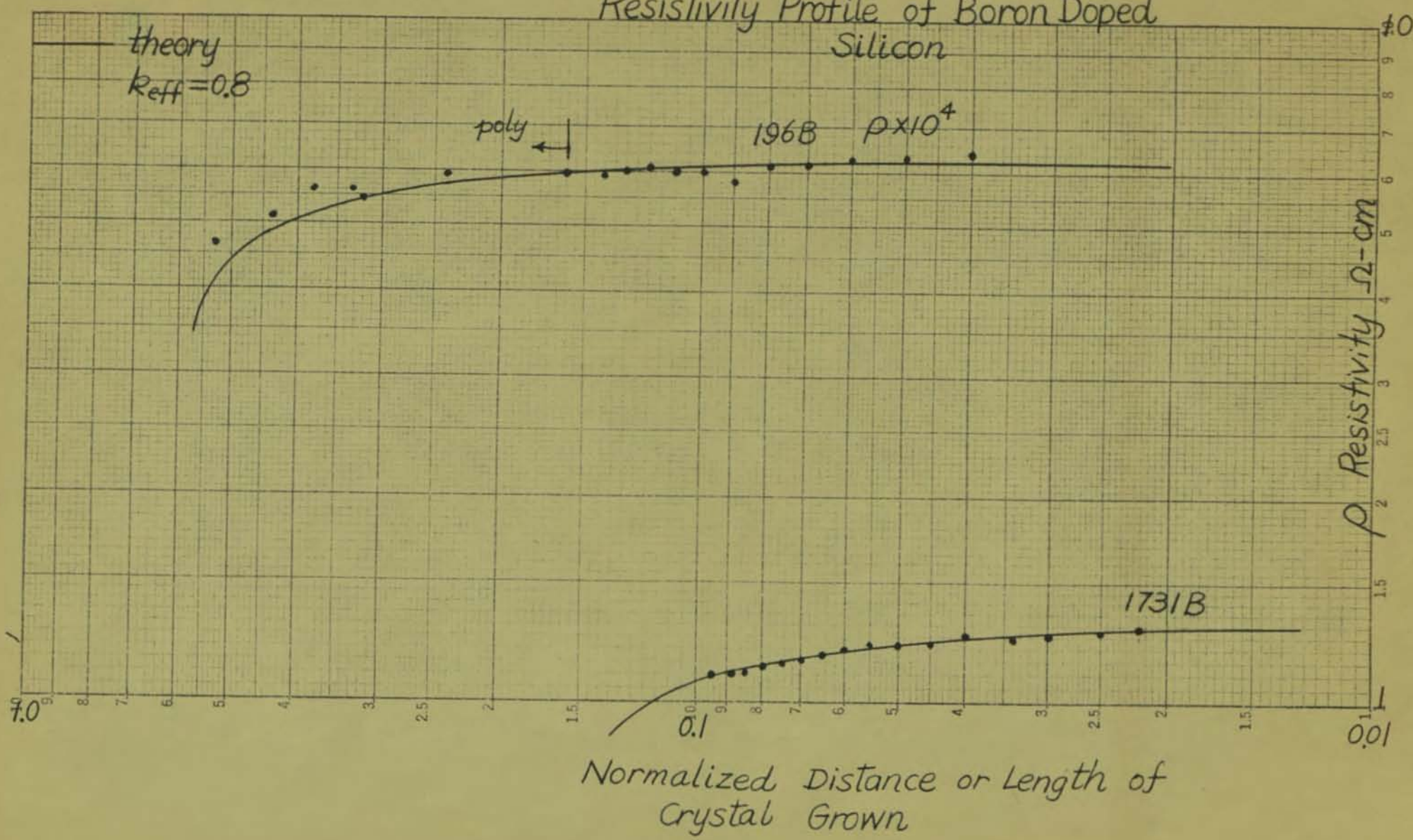
1731P

$\rho \times 10^3$ 2021P

Normalized Length of Crystal
Grown



Resistivity Profile of Boron Doped Silicon



NO. 31-226. 30 DIVISIONS PER INCH (120 DIVISIONS) BY FOUR CYCLES RATIO RULING



CODEX BOOK COMPANY, INC., NORWOOD, MASSACHUSETTS

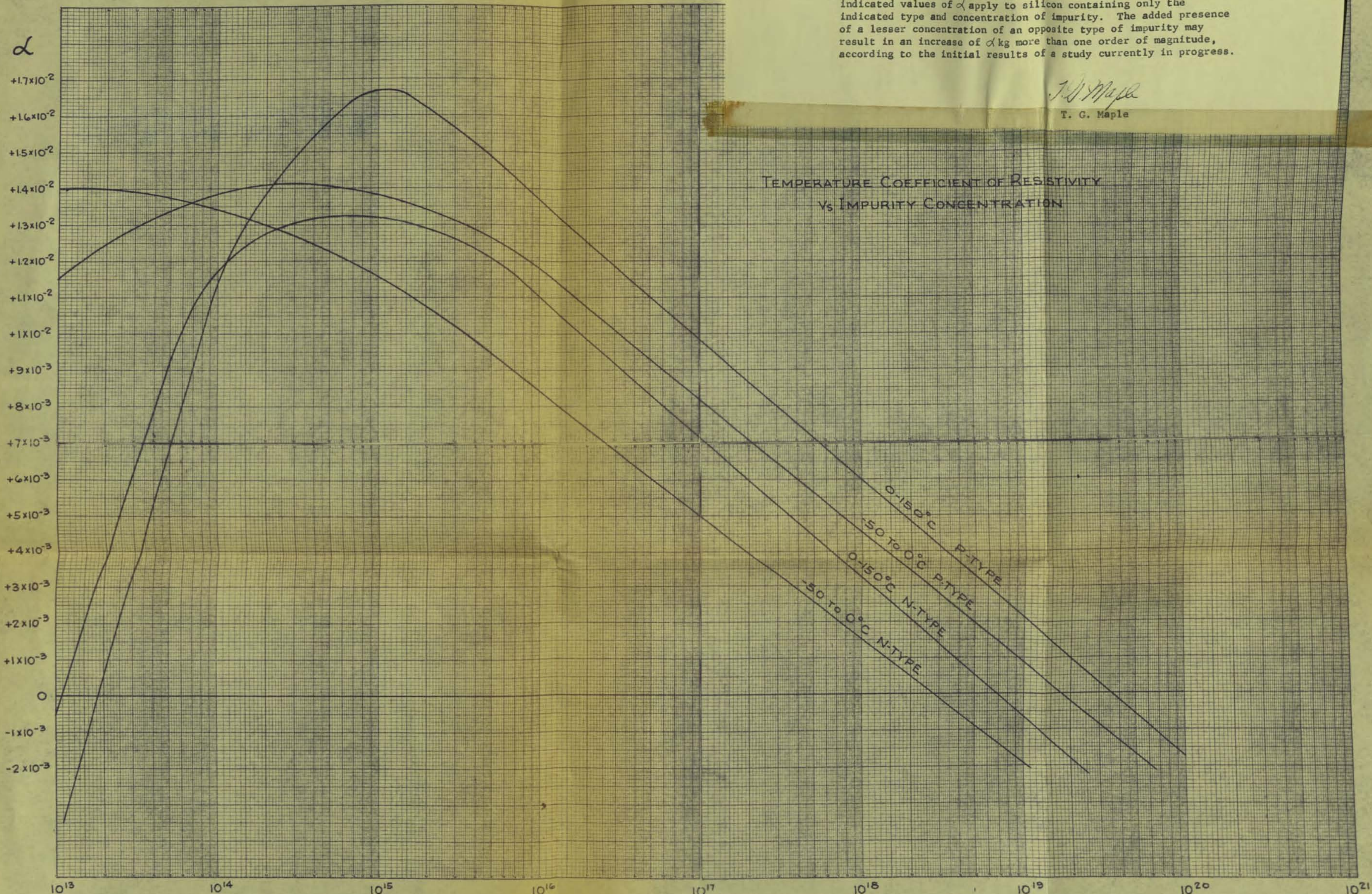
NC

The attached chart of Temperature Coefficient of Resistivity vs. Impurity Concentration was prepared by drawing smooth curves through points calculated from the figures of conductance vs. temperature shown on page 51, W. W. Gartner, "Transistors-Principles, Design and Applications", Van Nostrand 1960.

Caution must be exercised in the use of the chart because the indicated values of α apply to silicon containing only the indicated type and concentration of impurity. The added presence of a lesser concentration of an opposite type of impurity may result in an increase of α kg more than one order of magnitude, according to the initial results of a study currently in progress.

J.S. Mapel

T. G. Maple



WATER PRESSURE
CURVES

- (440) Treon, Crutchfield, and Kitamiller, *J. Ind. Hyg. Toxicol.*, **25**, 199-214 (1943).
 (441) Tschugnoff, *Ber.*, **33**, 735-6 (1900).
 (442) Ultee, *Ibid.*, **39**, 1856-8 (1906).
 (443) Van der Meulen and Mann, *J. Am. Chem. Soc.*, **53**, 481-3 (1931).
 (444) Vanstone, *J. Chem. Soc.*, **97**, 429-43 (1910).
 (445) Vaughan, *J. Am. Chem. Soc.*, **54**, 3803-76 (1932).
 (446) Venable, *Ber.*, **13** (2), 1649-52 (1880).
 (447) Verschoyle, *Trans. Roy. Soc. (London)*, **A230**, 189 (1931).
 (448) Villard, *Ann. chim. phys.*, [7] **10**, 387 (1897).
 (449) Villard, *Compt. rend.*, **120**, 1262-5 (1895).
 (450) Villiers, *Bull. soc. chim.*, **34**, 25-7 (1880).
 (451) Vincent and Chappuis, *Compt. rend.*, **100**, 1216-8 (1885).
 (452) Volmer and Kirchoff, *Z. physik. Chem.*, **115**, 233-8 (1925).
 (453) Von Rechenberg, "Destillation", Leipzig, 1923.
 (454) Von Siemens, *Ann. Physik.*, [4] **42**, 871-88 (1913).
 (455) Wade and Merriman, *J. Chem. Soc.*, **101**, 2438-43 (1919).
 (456) Walbaum, *Ber.*, **33**, 2299-302 (1900).
 (457) Walbaum, *J. prakt. Chem.*, **II**, **73**, 488-93 (1906).
 (458) Walbaum and Stephan, *Ber.*, **33**, 2302-8 (1900).
 (459) Walden, *Z. physik. Chem.*, **70**, 569-619 (1910).
 (460) Wallach, *Ann.*, **275**, 171 (1893).
 (461) *Ibid.*, **336**, 1-46 (1904).
 (462) Wallach et al., *Ibid.*, **279**, 366-97 (1894).
 (463) Weber, *Verlag Akad. Wissenschaften*, **22**, 380 (1914).
 (464) Wenzel and Pirak, *Collection Czechoslov. Chem. Commun.*, **6**, 54-9 (1934).
 (465) Whitmore and Fleming, *J. Am. Chem. Soc.*, **55**, 3803-6 (1933).
 (466) Whitmore et al., *Ibid.*, **68**, 475-81 (1946).
 (467) Wiberg and Söderlin, *Z. Elektrochem.*, **41**, 181-3 (1935).
 (468) Wilbrand and Beilstein, *Z. Chemie*, **7**, 153-60 (1884).
 (469) Wilcock, *J. Am. Chem. Soc.*, **68**, 691-6 (1946).
 (470) Williams, *Ibid.*, **47**, 2044-52 (1925).
 (471) Willingham et al., *J. Research Natl. Bur. Standards*, **32**, 1-19 (1945).
 (472) Wiedemann, *Ann.*, **275**, 309-82 (1893).
 (473) Wittenberg and Mayer, *Ber.*, **16**, 500-6 (1883).
 (474) Woringer, *Z. physik. Chem.*, **34**, 257-69 (1900).
 (475) Wöhler and Grotian, *Wied Ann.*, **11**, 545-604 (1829).
 (476) Yost and Stone, *J. Am. Chem. Soc.*, **55**, 1889-95 (1933).
 (477) Young, *J. Chem. Soc.*, **55**, 483-8 (1899).
 (478) *Ibid.*, **55**, 486-521 (1899).
 (479) *Ibid.*, **59**, 621-6 (1891).
 (480) *Ibid.*, **59**, 903-11 (1891).
 (481) *Ibid.*, **59**, 911-34 (1891).
 (482) *Ibid.*, **71**, 446-67 (1897).
 (483) *Ibid.*, **73**, 678-81 (1898).
 (483a) *Ibid.*, **77**, 1146-61 (1900).
 (484) Young, *Proc. Roy. Irish Acad.*, **38B**, 65-92 (1928).
 (485) Young, *Proc. Roy. Dublin Soc.*, **12**, 374-432 (1910).
 (486) Young, *Z. physik. Chem.*, **29**, 193-241 (1899).
 (487) Young and Forsey, *J. Chem. Soc.*, **75**, 873-83 (1899).
 (488) *Ibid.*, **77**, 1156-61 (1900).
 (489) *Ibid.*, **81**, 703-4 (1902).
 (490) Young and Nalma, *IND. ENG. CHEM.*, **21**, 321-2 (1929).
 (491) Young and Thomas, *J. Chem. Soc.*, **63**, 1191-262 (1883).
 (492) *Ibid.*, **71**, 628-4 (1897).
 (493) Zeleny and Heath, *Physik. Z.*, **7**, 667-71 (1906).
 (494) Zincke, *Ann.*, **302**, 1-31 (1880).

(Vapor Pressure of Pure Substances)

INORGANIC COMPOUNDS

The preceding paper catalogued vapor pressure data of organic compounds. This article presents vapor pressure data for about 300 inorganic compounds and completes the coverage of this field at this time.

THE foregoing report (441) discussed the need for accurate vapor pressure data when certain physical laws are put into practical application. One of the constant cries of modern times is for more extensive and better data. To a fair extent, a new plant is no better than the data used in its design. These two reports are intended as a start toward the improvement of this circumstance.

The methodical exhaustion of the sources of vapor pressure data was begun some six years ago. *Chemical Abstracts* was searched through 1942, but the coverage since then has been incomplete. In the vast majority of cases the original documents were consulted. Existing collections of vapor pressure data (9, 199, 249, 465) were of great help. In this connection special attention should be focused on the excellent compilation of Kelley (229), which has bolstered our work admirably.

The treatment of data follows the style, format, and general plan of the preceding paper. The analytical method was retained and was based on semilogarithmic charts measuring 30 × 42 inches (where 1 mm. = 1° C.) and colored map tacks representing the plotted points over which a taut thread was stretched. This resulted in the introduction of a gentle curvature to the vapor pressure line, but sufficient tacks were inserted so that the curve was virtually continuous and without angles. For the permanent gases (those materials below -100° C.), the lines were penciled in with the help of a French curve, but, in view of the uncertainties in temperature measurement above 500° C. (becoming less certain with increase of temperature), it was felt that the penciling of the curves was unnecessary. Where the tempera-

ture fell within the range -150° C. to +400° C. the Cox chart previously referred to was used.

So that ambiguity will be minimized, the name recognized by *Chemical Abstracts* has been used. The arrangement in the tables is alphabetical according to the name of the compound and the formula is also added so that there will be no doubt as to the substance meant.

Table I contains pressures (in millimeters of mercury) under 1 atmosphere, and Table II contains pressures (in atmospheres) over one atmosphere. All temperatures are in ° C. Since there is a discontinuity in a vapor pressure curve at the melting point, the melting point of the substance, where known, is listed in Table I. Since the vapor pressure curve ends at the critical point, Table II lists the critical temperature and pressure.

Assembling the results of many workers, as has been done here, leads to uncertainty as to the accuracy of the data. The temperature range is virtually from absolute zero to the highest temperatures man has devised. The lower part of the temperature scale is accurate, but as higher temperatures are reached, the uncertainty gap widens. In the opinion of the writer the figures given here represent the best experimental data possible with the graphic methods employed. The writer is certain that, as more reliable experimental measurements are made, a few of the figures given here should be revised.

NOMENCLATURE

d = decomposes	p = polymerizes
M.P. = melting point	s = solid
P _c = critical pressure	T _c = critical temperature

Table I. Pressures Lachan One Atmosphere

Formula	Name	Temperature, °C.										M.P.	Citation No.	
		1 mm.	5 mm.	10 mm.	20 mm.	40 mm.	60 mm.	100 mm.	200 mm.	400 mm.	760 mm.			
Al	Aluminum	1284	1421	1487	1555	1635	1654	1749	1844	1947	2056	650	(155, 222, 459)	
Al ₂ Br ₃	Aluminum borohydride	-	-52.2	-42.9	-32.5	-20.9	-13.4	-2.9	+11.2	28.1	45.9	-64.5	(220)	
Al ₂ Br ₅	Aluminum bromide	81.2	103.8	118.0	134.0	150.6	161.7	176.1	199.8	227.0	250.3	97.5	(8, 127, 222)	
AlCl ₃	Aluminum chloride	100.0	116.4	123.8	131.8	139.9	145.4	152.0	161.8	171.6	180.2	192.4	(127, 128, 222, 264, 409, 410, 437)	
AlF ₃	Aluminum fluoride	1238	1298	1324	1350	1378	1398	1422	1457	1496	1537	1640	(558)	
Al ₂ I ₃	Aluminum iodide	178.0	207.7	225.8	244.2	265.0	277.8	294.5	322.0	354.0	385.6	(187, 222)		
Al ₂ O ₃	Aluminum oxide	2148	2306	2385	2405	2549	2599	2655	2765	2874	2977	3050	(220, 222, 222)	
NH ₃	Ammonia	-109.1	-97.5	-91.9	-85.8	-72.2	-74.3	-68.4	-57.0	-45.4	-33.6	-77.7	(45, 62, 25, 49, 61, 88, 112, 178, 198, 225, 251, 279, 306, 334, 429)	
ND ₃	Deutero ammonia	29.2	49.4	59.2	69.4	80.1	-74.0	-67.4	-57.0	-45.4	-33.4	-74.0	(445)	
NH ₄ N ₃	Ammonium azide	-	-	-	-	-	-	-	-	-	-	-	(151)	
NH ₄ Br	Ammonium bromide	198.3	234.5	252.0	270.6	290.0	303.8	320.0	345.3	370.9	396.0	-	(405)	
NH ₄ CO ₂ NH ₃	Ammonium carbamate	-25.1	-10.4	-2.9	+5.5	14.0	19.6	26.7	37.2	48.0	58.3	(48, 107)		
NH ₄ Cl	Ammonium chloride	160.4	193.8	209.8	220.1	245.0	255.2	271.5	293.2	316.5	337.8	520	(555, 405)	
NH ₄ H ₂ S	Ammonium hydrogen sulfide	-51.1	-36.0	-28.7	-20.8	-12.3	-7.0	0.0	+10.5	21.8	33.3	-	(400)	
NH ₄ I	Ammonium iodide	210.9	247.0	263.5	282.8	302.8	316.0	331.8	355.8	381.0	404.9	-	(405)	
NH ₄ CN	Ammonium cyanide	-50.6	-35.7	-28.6	-20.9	-12.6	-7.4	-0.5	+9.6	20.5	31.7	35	(101)	
Sb	Antimony	855	984	1033	1084	1141	1176	1223	1288	1364	1440	1630.5	(168, 220, 222, 318, 456)	
SbBr ₃	Antimony tribromide	93.9	120.0	142.7	155.3	177.4	185.1	203.5	225.7	250.2	275.0	295.6	(9, 102)	
SbCl ₃	Antimony trichloride	49.2	71.4	85.2	100.6	117.8	128.3	143.3	165.0	192.2	219.0	234.4	(8, 9, 45, 222)	
SbCl ₅	Antimony pentachloride	22.7	45.6	61.8	75.8	91.0	101.0	114.1	d	-	-	2.8	(8, 9, 45, 222)	
SbI ₃	Antimony triiodide	163.6	203.8	223.5	244.8	267.8	282.5	303.5	333.8	368.5	401.0	167	(9, 102)	
Sb ₂ O ₃	Antimony trioxide	574.5	626	666	729	812	873	957	1035	1242	1425	620	(183, 222)	
A	Argon	-218.26	-213.9	-210.9	-207.9	-204.9	-202.9	-200.5	-195.5	-190.5	-185.5	-180.2	(41, 55, 84, 86, 125, 220, 222, 312, 406)	
As ₂ Me (metallic)	-	572	615	637	654	673	693	713	733	753	773	813	(145, 194, 220, 312, 342, 367)	
AsBr ₃	Arsenic tribromide	41.8	70.6	85.2	101.3	118.7	130.0	145.2	167.7	193.6	220.0	-	(2)	
AsCl ₃	Arsenic trichloride	-11.4	+11.4	+23.5	36.0	50.0	58.7	70.9	84.2	109.7	130.4	-18	(8, 80, 220, 222)	
AsF ₃	Arsenic trifluoride	-	-	-	-	-2.5	+4.2	13.2	26.7	41.4	55.3	-	(576)	
AsF ₅	Arsenic pentafluoride	-117.9	-105.0	-103.1	-98.0	-92.4	-88.8	-84.3	-75.5	-64.0	-52.8	-79.8	(222, 322)	
AsH ₃	Arsenic hydride (arsine)	-142.6	-130.8	-124.7	-117.7	-110.2	-104.8	-98.0	-87.2	-78.2	-62.1	-116.3	(816)	
As ₂ O ₃	Arsenic trioxide	212.5	242.6	-259.7	279.2	299.2	310.3	322.5	370.0	412.2	457.2	212.8	(829, 887, 373, 408, 409, 418, 479)	
Ba	Barium	-	-	984	1049	1120	1195	1240	1301	1403	1518	1635	850	(167, 222, 322)
BeBr ₂	Beryllium borohydride	+1.0	19.8	28.1	36.8	46.2	51.7	58.6	69.0	79.7	90.0	123	(60)	
BeBr ₃	Beryllium bromide	289	325	342	361	379	390	405	427	451	474	490	(229, 322)	
BeCl ₂	Beryllium chloride	291	328	346	365	384	395	411	438	461	487	405	(229, 322)	
BeI ₂	Beryllium iodide	283	322	341	361	382	394	411	435	461	487	488	(229, 322)	
Bi	Bismuth	1021	1099	1136	1177	1217	1240	1271	1319	1370	1420	271	(17, 185, 184, 185, 222, 225, 343)	
BiBr ₃	Bismuth tribromide	*	261	282	305	327	340	360	382	425	461	215	(116, 222)	
BiCl ₃	Bismuth trichloride	*	242	264	287	311	324	343	372	408	441	230	(116, 222, 224)	
BH ₂ CO	Borine carbonyl	-139.2	-127.3	-121.1	-114.1	-106.6	-101.9	-95.3	-85.5	-74.8	-64.0	-137.0	(29)	
BBr ₃	Boron tribromide	-41.4	-20.4	-10.1	+1.5	14.0	22.1	33.5	50.3	70.0	91.7	-45	(229, 421)	
BCl ₃	Boron trichloride	-91.5	-75.2	-66.9	-57.9	-47.8	-41.2	-32.4	-18.9	-3.6	+12.7	-107	(229, 305, 322, 430)	
BF ₃	Boron trifluoride	-154.6	-145.4	-141.3	-135.4	-131.0	-127.6	-123.0	-118.9	-108.3	-110.7	-126.8	(50, 118, 229, 319, 322)	
BeH ₂	Dihydroborane	-150.7	-149.5	-144.3	-138.5	-131.6	-127.2	-120.9	-111.2	-99.6	-86.5	-169	(229, 419, 424)	
Be ₂ H ₅	Diborane hydrobromide	-93.3	-75.3	-66.3	-56.4	-45.4	-38.2	-29.0	-15.4	0.0	+16.3	-104.2	(229, 424)	
Be ₂ H ₇ N ₃	Triborane triamine	-63.0	-45.0	-35.2	-25.0	-13.2	-5.8	+4.0	18.5	34.3	50.6	-58.2	(229, 427)	
Be ₂ H ₈	Tetrahydrotetraborane	-90.9	-73.1	-64.3	-54.8	-44.3	-37.4	-28.1	-14.0	+0.8	16.1	-119.9	(229, 425, 426, 428)	
Be ₂ H ₉	Dihydropentaborane	*	-40.4	-30.7	-20.0	-8.0	-0.4	+9.6	24.6	40.8	55.1	-47.0	(229, 426)	
Be ₂ H ₁₁	Tetrahydronitroborane	-50.2	-29.9	-19.9	-9.2	+2.7	10.2	20.1	34.8	51.2	67.0	-	(229, 426)	
Be ₂ H ₁₄	Dihydrodecaborane	60.0	80.8	90.2	100.0	117.4	127.8	142.3	163.8	187	199.6	-	(229, 426)	
Br	Bromine	-48.7	-32.6	-25.0	-16.8	-8.0	-0.6	+9.3	24.3	41.0	58.2	-7.3	(88, 102, 171, 205, 217, 229, 251, 331, 345, 351, 458, 487)	
BrF ₅	Bromine pentafluoride	-69.3	-51.0	-41.9	-32.0	-21.0	-14.0	-4.5	+9.9	28.7	40.0	-61.4	(229, 322)	
Cd	Cadmium	394	455	484	516	553	578	611	658	711	785	320.9	(17, 48, 61, 109, 111, 189, 185, 181, 210, 220, 245, 345)	
CdCl ₂	Cadmium chloride	*	618	656	695	736	762	797	847	908	967	568	(156, 220, 224)	
CdF ₂	Cadmium fluoride	1385	1504	1559	1617	1673	1709	1759	1834	1924	2024	520	(322)	
CdI ₂	Cadmium iodide	415	481	512	546	584	608	640	685	742	798	385	(229, 327)	
CdO	Cadmium oxide	1000	1100	1149	1200	1257	1295	1341	1409	1484	1559	-	(119, 184, 222)	
Ca	Calcium	*	926	983	1046	1111	1152	1207	1258	1355	1487	851	(167, 222, 315, 345, 355, 356)	
C	Carbon	3586	3828	3946	4069	4196	4273	4373	4516	4660	4827	-	(4, 176, 177, 220, 241, 242, 265, 327, 377, 445, 480)	
CB ₄	Carbon tetrabromide	-80.0	-30.0	-19.6	-8.2	+4.3	12.3	23.0	38.3	57.8	76.7	-22.6	(38)	
CCl ₄	Carbon tetrachloride	-184.6	-174.1	-169.3	-164.8	-155.8	-155.4	-150.7	-143.6	-135.5	-127.7	-183.7	(229, 370)	
CF ₄	Carbon tetrafluoride	-134.3	-124.4	-119.5	-114.4	-105.6	-104.8	-100.2	-93.0	-85.7	-78.2	-57.5	(5, 46, 117, 178, 179, 211, 220, 278, 292, 308, 334, 484, 487, 487, 490)	
CO ₂	Carbon dioxide	-	-	-	-	-	-	-	-	-	-	-	-	
CO ₃	Carbon suboxide	-94.8	-79.0	-71.0	-62.2	-53.0	-45.5	-36.9	-23.3	-8.9	+6.3	-107	(257, 435)	
CS ₂	Carbon disulfide	-73.8	-54.3	-44.7	-34.3	-22.5	-15.3	-5.1	+10.4	28.0	46.8	-110.8	(176, 222, 265, 325, 354, 355, 356, 480, 487, 490)	

(Continued on next page)

INDUSTRIAL AND ENGINEERING CHEMISTRY

Table I (continued)

Table I (Continued)

Formula	Name	Temperature, °C.										M.P.	Citation No.
		1 mm.	5 mm.	10 mm.	20 mm.	60 mm.	100 mm.	200 mm.	400 mm.	760 mm.			
H ₂ S	Hydrogen sulfide	-134.3*	-122.4*	-110.3*	-100.7*	-102.3*	-97.9*	-91.6*	-82.3	-71.8	-60.4	-55.5	(116, 157, 229, 255, 256, 262, 254, 418, 416)
H ₂ Tl	Hydrogen telluride	-42.2	-24.4	-15.2	-5.1	+6.0	-12.8	-22.0	-15.3	-49.6	-64.0	-89.7	(64, 229)
H ₂ NH	Hydrogen telluride	-90.4*	-82.4*	-75.4*	-67.8*	-59.1*	-43.7*	-45.7	-32.4	-17.2	-2.0	-49.0	(61, 229, 416)
NH ₂ OH	Hydroxylamine	*	39.0	47.2	*	64.6	70.0	77.5	87.9	99.2	110.0	34.0	(6, 26, 229)
I ₂	Iodine	36.7*	62.2*	73.2*	+4.7*	97.5*	105.4*	116.5	137.3	159.8	183.0	112.9	(10, 81, 22, 26, 156, 145, 155, 229, 254, 354, 356, 440, 447, 448)
IF ₅	Iodine pentafluoride	-15.2*	+1.8*	8.5	-5.1*	32.2	40.0	50.0	65.4	81.2	97.0	8.0	(561)
IF ₇	Iodine heptafluoride	87.0*	-70.7*	63.0*	-4.4*	48.3*	-39.4*	-31.9*	-20.7*	-8.3*	+4.0*	5.5	(229, 348)
Fe	Iron	1787	1957	2039	2148	2224	2283	2360	2475	2605	2735	1535	(165, 218, 249, 346)
Fe(CO) ₅	Iron pentacarbonyl	*	-6.5	+4.6	16.7	30.3	39.1	50.3	68.0	86.1	105.0	-21	(229, 460)
Kr	Krypton	-190.3*	-191.3*	-187.2*	-18.4*	-178.4*	-175.7*	-171.8*	-165.4*	-159.0*	-152.0	-156.7	(5, 221, 229, 318, 317, 329)
Pb	Lead	973	1099	1162	1224	1309	1358	1421	1519	1630	1744	327.5	(110, 155, 154, 165, 165, 172, 229, 256, 341, 345, 348, 460, 471)
PbBr ₃	Lead bromide	513	678	610	646	686	711	745	796	856	914	373	(186, 229, 165, 474)
PbCl ₃	Lead chloride	547	615	648	684	725	750	784	833	893	954	501	(105, 156, 207, 229, 465, 474)
PbF ₃	Lead fluoride	*	861	904	950	1003	1036	1080	1144	1219	1293	855	(229, 474)
PbI ₂	Lead iodide	479	540	571	605	644	668	701	750	807	872	402	(156, 209, 229)
PbO	Lead oxide	943	1039	1085	1134	1189	1222	1265	1330	1402	1472	890	(119, 229)
PbS	Lead sulfide	852*	928*	975*	1005*	1048*	1074*	1108*	1160	1221	1281	1114	(229, 388)
Li	Lithium	723	828	881	940	1003	1042	1097	1178	1273	1372	186	(56, 57, 107, 229, 257)
LiBr	Lithium bromide	748	840	885	939	994	1028	1076	1147	1226	1310	547	(229, 367, 475)
LiCl	Lithium chloride	783	860	932	987	1045	1081	1120	1203	1290	1382	614	(229, 364, 367, 475)
LiF	Lithium fluoride	1047	1156	1211	1270	1333	1372	1425	1503	1591	1681	870	(229, 371, 475)
LiI	Lithium iodide	723	802	841	883	927	953	993	1049	1110	1171	446	(229, 367, 475)
Mg	Magnesium	621*	702	743	789	838	868	900	967	1034	1107	651	(155, 167, 229, 355, 469)
MgCl ₂	Magnesium chloride	778	877	930	988	1050	1088	1142	1223	1316	1418	712	(229, 364)
Ma	Manganese	1292	1434	1505	1583	1666	1720	1792	1900	2029	2151	1260	(155, 165, 229, 349)
MaCl ₂	Manganese chloride	*	736	778	825	879	913	960	1028	1108	1190	650	(229, 354)
Hg	Mercury	126.2	164.8	184.0	204.6	228.8	242.0	261.7	290.7	323.0	357.0	-38.9	(26, 54, 109, 154, 159, 178, 181, 188, 185, 210, 229, 229, 340, 425, 471, 473, 477, 516, 518, 519, 520, 530, 532, 542, 545, 460, 474)
HgBr ₃	Mercuric bromide	126.5*	165.3*	179.8*	194.3*	211.5*	221.0*	237.8	262.7	290.0	319.0	237	(212, 229, 324, 344, 359, 458, 485)
HgCl ₃	Mercuric chloride	126.2*	166.0*	180.2*	195.8*	212.5*	222.2*	237.0*	256.5*	275.5*	304.0	277	(124, 212, 229, 324, 356, 387, 455, 485)
HgI ₃	Mercuric iodide	157.5*	189.2*	204.5*	220.0*	238.2*	249.0*	261.8	291.0	324.2	354.0	259	(98, 212, 229, 324, 359, 458, 485)
Mo	Molybdenum	3102	3393	3535	3690	3859	3964	4109	4322	4553	4804	2622	(212, 229, 258)
MoF ₆	Molybdenum hexafluoride	-65.5*	-49.0*	-40.8*	-32.0*	-22.1*	-16.2*	-8.0*	+4.1*	17.2	36.0	17	(229, 347)
MoO ₃	Molybdenum trioxide	734*	785*	814	851	892	917	955	1014	1082	1151	795	(120, 205, 229)
Ne	Neon	-257.3*	-255.5*	-254.6*	-253.7*	-252.6*	-251.9*	-251.0*	-249.7*	-248.1	-246.0	-248.7	(71, 229, 227, 485)
Ni	Nickel	1810	1979	2057	2143	2234	2289	2364	2473	2603	2732	1452	(212, 229, 349)
NiCl ₂	Nickel chloride	671*	731*	759*	789*	821*	840*	866*	904*	945*	987*	1001	(125, 229, 349)
Ni(CO) ₄	Nickel carbonyl	*	*	*	*	-23.0	-15.9	-6.0	+8.8	25.8	42.5	-25	(7, 95, 97, 229, 274)
N ₂	Nitrogen	-226.1*	-221.3*	-219.1*	-216.8*	-214.0*	-212.3*	-209.7	-205.6	-200.9	-195.8	-210.0	(15, 70, 80, 100, 125, 158, 173, 174, 195, 229, 298, 321, 465, 467, 489)
NF ₃	Nitrogen trifluoride	*	-175.5	-170.7	-165.7	-160.2	-156.5	-152.3	-145.2	-137.4	-129.0	-183.7	(229, 270)
NO	Nitric oxide	-184.5*	-180.6*	-178.2*	-175.3*	-171.7*	-168.9*	-165.0*	-162.3*	-158.8*	-151.7	-161	(1, 145, 170, 216, 229, 279, 292, 294)
N ₂ O	Nitrous oxide	-143.4*	-133.4*	-128.7*	-124.0*	-118.3*	-114.9*	-110.3*	-103.6*	-96.2*	-88.5	-90.9	(20, 58, 53, 68, 115, 158, 229, 247, 257, 464)
N ₂ O ₄	Nitrogen tetroxide	-55.6*	-42.7*	-36.7*	-30.4*	-23.9*	-19.9*	-14.7*	-5.0	+8.0	21.0	-9.3	(19, 108, 158, 229, 275, 317, 332, 374, 380, 385)
N ₂ O ₅	Nitrogen pentoxide	-36.8*	-23.0*	-16.7*	-10.0*	-2.9*	+1.8*	7.4*	15.6*	24.4*	32.4	30	(229, 229, 376)
NOCl	Nitrosoyl chloride	*	*	*	-60.2	-54.2	-46.3	-34.0	-20.3	-6.4	-64.5	(58, 229, 451)	
NOF	Nitrosoyl fluoride	-132.0	-120.3	-114.3	-107.8	-100.3	-95.7	-88.8	-79.2	-68.2	-56.0	-134	(229)
NO ₂ F	Nitrosoyl fluorine	-143.7*	-132.1	-126.2	-119.8	-112.8	-108.4	-102.3	-93.5	-83.2	-72.0	-139	(229)
O ₂ O ₄	Osmium tetroxide (white)	-5.6*	+15.6*	26.0*	37.4*	50.5	59.4	71.5	89.5	109.3	130.0	42	(229, 245, 229, 372, 468)
O ₂ O ₄	Osmium tetroxide (yellow)	3.2*	22.0	31.3*	41.0*	51.7*	59.4	71.5	89.5	109.3	130.0	56	(229, 245, 229, 372, 468)
O ₂	Oxygen	-219.1*	-213.4	-210.6	-207.5	-204.1	-201.9	-198.8	-194.0	-188.8	-183.1	-218.7	(15, 28, 88, 70, 86, 100, 114, 177, 174, 229, 229, 292, 295, 450, 456, 467, 488)
O ₃	Ozone	-180.4	-168.6	-163.2	-157.2	-150.7	-146.7	-141.0	-132.6	-122.5	-111.1	-251	(210, 227, 229, 414)
P	Phosphorus (yellow)	76.6	111.2	128.0	146.2	166.7	179.8	197.3	222.7	251.0	280.0	44.1	(78, 156, 219, 229, 265, 311)
P	Phosphorous (violet)	237*	271*	287*	306*	323*	334*	349*	370*	391*	417*	590	(186, 229, 229, 405, 408)

(Continued on next page)

Table 1 (continued)

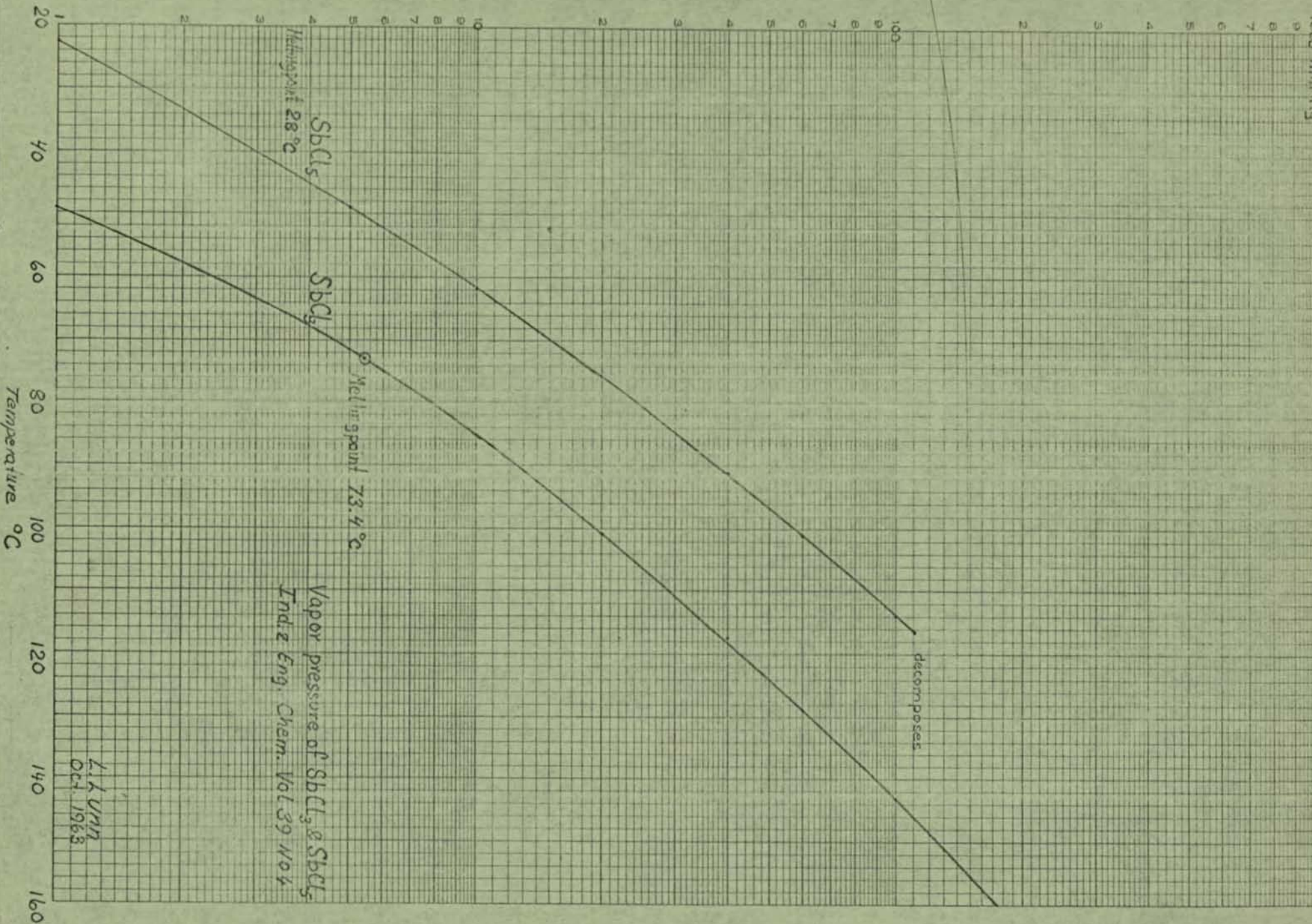
Table I (continued)

Formula	Name	Temperature, °C.												M.P.	Citation No.
		1 mm.	5 mm.	10 mm.	20 mm.	40 mm.	60 mm.	100 mm.	200 mm.	400 mm.	760 mm.				
Na	Sodium	439	511	549	589	633	662	701	758	823	892	97.5	(106, 154, 150, 160, 161, 163, 181, 889, 845, 857, 540, 543, 544, 557, 562, 567, 475)		
NaBr	Sodium bromide	806	903	952	1005	1063	1099	1148	1220	1304	1392	755	(829, 567, 475)		
NaCl	Sodium chloride	865	967	1017	1072	1131	1169	1220	1296	1379	1465	800	(128, 156, 168, 195, 829, 245, 264, 446, 478, 478)		
NaCN	Sodium cyanide	817	928	983	1046	1115	1156	1214	1307	1401	1497	564	(168, 229)		
NaF	Sodium fluoride	1077	1186	1240	1300	1363	1403	1455	1531	1617	1704	902	(829, 571, 475)		
NaOH	Sodium hydroxide	739	843	897	951	1017	1057	1111	1192	1286	1378	318	(829, 475)		
SnBr ₄	Stannic bromide	767	857	903	952	1005	1039	1083	1150	1225	1304	651	(156, 829, 567, 475)		
SnCl ₄	Stannic chloride	- 22.7	- 58.3	- 72.7	- 88.1	- 105.5	- 116.2	- 131.0	- 152.8	- 177.7	- 204.7	31.0	(9)		
SnI ₄	Stannic hydride	- 140.0	- 125.8	- 118.5	- 111.2	- 102.3	- 96.6	- 89.2	- 78.0	- 65.2	- 52.3	- 30.2	(829, 879, 481, 484, 494)		
SnCl ₃	Stannous chloride	-	156.0	175.8	196.2	218.8	234.2	254.2	283.5	315.5	348.0	144.5	(885)		
Br	Strontium	316	366	391	420	450	467	493	533	577	623	246.8	(829, 264)		
BrO	Strontium oxide	-	847	898	953	1018	1057	1111	1192	1285	1384	800	(167, 829, 565)		
S	Sulfur	2068.8	2198.8	2262.8	2333.8	2410.8	-	-	-	-	-	2430	(75, 229)		
SF ₆	Sulfur hexafluoride	-	-	-	-	-	-	-	-	-	-	112.8	(17, 54, 84, 86, 75, 157, 191, 829, 828, 878, 884, 583, 584, 585, 586, 458)		
SO ₂	Sulfur dioxide	- 132.7	- 120.6	- 114.7	- 108.4	- 101.5	- 96.8	- 90.9	- 82.3	- 72.6	- 63.5	- 50.2	(229, 258)		
SeCl ₄	Sulfur monochloride	- 95.5	- 83.0	- 76.8	- 69.7	- 60.5	- 54.6	- 46.9	- 35.4	- 23.0	- 10.0	- 73.2	(85, 53, 51, 65, 68, 140, 148, 176, 829, 801, 880, 554, 385, 415, 480)		
SO ₂ Cl ₂	Sulfuryl chloride	- 7.4	+ 15.7	27.5	40.0	54.1	63.2	75.3	93.5	115.4	138.0	- 80	(168, 229, 453)		
SO ₃	Sulfur trioxide (α)	- 35.1	- 24.8	- 13.4	- 1.0	+ 7.2	17.8	33.7	51.3	69.2	- 54.1	(829, 448, 449)			
SO ₃	Sulfur trioxide (β)	- 39.0	- 23.7	- 16.5	- 9.1	- 1.0	+ 4.0	10.5	20.5	32.6	44.8	15.8	(27, 161, 229, 411, 412)		
SO ₃	Sulfur trioxide (γ)	- 34.0	- 19.2	- 12.3	- 4.9	+ 3.2	8.0	14.3	23.7	32.6	44.8	32.3	(27, 161, 229, 411, 412)		
H ₂ SO ₄	Sulfuric acid	- 15.3	- 2.0	+ 4.3	11.1	17.9	21.4	28.0	35.8	44.0	51.6	62.1	(27, 161, 229, 411, 412)		
SOBr ₂	Thionyl bromide	145.8	178.0	194.2	211.5	229.7	241.5	257.0	279.8	305.0	330.0	10.5	(9)		
SOCl ₂	Thionyl chloride	- 52.9	- 32.4	- 21.9	- 10.5	+ 2.2	10.4	21.4	37.9	56.5	75.4	- 52.2	(829, 269)		
TaF ₅	Tantalum pentafluoride	-	-	-	-	-	-	-	-	-	-	111.5	(11, 15, 829)		
Te	Tellurium	520	605	650	697	753	789	838	910	997	1087	452	(101, 229)		
TeCl ₄	Tellurium tetrachloride	-	-	233	253	273	287	304	330	360	392	224	(829, 329)		
TeF ₆	Tellurium hexafluoride	- 111.3	- 98.8	- 92.4	- 86.0	- 78.4	- 73.8	- 67.9	- 57.3	- 48.2	- 38.6	- 37.8	(829, 358, 491)		
Tl	Thallium	825	931	983	1040	1103	1143	1196	1274	1364	1457	303.5	(145, 829, 355, 489)		
TlBr	Thallium bromide	-	490	822	559	598	621	653	703	759	819	460	(829, 465, 474)		
TlCl	Thallium chloride	-	487	617	550	589	612	645	694	748	807	430	(829, 465, 474)		
TlI	Thallium iodide	440	502	531	567	607	631	663	712	763	823	440	(829, 465, 474)		
Tl ₂	Tia	1492	1634	1703	1777	1855	1903	1968	2063	2169	2270	231.9	(155, 154, 155, 165, 829, 348, 488, 471)		
TiCl ₄	Titanium tetrachloride	- 13.9	+ 9.4	21.3	34.2	48.4	58.0	71.0	90.5	112.7	138.0	- 30	(11, 229)		
W	Tungsten	3900	4337	4507	4890	4885	5007	5168	5403	5636	5927	3370	(818, 829, 880, 498, 499)		
WF ₆	Tungsten hexafluoride	- 71.4	- 56.5	- 49.2	- 41.5	- 33.0	- 27.5	- 20.3	- 10.0	+ 1.2	17.3	- 0.5	(829, 347)		
UF ₆	Uranium hexafluoride	- 38.8	- 22.0	- 13.8	- 5.2	+ 4.4	10.4	18.2	30.0	42.7	55.7	69.2	(829, 336)		
VOCla	Vanadyl trichloride	- 23.2	+ 0.2	12.2	26.6	40.0	49.8	62.5	82.0	103.5	127.2	-	(128)		
H ₂ O	Water	- 17.3	+ 1.2	11.3	22.2	34.1	41.6	51.6	65.5	83.0	100.0	0.0	(81, 98, 104, 181, 189, 190, 817, 828, 829, 838, 303, 304, 378, 379, 404, 476, 481)		
Xe	Xenon	- 168.5	- 158.2	- 152.8	- 147.1	- 141.2	- 137.7	- 132.8	- 125.4	- 117.1	- 108.0	- 111.6	(5, 180, 829, 511, 518, 329)		
Zn	Zinc	487	558	593	632	673	700	736	788	844	907	419.4	(17, 48, 61, 109, 154, 155, 181, 810, 829, 835, 542, 543)		
ZnCl ₂	Zinc chloride	428	481	508	536	566	584	610	648	689	732	365	(828, 829, 864)		
ZnF ₂	Zinc fluoride	1243	1328	1359	1402	1448	1480	1527	1602	1690	1770	872	(365)		
ZrBr ₄	Zirconium tetrabromide	207	237	250	266	281	289	301	318	337	357	450	(829, 326)		
ZrCl ₄	Zirconium tetrachloride	190	217	230	243	259	265	279	295	312	331	437	(829, 326)		
ZrI ₄	Zirconium tetraiodide	264	297	311	329	344	355	369	389	409	431	499	(829, 326)		

Table II. Pressures Greater than One Atmosphere

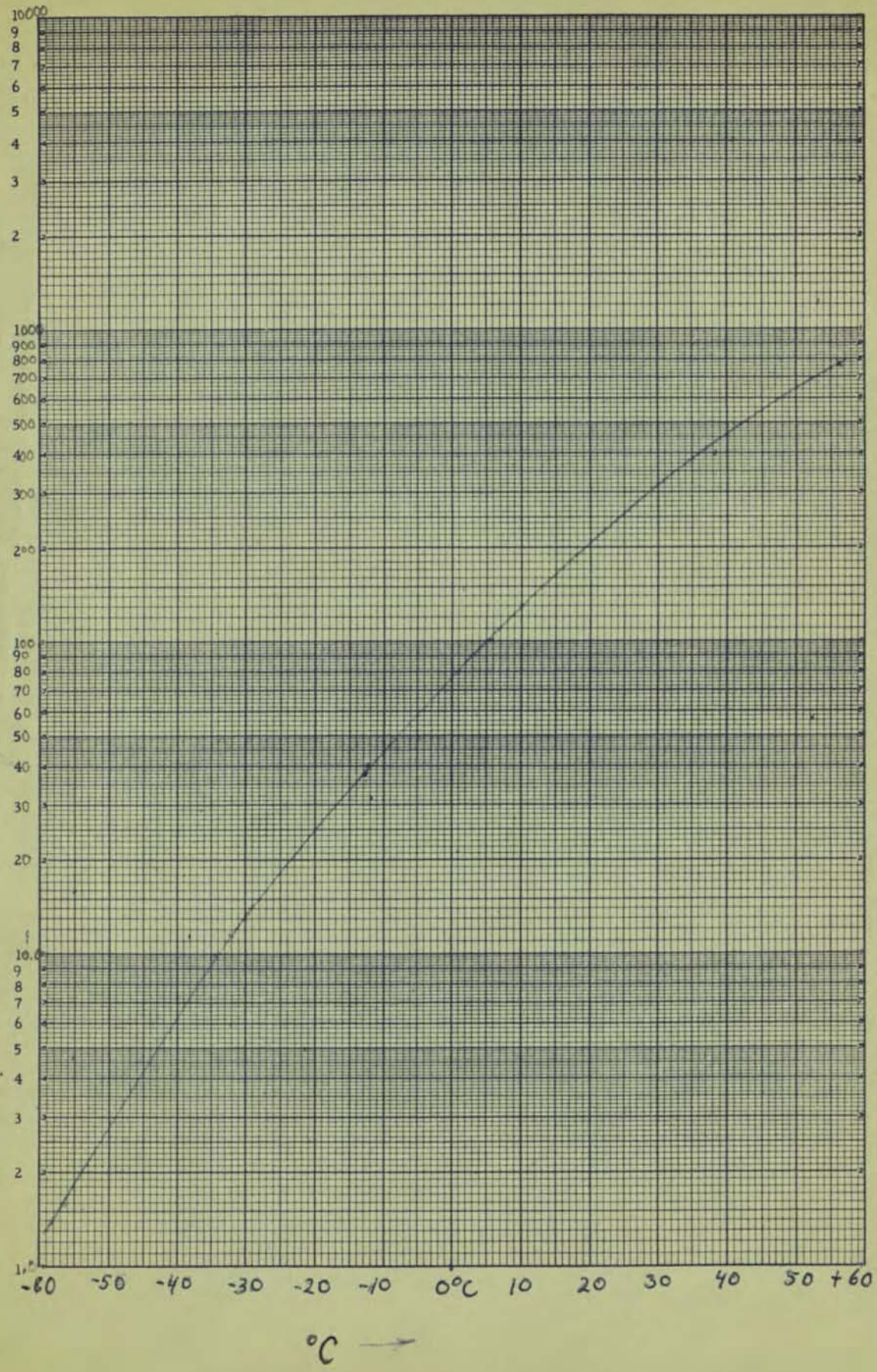
Formula	Name	Temperature, °C.										<i>T_e</i>	<i>P_e</i>	Citation No.
		1 atm.	2 atm.	5 atm.	10 atm.	20 atm.	30 atm.	40 atm.	50 atm.	60 atm.				
NH ₃	Ammonia	-33.6	-18.7	+4.7	25.7	50.1	66.1	78.9	89.3	98.3	132.4	111.5	(25, 26, 53, 49, 68, 88, 142, 176, 192, 225, 251, 279, 306, 334, 420)	
A	Argon	-185.6	-179.0	-166.7	-154.9	-141.3	-132.0	-124.9			-122.0	48.0	(41, 83, 155, 229, 256, 289, 406)	
BCl ₃	Boron trichloride	12.7	33.2	66.0	96.7	135.4	161.5				178.8	38.2	(229, 308, 334, 450)	
BF ₃	Boron trifluoride	-100.7	-89.4	-72.6	-57.7	-40.0	-28.4	-19.0			-12.2	49.2	(39, 102, 171, 205, 217, 229, 251, 251, 345, 351, 455, 457)	
Br ₂	Bromine	58.2	78.8	110.3	139.8	174.0	197.0	216.0	230.0	243.5	302.2	121		
CCl ₄	Carbon tetrachloride	76.7	102.0	141.7	178.0	222.0	251.2	276.0			283.1	45.0	(104, 179, 229, 334, 355, 415, 425)	
CO ₂	Carbon dioxide	-78.2	-69.1	-56.7	-39.5	-18.9	-5.3	+5.9	14.9	22.4	31.1	73.0	(5, 46, 117, 172, 175, 211, 229, 222, 228, 308, 334, 420, 464, 467, 477, 497)	
CS ₂	Carbon disulfide	46.5	69.1	104.8	136.3	175.5	201.5	222.8	240.0	256.0	273.0	72.9	(176, 229, 265, 333, 334, 420, 467, 490)	
CO	Carbon monoxide	-191.3	-183.5	-170.7	-161.0	-149.7	-141.9				-138.7	34.6	(16, 67, 77, 78, 87, 229, 293, 463)	
COCl ₂	Carbonyl chloride	+8.3	27.3	57.2	85.0	119.0	141.8	159.8	174.0		181.7	56.0	(14, 135, 229, 288, 309)	
CCl ₃ F	Chlorotrifluoromethane	-81.2	-66.7	-42.7	-18.5	+12.0	34.8	52.8			53	40.3	(102, 447)	
C ₂ N ₂	Cyanogen	-21.0	-4.4	+21.4	44.6	72.6	91.6	105.5	118.2		126.6	58.2	(74, 88, 102, 118, 313, 444)	
CCl ₂ F ₂	Dichlorodifluoromethane	-29.8	-12.2	+16.1	42.4	74.0	95.6				111.5	39.6	(102, 144)	
CHCl ₂ F	Dichlorofluoromethane	8.9	28.4	59.0	87.0	121.2	144.0	162.6	177.5		178.5	51.0	(335)	
CHClF ₂	Chlorodifluoromethane	-40.8	-24.7	+0.3	24.0	52.0	70.3	85.3			96.0	48.7	(40, 255)	
CCl ₃ F	Trichlorofluoromethane	23.7	44.1	77.3	108.2	146.7	172.0	194.0			198.0	43.2	(233)	
Cl ₂	Chlorine	-33.8	-16.9	+10.3	35.6	65.0	84.8	101.6	115.2	127.1	144.0	76.1	(139, 166, 171, 214, 229, 230, 512, 458)	
He	Helium	-268.6	-268.0								-267.9	2.26	(227, 228, 229, 500, 501)	
H ₂	Hydrogen	-252.5	-250.2	-246.0	-241.8						-240.0	12.80	(58, 71, 173, 225, 229, 292, 459, 596, 454, 455)	
HBr	Hydrogen bromide	-66.5	-51.5	-29.1	-8.4	+16.8	33.9	48.1	60.0	70.6	90.0	84.4	(18, 105, 169, 229, 415, 416)	
HCl	Hydrogen chloride	-84.8	-71.4	-50.5	-31.7	-8.8	+5.9	17.8	27.9	36.2	51.4	81.6	(50, 69, 105, 118, 141, 169, 175, 229, 229, 415, 420)	
HCN	Hydrogen cyanide	25.9	45.8	75.8	102.7	135.0	153.8	169.9	183.5		183.5	50.0	(44, 154, 229, 258, 314, 397, 401)	
HI	Hydrogen iodide	-35.1	-18.9	+7.3	32.0	62.2	83.2	100.7	116.2	127.5	151.0	82.0	(103, 169, 229, 415, 416)	
H ₂ S	Hydrogen sulfide	-60.4	-45.9	-22.3	-0.4	+25.5	41.9	55.8	66.7	76.3	100.3	88.9	(118, 157, 229, 258, 258, 292, 312, 415, 416)	
H ₂ Se	Hydrogen selenide	-41.1	-25.2	0.0	+23.4	50.8	69.7	84.6	97.2	108.7	137	91.0	(57, 201, 229, 229, 417)	
Kr	Krypton	-152.0	-143.5	-130.0	-118.0	-101.7	-88.8	-78.4	-66.5		-63	54	(5, 221, 229, 315, 317, 320)	
Ne	Neon	-246.0	-243.8	-239.9	-236.0	-230.8					-228.3	26.9	(71, 229, 297, 455)	
N ₂	Nitrogen	-195.8	-189.2	-179.1	-169.8	-157.6	-148.3				-147.2	33.5	(15, 70, 86, 100, 125, 158, 175, 174, 193, 229, 229, 321, 403, 407, 480)	
NO	Nitric oxide	-151.7	-145.1	-135.7	-127.3	-118.8	-109.0	-103.2	99.0	94.8	-92.9	64.6	(1, 125, 170, 216, 229, 229, 292, 294)	
N ₂ O	Nitrous oxide	-88.5	-76.8	-58.0	-40.7	-18.8	4.3	+8.0	18.0	27.4	36.5	71.7	(29, 52, 53, 62, 115, 188, 229, 247, 327, 414)	
N ₂ O ₄	Nitrogen tetroxide	21.0	37.3	59.8	79.4	100.3	112.3	121	127.0	132.2	158	99	(19, 105, 138, 229, 229, 317, 332, 374, 380, 481)	
O ₂	Oxygen	-183.1	-176.0	-164.5	-153.2	-140.0	-130.7	-124			-118.9	49.7	(15, 25, 26, 27, 46, 110, 114, 172, 174, 229, 229, 242, 295, 420, 456, 467, 481)	
SiF ₄	Silicon tetrafluoride	-94.8	-84.4	-67.9	-52.6	-33.4	-21.2				-14.2	36.7	(40, 179, 410, 547)	
SiClF ₃	Chlorotrifluorosilane	-70.0	-57.3	-37.7	-18.6	+4.1	19.4				34.8	34.2	(40, 229, 302)	
SiCl ₂ F ₃	Dichlorodifluorosilane	-31.8	-15.1	+11.6	36.6	66.2	86.0				95.8	34.5	(40, 229, 302)	
SiCl ₃ F	Fluorotrichlorosilane	12.2	32.4	64.6	94.2	131.8	156.0				165.3	35.3	(40, 229, 302)	
RnCl ₂	Stannic chloride	113.0	141.3	184.3	223.0	270.0	299.8				318.7	37.9	(29, 479, 481, 494, 496)	
SO ₂	Sulfur dioxide	-10.0	+6.3	32.1	55.5	83.8	102.6	118	130.2	141.7	157.2	77.7	(5, 55, 51, 65, 68, 140, 142, 175, 176, 201, 280, 334, 335, 415, 480)	
SO ₃	Sulfur trioxide	44.8	60.0	82.5	104.0	138.0	157.8	175.0	187.8	198.0	218.3	83.6	(27, 151, 229, 229, 418)	
H ₂ O	Water	100.0	120.1	152.4	180.5	213.1	234.6	251.1	264.7	276.5	274.2	218.0	(81, 95, 102, 121, 189, 190, 217, 222, 229, 232, 305, 304, 324, 484)	

1000 mm. Hg



mm Hg

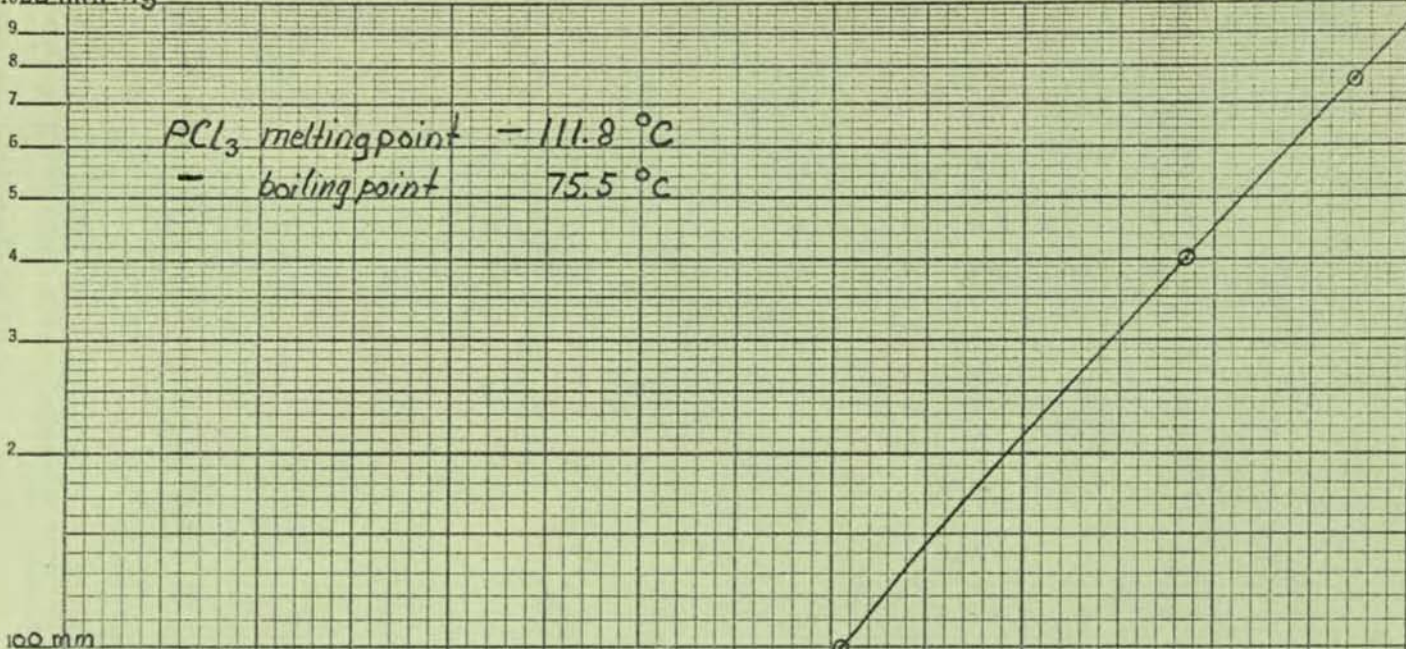
Log Pressure, mm Hg, 5, Cl 4



Larsel Lund

100 mm Hg

PCl_3 melting point -111.8°C
boiling point 75.5°C



100 mm

1

VAPOR PRESSURE X TEMPERATURE

Log P. (2 Cycle) $\times \gamma(t^{\circ}\text{C.} + 230)$
FOR STRAIGHT-LINE PLOTTING

10^{-5} mm

0.001 (μ)

0.1

10

Lab

TRICRESYL PHOSPHATE

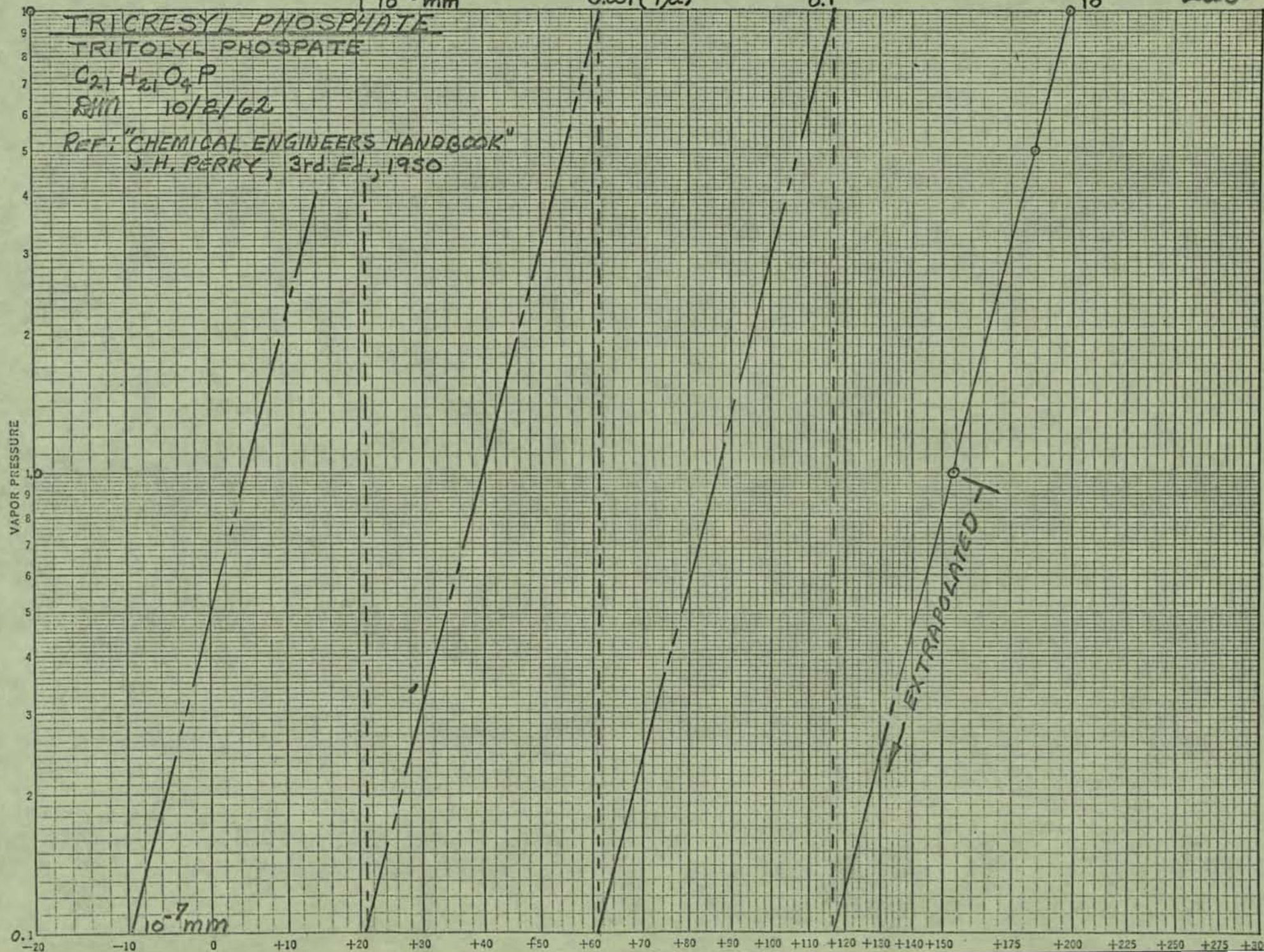
TRITOLYL PHOSPHATE

$C_{21}H_{21}O_4P$

8JIN 10/2/62

REF: "CHEMICAL ENGINEERS HANDBOOK"
J.H. PERRY, 3rd ED., 1950

VAPOR PRESSURE

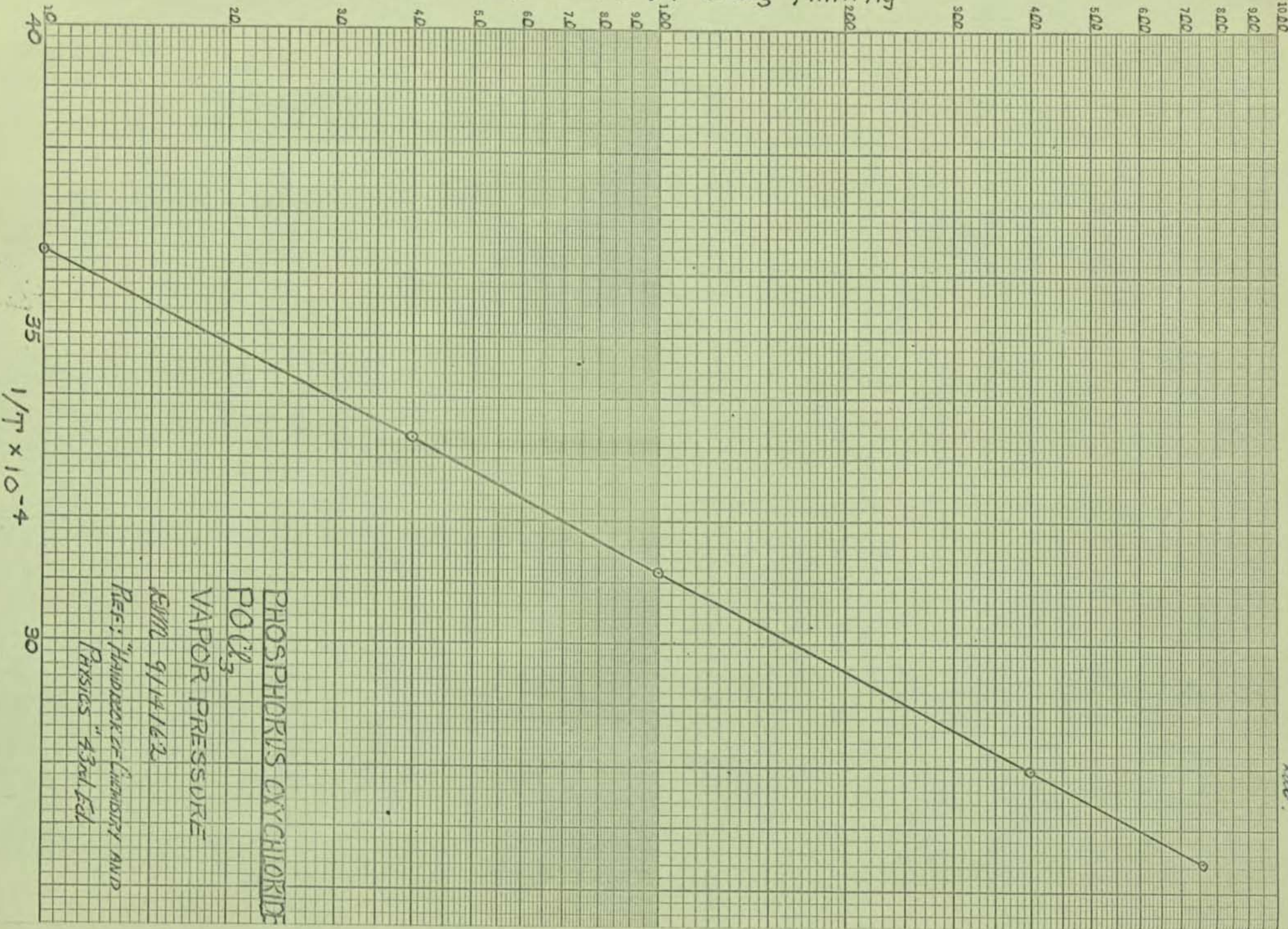


10^{-7} mm

TEMPERATURES IN DEGREES CELSIUS

Ko SEMI-LOGARITHMIC 358-61L
KEUFFEL & ESSER CO. MADE IN U.S.A.
2 CYCLES X 100 DIVISIONS

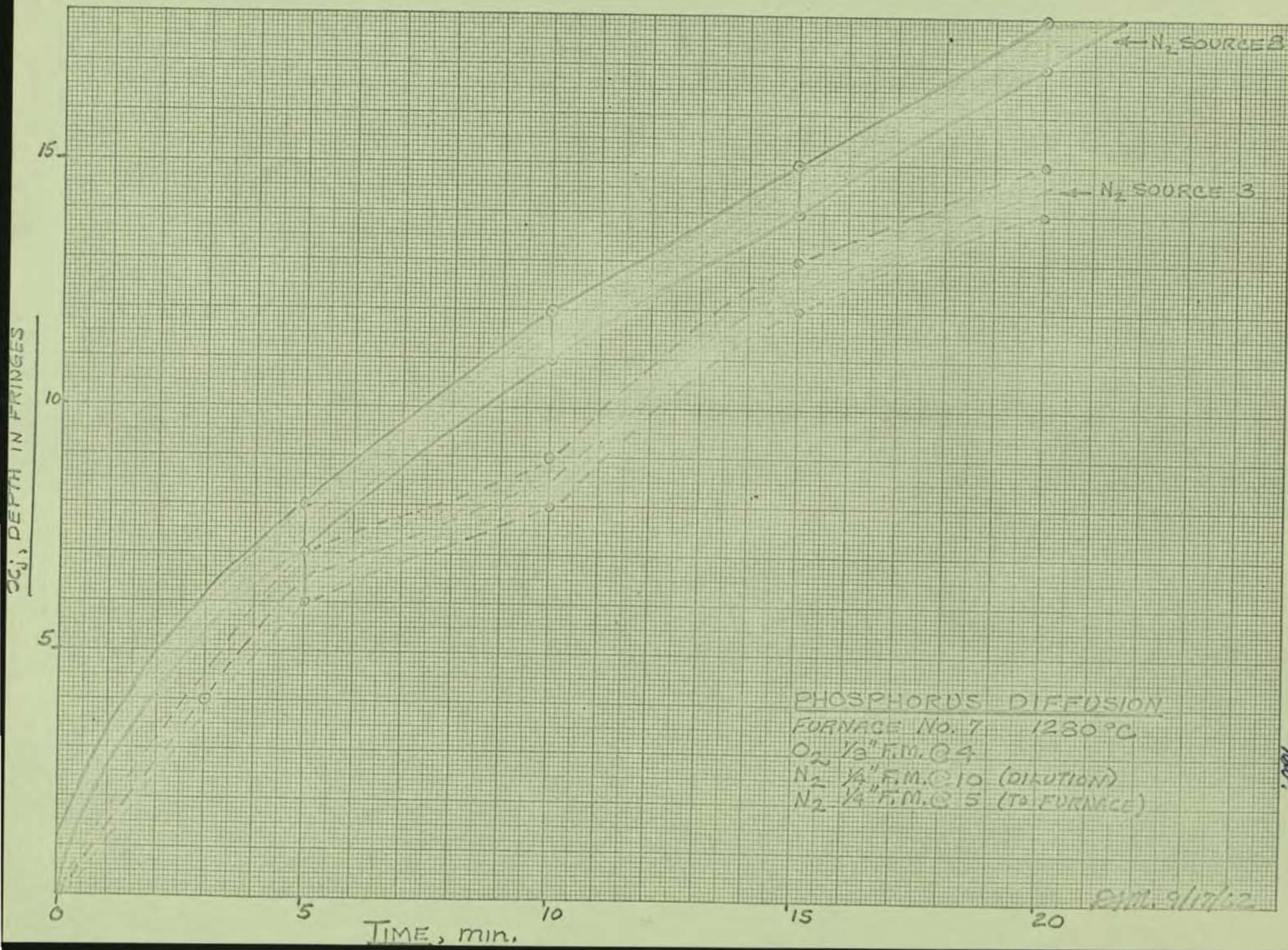
VAPOR PRESSURE: POCl_3 , mm Hg





10 X 10 TO THE CM.
KEUFFEL & ESSER CO.
MADE IN U.S.A.

359-14G

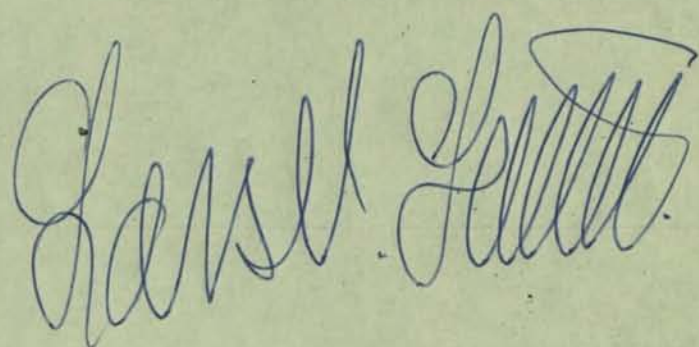


FLOW METERS

CALIBRATION CHART

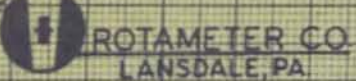
cc/min AIR METERED AT 14.7 psia & 70 F

1/2"			1/4"			1/8"			1/16"					
ALL TUBES			ALL TUBES			ALL TUBES			-20-, -16-, -12-			-10-, -08-		
SC READING	STN STL (17360)	GLASS (9340)	TANTALUM (8940)	STN STL (6160)	GLASS (3292)	TANTALUM (3165)	STN STL (2180)	SAPPHIRE (1550)	TANTALUM (1117)	STN STL (772)	SAPPHIRE (549)	TANTALUM (1117)	STN STL (772)	SAPPHIRE (549)
25	143500	73600	35200	23400	11750	5580	3660	2480						
20	112700	57900	27600	18400	9100	4325	2860	1910	681	426	271			
18	99600	51200	24450	16250	8050	3820	2510	1670	596	370	234			
16	87000	44500	21160	14100	6950	3270	2120	1420	510	315	196			
14	75000	38200	18200	12000	5900	2785	1790	1190	420	260	159			
12	62500	31700	15100	10000	4850	2292	1470	960	332	206	122			
10	50900	25700	12250	8050	3850	1835	1156	741	258	154	88	240	136	75
8	39100	19750	9360	6050	2860	1341	840	525	189.5	104	57	159	83.3	43.5
7	33600	16780	7990	5100	2370	1133	687	425	149	80	43	118.5	60	31
6	28300	14000	6660	4175	1900	900	538	325	116.1	57	31	82.5	41	20.7
5	23380	11050	5270	3320	1440	682	397	233	81.2	39	21	52	25.3	13
4	17670	8200	3880	2460	1010	472.5	263	147.5	50.75	25	13.5	29.8	13.5	7
3	12950	5700	2697	1650	600	279.7	145	75	30.1	14	7.5	7.64	5.3	2.75
2	8190	3405	1598	880	270	125.5	60	30	15.6	7	3.5		0.4	0.3



150

BROOKS



ROTAMETER CO.
LANSDALE, PA.

CALIBRATION CURVE

TUBE A-2-15-A

FLOAT SAPPHIRE

SERIAL NO.

MILLIMETERS

100

50

250

500

750

1000

1250

CC/MIN AIR AT 70°F & 14.7 PSIA

Alloy Furnace process 216.

Laser Data

150



BROOKS
INSTRUMENT COMPANY, INC.
HATFIELD, PENNSYLVANIA

CALIBRATION CURVE

TUBE A-2-15-B

FLOAT SAPPHIRE

SERIAL NO.

100

50

0

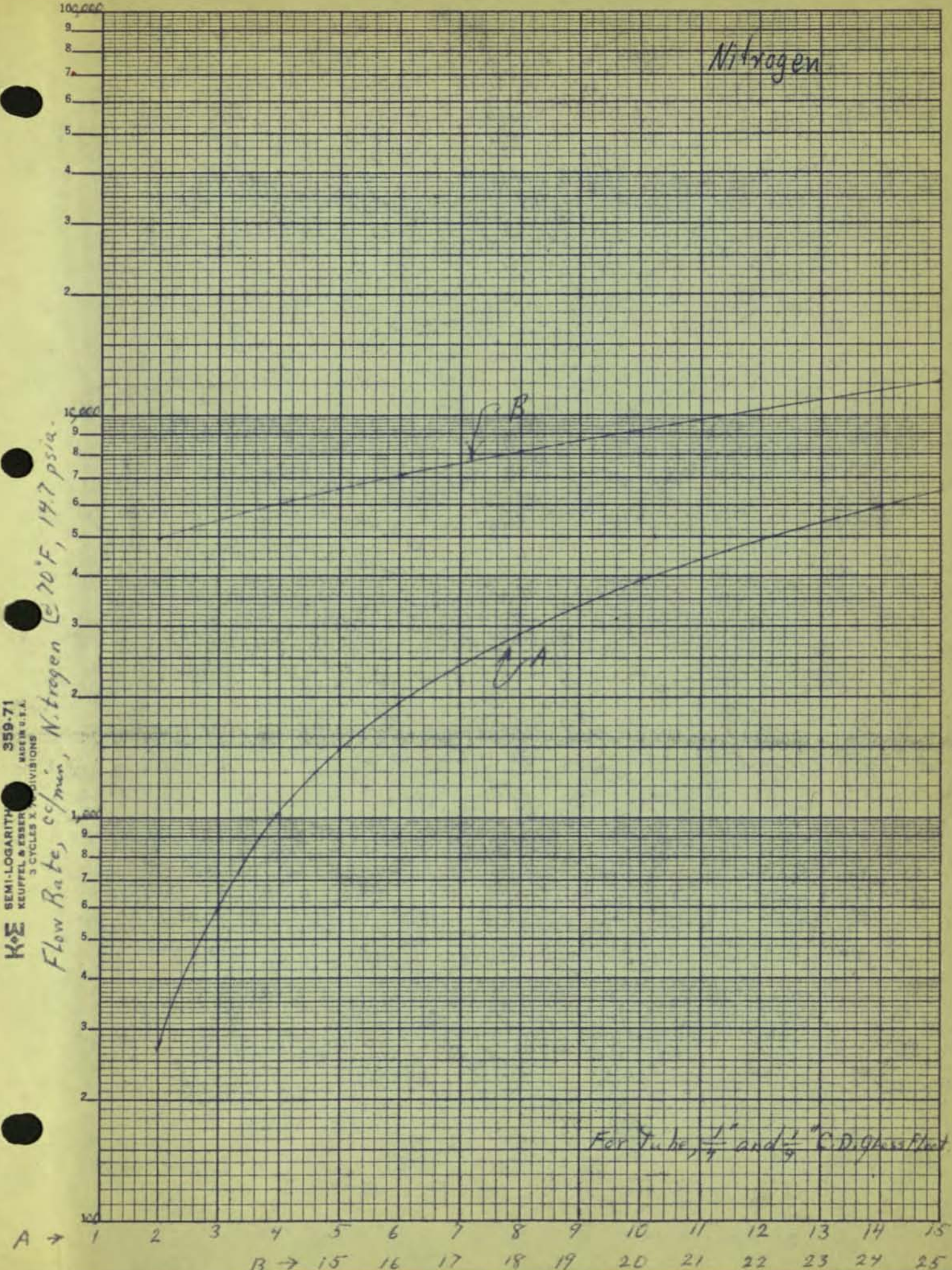
1000

2000

3000

CC/MIN AIR AT 70°F 1.7 PSIA

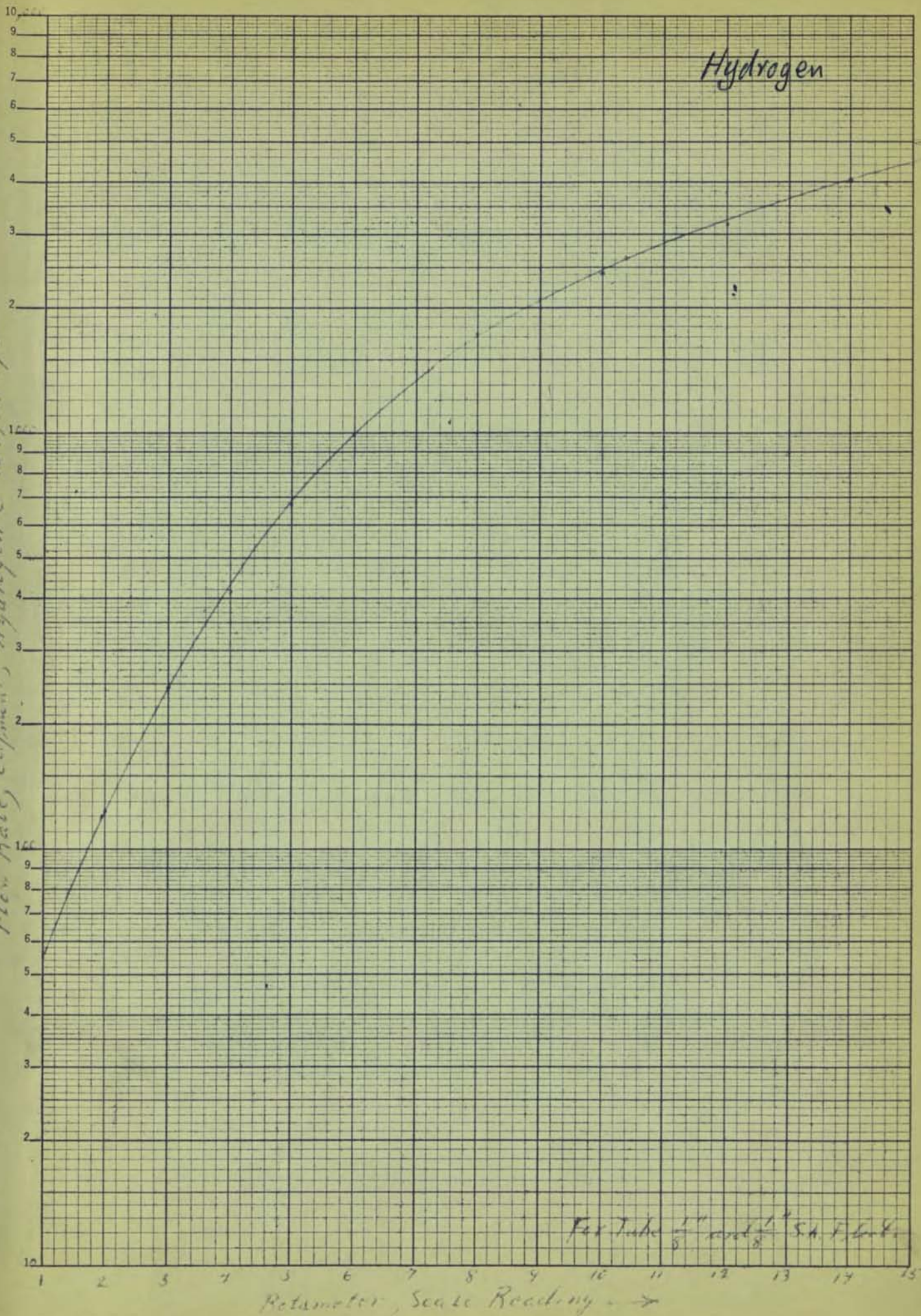
5-1860



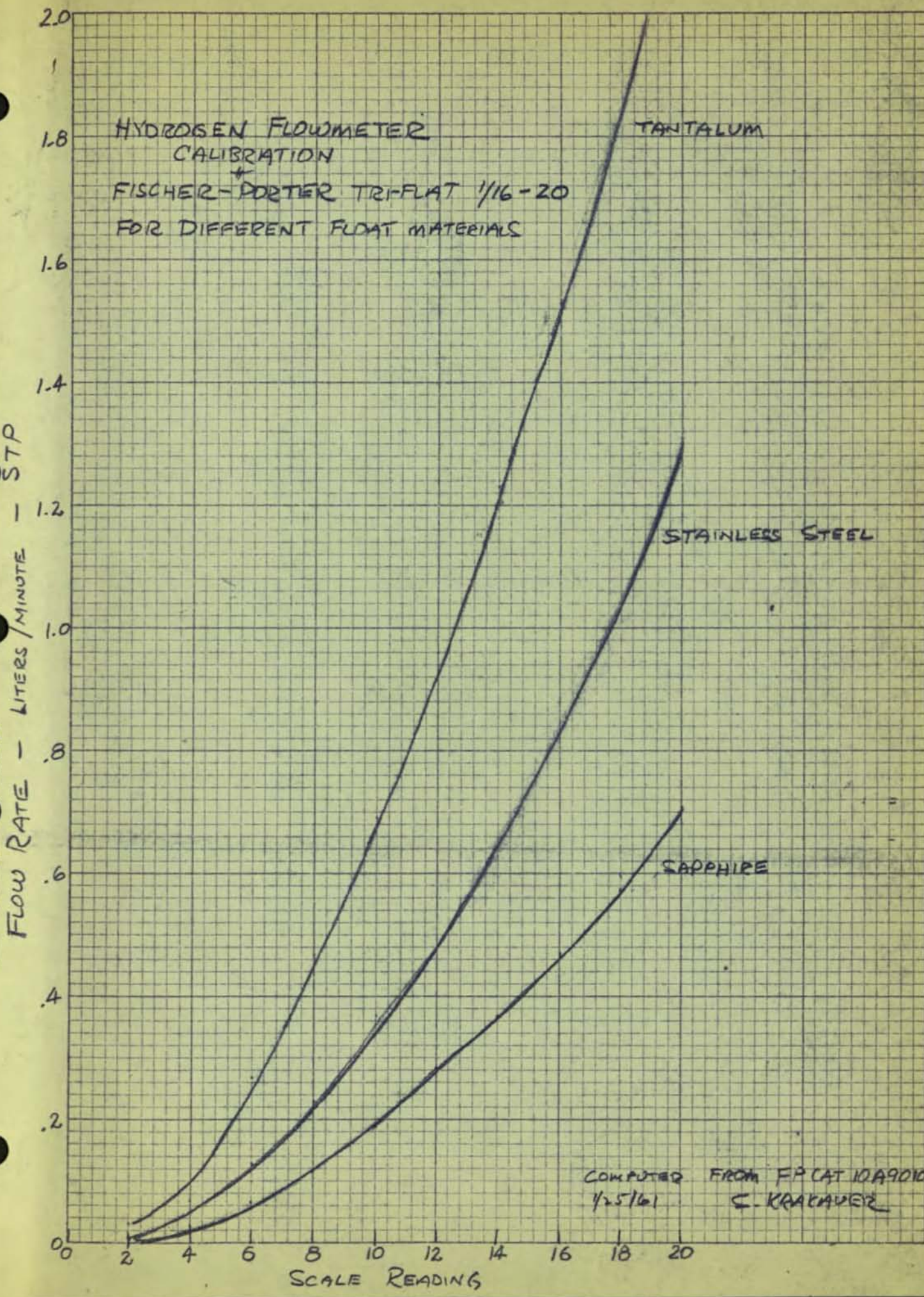
KoΣ SEMI-LOGARITHMIC

35971 KEUFFEL & ESKEFF, MADE IN U.S.A.
3 CYCLES X 10 DIVISIONS

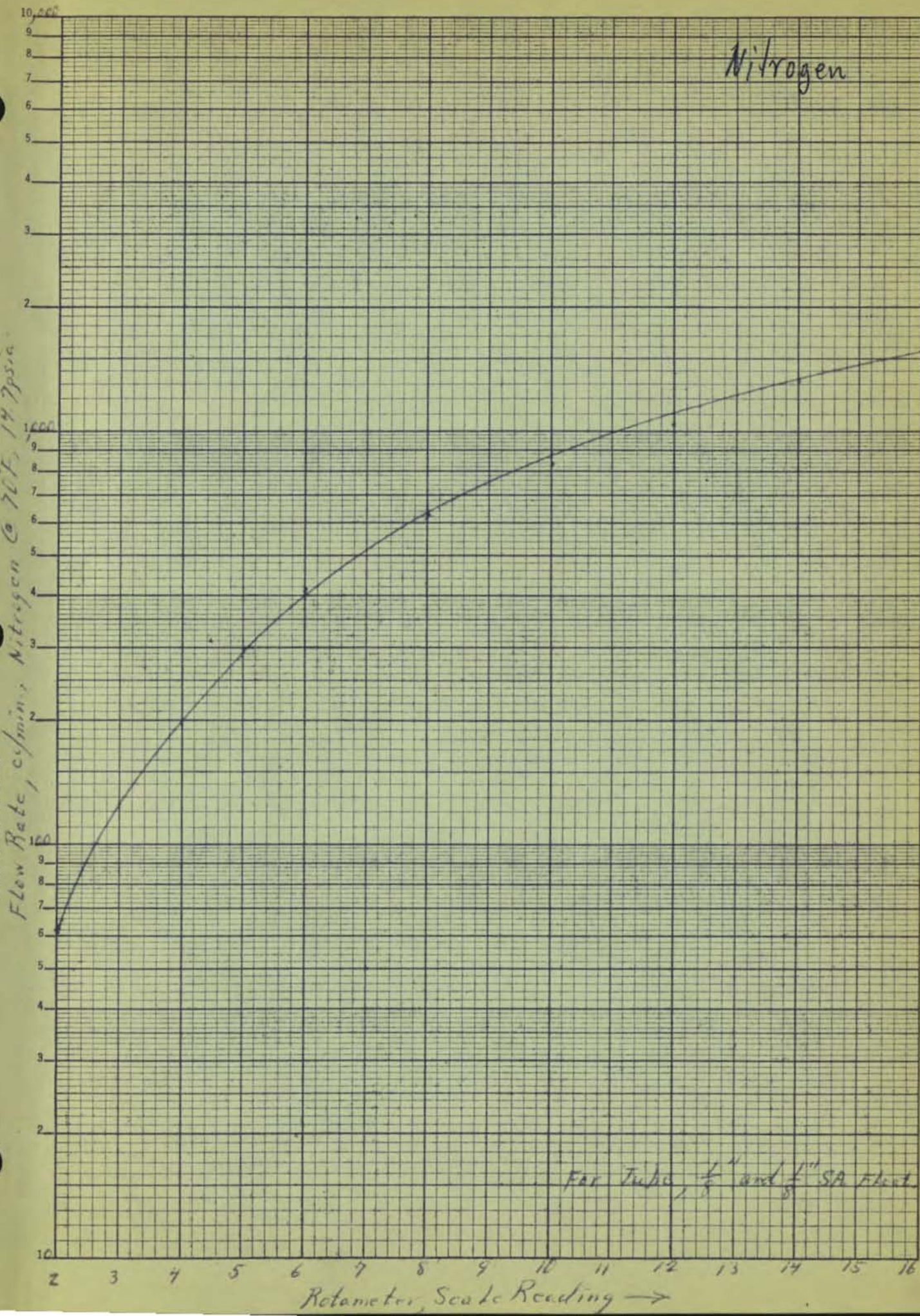
Flow Rate, Cc./sec., Hydrogen (C H₂) 14.7 psia



K&E 10 X 10 TO THE 359-5
KEUFFEL & SULLIVAN NEW YORK



KoE SEMI-LOGARITHMIC
KELPFEL & EBNER
MADE IN U.S.A.
3 CYCLES X 70 DIVISIONS

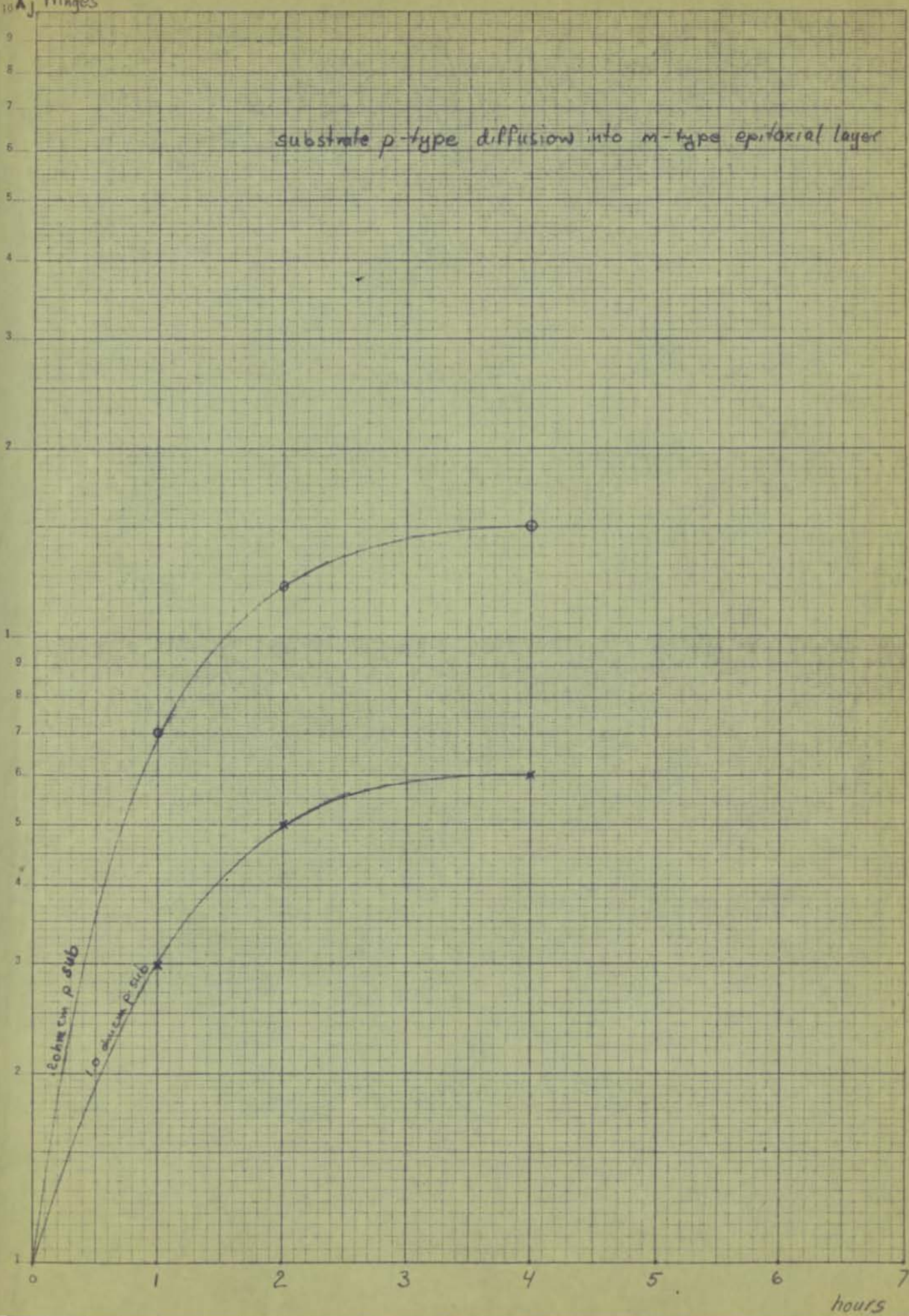


EPILOGY

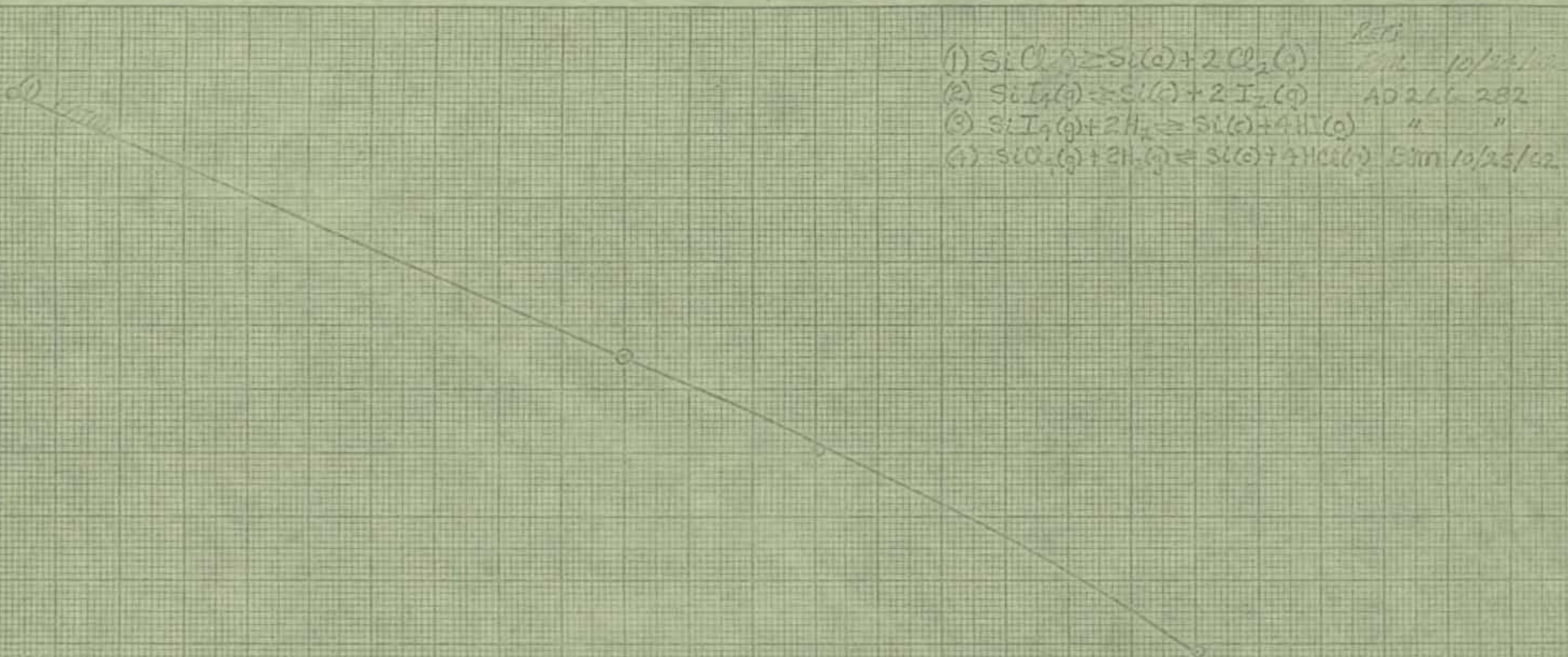
10^3 fringes

substrate p-type diffusion into n-type epitaxial layer

KOER
SEMILOGARITHMIC
REUTHER & LASSER CO.
2 CYCLES X 70 DIVISIONS
ALUMINUM 5



+150



- Ref:
- (1) $SiO_2(s) \geq Si(l) + 2 O_2(g)$ Date 10/25/42
 - (2) $SiI_4(l) \geq Si(l) + 2 I_2(g)$ AD 266-282
 - (3) $SiI_4(g) + 2 H_2 \geq Si(l) + 4 HI(g)$ " "
 - (4) $SiO_2(g) + 2 H_2(g) \leq Si(l) + 2 H_2O(g)$ E'm 10/25/42

+100

+50

ΔF
KCAL
MOLE

-30

0

500

1000

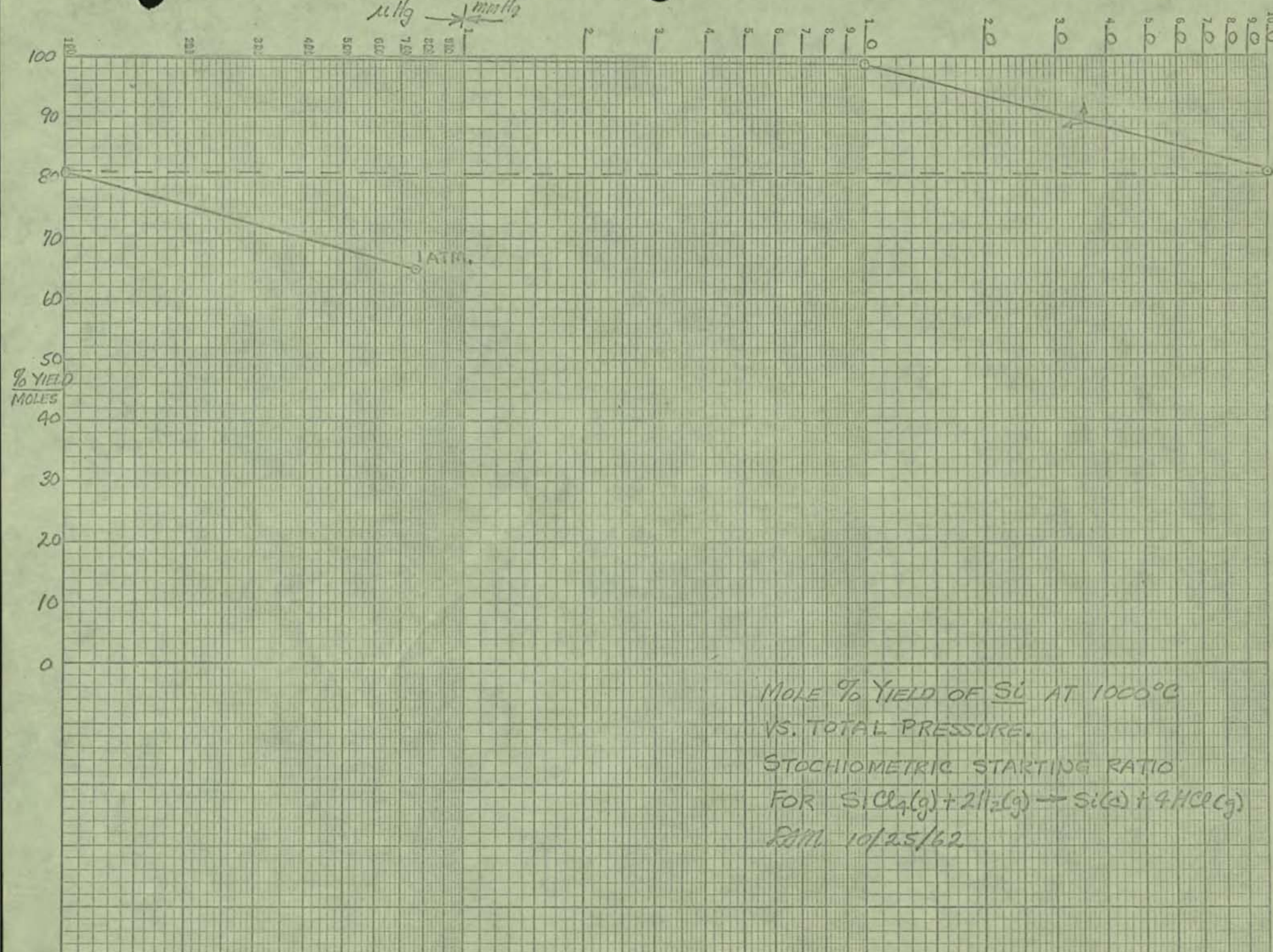
2000

2500

T °C

KoE SEMI-LOGARITHMIC 358-71L
KEUFFEL & ESSER CO., MADE IN U.S.A.
3 CYCLES X 150 DIVISIONS

1000
mmHg → mmHg



MOLE % YIELD OF Si AT 1000°C
VS. TOTAL PRESSURE.

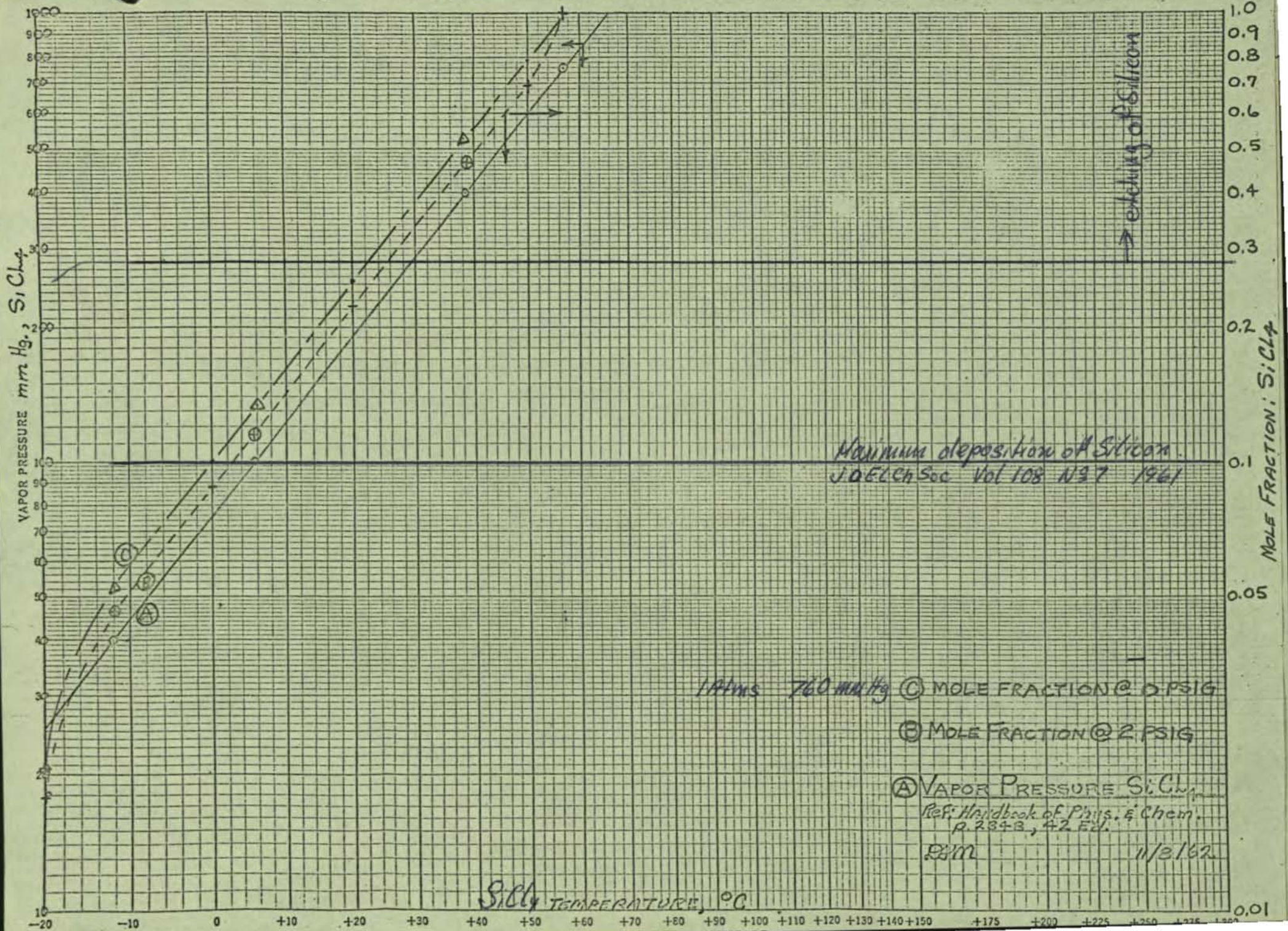
STOCHIOMETRIC STARTING RATIO

FOR $\text{SiCl}_4(\text{g}) + 2\text{H}_2(\text{g}) \rightarrow \text{Si}(\text{s}) + 4\text{HCl}(\text{g})$

DATE 10/25/62

N.Y. 16021
Serial Job 41763

VAPOR PRESSURE X TEMPERATURE
 $\log P$. (2 Cyc.) $\times Y(t^{\circ}\text{C.} + 20^{\circ})$
 FOR STRAIGHT-LINE PLOTTING



ALLOYING

Junction Capacity vs. Voltage
for Various Resistivities
of n-type Si alloyed devices

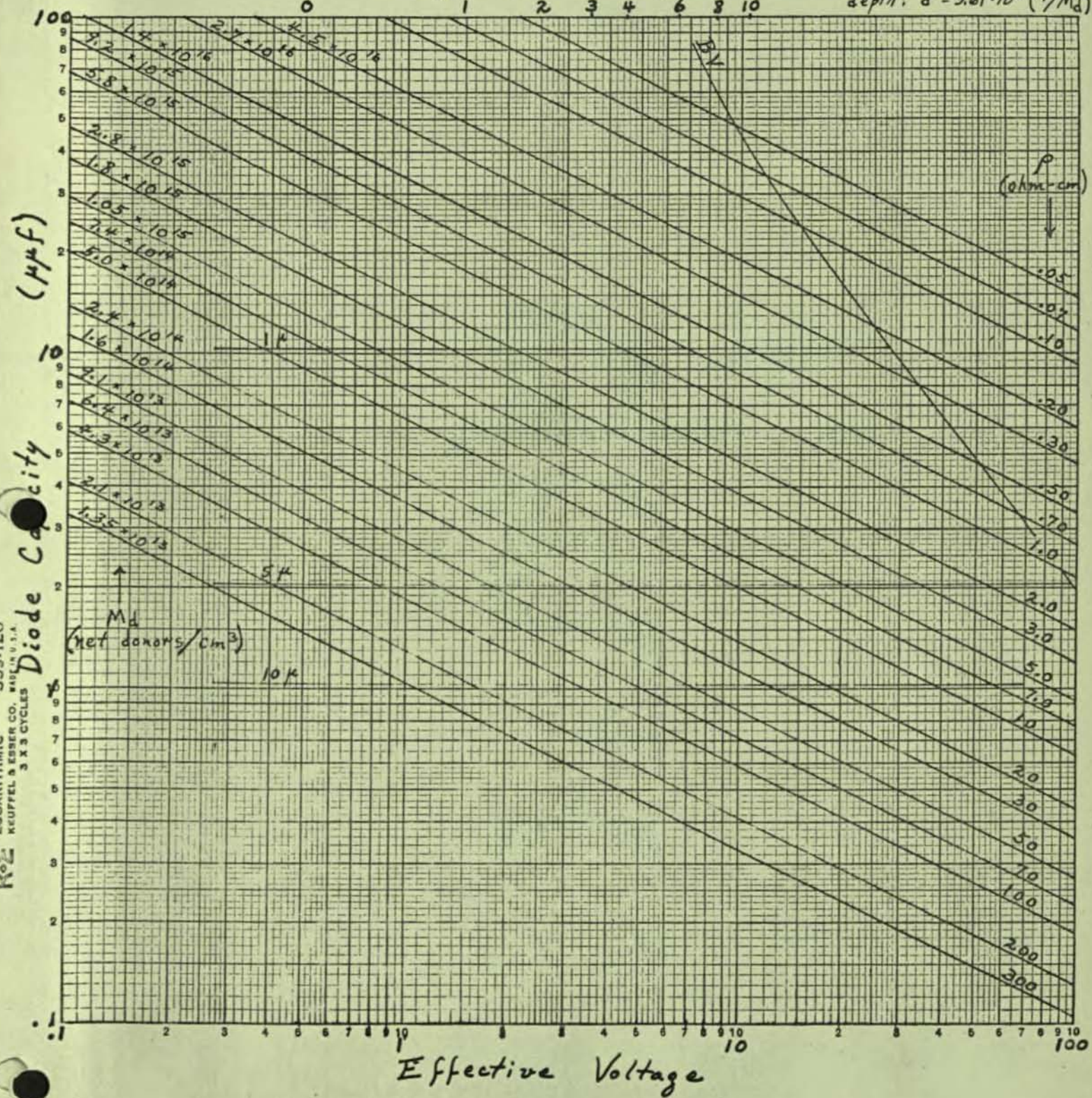
$$C^2 = 7.995 \times 10^{-14} M_d / N$$

for diode area = .0995 mm²

Md vs. P graph 1-9-61 WRL used
horiz. lines show depletion
depth: $d = 3.61 \times 10^7 (V/M_d)^{1/2}$

~ Applied Voltage

0 1 2 3 4 6 8 10

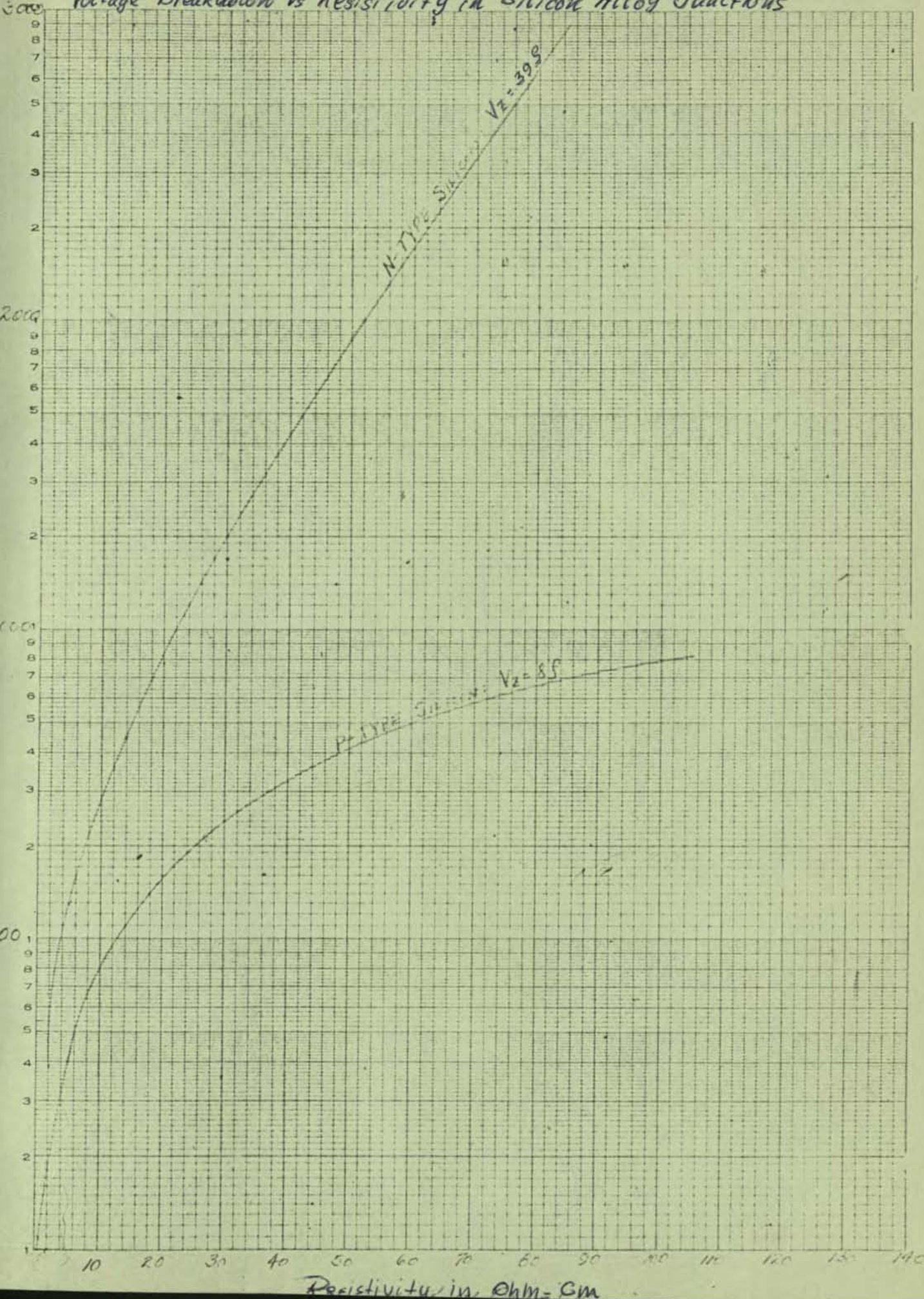


1-10-61
G.H.

Voltage Breakdown Vs Resistivity in Silicon Alloy Junctions

NO. 340-LTC DITZGEN GRAPH NAME 4
EUDENE DITZGEN CO.
4 DIVIDES X 10 DIVISIONS PER INCH
4 CYCLES X 10 DIVISIONS PER INCH

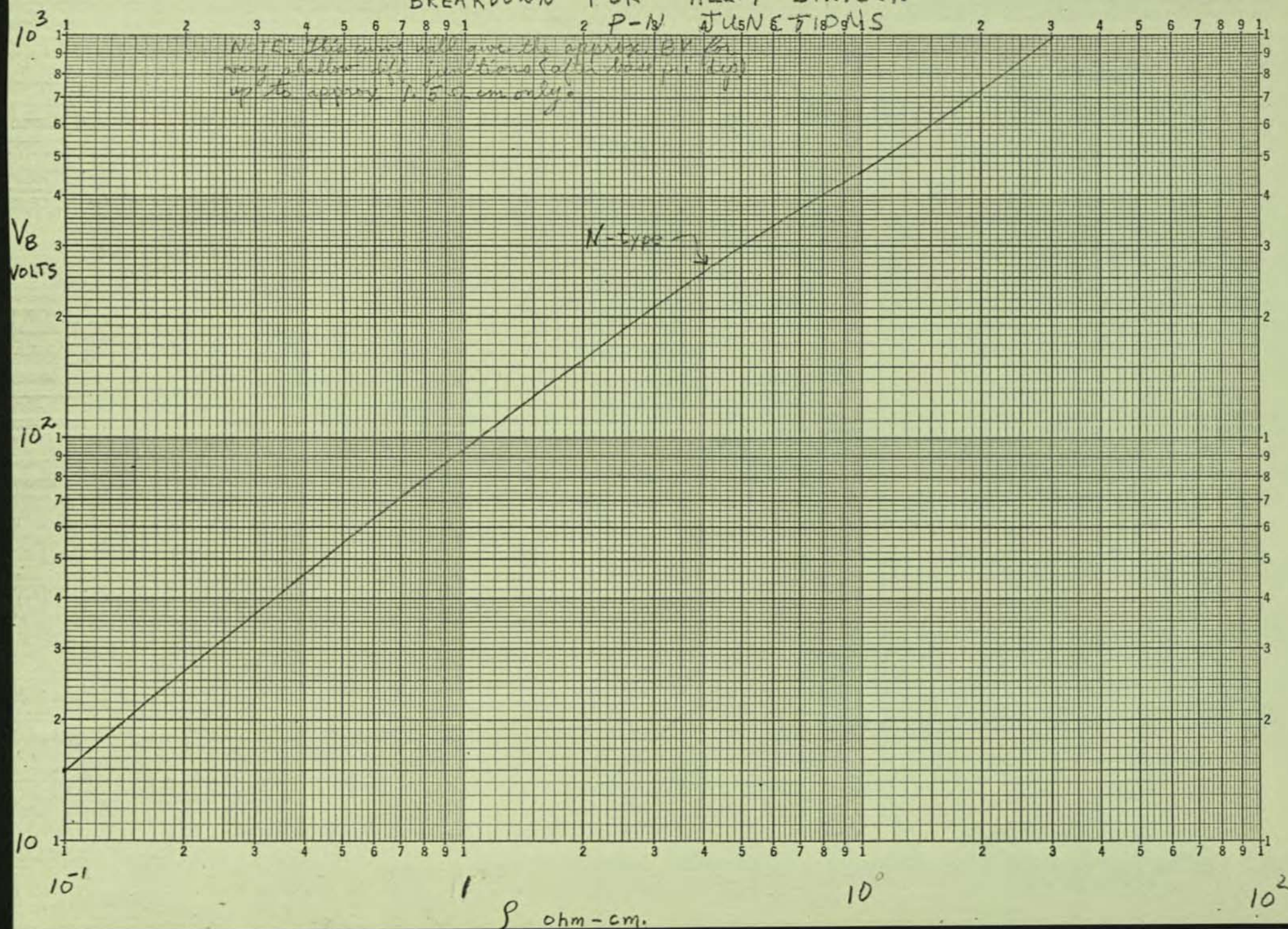
Voltage Breakdown, V_B



BREAKDOWN FOR ALLOY SILICON

P-18 JULY 5 1945

NOTE: The graph will give the approximate breakdown voltage for various thicknesses (of a base 1 cm. thick) up to approximately 1.5 cm. only.



OXIDATION

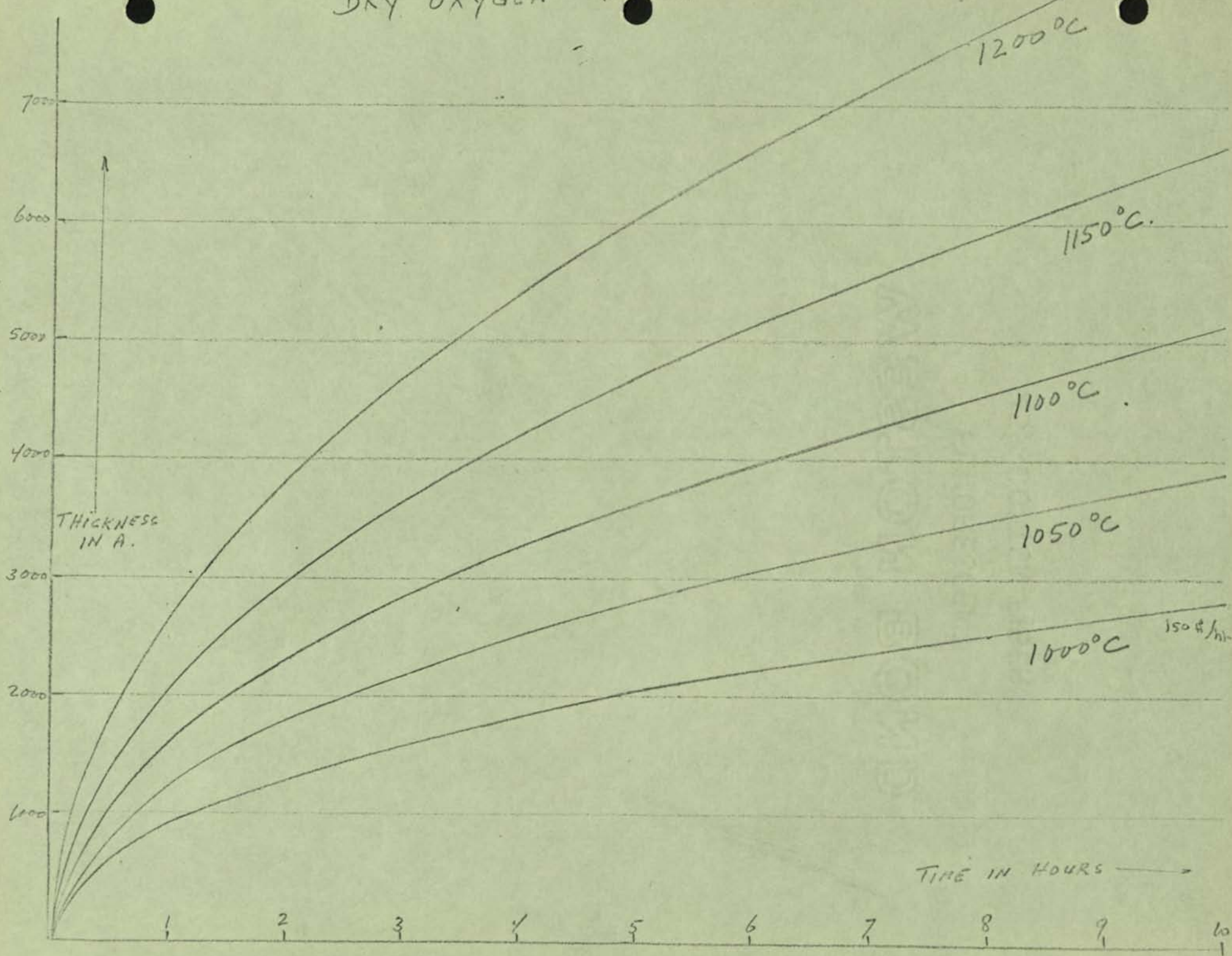
Lars L. Lönn.

only through Oxide layer.

kr 2/15/62

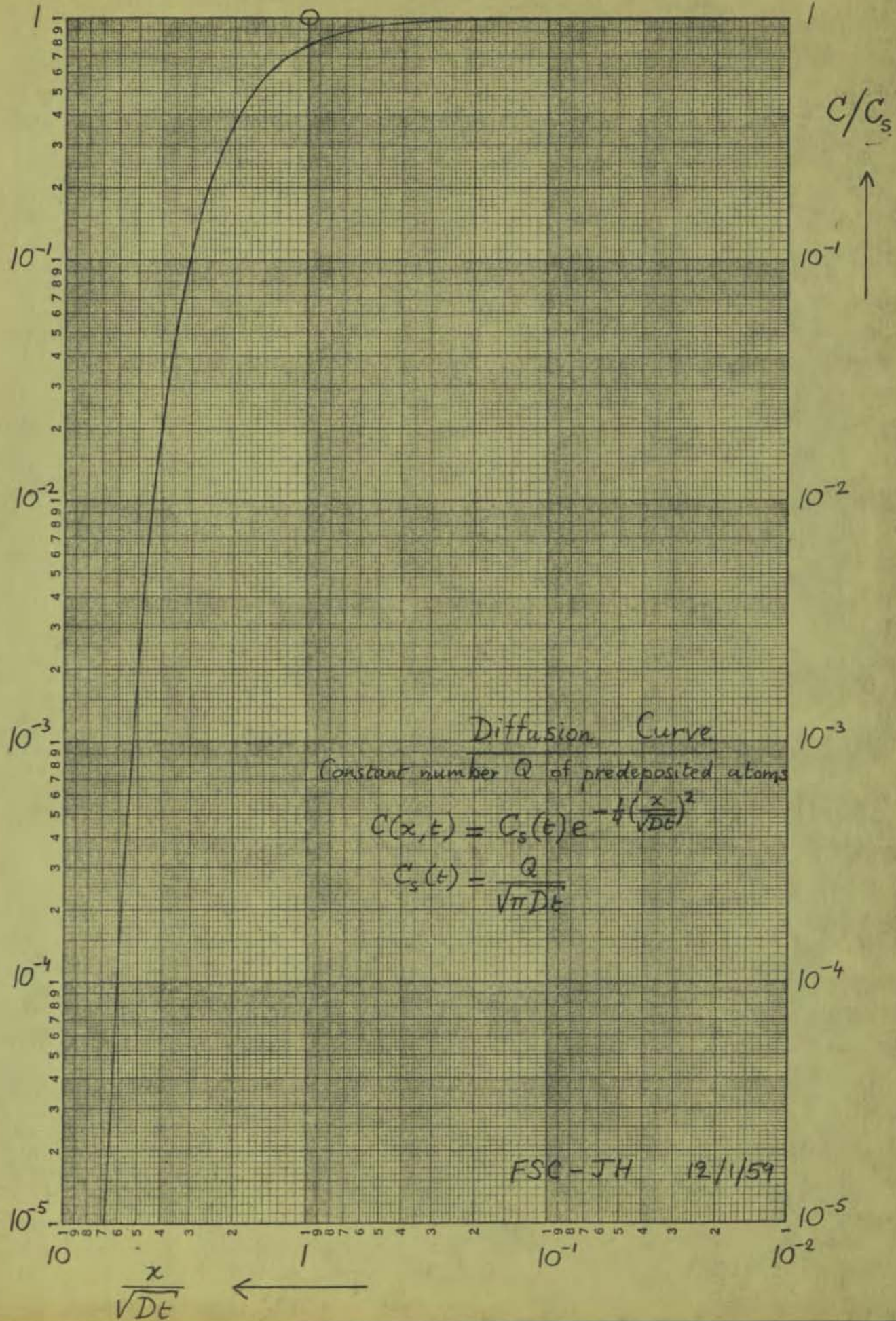
DRY OXYGEN 1 ATM.

500 A.



<u>Order</u>	<u>Color</u>	<u>Thickness in Angstrom Units</u>
I	Brownish white	685
	Clear brown	733
	Dark brown	795
	Red brown	850
	Dark purple	884
	Dark violet	925
	Dark blue	959
	Clearish blue to greenish	1120
	Still clear blue	1610
II	Pale blue green	1680
	Pale green	1760
	Clear yellow green	1860
	Clear yellow	1930
	Golden yellow	2060
	Orange	2410
	Red	2550
	Deep purple	2650
	Violet	2800
	Blue	2980
	Clearish blue	3180
	Bluish green	3360

DIFFUSION



$10^{-6} \quad 10^{-7} \quad 10^{-8}$ 10^{-9} $\times 10^{-4}$ $\times 10^{-2}$ 10^{-7} 10^{-5} 10^{-3} 10^{-1} 10^{-8} 10^{-6} 10^{-4} 10^{-2}

$$C = C_s \operatorname{erfc} \frac{X}{2\sqrt{Dt}}$$

$$\frac{Dt}{C_s} \frac{dC}{dX} = \frac{1}{\sqrt{\pi}} e^{-\frac{X^2}{4Dt}}$$

$$\frac{Dt}{C_s} \frac{dC}{dX}$$

c.g.s. units

$$\frac{X}{2\sqrt{Dt}}$$

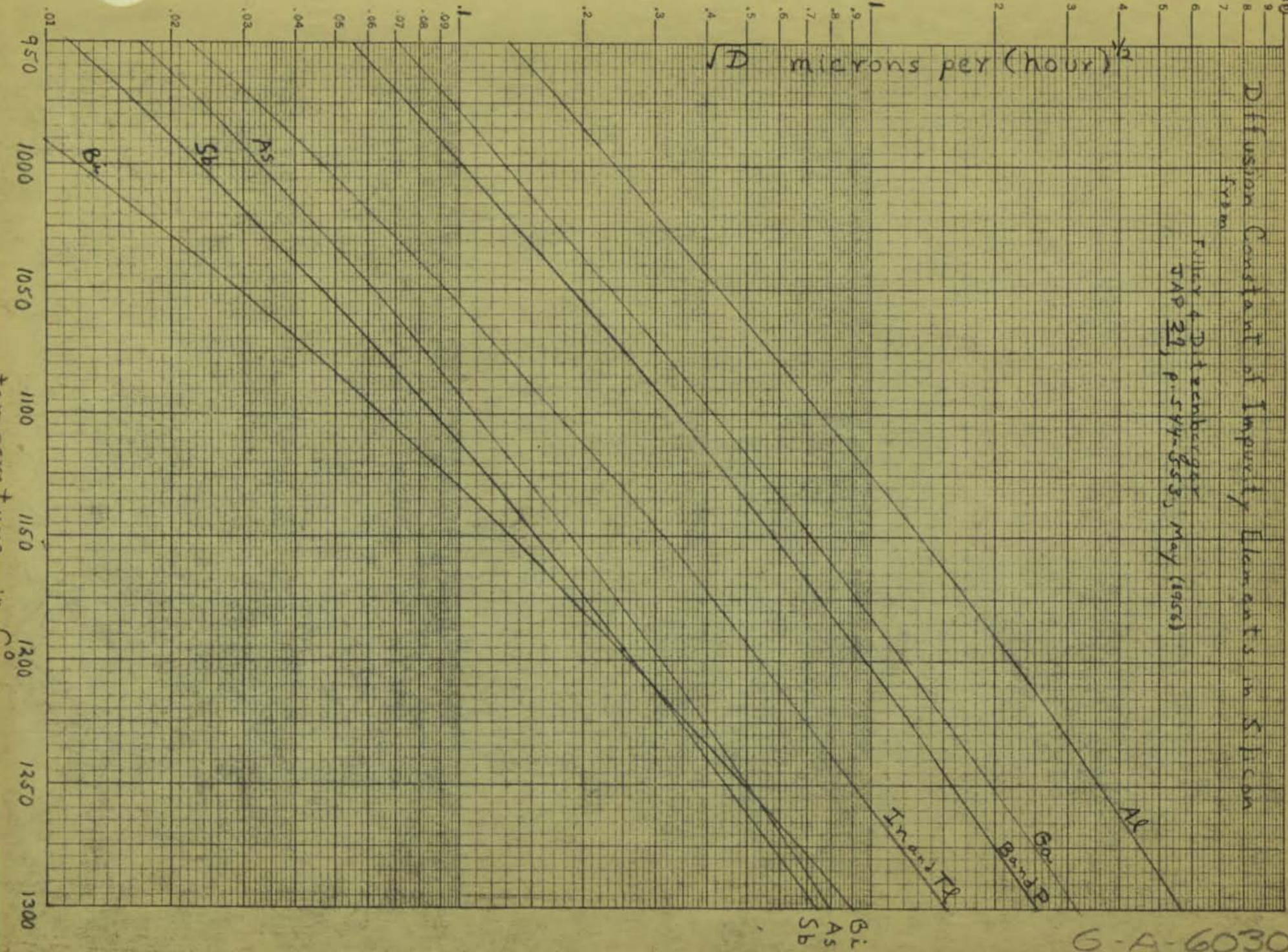
DERIVATIVE OF ERROR FUNCTION

359.71 KEUFFEL & ESBER CO.
Semi-Logarithmic, 3 Cycles X 10 to the Inch,
5th lines accented.
MADE IN U. S. A.

\sqrt{D} microns per (hour) $^{1/2}$

Diffusion Constant of Impurity Elements in Silicon

FULLY ADJUSTED
JAN 22, 1956, P. 544-353

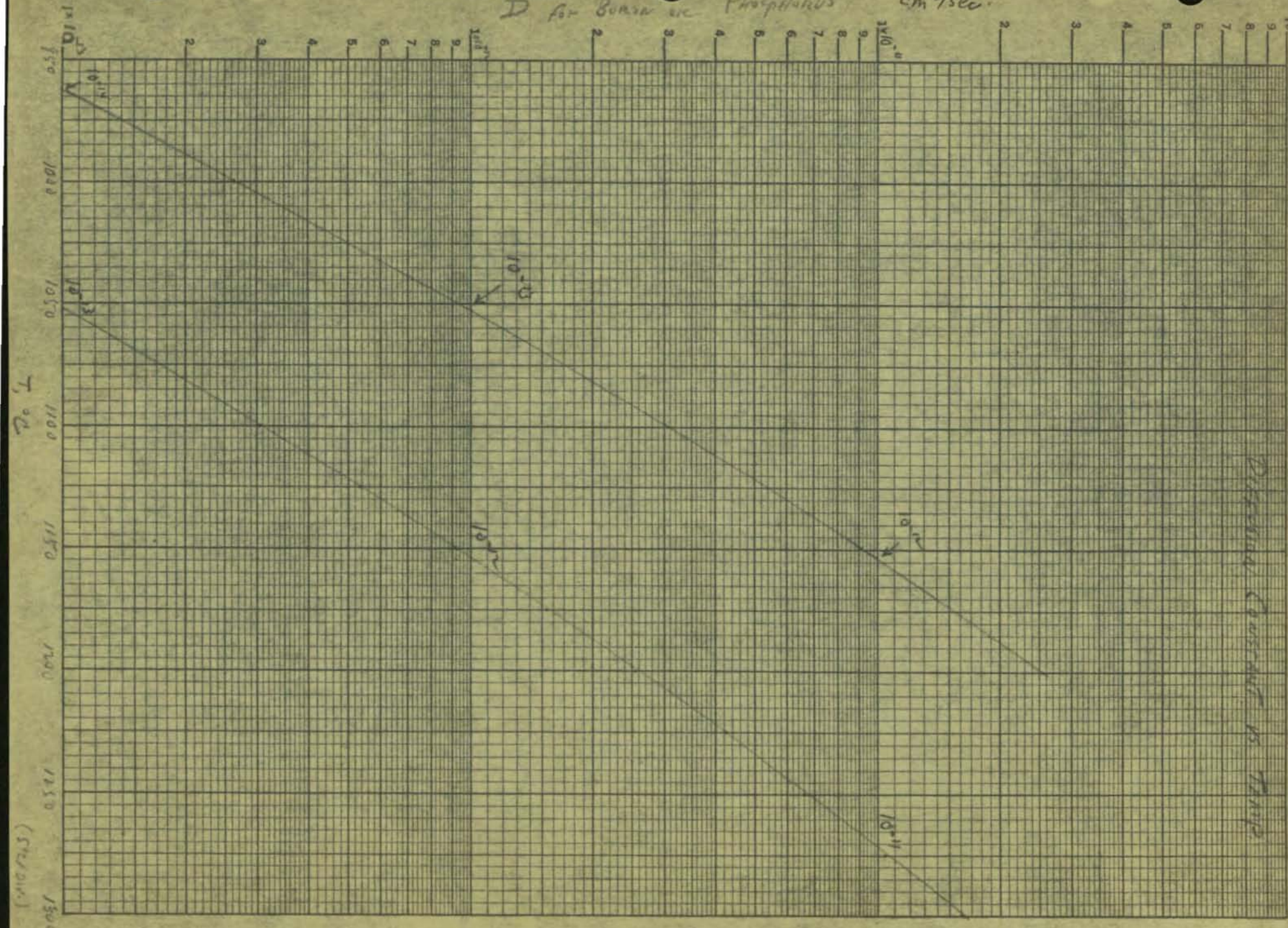


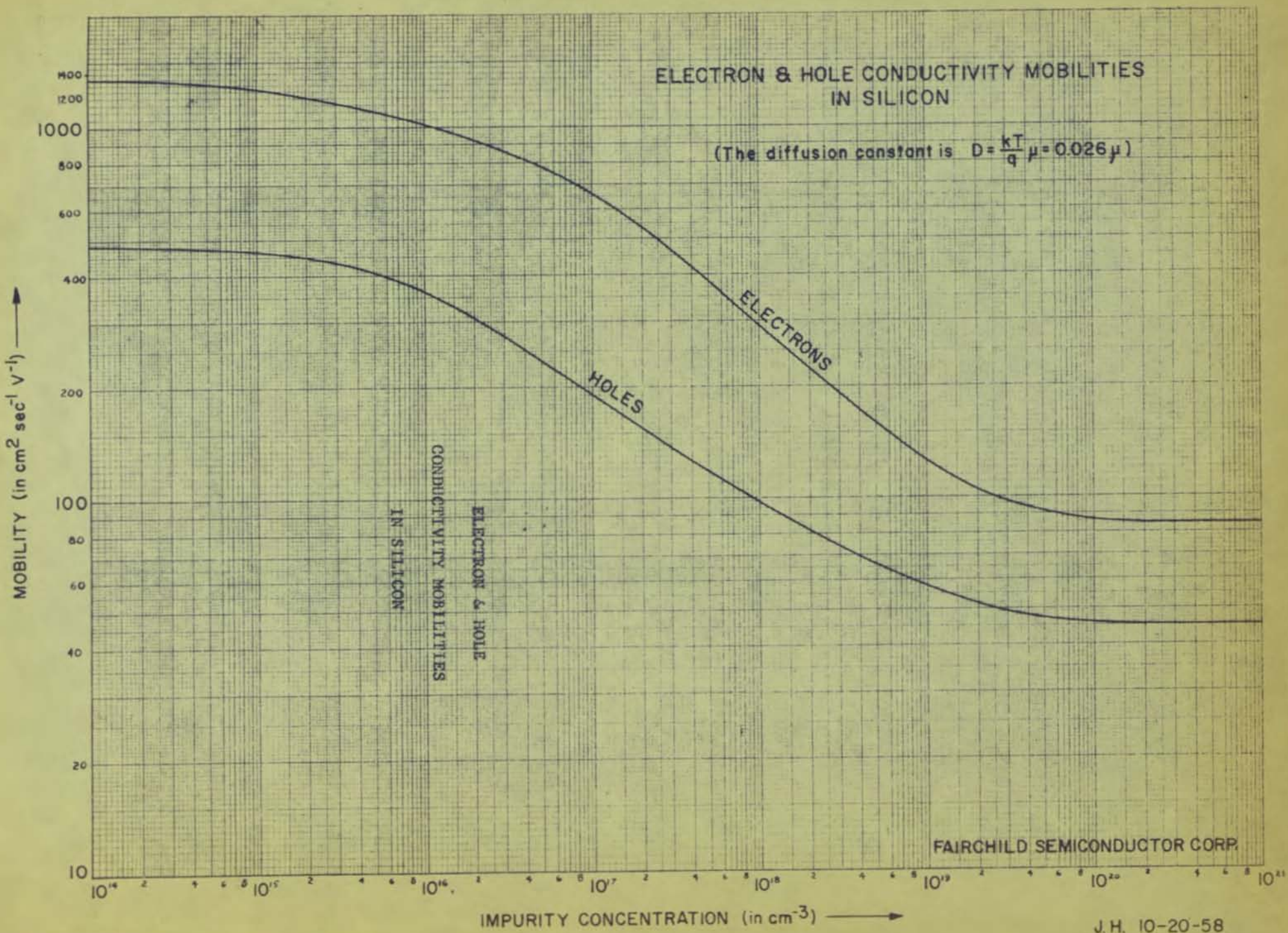
B
As
Sb

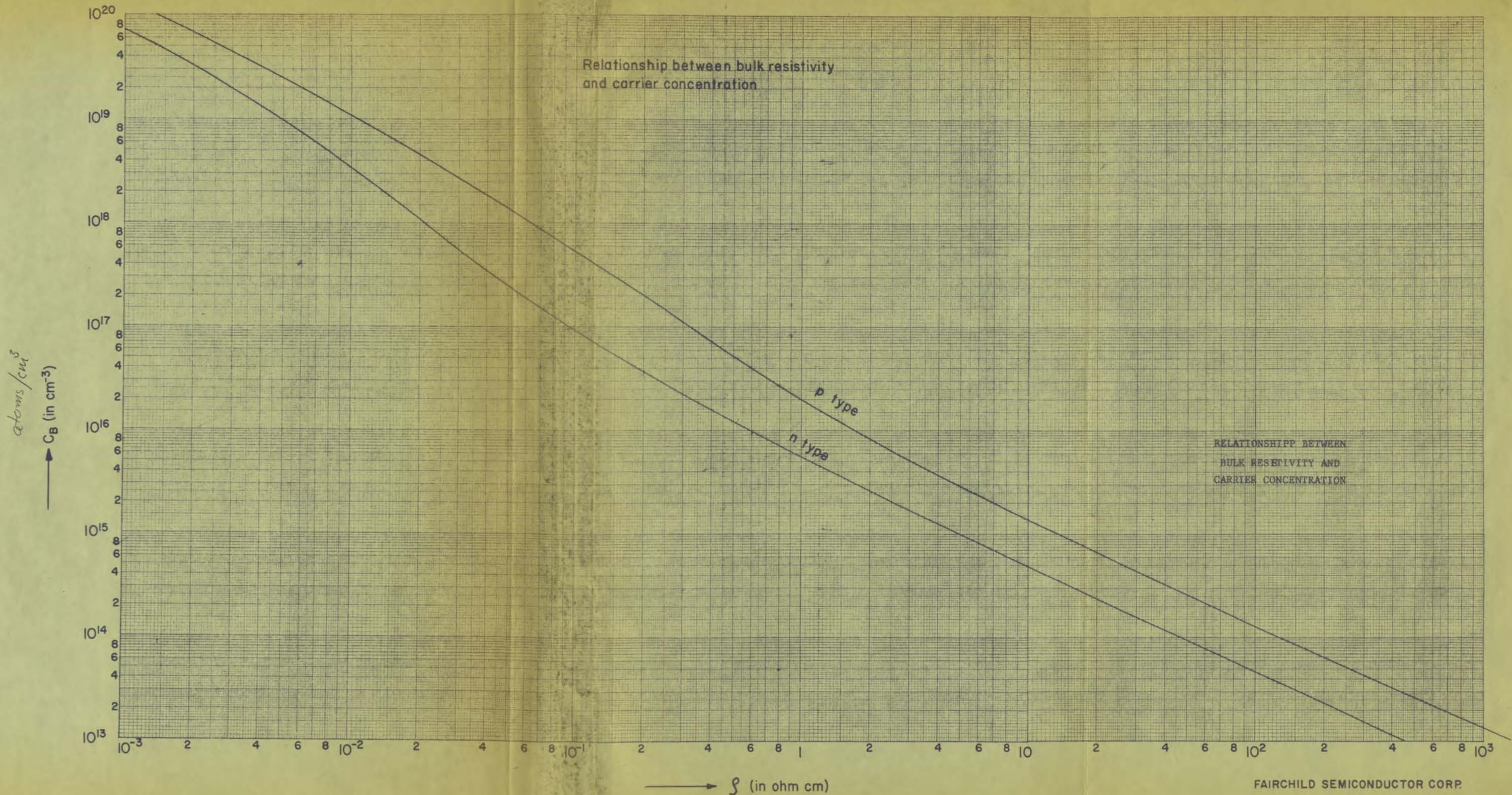
G-A-6030

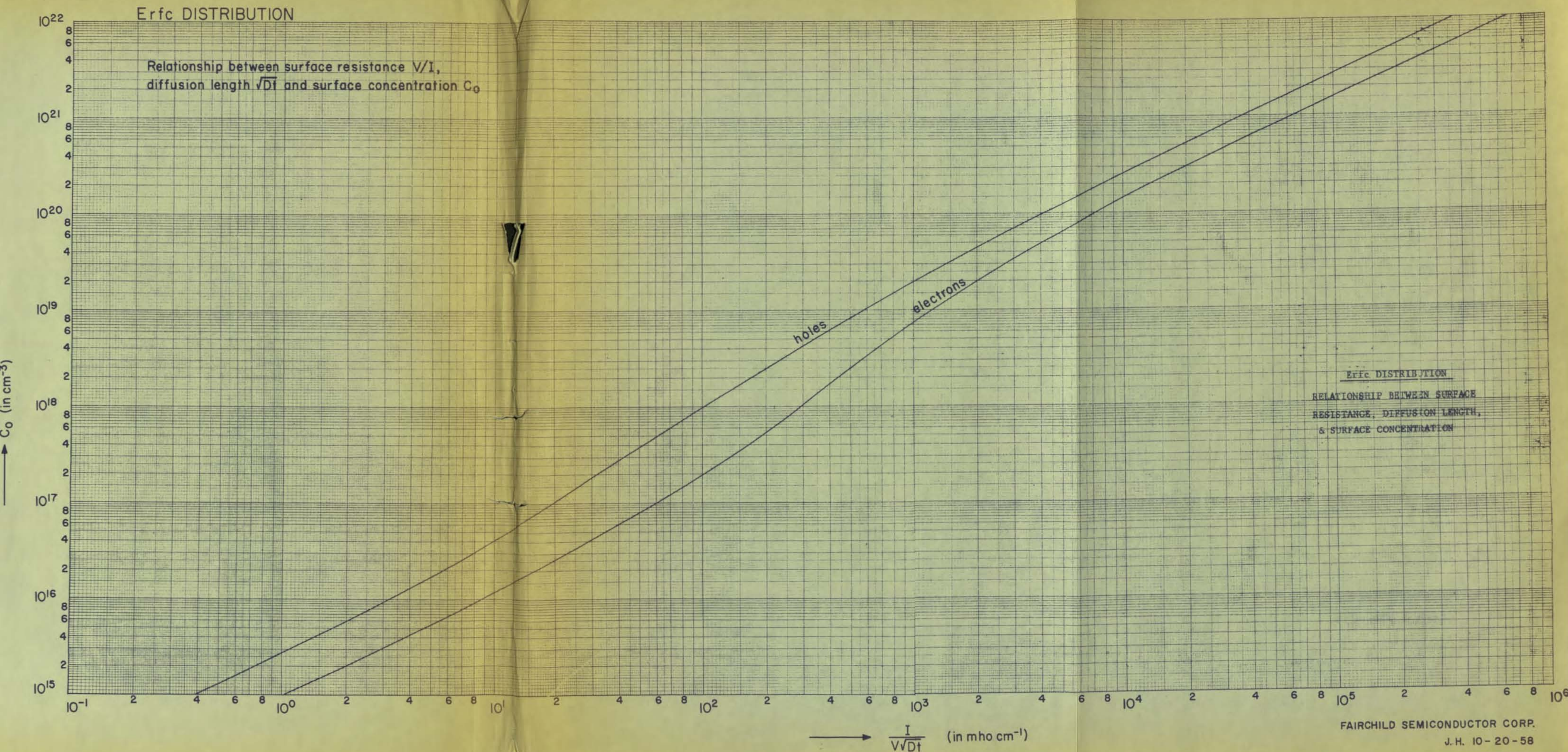
K-E SEMI-LOGARITHMIC 359-71
KEUFFEL & ESER CO. MADE IN U.S.A.
3 CYCLES X 70 DIVISIONS

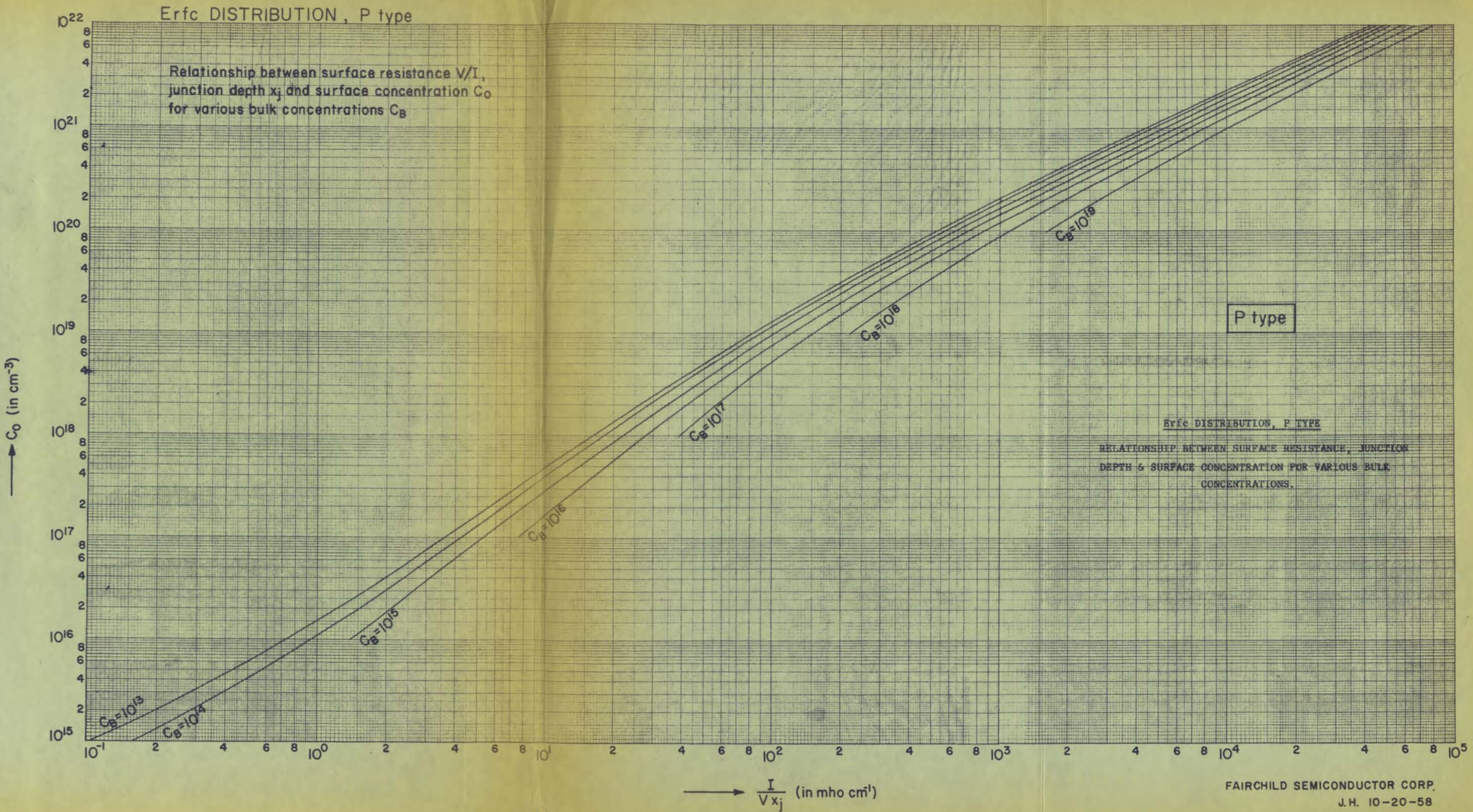
CO. MADE IN U.S.A.
70 DIVISIONS D for BURR WIRE PROSPERUS Cm⁻¹/sec.



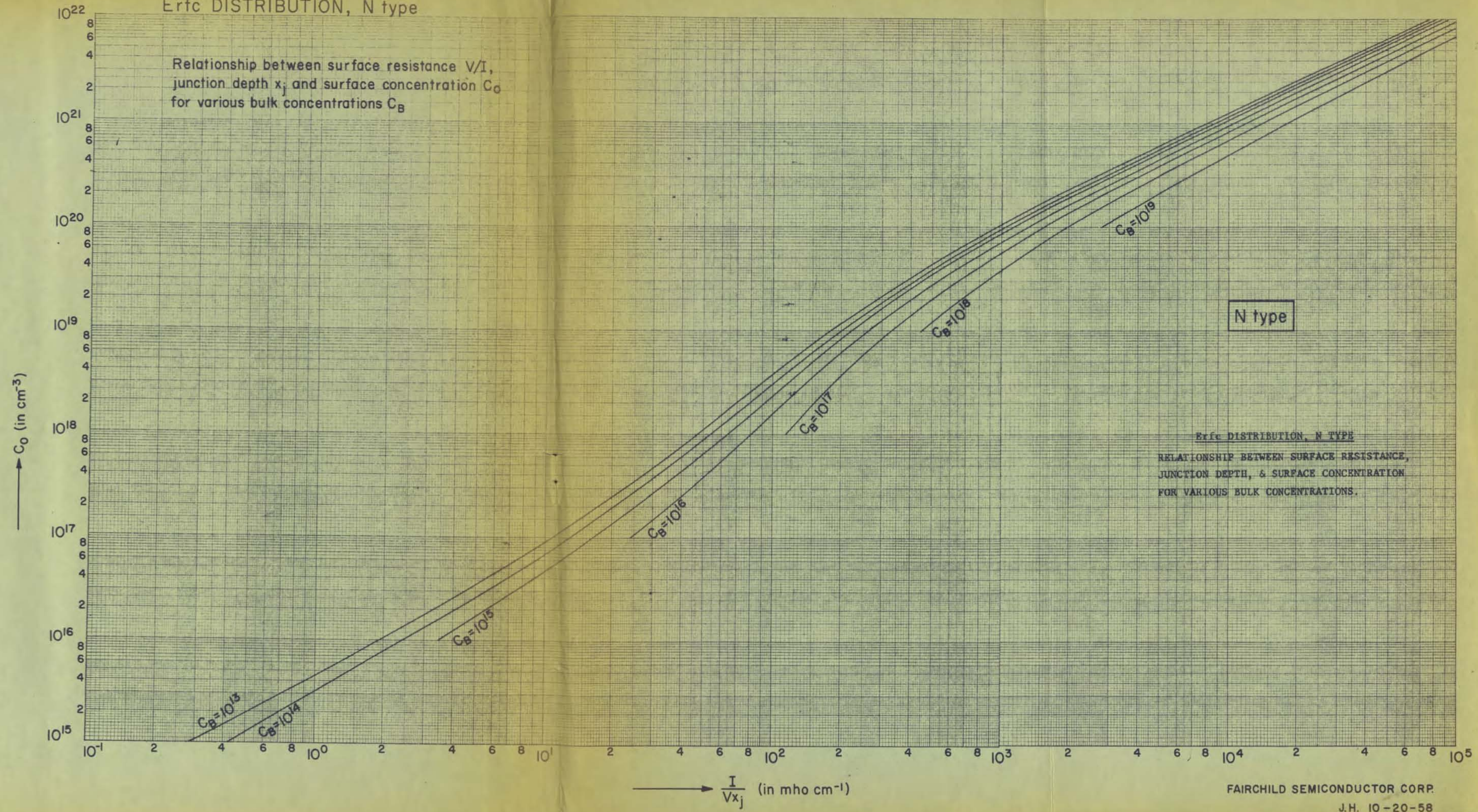


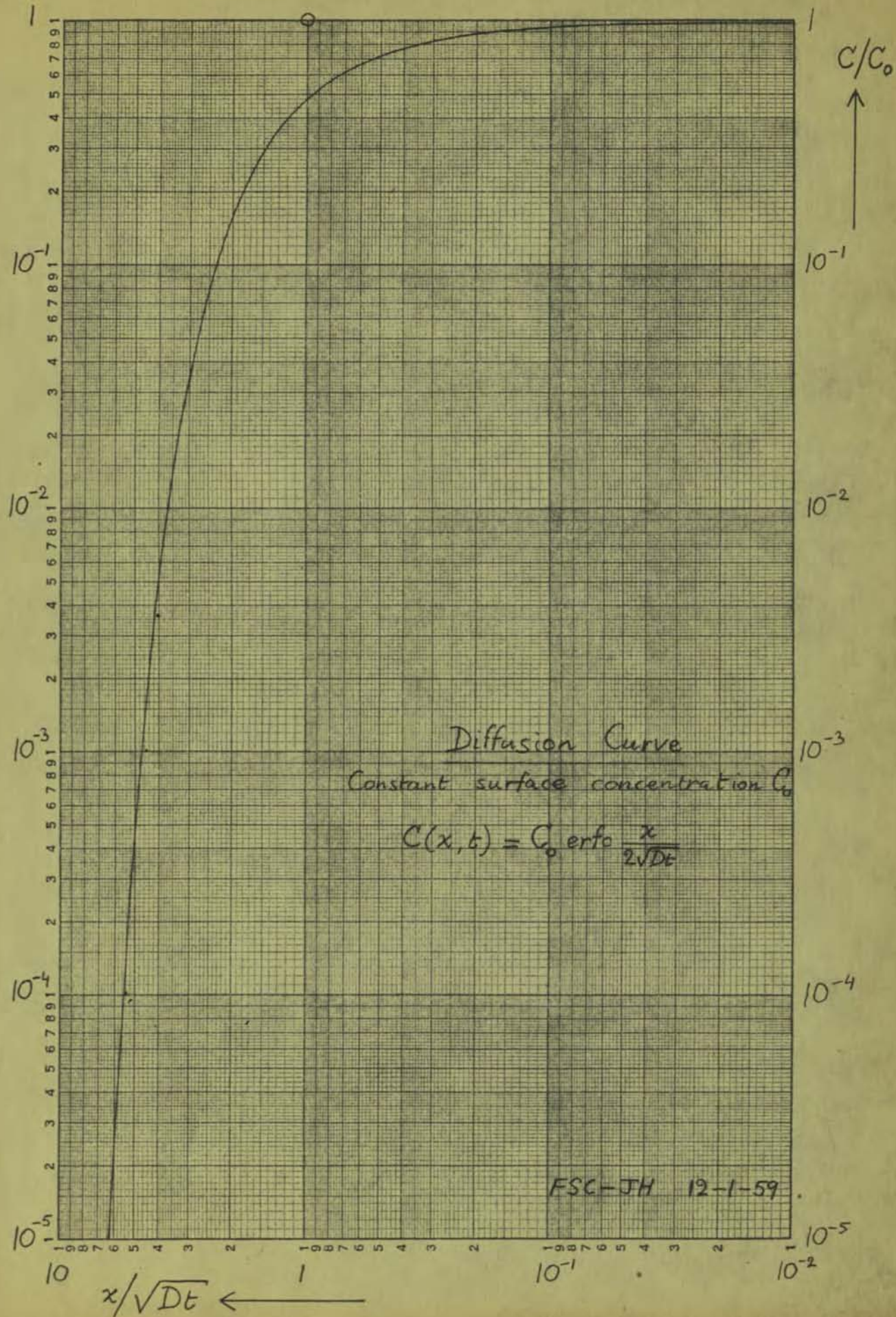


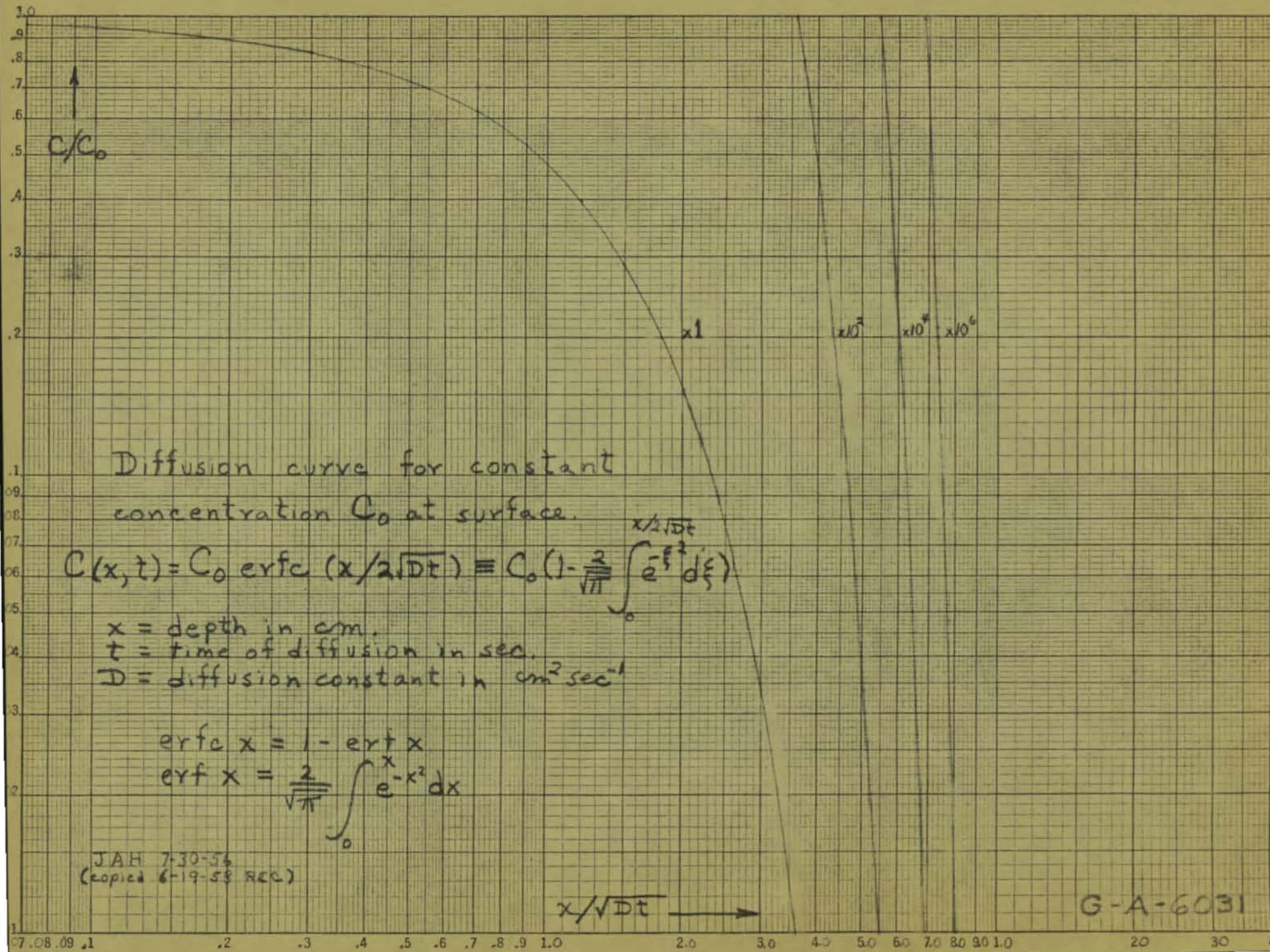




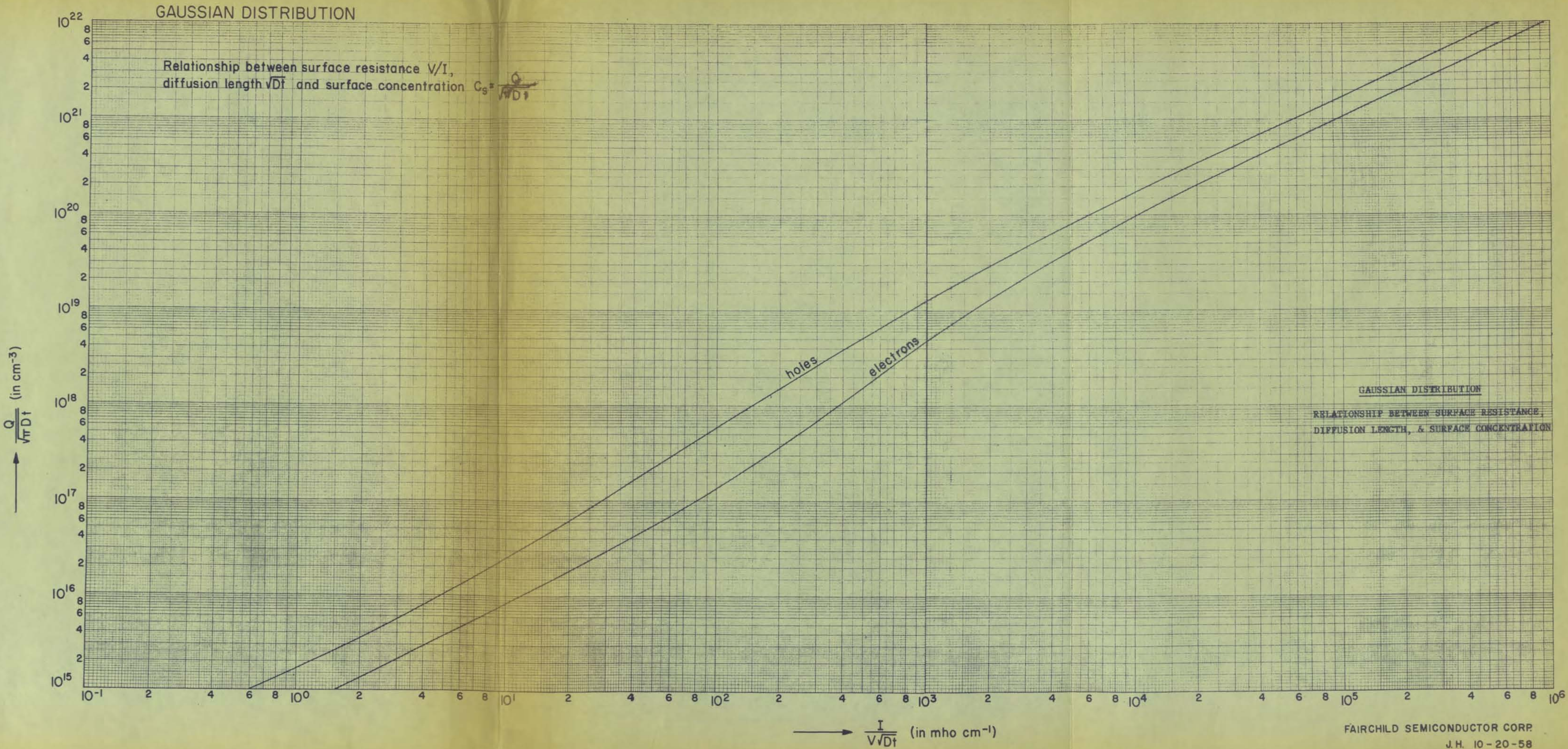
Erfc DISTRIBUTION, N type



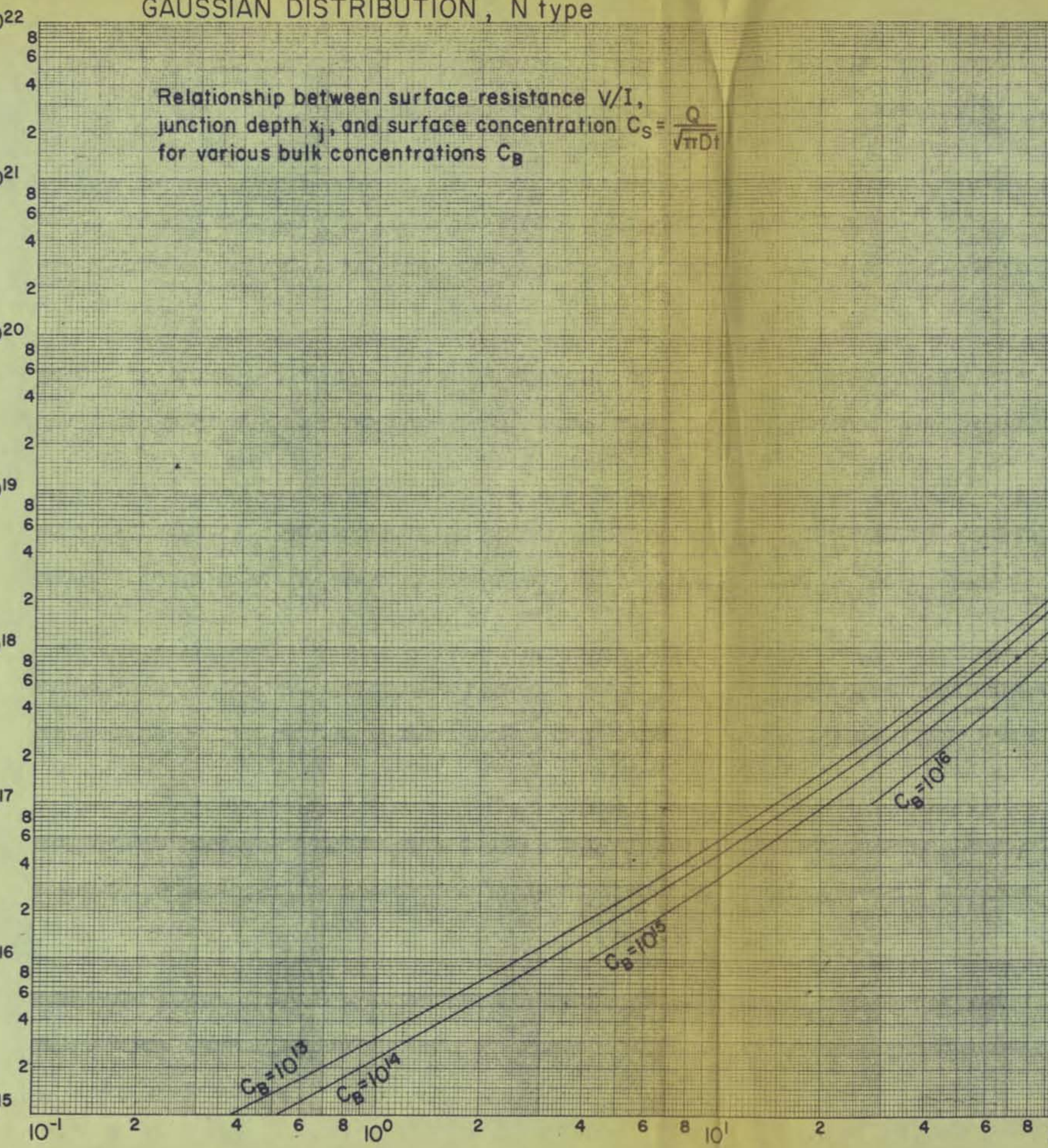




G-A-6031



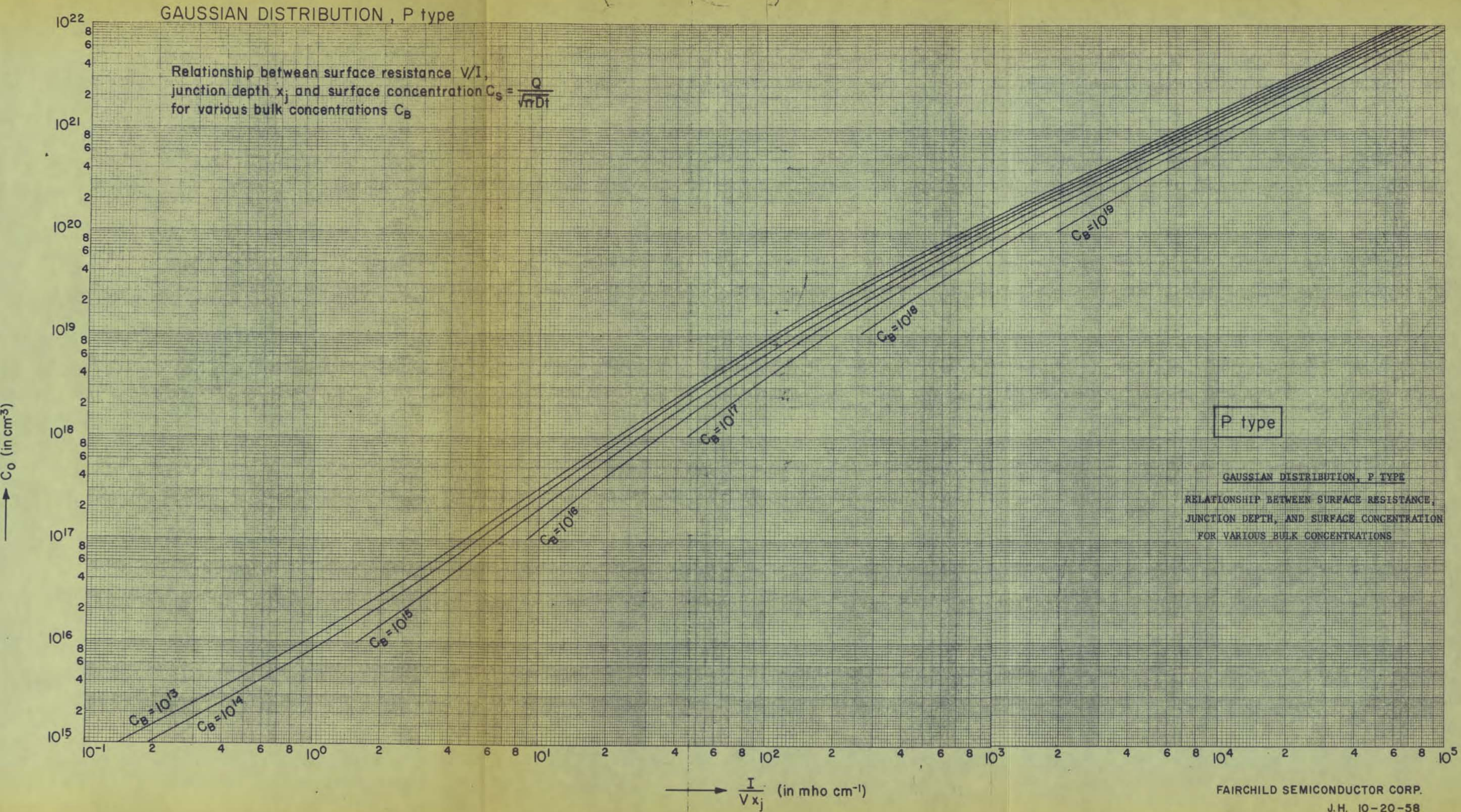
GAUSSIAN DISTRIBUTION, N type

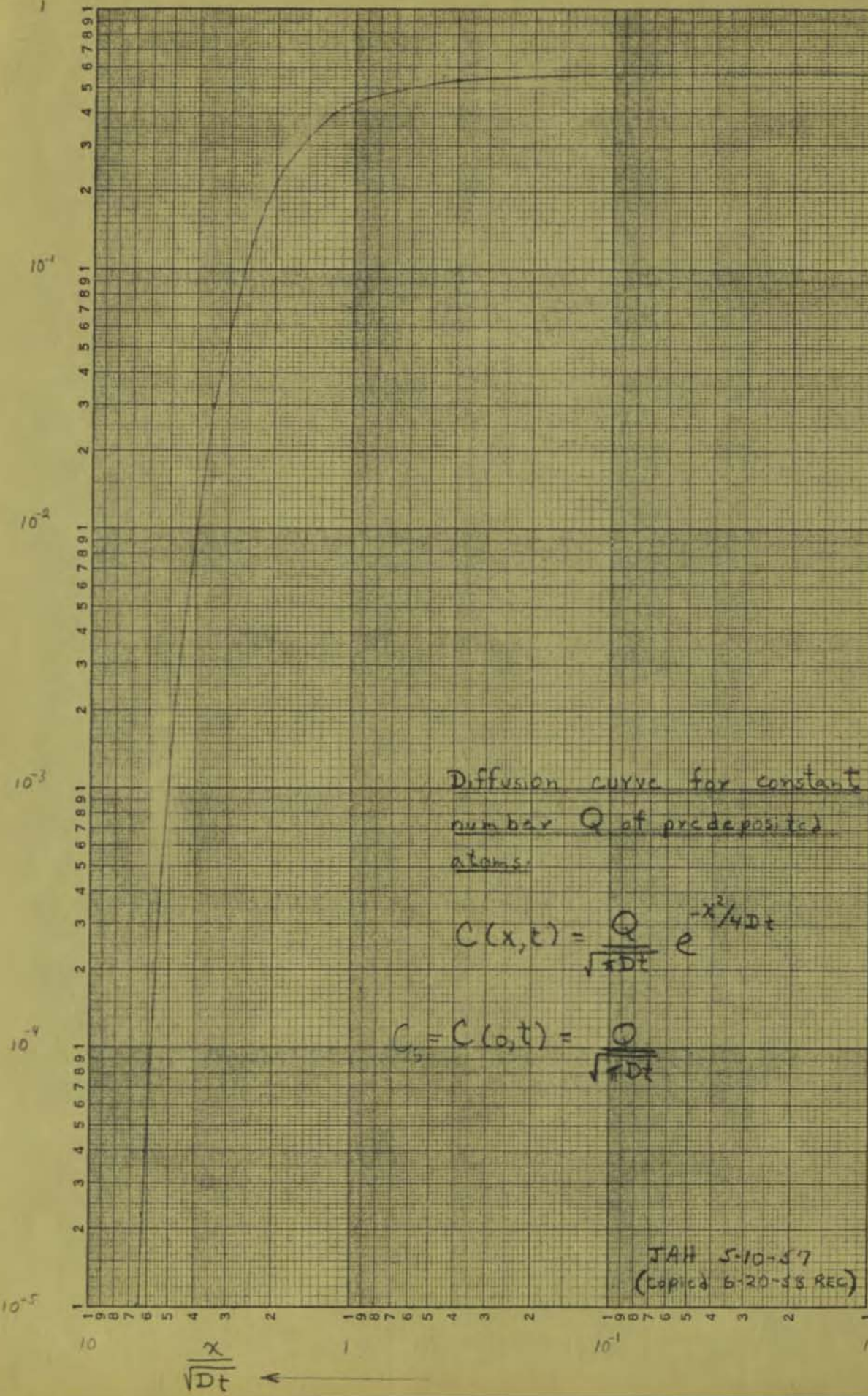


N type

GAUSSIAN DISTRIBUTION, N TYPE

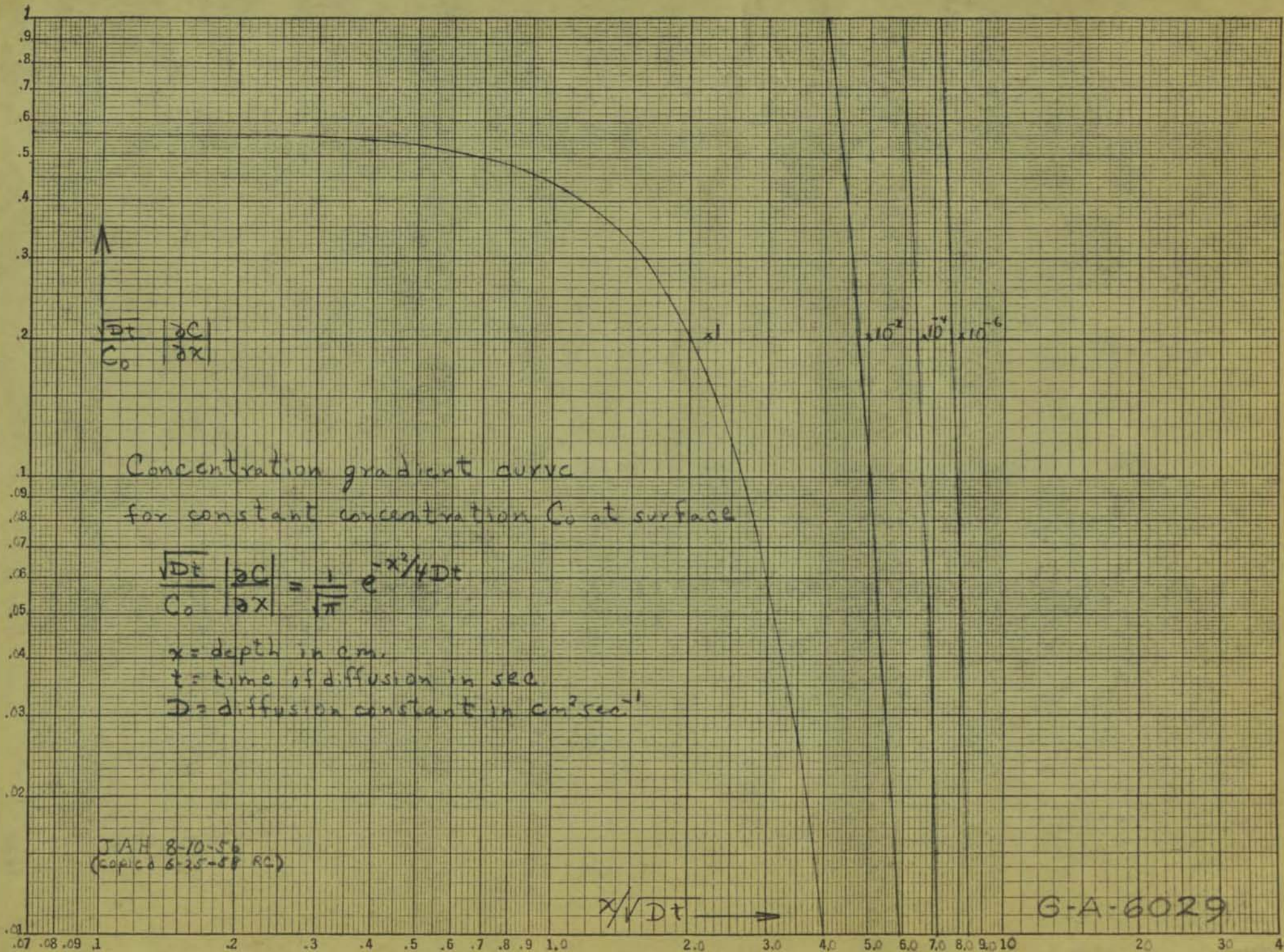
RELATIONSHIP BETWEEN SURFACE RESISTANCE,
JUNCTION DEPTH, AND SURFACE CONCENTRATION
FOR VARIOUS BULK CONCENTRATIONS.

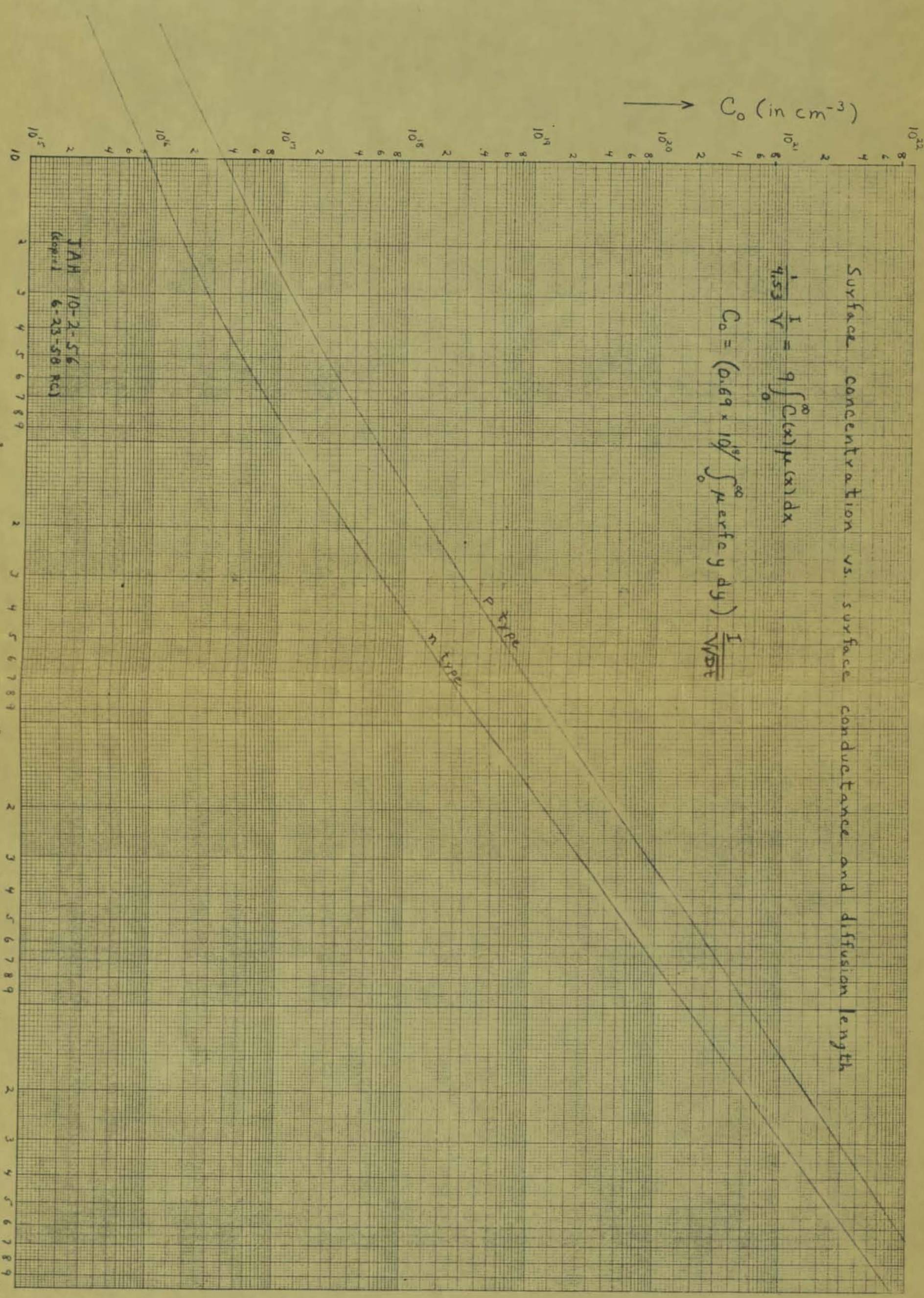




$\frac{Q}{\sqrt{4\pi Dt}}$

6-A-6033





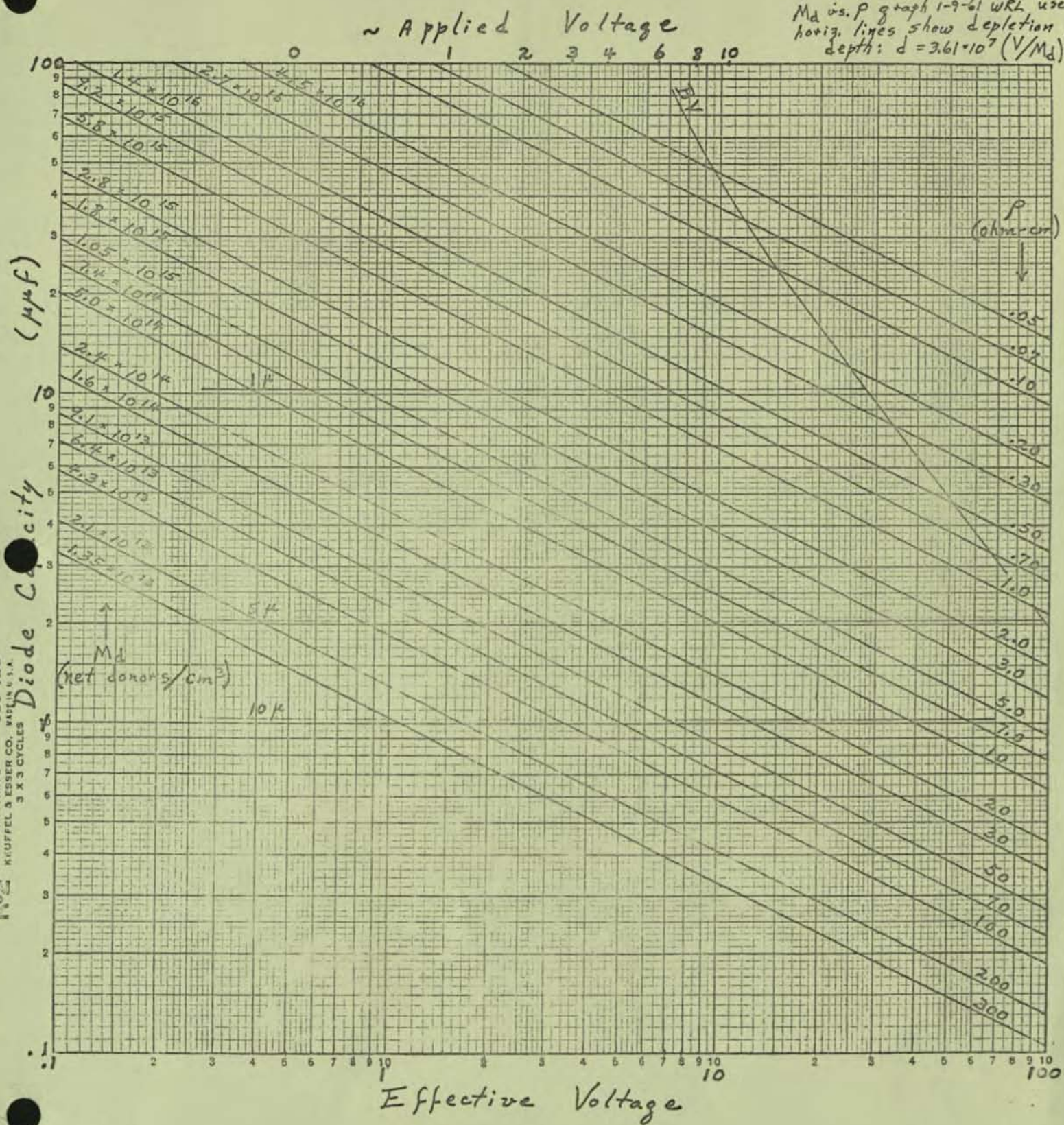
Lars L. Leib's

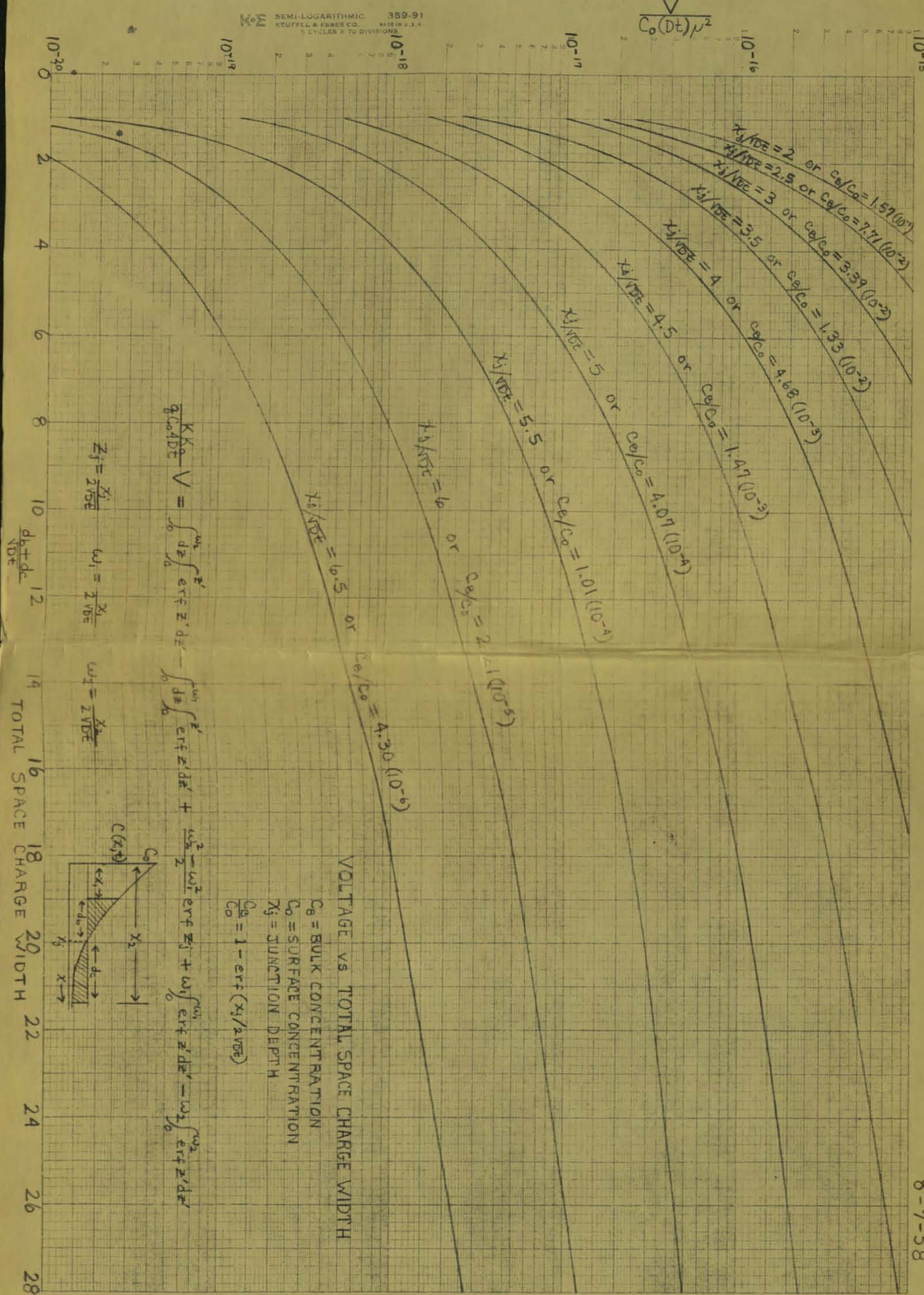
Junction Capacity vs. Voltage
for Various Resistivities
of n-type Si

$$C^2 = 7.995 \times 10^{-14} M_d / N$$

for diode area = .0995 mm²

M_d vs. P graph 1-9-61 WRL used
horiz. lines show depletion
depth: $d = 3.61 \times 10^5 (V/M_d)^{1/2}$





SPACE CHARGE WIDTH IN BASE

2.0

2

4

6

$d_b/\sqrt{D_E}$

8

10

12

14

16

1.8

2.0

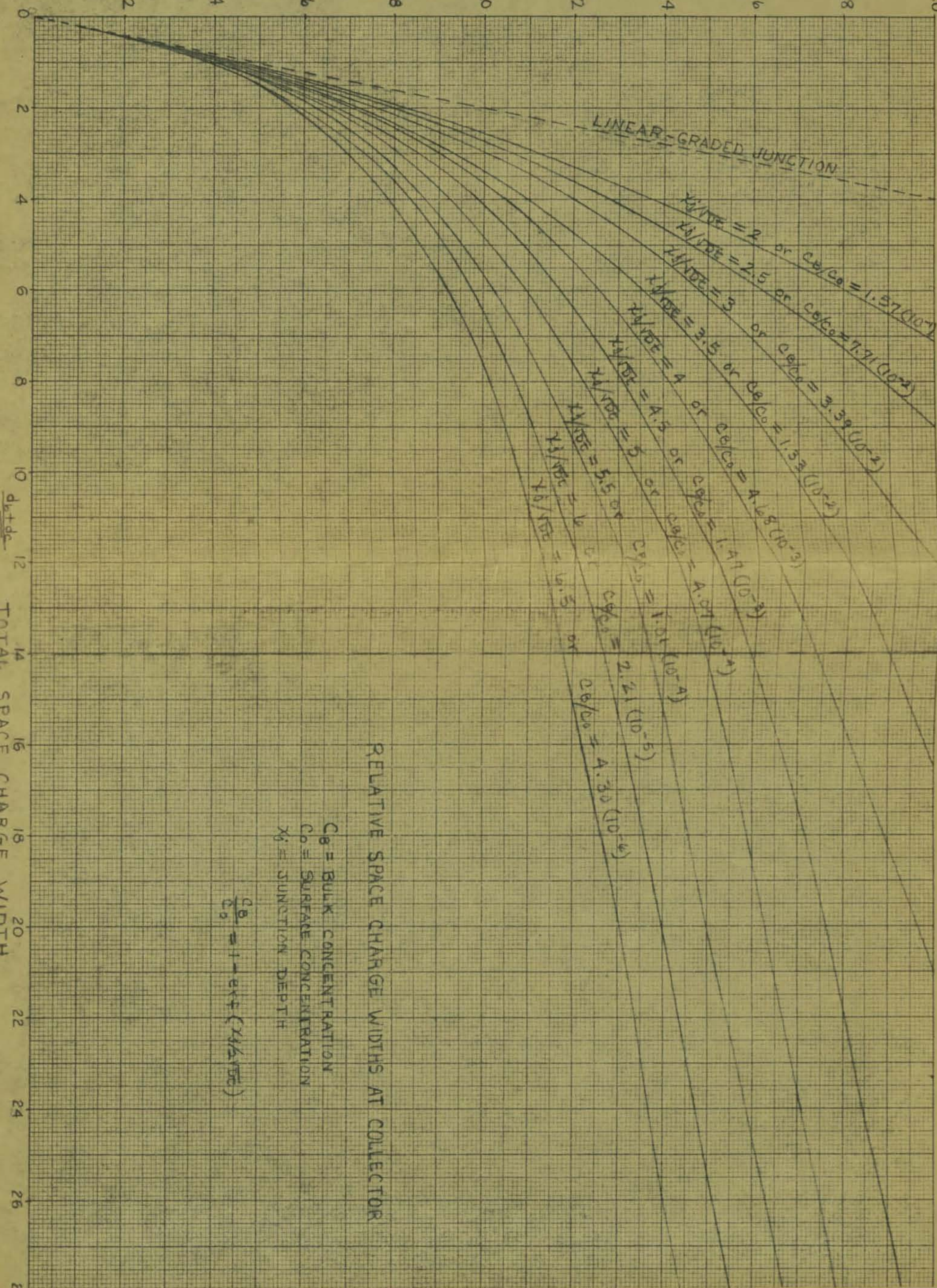
LINEAR-GRADED JUNCTION

$$\begin{aligned} \frac{d_b}{\sqrt{D_E}} &= 4 \quad \text{or} \quad \frac{C_B}{C_0} = 1.97(10^4) \\ \frac{d_b}{\sqrt{D_E}} &= 2.5 \quad \text{or} \quad \frac{C_B}{C_0} = 3.39(10^4) \\ \frac{d_b}{\sqrt{D_E}} &= 2 \quad \text{or} \quad \frac{C_B}{C_0} = 1.52(10^4) \\ \frac{d_b}{\sqrt{D_E}} &= 1.5 \quad \text{or} \quad \frac{C_B}{C_0} = 1.06(10^4) \\ \frac{d_b}{\sqrt{D_E}} &= 1 \quad \text{or} \quad \frac{C_B}{C_0} = 1.41(10^4) \\ \frac{d_b}{\sqrt{D_E}} &= 0.5 \quad \text{or} \quad \frac{C_B}{C_0} = 1.01(10^4) \\ \frac{d_b}{\sqrt{D_E}} &= A \quad \text{or} \quad \frac{C_B}{C_0} = A \cdot 2.1(10^4) \\ \frac{d_b}{\sqrt{D_E}} &= A \cdot 0.5 \quad \text{or} \quad C_B = 1.01(10^4) \\ \frac{d_b}{\sqrt{D_E}} &= 0.5 \quad \text{or} \quad C_B = 2.2(10^4) \\ \frac{d_b}{\sqrt{D_E}} &= 0.2 \quad \text{or} \quad C_B = 26/0.2 = 130(10^4) \\ \frac{d_b}{\sqrt{D_E}} &= 0.1 \quad \text{or} \quad C_B = 26/0.1 = 260(10^4) \\ \frac{d_b}{\sqrt{D_E}} &= 0.05 \quad \text{or} \quad C_B = 26/0.05 = 520(10^4) \end{aligned}$$

RELATIVE SPACE CHARGE WIDTHS AT COLLECTOR

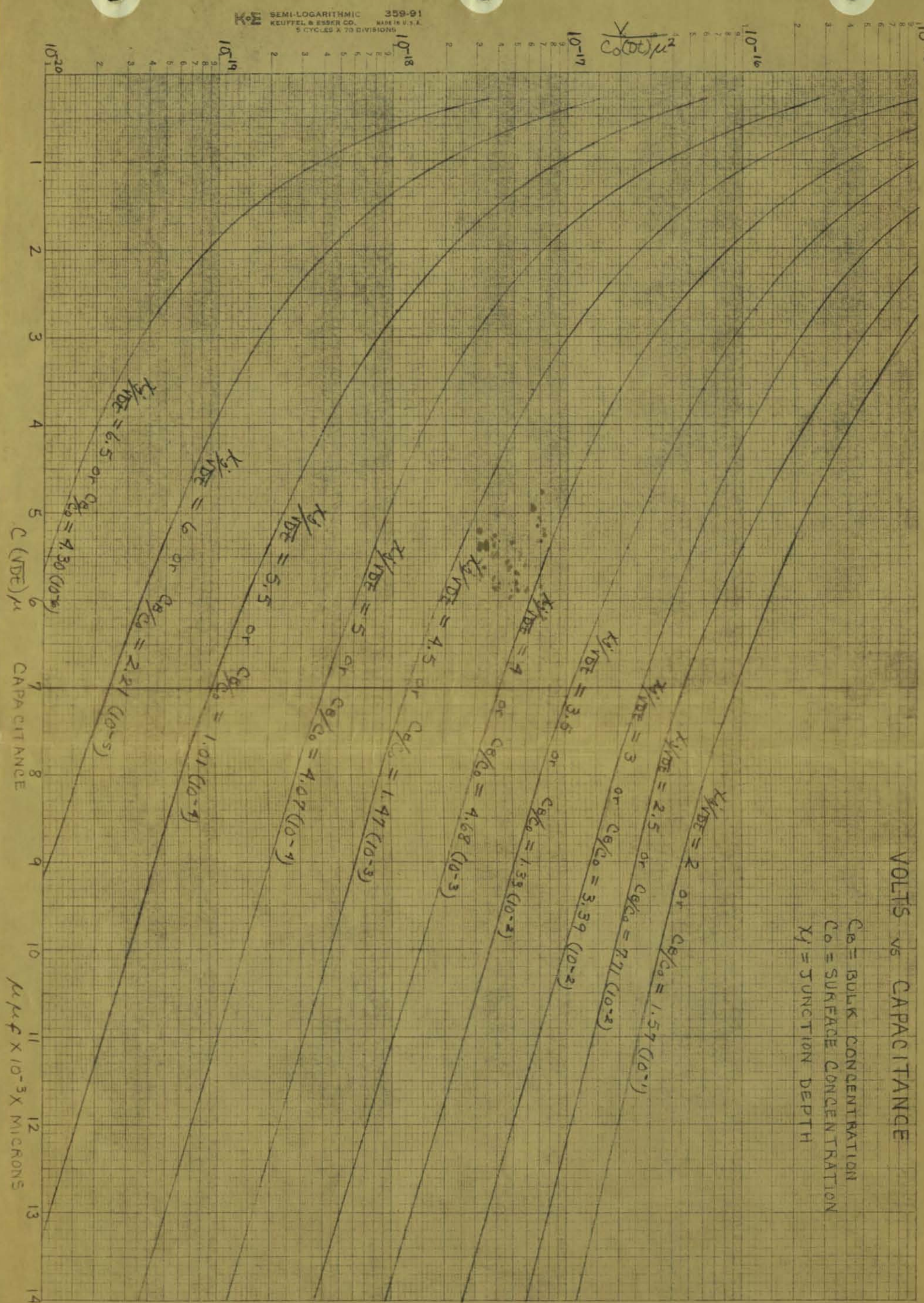
C_B = BULK CONCENTRATION
 C_0 = SURFACE CONCENTRATION
 x_0 = JUNCTION DEPTH

$$\frac{C_B}{C_0} = 1 - e^{-x_0/(2\sqrt{D_E})}$$



VOLTS vs CAPACITANCE

C_B = BULK CONCENTRATION
 C_0 = SURFACE CONCENTRATION
 X_J = JUNCTION DEPTH



VOLTAGE RATINGS FOR DOUBLE DIFFUSED SILICON SWITCHING TRANSISTORS

BY V.H. GRINICH

DEFINITIONS

The various voltages and resistances appropriate to this discussion are defined by the circuit diagram in Figure 1. The example illustrates the polarities appropriate for an n-p-n transistor. The important consideration is what values can be used for V_{CC} and R_L for given values of V_{BB} and R_B without endangering the transistor. As examples we illustrate the points by showing typical curves for a Fairchild 2N697 Double Diffused Silicon Mesa Transistor.

For grounded base operation the collector current-voltage plot with open emitter is shown in Figure 2. No appreciable current flows at voltages below the collector-base diode breakdown voltage, BV_{CBO} . Used in this manner there is negligible negative resistance region (neglecting thermal effects, which are small in the operating temperature range for the device), so the device can be operated at peak voltages up to the order of BV_{CBO} . This is the important limit in many amplifier* and oscillator applications. It is, therefore, a reasonable parameter from which to establish a voltage rating for devices used in this sort of application.

Figure 3 is a v-i plot for grounded emitter operation with base open. In this case, a negative resistance region will exist at normal temperatures. The peak voltage, BV_{CEO} , is a function of BV_{CBO} and current gain at this point. As the current is increased, the voltage drops and continues through a minimum. The exact current at which the minimum is located depends upon variation of current gain with collector current. For the 2N697 the broad, flat minimum occurs in the vicinity of 50 ma.** This minimum voltage, called the lower limiting voltage, LV_{CEO} , for n-p-n silicon transistors is related approximately to BV_{CBO} and h_{FE} , the large signal current gain by

$$LV_{CEO} = \frac{BV_{CBO}}{(h_{FE})^{1/n}}$$

where n is a function of BV_{CBO} .

SGS-FAIRCHILD - LONDON - MILAN - PARIS - STOCKHOLM - STUTTGART

In using a transistor as a switch with a resistive load and allowing the base to open, it is important that the load line remains at all times below and to the left of the curve in Figure 3; otherwise, the transistor will not return to the "off" state when the base is opened. This mode of operation puts the most severe restriction on the maximum voltage that can be used. Essentially, in this extreme case, when switching moderate or high currents where R_L is small, the voltage V_{CC} cannot exceed LV_{CEO} . Fortunately, LV_{CEO} is a bulk property of the device not subject to degradation with life.

Figure 4 shows the case for a short between base and emitter. In this case, no appreciable current flows below BV_{CES} ($=BV_{CBO}$). The current then increases at about the same voltage until at current I_{C1} the voltage drop across the internal base spreading resistance (r_{BB}) causes the emitter-base diode to become forward biased at the point farthest removed from the base contact. The voltage then drops to LV_{CES} with increased current because of the avalanche multiplication associated with current flow through this new path. On reducing the current the voltage remains low until it reaches I_{C2} where the voltage again returns to the upper curve. In general I_{C2} is below I_{C1} . The hysteresis is related to the different current flow paths which made r_{BB} effectively higher approaching from the high current side than from the lower.

Because some of the current flows out the base lead in this case, LV_{CES} is in general significantly higher than LV_{CEO} . The difference is a function of r_{BB} , h_{FE} , and r_{EE} , the emitter spreading resistance.

This case (of $V_{BB} = R_B = 0$) is of considerable importance since it closely represents many practical situations. As an example, in core switching circuitry where the base drive is supplied by cores, the d-c impedance from base to ground is that of the core winding which is essentially a d-c short. In this case for $R_L = 0$, the use of a V_{CC} less than LV_{CES} is a necessary condition for a conservative design. Other conditions such as additional voltages induced in the collector circuit and the exact value of R_L will determine the final value of V_{CC} in the particular application.

Other examples where LV_{CES} is the proper rating would be in a transformer input Class B grounded emitter power amplifier where the d-c resistance of the winding from base to emitter is negligible.

In place of a short (or near short) between base and emitter, a resistor R may be included. In this case the appropriate ratings are called BV_{CER} and LV_{CER} . The values of BV_{CER} and LV_{CER} are between BV_{CEO} and BV_{CES} or LV_{CEO} and LV_{CES} , respectively. For $R = 10\Omega$ the value of LV_{CER} is typically equal to LV_{CES} . This value of resistance also guarantees that all units will be "locked" on the low voltage leg of the v-i curve with 100 ma of collector current.

In Figure 5, a curve of LV_{CER} at $I_c = 100$ ma is plotted for a typical 2N697 transistor. For values of $R > 5$ K, LV_{CER} is very nearly equal to LV_{CEO} . For values of $R < 100\Omega$, it is nearly the same as LV_{CES} .

By holding off the base, it is possible to use the transistor at higher voltages. Figure 6 illustrates typical results with the 2N697 for the base held off through several values of base resistance. No simple method to relate the voltage to transistor parameters under these conditions is known. Appropriate data should be taken before using this manner. In this case, the breakdown voltage is BV_{CEX} and the minimum voltage LV_{CEX} .

A general statement one can make regarding BV_{CEX} for a negative value of V_{BB} is that it is limited to less than $(BV_{CBO} - V_{BB})$, since at this voltage the collector-base diode breakdown occurs. The lower boundary of BV_{CEX} is BV_{CEO} for V_{BB} negative. The lower boundary of LV_{CEX} is LV_{CEO} and the upper bound is $BV_{CBO} - V_{BB}$. Another practical limit occurs when the current pulled through the base is so large that the voltage drop across r_{bb} causes the emitter base diode to break down at the point where the base contact comes closest to the emitter junction. Ratings for BV_{CEX} and LV_{CEX} are non-conservative, since when used near these maximum voltages in this manner, a power failure in the hold-off voltage with collector voltage still applied can allow the transistor to get into the negative resistance region and burn out if the collector current is not limited.

* Linearity considerations may dictate a lower value for amplifier use.

** Measurements made on breakdown voltages at high currents should be made at a very low duty cycle with short pulses in order to keep the dissipation and temperature rise low.

MEASUREMENT

BV_{CBO} can be measured by forcing a collector current and measuring the collector-to-base voltage. For use as an absolute maximum rating, one need only be sure that the power dissipation of the device not be exceeded, although it is convenient to measure at a much lower current - of the order of microamps.

Using the same techniques as for BV_{CBO} , BV_{CEO} must be measured at a sufficiently low current so that the device is not in a negative resistance region which will cause oscillations. This requires currents of about 10μ amp for the 2N697.

BV_{CES} can be measured at currents considerably higher than used in the measurement of a BV_{CEO} . The same method of measurement is used.

LV_{CEO} and LV_{CES} are high power dissipation measurements and ordinarily must be done on a low duty cycle with short pulses. A circuit for measuring these parameters is shown in Figure 7. In order to be sure of getting on the right region of the characteristics, a current pulse into the base turns the device "on" in each case. For LV_{CES} a switching core is used as the base pulse generator. Inserting a diode with the proper polarity in the base leads makes this a LV_{CEO} test. Paralleling the diode by a resistor R makes it a LV_{CER} test. BV_{CER} , BV_{CEX} and LV_{CEX} can be measured in similar ways.

To illustrate typical magnitudes and differences between these various breakdown voltages, Table I summarizes the data on a group of 2N697 transistors.

CONCLUSIONS

Voltage ratings of transistors as switches require close examination of circuit conditions. This refers to both d-c and dynamic conditions.

The highest collector voltage rating is that of the collector-to-base breakdown voltage BV_{CBO} . This is a useful rating in many oscillator and amplifier circuits.

The lowest collector voltage rating in any practical switching circuit is the lower limiting voltage LV_{CEO} . This corresponds to the case where a very high impedance path lies between the base and emitter and no turn-off current is used ($R_B = \infty$; $V_{BB} = 0$).

For many practical applications of Fairchild 2N696 and 2N697 Diffused Silicon Transistors, the conditions of $R_B = 10\Omega$ is very nearly met. Then the appropriate collector voltage rating for switching currents in the order of tens and hundreds of milliamperes is LV_{CER} . Hence, Fairchild Semiconductor has inaugurated this as one of the voltage ratings for the 2N696 and 2N697.

For the case where the current switched is small so that the load line passes completely under the second part of the v-i curve (for the 2N696 and 2N697 this is in the order of milliamperes) the rating BV_{CES} could be used for the case $V_B = 0$ and R_B is negligible.

For the variety of other conditions that can exist where $R_B > 10\Omega$ or $R_B \neq \infty$, the appropriate tests should be made if the most conservative rating is not used.

TABLE I

Typical Breakdown and Asymptotic Voltages
for Fairchild 2N697 Diffused Silicon Transistors

	Conditions	Typical Value (volts)
BV_{CEO}	$I_C = 10\mu A$	75
BV_{CBO}	$I_C = 100\mu A$	120
LV_{CEO}	$I_C = 100 ma, 167\mu s pulse,$ $1\% \text{ Duty Cycle}$	35
LV_{CER}	$I_C = 100 ma, R = 10\Omega, 167\mu s pulse$ $1\% \text{ Duty Cycle}$	70

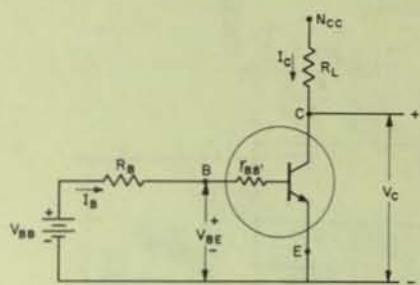


Fig. 1 Definitions of Circuit and Device Variables.

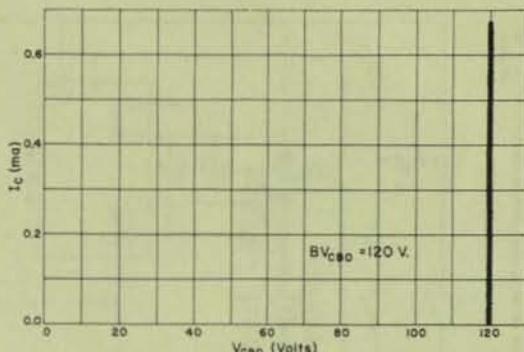


Fig. 2 I_C versus V_{CE} for $I_E = 0$
for a typical Fairchild 2N697

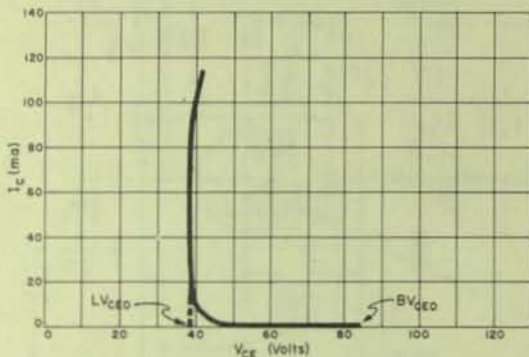


Fig. 3 BV_{CEO} and LV_{CEO}
for a typical Fairchild 2N697

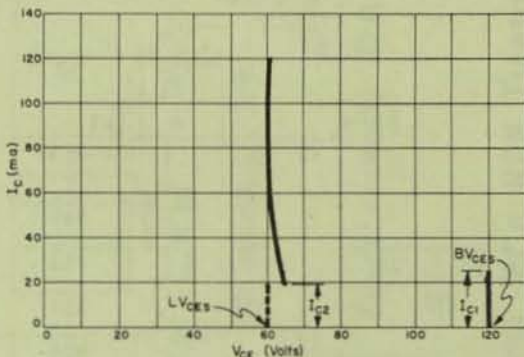


Fig. 4 BV_{CES} and LV_{CES}
for a typical Fairchild 2N697

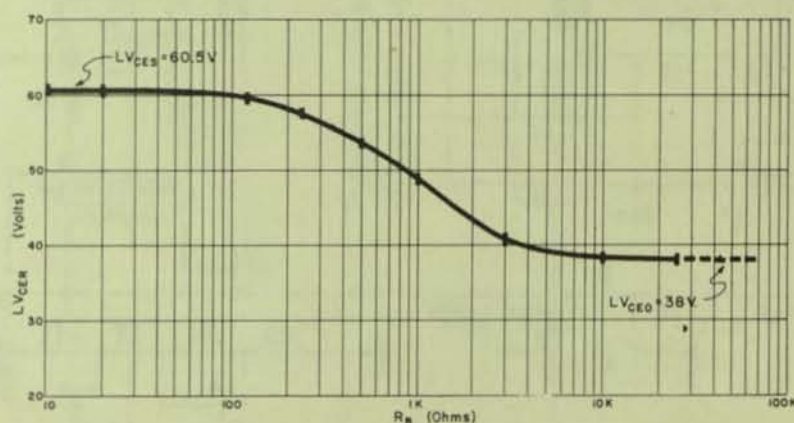
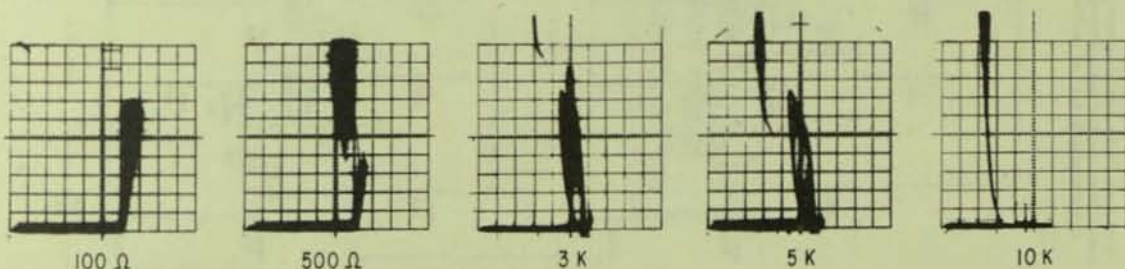


Fig. 5 LV_{CER} versus R_B for a typical Fairchild 2N697
at 100 mA, 167 μ s pulse, 1% duty cycle

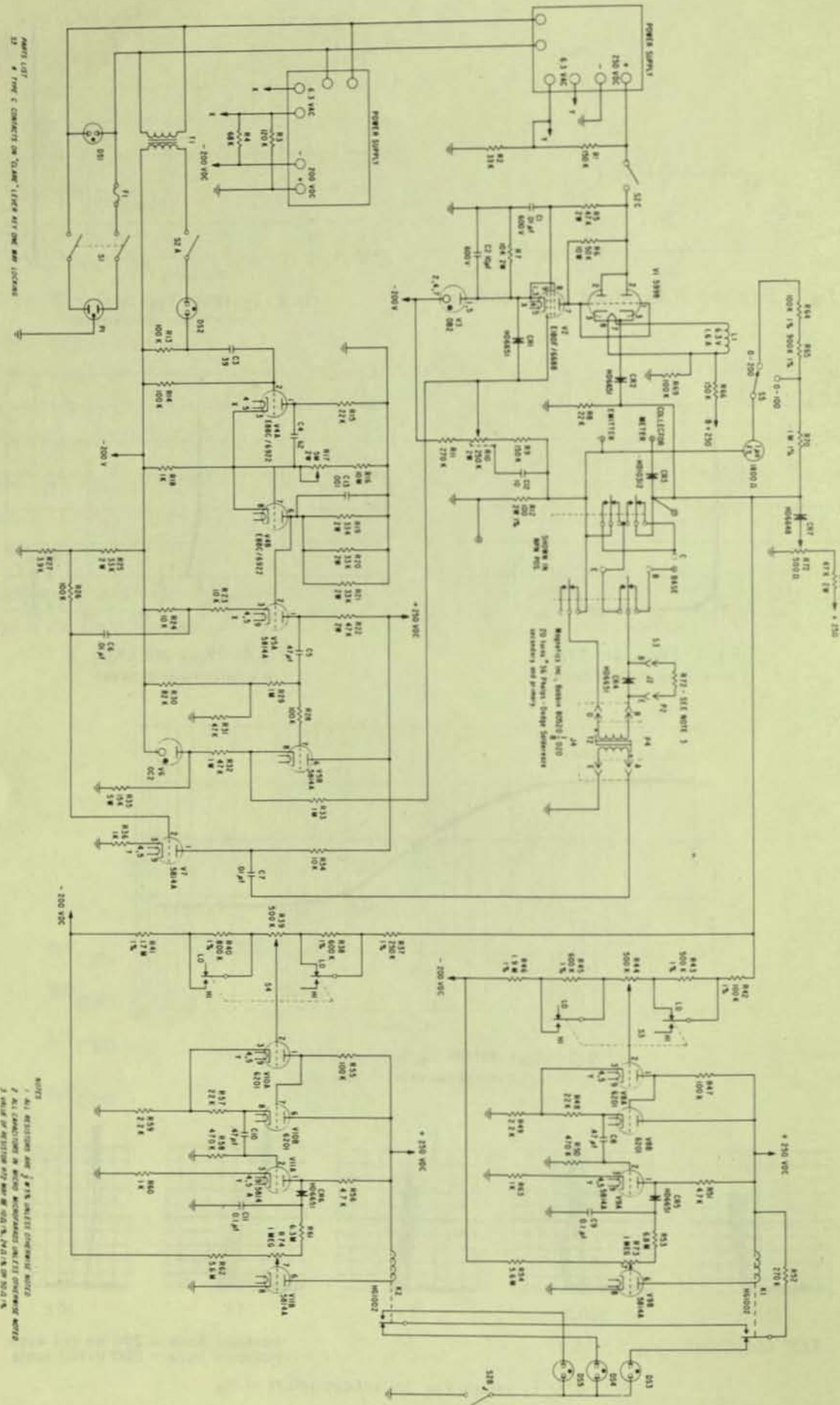


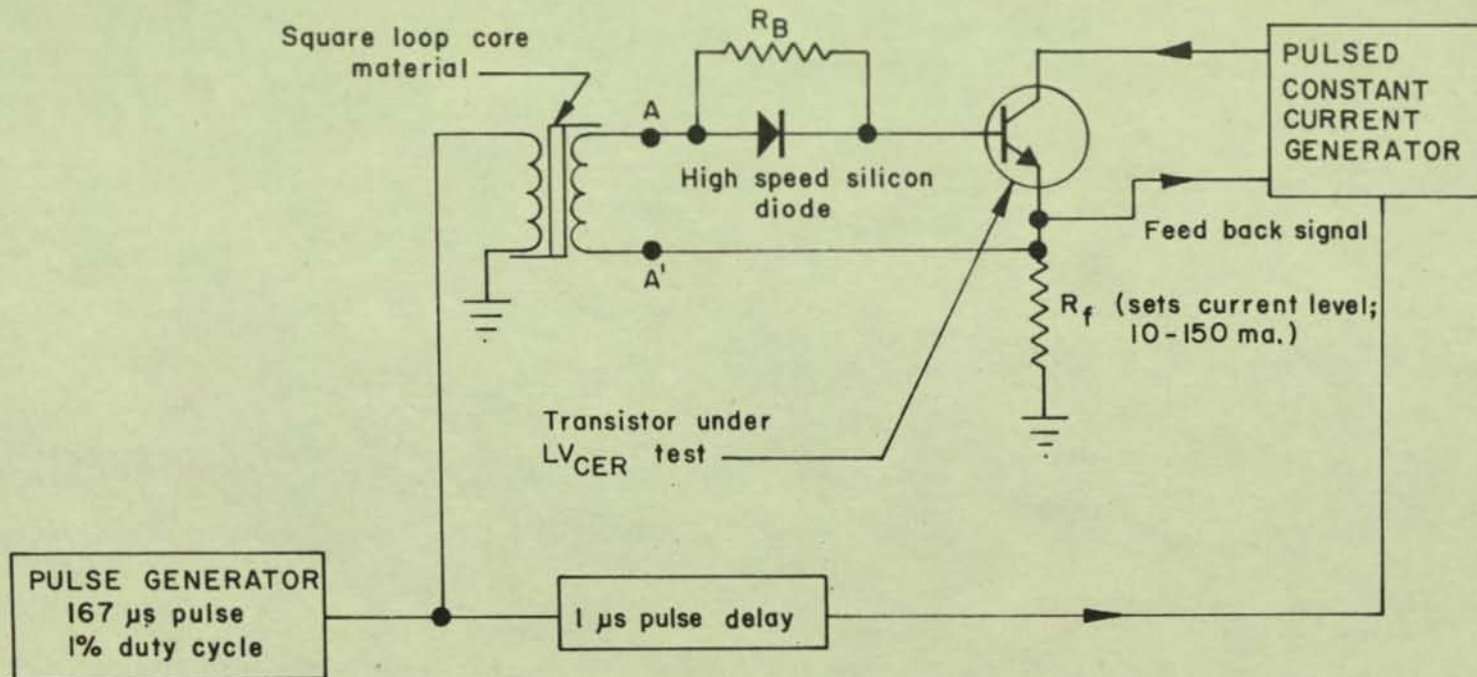
TEST CONDITIONS : $V_{BB} = -1.5$ V

Vertical Scale = 200 mA full scale
Horizontal Scale = 200 V full scale

Fig. 6 I_C versus V_{CE} for various values of R_B

Fig. 7 SCHEMATIC LVGER
 $R = 10\Omega$; $I_C = 100\text{mA}$



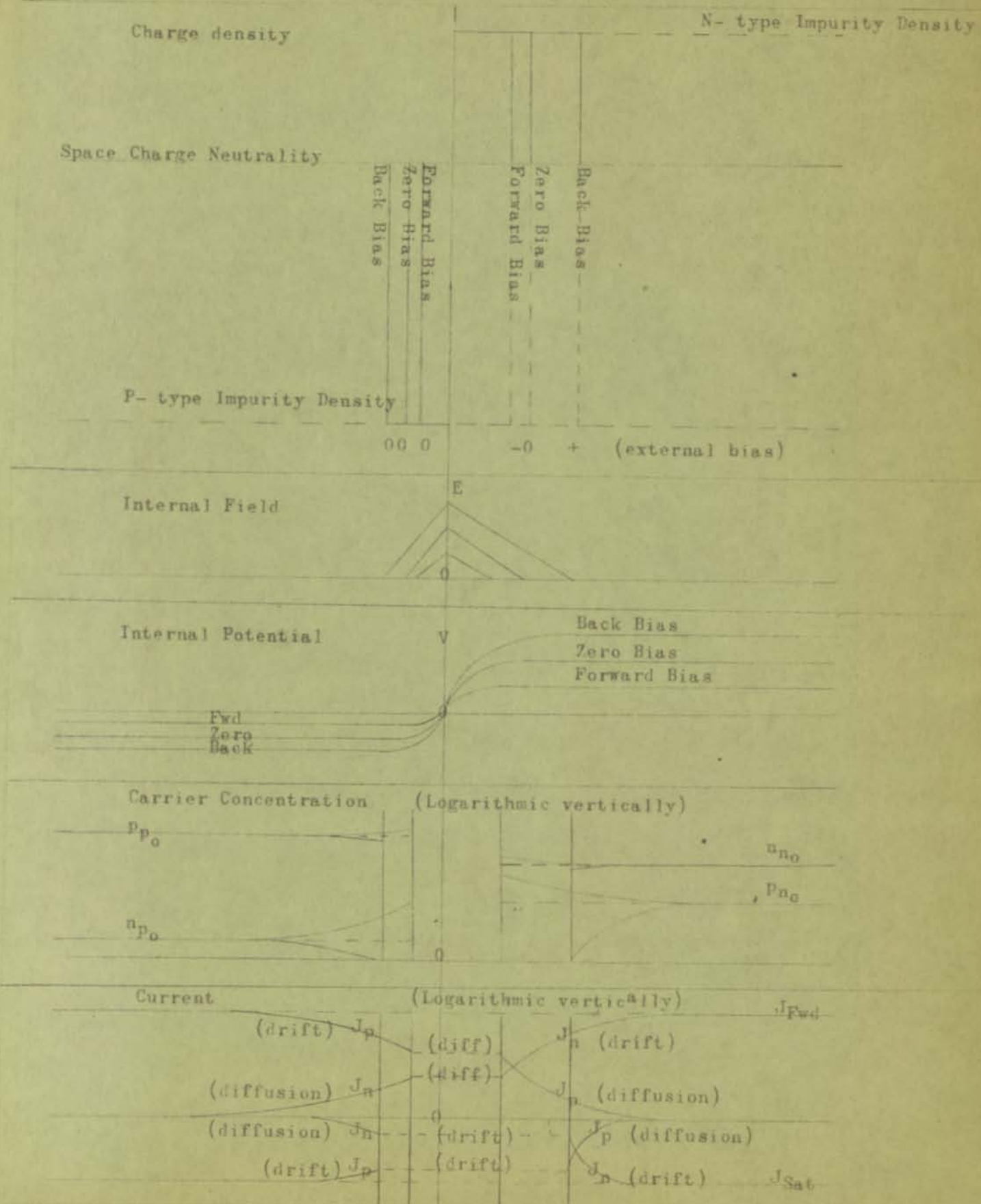


At terminals A-A': open circuit voltage
is 2.5v p-p, with 2 μ s
pulse duration.

R_B is normally 10 Ω

Fig. 7A Block Diagram of LV_{CER} Tester for a NPN Transistor.

FORWARD, ZERO, & BACK BIASED ABRUPT P-N JUNCTION



DEVICE PHYSICS REFERENCE NOTES

NOMENCLATURE & SYMBOLS

P = thermal equilibrium concentration of holes
 N = " " " " electrons
 n_i = " " " " or holes in intrinsic material
 ϵ_0 = permittivity of vacuum = 8.85×10^{-12} farad/meter
 ϵ = permittivity
 ϵ_r = relative dielectric constant ($\epsilon_r, Si = 12, \epsilon_r, Ge = 16$)
 N_A = acceptor dopant concentration
 N_D = donor
 X_p = depletion region width from metallurgical junction in P-type semiconductor
 X_n = " " " " " " N " "
 V_B = contact potential
 V = externally applied voltage in forward direction
 V_D = barrier voltage = contact potential minus applied voltage
 q = charge of electron = -1.6×10^{-19} coulomb
 k = Boltzmann's constant = 1.38×10^{-23} joule / °K
 T = absolute temperature (°K)
 C = capacitance per unit area
 Q = charge per unit area
 D = diffusion constant of holes
 D^P = " " " electrons
 τ = lifetime
 L_A = constant of linear junction relationship
 J = current per unit area
 J_s = minority carrier diffusion current per unit area (saturation)
 L_p = diffusion length of holes
 L_n = " " " electrons
 p_p = hole concentration in P-type material
 p_n = " " " N " "
 n_p = electron " " P " "
 n_n = " " " N " "
 BV_D = avalanche breakdown voltage
 m = empirical constant in avalanche equation
 n₁ = electron density in excess of thermal equilibrium density at edge of depletion layer on P side
 p₂ = hole " " " " " " " " " " N "
 μ_n = mobility of electrons
 μ_p = " " holes
 n₀^P = electron concentration at thermal equilibrium
 p₀^N = hole " " " " "
 σ = conductivity = $1/\rho$
 ρ = resistivity

REFERENCE EQUATIONS

1. Mass action law in homogeneous region

$$NP = n_i^2 = M_c M_v \exp(\xi_g / kT) \text{ where } M_c = \text{energy state density in conduction band}$$

and $M_v = " " " " " \text{valence}$

2. Einstein equations of mobility

$$\mu_n = qD_n/kT$$

$$\mu_p = qD_p/kT$$

3. Conductivity equations

$$J_{\text{drift}} = \sigma E = E/\rho = qE(P\mu_p + N\mu_n)$$

$$J_{\text{diff}} = q(D_n \nabla N - D_p \nabla P)$$

$$J = J_{\text{drift}} + J_{\text{diff}}$$

4. Rectifier equation or small current equation

$$J = J_s [\exp(qV/kT) - 1] \text{ where}$$

$$J_s = q(D_p p_n / L_p + D_n n_p / L_n) \text{ and}$$

$$L_p = (D_p \tau_p)^{1/2} \text{ and}$$

$$L_n = (D_n \tau_n)^{1/2}$$

5. Back Bias current near avalanche breakdown

$$J = \frac{-J_s}{1 - (-V/BV_D)^m} \text{ where } 1.5 < m < 4 \text{ for silicon}$$

6. Capacitance per unit area

Abrupt Junction:

$$C_{AJ} = dQ/dV = \epsilon / (X_p + X_n) = [q\epsilon M_A M_D / 2(M_A + M_D)]^{1/2} V_D^{-1/2}$$

Graded Junction:

$$C_{GJ} = dQ/dV = \epsilon / 2X_p = \epsilon / 2X_n = (q\epsilon^2 n_i / 12L_A)^{1/3} V_D^{-1/3} \text{ where}$$

7. Depletion Region widths

$$M_D - M_A = n_i x / L_A$$

Abrupt junction:

$$X_p = \left[\frac{q\epsilon V_D}{qM_A(1 + M_A/M_D)} \right]^{1/2}$$

$$X_n = \left[\frac{2\epsilon V_D}{qM_D(1 + M_D/M_A)} \right]^{1/2} \text{ where } V_D = V_B - V \text{ and}$$

$$V_B = \text{contact potential} = kT/q \ln(M_D M_A / n_i^2)$$

Graded junction:

$$X_p = X_n = (V_D^3 \epsilon L_A / 2q n_i)^{1/3} \text{ where the graded junction definition is}$$

$$M_D - M_A = n_i x / L_A$$

REFERENCE EQUATIONS

8. Excess minority carrier density at edge of depletion layer

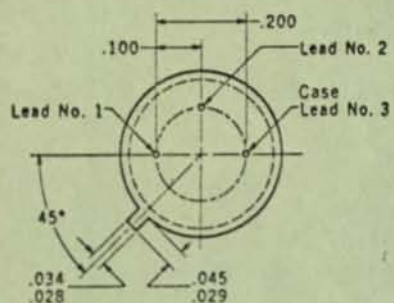
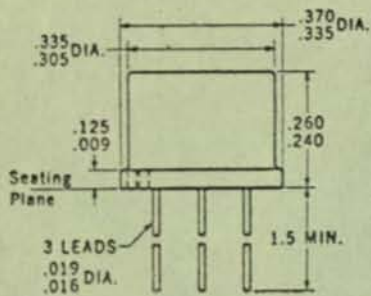
$n_1 = n_p [\exp(qV/kT) - 1]$ on uniform P-type side of junction

$p_2 = p_n [\exp(qV/kT) - 1]$ " " N " " " where

n_1 = electron density in excess of thermal equilibrium density at
edge of depletion region on P-type side, and

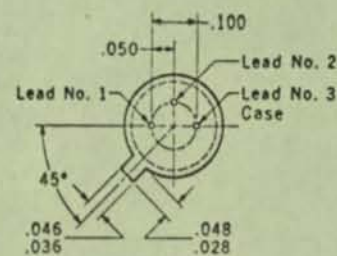
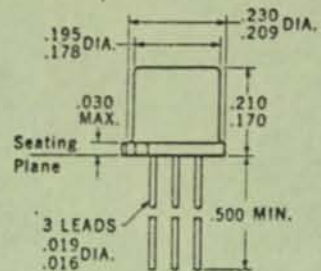
p_2 = hole density in excess of thermal equilibrium density at edge of
depletion region on N-type side

PHYSICAL DIMENSIONS A
in accordance with
JEDEC (TO-5) outline
(15 mil kovar)



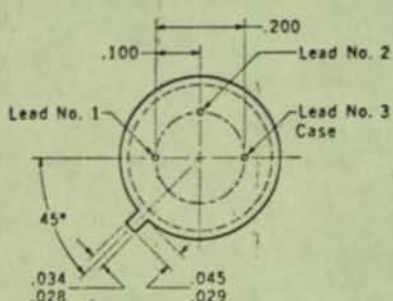
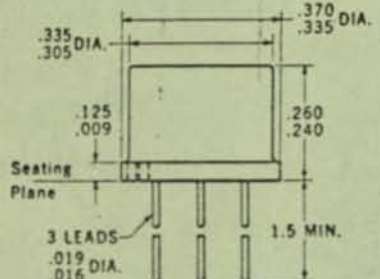
NOTES: All dimensions in inches
Leads are gold-plated kovar
Lead No. 3 internally connected to case
Package weight is 1.11 grams

PHYSICAL DIMENSIONS B
in accordance with
JEDEC (TO-18) outline
(8 mil kovar)



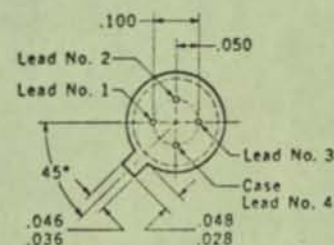
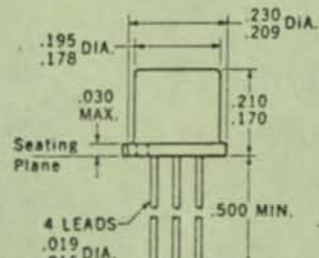
NOTES: All dimensions in inches
Same as "CB" except for lead length
Leads are gold-plated kovar
Lead No. 3 internally connected to case
Package weight is 0.44 gram

PHYSICAL DIMENSIONS C
in accordance with
JEDEC (TO-5) outline
(60 mil kovar)



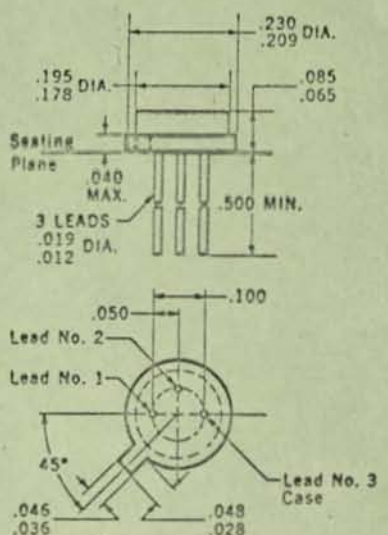
NOTES: All dimensions in inches
Leads are gold-plated kovar
Lead No. 3 internally connected to case
Package weight is 1.23 grams

PHYSICAL DIMENSIONS D
in accordance with
JEDEC (TO-72) outline
(Similar to packages
"F", "M" and "AV")
(8 mil kovar)



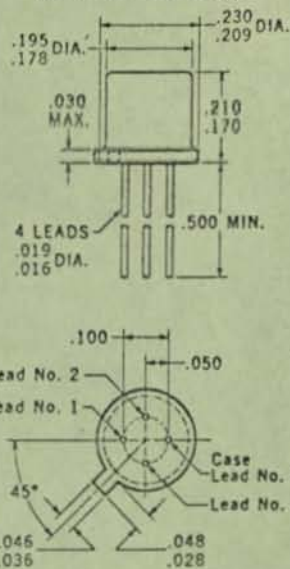
NOTES: All dimensions in inches
Dimensions similar to JEDEC TO-18 except
4 lead 90° spacing, bridge type
Leads are gold-plated kovar
Internal collector lead length is 110 mils
Collector club head length is 75 mils
Package weight is 0.50 gram

PHYSICAL DIMENSIONS E
in accordance with
JEDEC (TO-46) outline
(45 mil kovar)



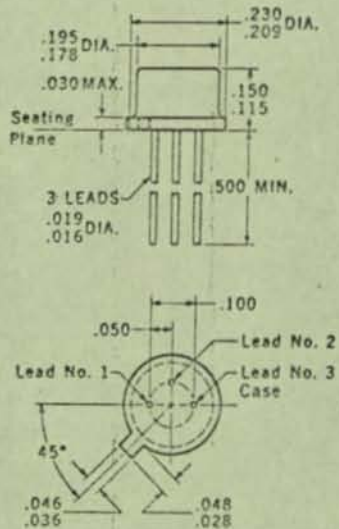
NOTES: All dimensions in inches
Lead No. 3 internally connected to case
Leads are gold-plated kovar
Package weight is 0.35 gram

PHYSICAL DIMENSIONS F
in accordance with
JEDEC (TO-72) outline
(Similar to packages
"D", "M" and "AV")
(8 mil kovar)



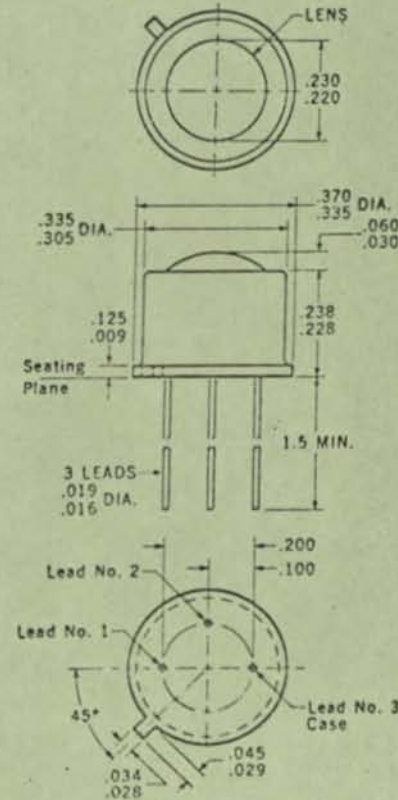
NOTES: All dimensions in inches
Dimensions similar to JEDEC TO-18 except 4
leads 90° spacing
Leads are gold-plated kovar
Package weight is 0.47 gram

PHYSICAL DIMENSIONS H
in accordance with
JEDEC (TO-52) outline
(8 mil kovar)



NOTES: All dimensions in inches
Leads are gold-plated kovar
Lead No. 3 internally connected to case
Package weight is 0.31 gram

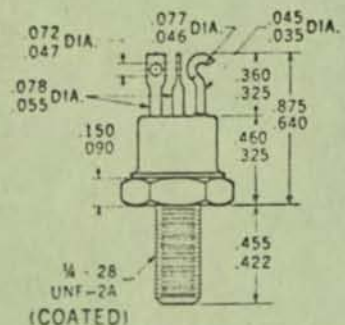
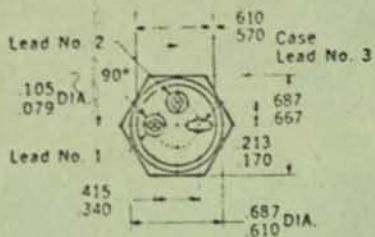
PHYSICAL DIMENSIONS I
(15 mil kovar)



NOTES: All dimensions in inches
Leads are gold-plated kovar
Lead No. 3 internally connected to case
Dimensions similar to JEDEC (TO-5) except
for short height and lens top
Package weight is 1.34 grams

PHYSICAL DIMENSIONS J

Similar* to JEDEC
(TO-61) outline



NOTES: All dimensions in inches
Header and stud are gold-plated copper

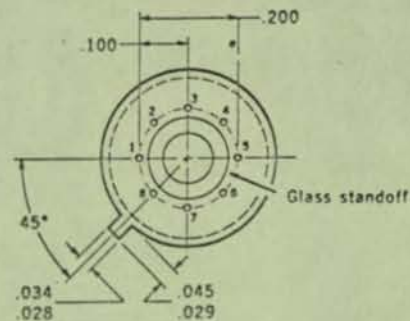
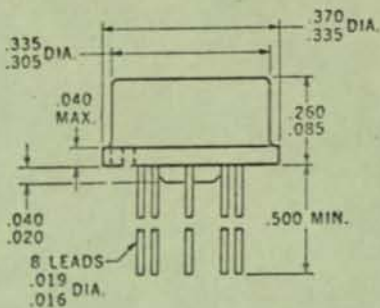
Cap is kovar

Disc is beryllia

*Identical to TO-61 with exception of lead solder lug
Package weight is 14.10 grams

PHYSICAL DIMENSIONS K

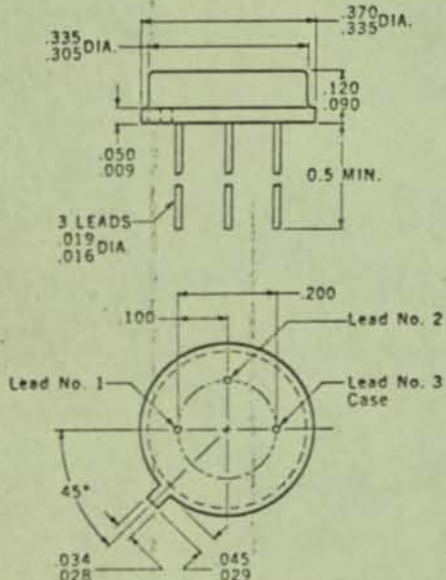
(15 mil kovar)



NOTES: All dimensions in inches
8 leads, 45° spacing, omitted pins are specified on individual specifications
Dimensions are similar to JEDEC (TO-5) except for 8 leads and short height
Leads are gold-plated kovar
Package weight is 0.95 grams

PHYSICAL DIMENSIONS L

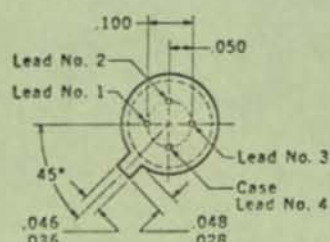
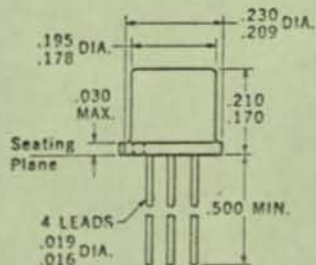
(60 mil kovar)



NOTES: All dimensions in inches
Dimensions similar to JEDEC TO-5 except for overall height
Lead No. 3 internally connected to case
Leads are gold-plated kovar
Package weight is 0.98 gram

PHYSICAL DIMENSIONS M

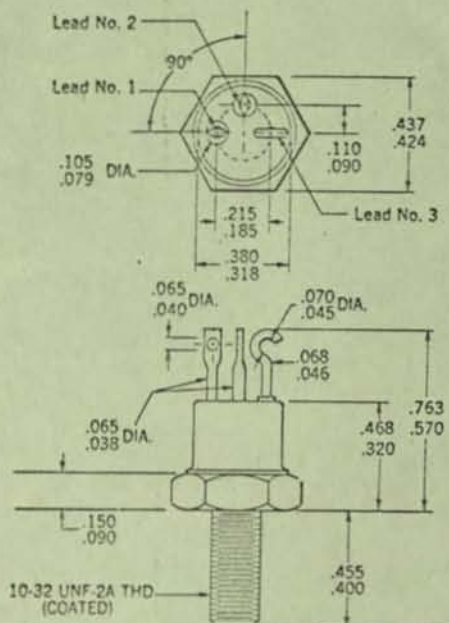
Single island package
in accordance with
JEDEC (TO-72) outline
(Similar to packages
"D", "F" and "AV")



NOTES: All dimensions in inches
Dimensions similar to JEDEC TO-18 except 4 leads
90° spacing, single island type
Leads are gold-plated kovar
Kovar island thickness = 15 mils
Package weight is 0.47 gram

PHYSICAL DIMENSIONS P

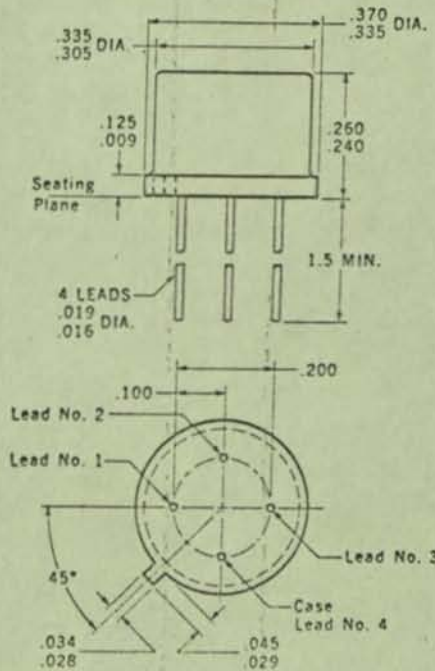
in accord with JEDEC
(TO-59) outline



NOTES: All dimensions in inches
Stud and header are gold-plated copper
Cap is gold-plated Kovar
Disc is silver tungsten
Package weight is 5.65 grams
Lead No. 3 electrically connected to case

PHYSICAL DIMENSIONS R

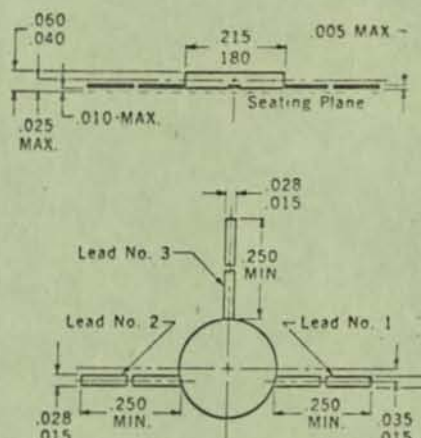
in accordance with
JEDEC(TO-33) outline
(15 mil kovar)



NOTES: All dimensions in inches
Leads are gold-plated Kovar
Internal collector lead length is 75 mils
Island is 60 mils wide, 80 mils long and 15
mils thick
Package weight is 1.22 grams

PHYSICAL DIMENSIONS Q

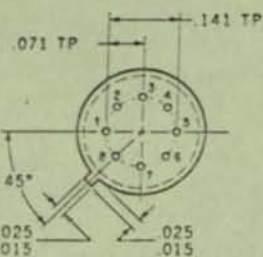
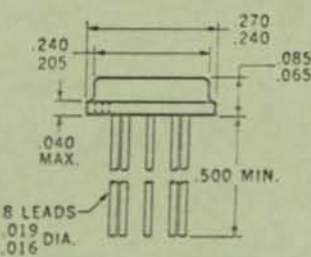
in accordance with
JEDEC (TO-50) outline



OTES: All dimensions in inches
Leads are gold-plated kovar
Base material is ceramic and is 10 mils thick
Package weight is 0.126 gram

PHYSICAL DIMENSIONS T

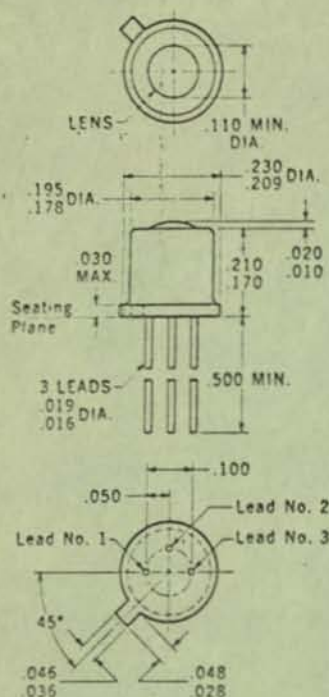
in accordance with
JEDEC (TO-70) outline
(45 mil kovar)



NOTES: All dimensions in inches
Leads are gold-plated kovar.
Dimensions are similar to JEDEC TO-47 except
8 lead 45° spacing
Omitted leads are specified on individual
specifications
Package weight is 0.67 gram

PHYSICAL DIMENSIONS U

(8 mil kovar)

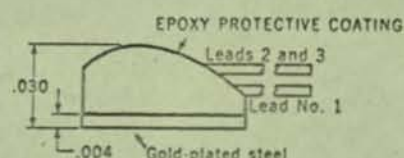
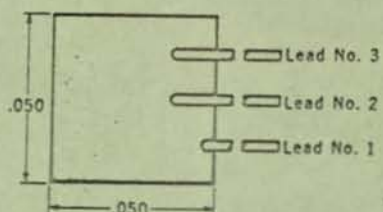


NOTES: All dimensions in inches

Lead No. 3 internally connected to case
Dimensions similar to JEDEC (TO-18) except
for lens top
Lead No. 2 omitted for 2 lead package
Leads are gold-plated kovar
3 lead package weight is 0.43 gram
2 lead package weight is 0.38 gram

PHYSICAL DIMENSIONS W

(Typical)

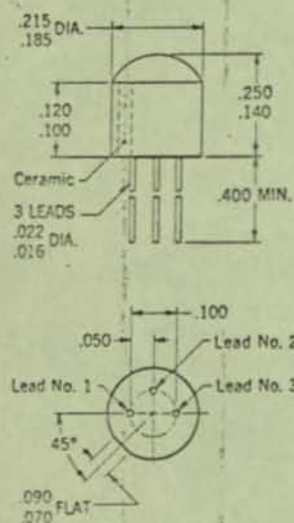


NOTES: All dimensions in inches

Leads are 1 mil diameter gold
Package weight is 0.004 gram

PHYSICAL DIMENSIONS Y

Epoxy package

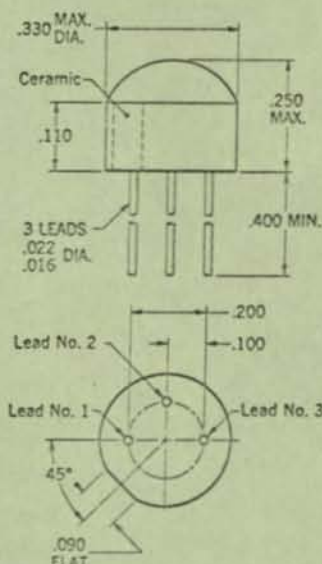


NOTES: All dimensions in inches

Ceramic Base
Internal collector lead length is 110 mils
Collector club head length is 85 mils
Emitter and Base leads are gold-plated nickel
Collector lead is gold-plated kovar
Package weight is 0.31 gram

PHYSICAL DIMENSIONS Z

Epoxy package

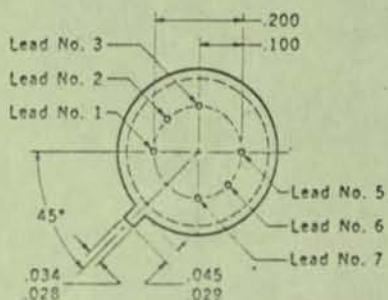
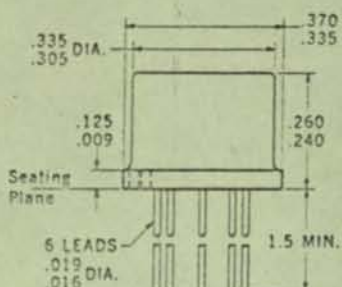


NOTES: All dimensions in inches

Leads are gold-plated kovar
Ceramic base
Internal collector lead length is 110 mils
Collector club head length is 180 mils
Package weight is 0.68 gram

PHYSICAL DIMENSIONS AA

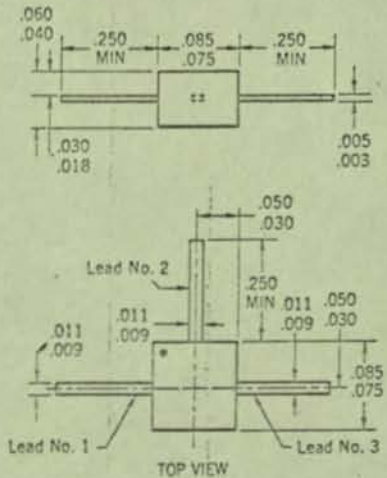
Adjacent two
island package



NOTES: All dimensions in inches
Dimensions similar to JEDEC TO-5 except 8 lead 45° spacing, leads 4 and 8 omitted
Lead No. 1 internally connected to one island,
Lead No. 7 internally connected to other island
Leads are gold-plated kovar
Kovar island thickness = 15 mils
Package weight is 1.23 grams

PHYSICAL DIMENSIONS AC

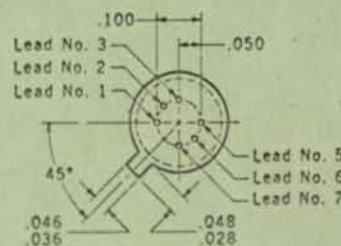
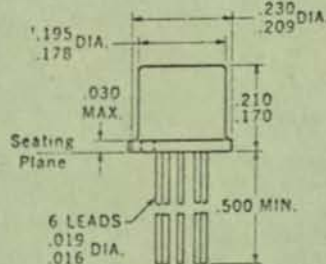
HERMETTM package



NOTES: All dimensions in inches
Leads are gold-plated nickel alloy
Package weight is 0.015 gram

PHYSICAL DIMENSIONS AB

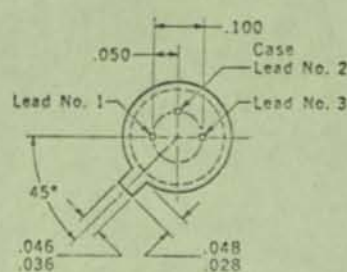
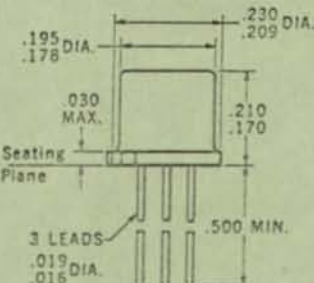
Opposed two
island package



NOTES: All dimensions in inches
Dimensions similar to JEDEC TO-18 except
8 lead 45° spacing, leads 4 and 8 omitted
Lead No. 3 internally connected to one island,
Lead No. 7 internally connected to other island
Leads are gold-plated kovar
Kovar island thickness = 15 mils
Package weight is 0.60 gram

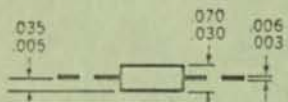
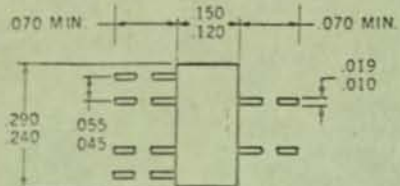
PHYSICAL DIMENSIONS AD

in accordance with JEDEC (TO-18) outline (8 mil kovar)



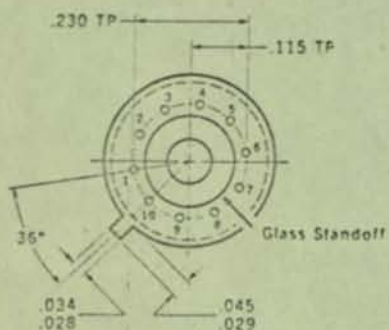
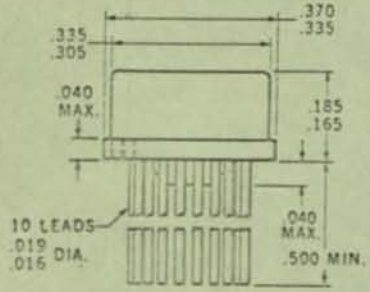
NOTES: All dimensions in inches
Leads are gold-plated kovar
Identical to package "B" except that lead No. 2 is internally connected to case
Package weight is 0.44 gram

PHYSICAL DIMENSIONS AE
 in accordance with
 JEDEC (TO-89) outline
 Network Package



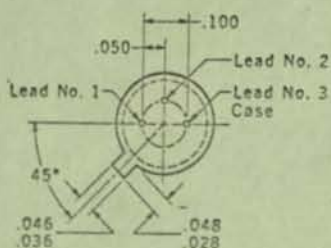
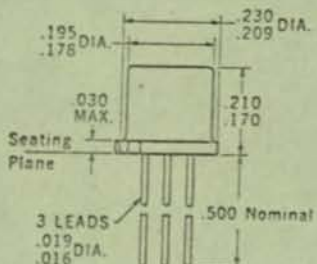
NOTES: All dimensions in inches
 Leads are gold-plated kovar
 Base material is gold-plated kovar
 4 mils in thickness. Chips are mounted on a
 4 mil thick gold-plated kovar slab which is
 separated from the base material by a 6 to
 7.5 mil ceramic insulator
 Package weight is .09 gram

PHYSICAL DIMENSIONS AG
 (15 mil kovar)
 in accordance with
 JEDEC (TO-100) outline



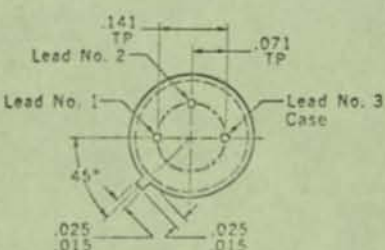
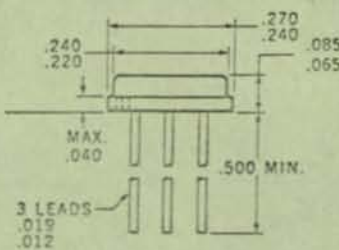
NOTES: All dimensions in inches
 Leads are gold-plated kovar
 Dimensions similar to TO-5 except 10 leads
 36° spacing and short height
 Package weight is 1.02 grams

PHYSICAL DIMENSIONS AF
 Similar* to JEDEC
 (TO-18) outline
 (8 mil kovar)



NOTES: All dimensions in inches
 OBSOLETE — For information only
 Leads are gold-plated kovar
 Lead No. 3 internally connected to case
 Package weight is 0.34 gram
 *Identical to package "B", except that lead length is specified 0.5 inch nominal instead of 0.5 inch minimum

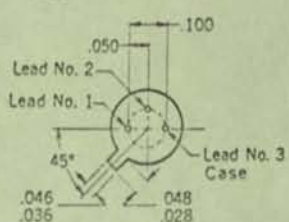
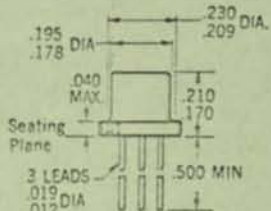
PHYSICAL DIMENSIONS AH
 in accordance with
 JEDEC (TO-47) outline
 (45 mil kovar)



NOTES: All dimensions in inches
 Leads are gold-plated kovar
 Lead No. 3 internally connected to case
 Package weight is 0.55 gram

PHYSICAL DIMENSIONS AI

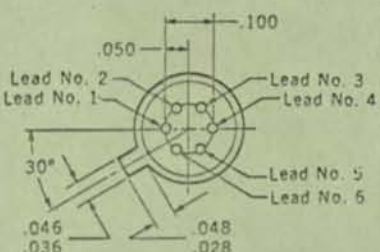
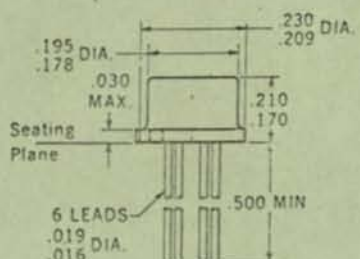
(45 mil kovar)



NOTES: All dimensions in inches
 TO-46 header with TO-18 cap
 Lead No. 3 Internally connected to case
 Leads are gold-plated kovar
 Package weight is 0.43 gram

PHYSICAL DIMENSIONS AJ

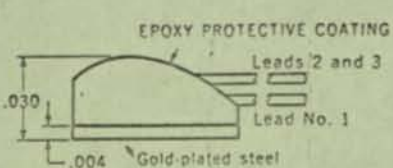
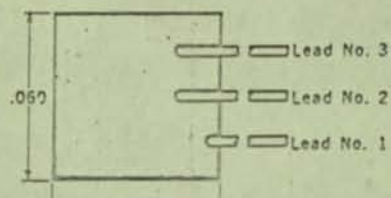
Adjacent two island package
 (8 mil kovar)



NOTES: All dimensions in inches
 Dimensions similar to JEDEC TO-18 except 6 lead,
 60° spacing
 Lead No. 1 internally connected to one island,
 Lead No. 5 internally connected to other island
 Package weight is 0.60 gram

PHYSICAL DIMENSIONS AK

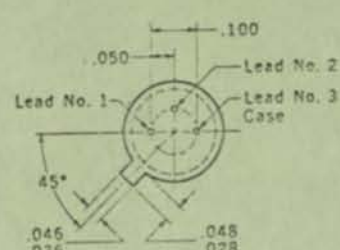
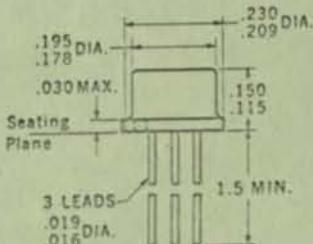
(Typical)



NOTES: All dimensions in inches
 Leads are 2 mil diameter gold
 Package weight is 0.006 gram

PHYSICAL DIMENSIONS* AL

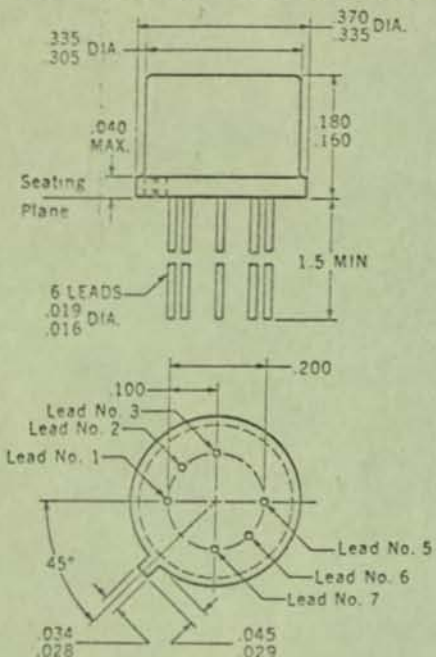
(8 mil kovar)



NOTES: All dimensions in inches
 *Identical to the "H" package JEDEC TO-52 except
 minimum lead length
 Leads are gold-plated kovar
 Lead No. 3 internally connected to case
 Package weight is 0.40 gram.

PHYSICAL DIMENSIONS AM

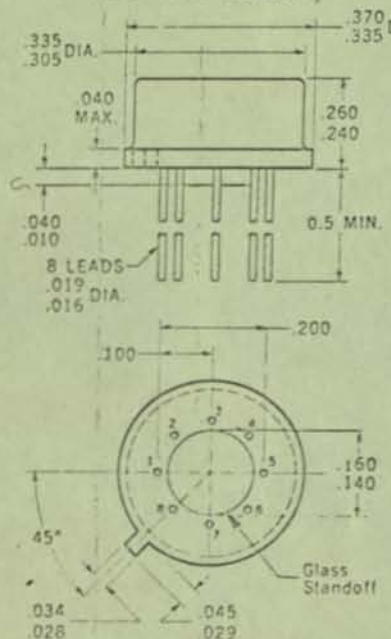
Adjacent two island package
in accord with JEDEC TO-78



NOTES: All dimensions in inches
Dimensions similar to JEDEC TO-5 except short height.
8 lead 45° spacing, leads 4 and 8 omitted
Identical to "AA" package except for height
Lead No. 1 internally connected to one island,
Lead No. 7 internally connected to other island
Leads are gold-plated kovar
Kovar island thickness = 15 mils
Package weight is 1.08 grams

PHYSICAL DIMENSIONS AP

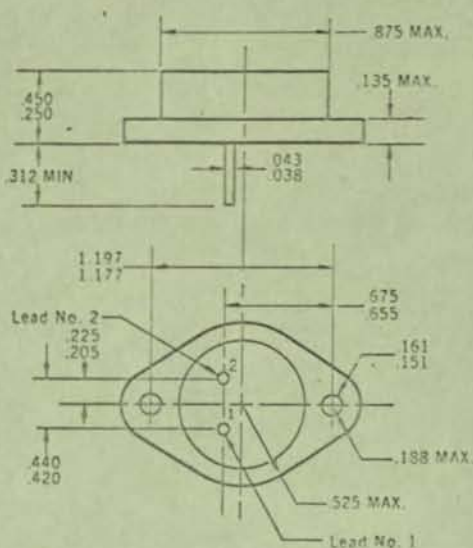
in accordance with
JEDEC (TO-76) outline
(15 mil kovar)



NOTES: All dimensions in inches
Same as K package except for standard
TO-5 height
8 leads, 45° spacing, omitted pins are
specified on individual specifications
Dimensions are similar to JEDEC (TO-5)
except for 8 leads
Leads are gold-plated kovar
Package weight is 1.22 grams

PHYSICAL DIMENSIONS AN

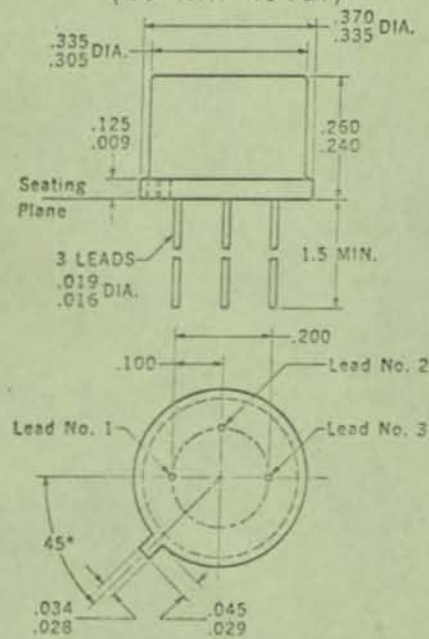
in accordance with
JEDEC (TO-3) outline



NOTES: All dimensions in inches
Leads 1 & 2 electrically isolated from case
Case is third electrical connection
Leads are nickel-alloy
Package weight 8.71 grams

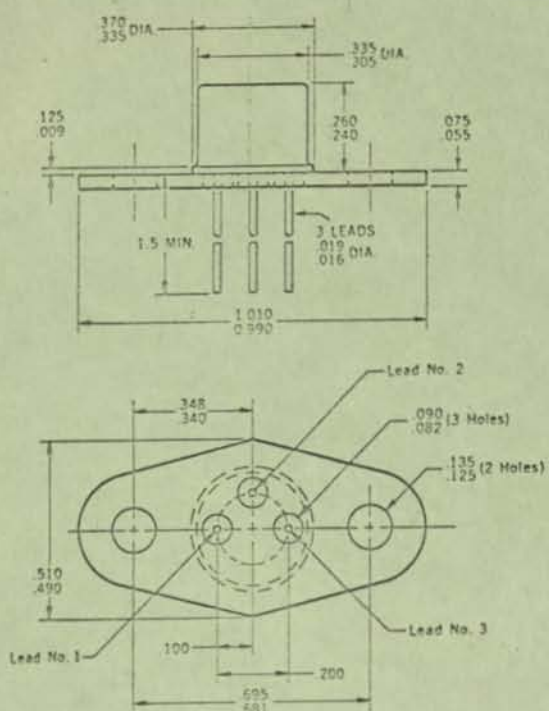
PHYSICAL DIMENSIONS AQ

in accordance with
JEDEC (TO-5) outline
(15 mil kovar)



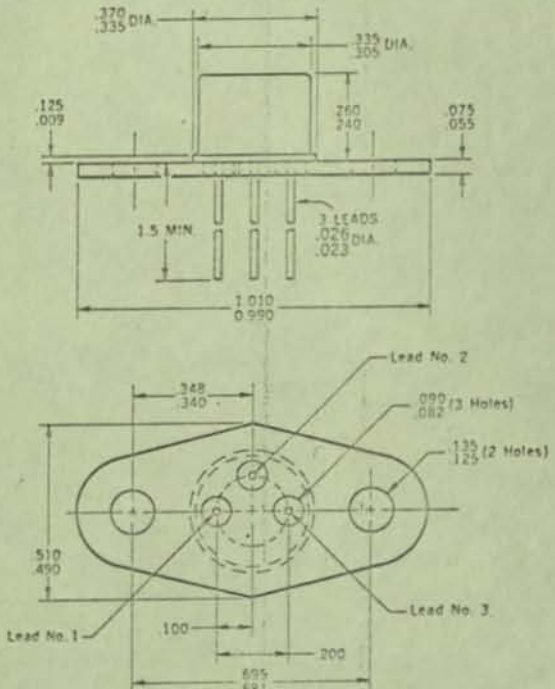
NOTES: All dimensions in inches
Same as "AS" except for lead diameter
Leads are gold-plated kovar
Solid kovar header
This package also used as part of
"AR" assembly
Collector internally connected to case
Package weight is 0.75 gram

PHYSICAL DIMENSIONS AR



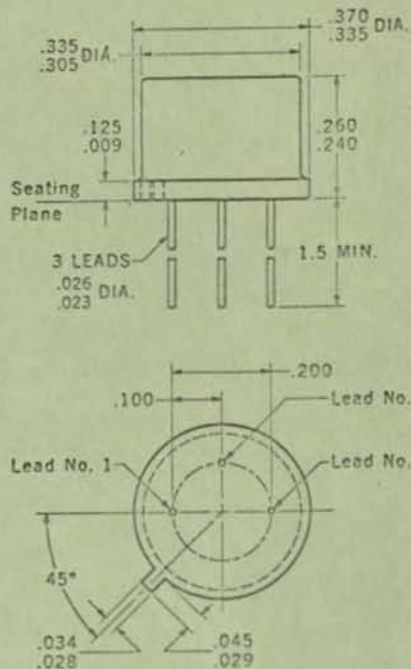
NOTES: All dimensions in inches
 Same as "AQ" except for addition of flange
 Leads are gold-plated copper
 Emitter and Base flange holes countersunk
 to 0.141 ± 0.005 on seating plane
 Collector internally connected to case
 Solid Kovar header
 Package weight 3.84 grams

PHYSICAL DIMENSIONS AT



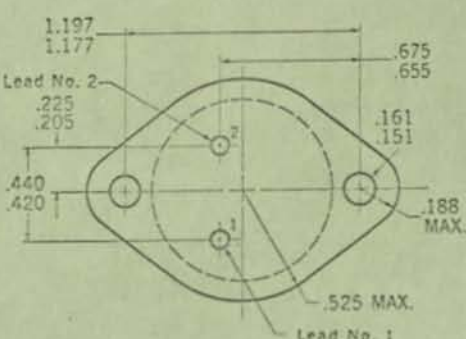
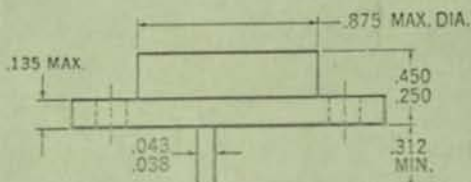
NOTES: All dimensions in inches
 Same as "AS" except for addition of flange
 Leads are gold-plated kovar
 Flange is nickel-plated copper
 Emitter and Base flange holes countersunk
 to 0.141 ± 0.005 on seating plane
 Collector internally connected to case
 Solid kovar header
 Package weight is 4.1 grams

**PHYSICAL DIMENSIONS AS
(15 mil kovar)**



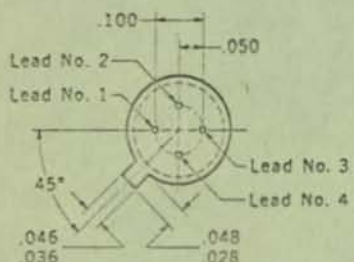
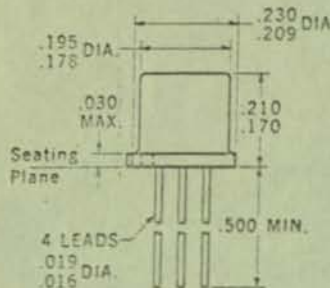
NOTES: All dimensions in inches
Same as "AQ" except for lead diameter
Leads are gold-plated kovar
Solid kovar header
This package also used as part of
"AT" assembly
Package weight is 0.98 gram

PHYSICAL DIMENSIONS in accordance with JEDEC (TO-3) outline



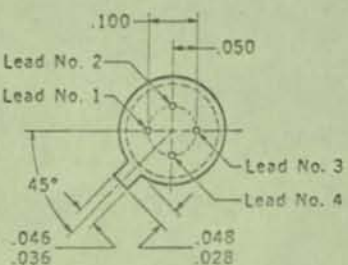
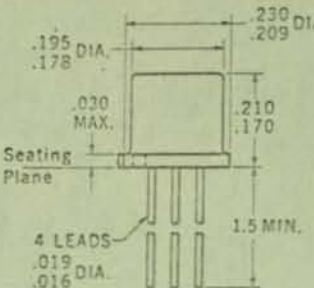
NOTES: All dimensions in inches
Identical to "AN" except for base thickness
Leads 1 and 2 electrically isolated from case
Case is third electrical connection
Leads are gold-plated nickel alloy
Package weight 8.8 grams
Steel flange

PHYSICAL DIMENSIONS AV
in accordance with
JEDEC (TO-72) outline



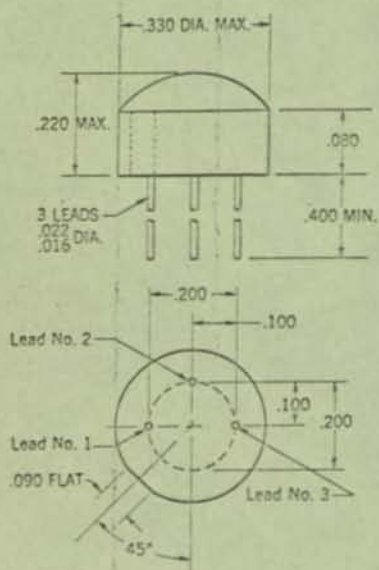
NOTES: All dimensions in inches
Identical to "AW" except for lead length
Similar to packages "D," "F" and "M"
Nail head collector
Leads are gold-plated kovar
Lead No. 3 electrically isolated from case
Package weight is 0.36 gram

PHYSICAL DIMENSIONS AW
in accord with
JEDEC (TO-72) outline



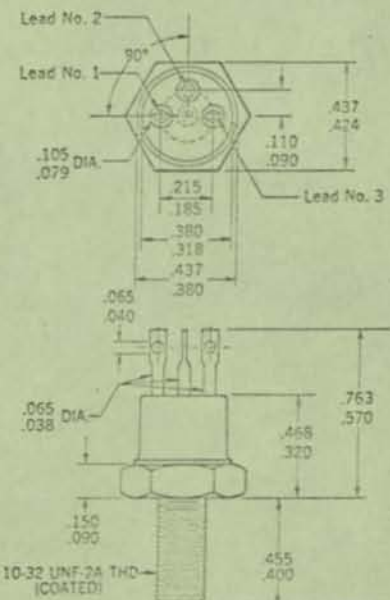
NOTES: All dimensions in inches
Identical to "AV" except for lead length
Similar to packages "D," "F" and "M"
Nail head collector
Leads are gold-plated kovar
Lead No. 3 electrically isolated from case
Package weight is 0.5 gram

PHYSICAL DIMENSIONS AZ
Epoxy package



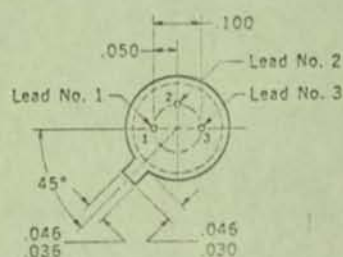
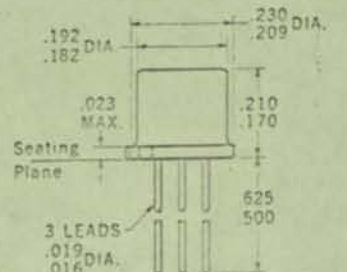
NOTES: All dimensions in inches
Internal collector lead length is .080
Same as "Z" package except for height
Leads 1 and 2 are gold-plated nickel
Lead No. 3 is gold-plated kovar
Ceramic base
Package weight is 0.5 gram

PHYSICAL DIMENSIONS BA
ISOLATED COLLECTOR
in accord with JEDEC (TO-59) outline



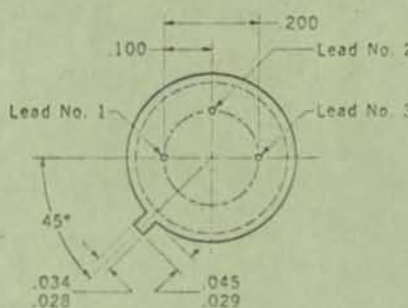
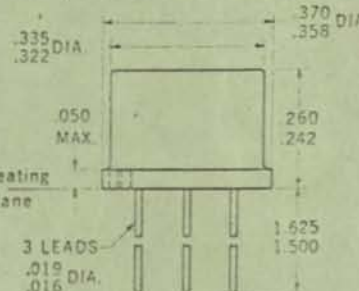
NOTES: All dimensions in inches
Stud and header are gold-plated copper
Cap is gold-plated kovar
All leads electrically isolated from case by beryllia disc
Package weight is 5.65 grams

PHYSICAL DIMENSIONS BB
in accordance with
JEDEC (TO-56) outline



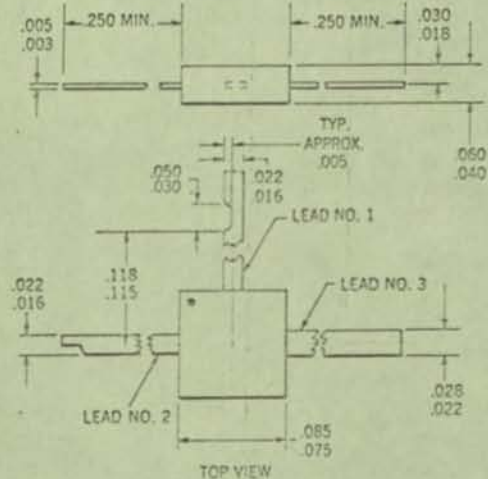
NOTES: All dimensions in inches
Leads are gold-plated kovar
Collector internally connected to case
Package weight is 0.43 gram

PHYSICAL DIMENSIONS BC
in accordance with
JEDEC (TO-55) outline
(15 mil kovar)



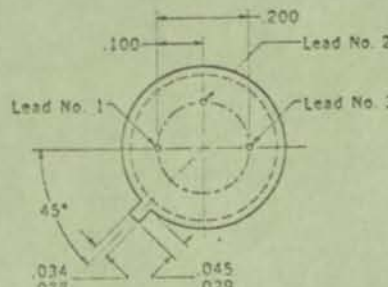
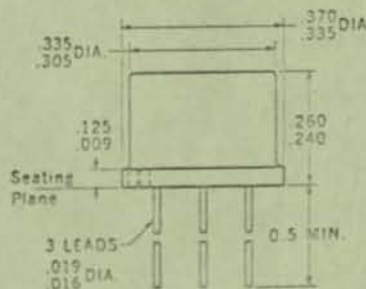
NOTES: All dimensions in inches
Leads are gold-plated kovar
Lead No. 3 internally connected to case
Package weight is 1.23 grams

PHYSICAL DIMENSIONS BD
HERMETTM package



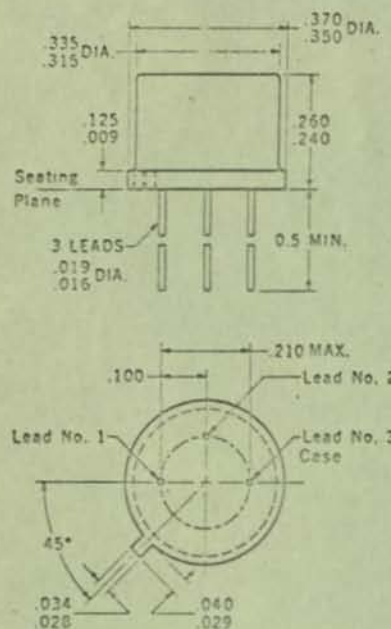
NOTES: All dimensions in inches
Leads are gold-plated nickel alloy
Package weight is 0.034 gram

PHYSICAL DIMENSIONS BE
in accord with JEDEC
(TO-39) outline
(15 mil kovar)



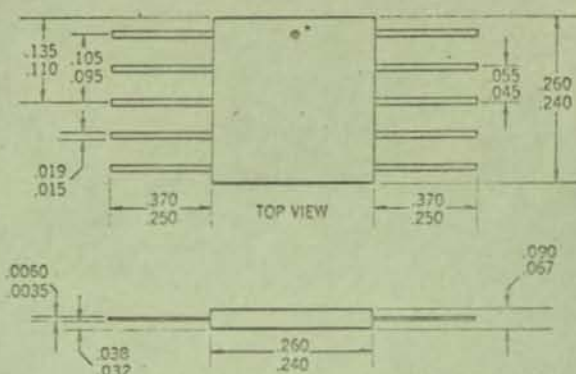
NOTES: All dimensions in inches
Identical to package "A" except for lead length
Leads are gold-plated kovar
Lead No. 3 internally connected to case
Package weight is 1.11 grams

PHYSICAL DIMENSIONS BF
 in accord with JEDEC
 (TO-39) outline
 (50 mil kovar)



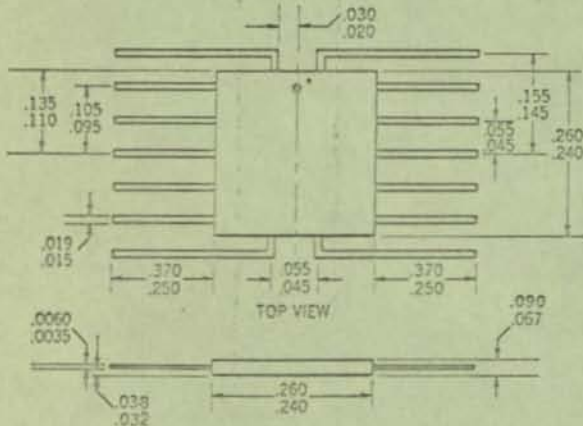
NOTES: All dimensions in inches
 Identical to package "C" except for lead length
 Leads are gold-plated kovar
 Lead No. 3 internally connected to case
 Package weight is 1.23 grams

PHYSICAL DIMENSIONS BG



NOTES: All dimensions in inches
 *Alternate marking of dot in upper left hand corner is also acceptable
 Package weight is approximately 0.7 gram

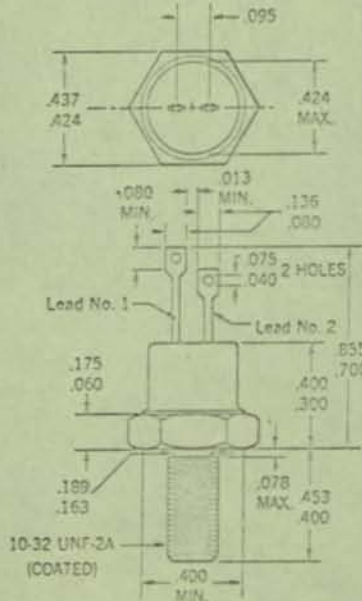
PHYSICAL DIMENSIONS BH



NOTES: All dimensions in inches
 *Alternate marking of dot in upper left hand corner is also acceptable
 Package weight is approximately 0.718 gram

PHYSICAL DIMENSIONS BI
 in accordance with JEDEC

(TO-64) outline

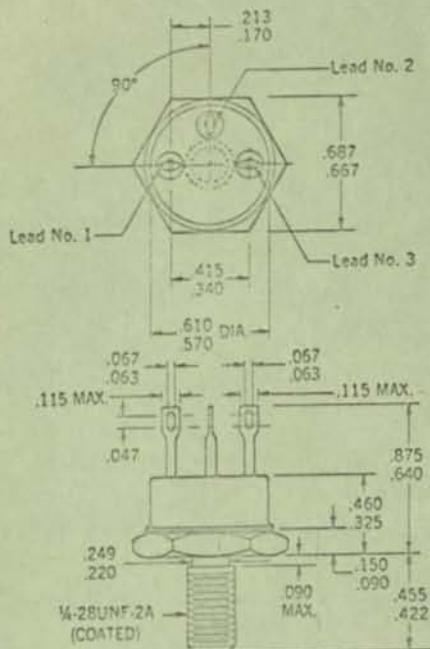


NOTES: All dimensions in inches
 Anode connected to case
 Stud and header are nickel-plated copper
 Cap is nickel-plated steel
 Package weight is 5.3 grams

PHYSICAL DIMENSIONS BJ

ISOLATED COLLECTOR

Similar to JEDEC (TO-61) outline*



NOTES: All dimensions in inches

Stud and header are copper

Cap is Kovar

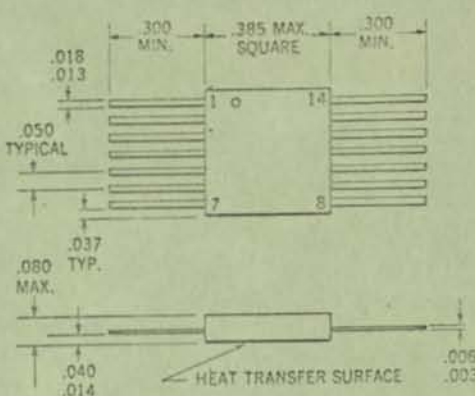
All leads electrically isolated from case

Disc is beryllia

Package weight is 14.1 grams

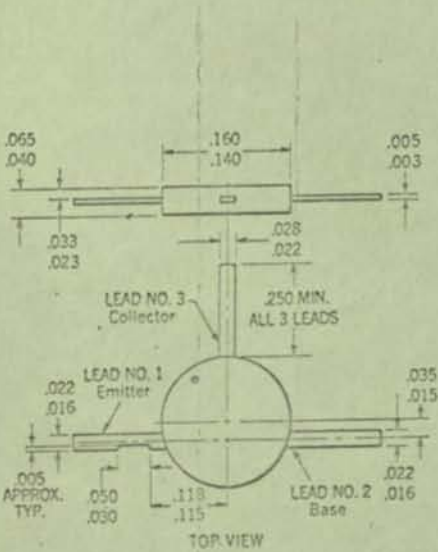
*Identical to TO-61 except for lead solder lugs

PHYSICAL DIMENSIONS BK



NOTES: All dimensions in inches
 Leads are gold-plated KOVAR
 Package weight is 0.55 gram

PHYSICAL DIMENSIONS BN



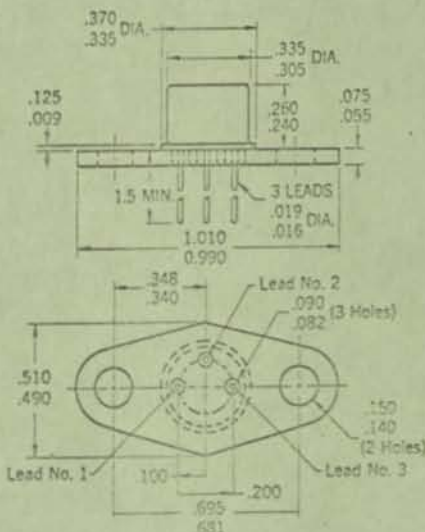
NOTES: All dimensions in inches

Leads are gold-plated nickel-iron

*Similar to JEDEC TO-51

Package weight is 0.04 gram

PHYSICAL DIMENSIONS BR



NOTES: All dimensions in inches

Same as "AQ" except for addition of flange

Identical to "AR" except for size of flange holes

Leads are gold-plated copper

Emiter and base flange holes countersunk to 0.141 ± 0.005 on seating plane

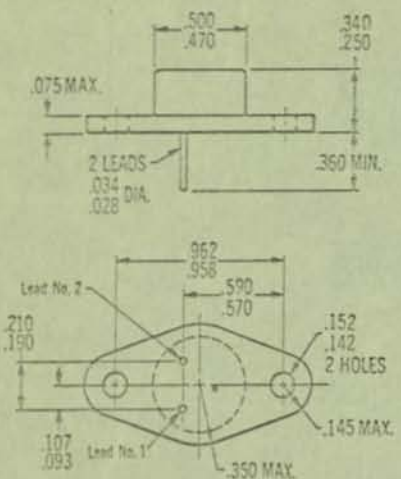
Collector internally connected to case

Solid Kovar header

Package weight 3.84 grams

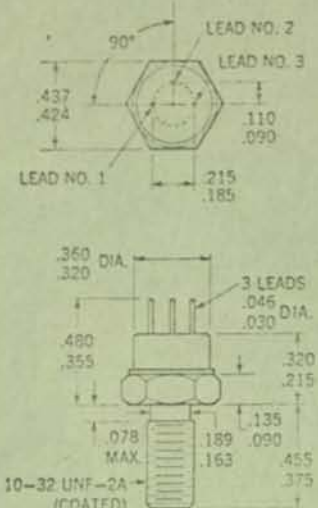
PHYSICAL DIMENSIONS BU

Identical to (TO-66)
except for flange thickness



PHYSICAL DIMENSIONS BV

in accordance with
JEDEC (TO-60)



NOTES: All dimensions in inches
Leads are gold-plated KOVAR *isolated from case*
All leads electrically connected to case
Package weight is 4.8 grams

NOTES: All dimensions in inches

Leads are gold or nickel-plated nickel alloy
Identical to "CU" except die mounting pedestal is steel

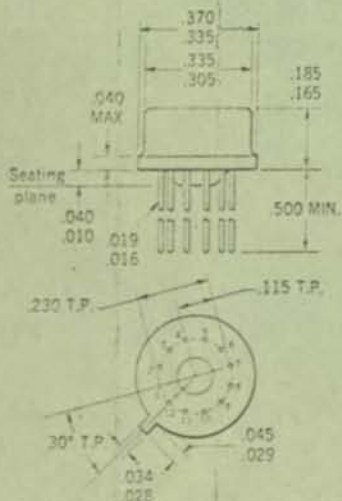
Leads 1 and 2 electrically isolated from case

Case is third electrical connection

Package weight is 6.192 grams

PHYSICAL DIMENSIONS BW

in accordance with
JEDEC (TO-101)



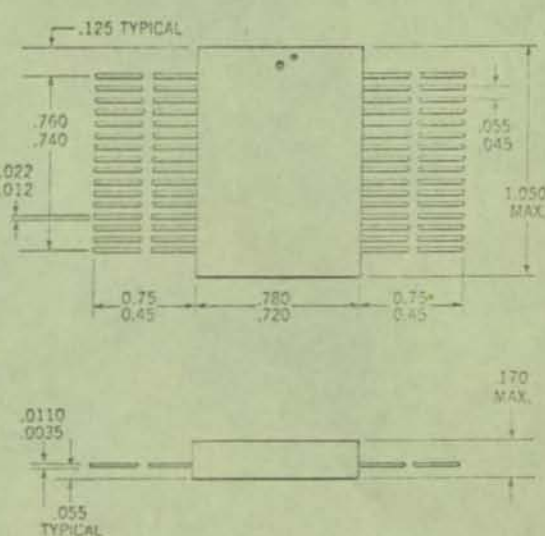
NOTES: All dimensions in inches

Leads are gold-plated KOVAR

Lead No. 6 internally connected to case

Package weight is 1.08 grams

PHYSICAL DIMENSIONS BY



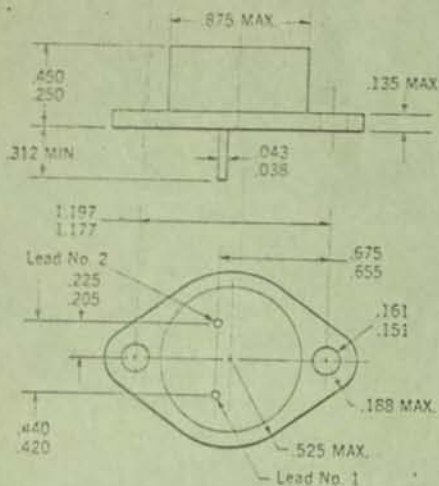
NOTES: All dimensions in inches

*Alternate marking of dot in upper left hand corner is also acceptable

Package weight is approximately 5.0 grams

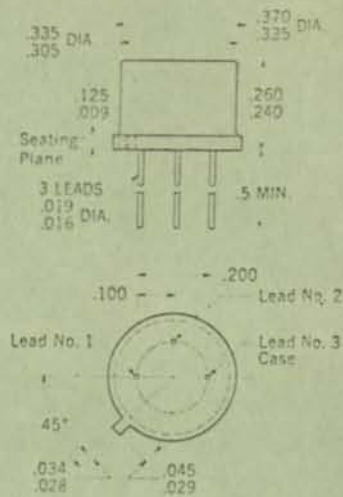
PHYSICAL DIMENSIONS
in accordance with
JEDEC (TO-3)

BZ



NOTES: All dimensions in inches
Leads 1 & 2 electrically isolated from case
Case is third electrical connection
Leads are nickel alloy
Package weight 16.5 grams
Copper flange

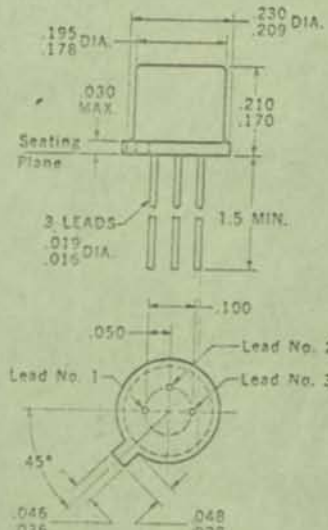
PHYSICAL DIMENSIONS
Similar to
JEDEC (TO-5) outline
low RTH package



NOTES: All dimensions in inches
Leads are gold-plated kovar
Lead No. 3 internally connected to case
Package weight is 1.3 grams

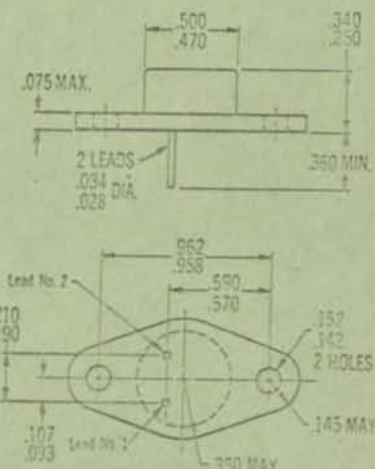
PHYSICAL DIMENSIONS CB
Similar to JEDEC
(TO-18) outline*

.8 mil kovar



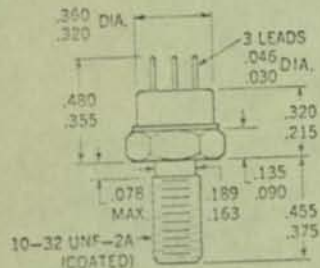
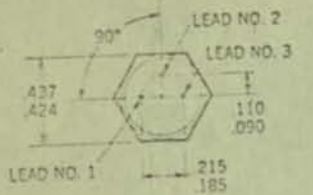
NOTES: All dimensions in inches
Leads are gold-plated kovar
Lead No. 3 internally connected to case
Package weight is 0.44 gram
*Identical to package "B" except for 1 1/2 inch minimum lead length

PHYSICAL DIMENSIONS CU
Identical to (TO-66)
except for flange thickness



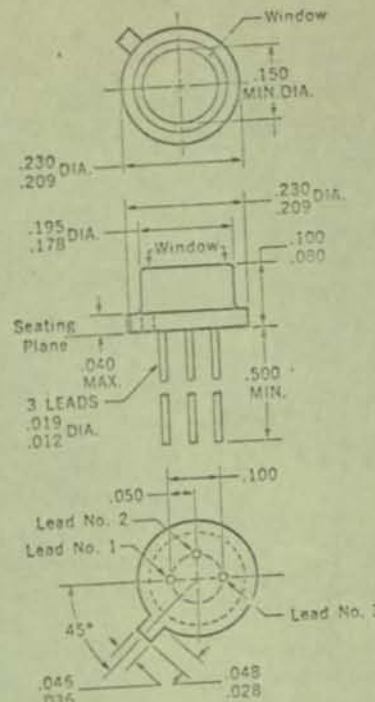
NOTES: All dimensions in inches
Leads are gold or nickel-plated nickel alloy
Identical to "BU" except die mounting pedestal is copper
Leads 1 and 2 electrically isolated from case
Case is third electrical connection
Package weight is 6.192 grains

PHYSICAL DIMENSIONS CV
in accordance with
JEDEC (TO-60)



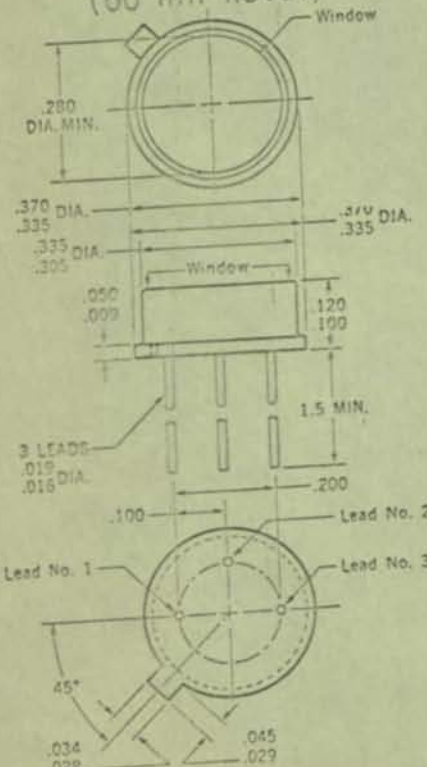
NOTES: All dimensions in inches
Leads are gold-plated kovar
Emitter is electrically connected to case
Package weight is 4.8 grams

PHYSICAL DIMENSIONS LB
(45 mil kovar)



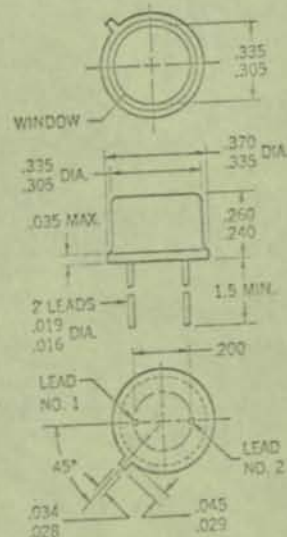
NOTES: All dimensions in inches
Dimensions similar to JEDEC TO-46 except for
overall height and semi-rigid silicone
resin window
Lead No. 3 internally connected to case
Leads are gold-plated kovar
Package weight is 0.317 gram

PHYSICAL DIMENSIONS LC
(60 mil kovar)



NOTES: All dimensions in inches
Dimensions similar to JEDEC TO-5 except for
overall height and semi-rigid silicone
resin window
Lead No. 3 internally connected to case
Leads are gold-plated kovar
Package weight is 1.0 gram

PHYSICAL DIMENSIONS PP
(15 mil kovar)



NOTES: All dimensions in inches
Leads are gold-plated kovar
Both leads are electrically isolated from case
Dimensions similar to JEDEC (TO-5) except
for 2 leads and window top
Package weight is 1.056 grams

Product Information

2.

Specification Parameters

Parameter	Test Conditions (must be specified)		Meaning of Specification
BV_{GSS}	I_G	$V_{DS} = 0$	Breakdown voltage from gate to channel. Drain and source are shorted, and a reverse bias is placed across the gate-channel junction.
BV_{GDS}	I_G	$V_{DS} = 0$	Identical to BV_{GSS} .
BV_{GDO}	I_D	$I_S = 0$	Breakdown voltage from gate to drain with source open.
BV_{SGO}	I_S	$I_D = 0$	Breakdown voltage from gate to source with drain open.
BV_{DSS}	I_D	$V_{GS} = 0$	Breakdown from drain to source with $V_{GS} = 0$. This is normally specified for enhancement MOS devices. It represents breakdown from drain to substrate.
BV_{DGS}			
BV_{DSX}	I_D	V_{GS}	Breakdown from drain to source with $V_{GS} \neq 0$. It represents breakdown from drain to substrate.
BV_{SDS}	I_S	$V_{DG} = 0$	Breakdown voltage from source to drain with $V_{DG} = 0$.
I_{GSS}	V_{GS}	$V_{DS} = 0$	Gate-channel leakage with $V_{DS} = 0$.
I_{DGO}	V_{GD}	$I_S = 0$	Drain-to-gate leakage current with source open.

.../

Product Information

3.

Specification Parameters

Parameter	Test Conditions (must be specified)	Meaning of Specification
I_{SGO}	V_{SG} $I_D = 0$	Source-to-gate leakage current with drain open.
I_G	V_{DS} or V_{DG} V_{GS}	Gate leakage current under certain operating conditions. It is usually somewhat lower than I_{DGO} since I_{DGO} is the limiting case of I_G .
I_{SDS}	V_{SD} $V_{GD} = 0$	Source-to-drain leakage current with zero gate-drain voltage.
I_{DSS}	V_{DS} $V_{GS} = 0$	Drain saturation current, the value of I_D measured above the knee of the V_{DS} - I_D characteristic curve where $V_{DS} \geq V_P$. I_{DSS} is actually defined as I_D at the V_{DS} required for channel pinch-off. In enhancement MOS devices, I_{DSS} is essentially the drain-substrate leakage plus any residual drain-source channel current.
I_D (ON)	V_{DS} V_{GS}	Drain current under specified bias conditions. Specified for enhancement MOS devices as a max intended operating drain current when V_{GS} is biased for max channel conduction.

.../

Specification Parameters

Parameter	Test Conditions (must be specified)	Meaning of Specification	
I_D	V_{DS} or V_{DG} V_{GS} or V_{SG}	Drain-source current under certain specified operating conditions.	
I_D (OFF)	V_{DS}	V_{GS}	Drain-gate leakage current with $V_{GS} \geq V_{GS(OFF)}$. $I_D(OFF)$ is slightly lower than I_{DGO} .
$V_{GS(OFF)}$	V_{DS}	$I_D(OFF)$	Gate cut-off voltage. Gate-source voltage required to cut-off channel current.
V_P			Pinch-off voltage, interchangeable with $V_{GS(OFF)}$.
$V_{GS(th)}$, V_T	V_{DS}	I_D	Gate-threshold voltage. Gate-source voltage required to initiate channel conduction in enhancement MOS devices.
V_{GS}	V_{DS}	I_D	Gate-source voltage at any given operating point.
$ V_{GS1} - V_{GS2} $	V_{DS}	I_D	Magnitude of gate-to-gate differential offset voltage in differential (matched) pairs.
$\Delta \left \frac{V_{GS1} - V_{GS2}}{\Delta T} \right $	T_{A1} & T_{A2}		Incremental change in $V_{GS1} - V_{GS2}$ expressed in $\mu\text{V}/^\circ\text{C}$.
$\frac{I_{DSS1}}{I_{DSS2}}$	V_{DS}		Match in I_{DSS} of differential pairs, expressed as a fraction.

.../

Product Information

5.

Specification Parameters

Parameter	Test Conditions (must be specified)	Meaning of Specification
$ I_{G1} - I_{G2} $	V_{DS} and V_{GS} V_{DG} and/or I_D T_A	Magnitude of match in I_G for differential pairs. Usually specified at an elevated temperature near 100°C.
$r_{DS(ON)}$	I_D V_{DS} and/or V_{GS}	Static drain-source resistance when biased to full ON conditions (maximum operating I_D). This resistance is defined in the ohmic region.
r_o	$V_{GS} = 0$	Minimum value of the $r_{DS(ON)}$ for $V_{GS} = 0$ (only for FET devices).

Product Information

6.

Small Signal Characteristics of FET's

Parameter	Test Conditions (must be specified)	Meaning of Specification
$r_{ds(on)}$	V_{GS} $V_{DS} = 0$ or I_S frequency	Drain-to-source resistance when the gate is biased to full ON conduction. This resistance is defined in the saturation region.
Y_{fs}	V_{DS} V_{GS} frequency	Common-source forward trans- fer admittance. Measured at $V_{GS} = 0$ unless otherwise speci- fied.
g_m , g_{fs}	V_{GS} V_{DS} frequency	Common-source forward trans- fer conductance. This is perhaps a more inform- ative term than Y_{fs} . At 1 KH _Z , $Y_{fs} \approx g_{fs}$. However, at high frequencies, Y_{fs} includes the ef- fect of gate-drain capacity, and it may therefore be misleadingly high. The term g_{fs} should be used for all high frequency measurements..
g_{mo}		Same as g_m , but specifically at a $V_{GS} = 0$.
Y_{iss}	V_{DS} V_{GS} $v_{ds} = 0$ frequency	Common-source input admittance with output shorted. Important for high frequency operation.

.../

Product Information

7.

Small Signal Characteristics of FET's

Parameter	Test Conditions (must be specified)	Meaning of Specification
G_{iss}	V_{DS} V_{GS} v_{ds} frequency	Common-source input conductance with output shorted. This must be specified for high frequency applications, as $g_{iss} \equiv 1/\mu$.
g_{is}		Same as g_{iss} .
Y_{OSS}	V_{DS} V_{GS} $V_{gs} = 0$ frequency	Output admittance, input shorted.
g_{OSS}	V_{DS} V_{GS} $V_{gs} = 0$ frequency	Common-source output conductance, input shorted.
C_{iss}	V_{DS} V_{GS} $V_{ds} = 0$	Common-source input capacitance, output shorted $C_{iss} = C_{dg} + C_{gs}$
C_{gss}	$V_{DS} = V_{GS}$ $v_{do} = 0$ frequency	Gate-source capacitance.
C_{rss}, C_{rs}	V_{DS} V_{GS} frequency	Reverse transfer capacitance.
C_{dg}	V_{DS} V_{GS} frequency	Actual value of drain-gate capacitance.

.../

Product Information

8.

Small Signal Characteristics of FET's

Parameter	Test Conditions (must be specified)	Meaning of Specification
C_{gs}	Value in equivalent circuit	Actual value of gate-capacitance.
C_{ds}	-do-	Actual value of drain-source capacitance, essentially header capacitance.
C_{oss}	$V_{DS} = V_{GS}$ $V_{gs} = 0$ frequency	Common-source output capacitance, input shorted. $C_{oss} = C_{rss} + C_{ds}$
C_{os}	$V_{DS} = V_{GS}$ $V_{gs} = 0$ frequency	Same as C_{oss} if $V_{GS} = 0$.
C_{dgs}	-do-	Same as C_{oss} .

Product Information

9.

FET Performance Parameters

Parameter	Test Conditions (must be specified)	Meaning of Specification
$t_{\text{delay(on)}}$	$\left\{ \begin{array}{l} V_{DD} \\ I_{D(\text{ON})} \\ V_{GS(\text{ON})} \\ \text{pulse characteristics} \end{array} \right.$	Delay time before turn on when pulsed from OFF to ON condition.
t_{rise}		Rise time when pulsed from OFF to ON condition.
t_{on}		$t_{\text{rise}} + t_{\text{delay(on)}}$
$t_{\text{delay(off)}}$	$\left\{ \begin{array}{l} V_{GS(\text{ON})} \quad V_{GS(\text{OFF})} \\ V_{DD} \quad I_{D(\text{on})} \\ \text{input pulse characteristics} \end{array} \right.$	Delay time before turn off when pulsed from ON to OFF condition.
t_{fall}		Fall time pulsed from ON to OFF condition.
t_{off}		$t_{\text{fall}} + t_{\text{delay(on)}}$
e_n	V_{DS} V_{GS} or I_D frequency bandwidth frequency	Common-source equivalent short-circuit input noise voltage. Measured at the output with the input shorted, and referred to the input. Expressed as rms volts per root cycle, $\mu\text{V}/\sqrt{\text{Hz}}$. A function of frequency, so frequency value must be stated.
i_n	V_{DS} V_{GS} or I_D frequency bandwidth	Common-source equivalent open circuit input noise current. Expressed as $\text{pA}/\sqrt{\text{Hz}}$, a function of frequency.

.../

Product Information

10.

FET Performance Parameters

Parameter	Test Conditions (must be specified)	Meaning of Specification
PG	frequency V_{DS} ; P_{in} I_D	Neutralised Power Gain. It expresses the power gain of the device when its reverse transmission is neutralised by an equal and apposite external circuit (neutralisation circuit).
NF	V_{DS} V_{GS} or I_D R_s generator frequency bandwidth	Noise figure. This represents a ratio between input signal to noise and output signal to noise. NF is a function both of frequency and generator resistance R_s . Both must be stated or the specification is meaningless. When properly qualified, NF includes the effects of both e_n and i_n .

Product Information

Our FET and MOS-FET Characteristics

Line	Type	I_{GSS} (max)	I_{DSS} (max)	$Y_{FS} (g_m)$ at 1 KH _z (min)	$R_{ds(on)}$ (max)	V_p or V_{TH} (max)	Structure	Notes
0028	BSX 83 BSX 84		0.5 nA 0.5 nA	400 / umhos 700 / umhos	1.5 KOhm 1 KOhm	-6 V -6 V	P-Channel MOS P-Channel MOS	Enhancement Mode Enhancement Mode
0049	BSX 85 BSX 86			1500 / umhos 2500 / umhos	500 Ohm 250 Ohm	-6V -6V	Dual P-MOS Dual P-MOS	Enhancement Mode Enhancement Mode
0057	BFX 78	10 pA	25 mA	6000 / umhos			N-MOS	Depletion Mode- High P _G (20 dB) and low noise (2.7 dB) at 100 MHz
0030	Not yet announced	1 nA	30 mA	4000 / umhos	350 Ohm	15	P-Channel FET	Very low noise (1.5 dB at 0.1- 100 kHz).